

Measurement, Analysis, and Modeling of Non-Isothermal

Low-Velocity Displacement Ventilation Jets

Laurent Magnier-Bergeron

A Thesis

In the Department

of

Building, Civil and Environmental Engineering

Presented in Partial Fulfillment of the Requirements

For the Degree of

Doctor of Philosophy (Building, Civil and Environmental Engineering) at

Concordia University

Montreal, Quebec, Canada

December 2015

© Laurent Magnier-Bergeron, 2015

ABSTRACT

Title: Measurement, Analysis, and Modeling of Non-Isothermal Low-Velocity Displacement

Ventilation Jets

Laurent Magnier-Bergeron, Ph.D.

Concordia University, 2015

Displacement Ventilation (DV) is an air distribution method recognized to enhance indoor air quality, while having a great potential for energy savings, due to stratification, higher supply air temperature and opportunity of free cooling. A frequent complaint associated with displacement ventilation is however the draft discomfort caused by the colder air movement at foot level, and the local discomfort due to an excessive temperature difference between head and ankle. Insufficient information is currently available regarding the variations of temperature and velocity inside a DV jet. Correlation models also need to be developed to report the variation of air speed in the jet.

In this thesis, the DV jet is analyzed in depth through, first, experimental measurements and, then, the development of correlation models. Measurements are performed in an environmental chamber to study the DV jet coming from two different wall-mounted DV diffusers, for different supply conditions. The variations of air speed and temperature in the longitudinal, transversal, and horizontal planes are measured and analyzed. The thermal characteristics are discussed in terms of local thermal comfort.

In the second part of the thesis, the experimental data are analyzed towards developing new models for the distribution of air speed and temperature in the air jets. A new mathematical model is proposed for the variation of air speed in the secondary zone of the jet, as well as a new model is suggested for the vertical air speed profile. The variation of the thickness of the DV jet is also studied. A new mathematical model is proposed to account for the variation of minimal air temperature in the jet. The variations of air speed and temperature in the transversal direction are also discussed. Finally, the contributions are summarized and future work is proposed.

À Gabrielle

À la vie

Acknowledgements

I would like first to thank my supervisors Radu Zmeureanu and Dominique Derome for their patience, support, and guidance. They believed in me and gave me the opportunity to do this thesis, helped me and trained me along the way, always provided me with useful comments, and made me a better researcher. This thesis would not have been finished if not for the respect I have for them. I would also like to thank Dr Haghghat, my MASc thesis's supervisor; without him and his supervision style, I would have never been an efficient and independent researcher. I would also like to thank my colleagues from NRC, NRCan, and EHPrice: Michel Tardif, Iain McDonalds, Bouaelm Ouazia, Daniel Booth, Liang Zhou, Brad Tully, and Julian Rimmer. A special thank also has to go to Concordia technicians and IT, especially Joe, Luc, and Sylvain. I would also like to thank l'Agence de l'Efficacité Énergétique for its financial support.

On a personal level, I thank Gabrielle, for everything. Everything she did, everything she said, everything she was. If there is a heaven, you are there now. I also thank Kate, who helps me on so many levels, supports me, and helped me go through the end of my thesis. I love you both. I thank my families; the one in France: Maman, Papa, Claire, Stéphane; the one in Québec: Marc, Danielle, Marie-Eve and Thomas; and the one in the US: Trudy, Alex, and Meghan. I thank my friends from Concordia, especially Zmeureanu's, Athienitis's, and Haghghat's offices. All of you helped, but my heart goes especially for (in no particular order) Arash, Alex, Costa, Véronique, José, Arash, Marie-Claude, Justin, Jason, Ahmed, Andreea, Mathieu, Diane, Arash, Parham, Xiao-Nan. You made all that craziness bearable and enjoyable. My deepest thanks also go to Isabelle, Justine, Alice, Anne-Sophie, and Jerome, for the profound help and caring they gave me. You were my faith when I lost it. I finally need to thank Maryse Labbé, my psychotherapist, who helped me with my depression and anxiety, and helped me heal my wounds.

Thanks to all those, and all those I am forgetting but whom I do not forget.

1.Contents

TABLE OF CONTENTS.....	vii
LIST OF FIGURES.....	xi
LIST OF TABLES.....	xv
LIST OF SYMBOLS.....	xix
1. CHAPTER 1: INTRODUCTION.....	1
1.1 Problem statement.....	1
1.2 Objectives of this thesis.....	3
2. CHAPTER 2: LITERATURE REVIEW.....	5
2.1 Introduction.....	5
2.1.1 Overview of a displacement ventilation jet.....	5
2.1.2 Thermal comfort.....	6
2.2 Velocity distribution in the DV jet.....	8
2.2.1 Velocity increase in the primary zone.....	8
2.2.2 Velocity decay in the secondary zone.....	10
Nielsen model.....	10
Nordtest model.....	11
Sandberg and Blomqvist theoretical model.....	12
Discussion.....	13
2.2.3 Vertical velocity profile in the secondary zone.....	14
2.2.4 Transversal velocity profiles.....	16

2.3 Temperature distribution	17
2.3.1 Temperature at floor level	17
2.3.2 Temperature variation inside the DV jet	18
2.4 Summary of the literature	20
3. CHAPTER 3: EXPERIMENTAL PROTOCOL.....	21
3.1 Testing facility and instrument	21
3.1.1 Testing facility	21
3.1.2 Measuring instruments	23
3.1.3 Testing conditions	24
3.1.4 Measurements outside the jet	24
3.2 Measurements locations in a DV jet for the two diffusers	26
3.2.1 Diffusers studied and supply conditions	26
3.2.2 Measurements in front of the diffuser	27
3.2.3 Measurements in the DV jet for non-isothermal supply conditions.....	28
3.3 Additional measurement for the 0.6 m x 0.6 m diffuser	30
4. CHAPTER 4: EXPERIMENTAL RESULTS	33
4.1 Experimental results for the diffuser of size 0.6 m x 0.6 m for under-temperatures of 2.4°C and 5.0°C	33
4.1.1 Measurements in front of the diffuser	34
4.1.2 Measurements in the longitudinal vertical plane, Plane L	37
Air speed.....	37
Air temperature	40
4.1.3 Measurements in the transversal vertical plane, Plane T	43
4.1.4 Measurements in a horizontal plane, plane H	45

4.1.5 Additional discussion	47
Vortices	47
Turbulence intensity	47
Particle Image Velocimetry (PIV)	47
Draft rate	48
Vertical Air Temperature Difference	48
4.2 Experimental measurements on the large diffuser (1.2 m x 0.6m)	49
4.2.1 Air speed measurements in the vertical longitudinal plane	50
4.2.2 Temperature distribution in the horizontal plane at 0.05 m from the floor	51
4.2.3 Comparison of the two diffusers tested	53
4.3 Additional measurements on the 0.6 m x 0.6 m diffuser	57
4.3.1 Measurements at 0.05 m in front of the diffuser	57
4.3.2 Air speed and temperature profiles in the vertical longitudinal plane	60
4.3.4 Characteristics of the DV jet at the end of the primary zone	62
4.4 Summary	66
5. CHAPTER 5: DATA ANALYSIS AND CORRELATIONS	68
5.1 Analysis of existing models for air speed decay in a DV jet	68
5.2 Determination of the maximal air speed at the end of the primary zone	73
5.2.1 Determination of the maximal air speed in a DV jet without air entrainment	73
Conservation of energy in the primary zone	74
Kinetic and potential energies at 0.05 m from the diffuser	75
Kinetic and potential energies of the DV jet at the end of the primary zone	77
Maximum air speed at the end of the primary zone assuming no entrainment	81
5.2.2 Correction for the entrainment of room air	82

Conservation of momentum in the jet	82
Calculation of the momentum terms	83
Final equation for the maximum air speed at the end of the primary zone of a DV jet	86
5.2.3 Validation with experimental data	86
Identification of variables used in Equation 5-39	87
Comparison with experimental data	88
5.3 Normalization and correlation for the air speed in the secondary zone	89
5.3.1 Data used for the study of the secondary zone	90
5.3.2 Normalization of air speed in the secondary zone.....	91
5.3.3 Graphical representation of the normalization model	92
5.3.4 Regression for the normalized air speed profile	93
5.3.5 Conclusion and discussion	94
5.4 Combination of the primary zone and secondary zone models	96
5.4.1 Maximum air speed in the secondary zone	96
5.4.2 Validation of the maximum air speed profile equation	96
5.4.3. Discussion	98
5.5 Analysis of the vertical air speed profile	99
5.5.1 Normalization of experimental data	100
5.5.2 Wall-jet vertical profile.....	103
5.5.3 A new proposed vertical profile specific to displacement ventilation jets.....	106
5.6 Thickness variations in a DV jet.....	109
5.6.1 Variation of the jet thickness with the distance from the diffuser	110
5.6.3 Proposed correlation for the jet thickness along the longitudinal axis	113
Minimum thickness in the DV jet.....	114

Variation in jet thickness from the minimum thickness δ_{\min}	118
General model of the thickness in the secondary zone of a DV jet	121
Discussion	123
5.6.2 Thickness of a DV jet in the transversal plane	124
Variation in jet thickness over the transversal axis	124
Correlation for the jet thickness in the transversal plane	125
5.7 Analysis of the transversal air speed profile	127
5.7.1 Experimental data used and normalization	127
5.7.2 Vertical transversal plane	128
5.7.3 Transversal profiles of air speed in the horizontal plane	130
Additional discussion	132
5.8 Analysis of the temperature distribution in the DV jet	134
5.8.1 Variation of temperature along the longitudinal axis	134
Variation of temperature in the primary zone	134
Normalization of the minimal air temperature in the secondary zone	135
Regression on the normalized profile of temperature	138
Final formulation for the longitudinal profile of minimum air temperature in the secondary zone of a DV jet	139
5.8.2 Discussion on the transversal and vertical profiles of temperature in the jet	141
5.9 Conclusion	145
5.9.1 Final equation for the air speed in the secondary zone of a DV jet	145
5.9.2 Final equation for the air temperature in the secondary zone of a DV jet	147
6. CHAPTER 6: CONTRIBUTIONS AND FUTURE WORK	149
6.1 Summary and contributions	149

6.2 Future work	151
7. APPENDIX	164

List of figures

Figure 1-1: Illustration of Displacement Ventilation..... 2

Figure 2-1: Schematic view of the two flow regions in a DV jet..... 6

Figure 2-2: Theoretical vertical velocity profile in a DV jet (based on Rajaratnam, 1976) 14

Figure 3-1: Schematic view a) of the environmental chamber; b) of the exhaust system 22

Figure 3-2: Motorized rail and anemometer used for measurements inside the jet..... 24

Figure 3-3: Schematic view of the axes of measurements for the DF1W 0.6 m x 0.6 m diffuser 28

Figure 3-4: Measurement planes for non-isothermal jet measurements 29

Figure 3-5: Measurement locations for non-isothermal jet measurements (Top view) 30

Figure 4-1: : Air speed (left) and temperature (right) measurements at 0.05 m from the diffuser (a, b) on the complete grid for $\Delta T=5.0^{\circ}\text{C}$; (c, d) on a vertical axis passing by the center of the diffuser for both supply conditions; (e, f) on the horizontal axis passing by the center of the diffuser for both supply conditions 36

Figure 4-2: Air speed distribution in Plane L for $\Delta T=2.4^{\circ}\text{C}$ (a) and $\Delta T=5.0^{\circ}\text{C}$ (b), the vertical white line refers to the maximum air speed attained. 38

Figure 4-3: Air speed profiles at different heights in plane L for $\Delta T=2.4^{\circ}\text{C}$ (a) and $\Delta T=5.0^{\circ}\text{C}$ (b)..... 39

Figure 4-4: Vertical air speed profiles in the primary and secondary zones for $\Delta T=2.4^{\circ}\text{C}$ (a) and $\Delta T=5.0^{\circ}\text{C}$ (b)... 40

Figure 4-5: Temperature distribution in Plane L for $\Delta T=2.4^{\circ}\text{C}$ (a) and $\Delta T=5.0^{\circ}\text{C}$ (b) 41

Figure 4-6: Air temperature profiles at different heights (left axis) and floor surface temperature (right axis) in Plane L for $\Delta T=2.4^{\circ}\text{C}$ (a) and $\Delta T=5.0^{\circ}\text{C}$ (b)..... 42

Figure 4-7: Vertical temperature profiles at different distances from the diffuser for $\Delta T=2.4^{\circ}\text{C}$ (a) and $\Delta T=5.0^{\circ}\text{C}$ (b)..... 42

Figure 4-8: Air speed (left) and temperature (right) distributions in Plane T for $\Delta T=2.4^{\circ}\text{C}$ (a, b) and $\Delta T=5.0^{\circ}\text{C}$ (c, d)..... 44

Figure 4-9: Air speed and temperature profiles at 2.16 m from the diffuser and at 0.05 m from the floor for both supply conditions..... 44

Figure 4-10: Air speed (left) and temperature (right) distributions at 0.05 m from the floor for $\Delta T=2.4^{\circ}\text{C}$ (a, b) and $\Delta T=5.0^{\circ}\text{C}$ (c, d).....	46
Figure 4-11: Transverse air speed profiles measured at a height of 0.05 m a) at different distances from the diffuser for $\Delta T=2.4^{\circ}\text{C}$; b) at 0.96 m and 2.16 m from the diffuser for both supply conditions	46
Figure 4-12 : VATD and maximum Draft Rate at floor level for both supply conditions	49
Figure 4-13 : Diffuseur DF1W 1.2m x 0.6 m	50
Figure 4-14: Air speed distribution in the vertical longitudinal plane for an under-temperature of 2.5°C (diffuser 1.2 m x 0.6 m).....	51
Figure 4-15: Air speed distribution in the vertical longitudinal plane for an under-temperature of 5.5°C (diffuser 1.2 m x 0.6 m).....	51
Figure 4-16: Temperature distribution in the horizontal plane at a height of 0.05 m for an under-temperature of 2.5°C (diffuser 1.2 m x 0.6 m).....	52
Figure 4-17: Temperature distribution in the horizontal plane at a height of 0.05 m for an under-temperature of 5.5°C (diffuser 1.2 m x 0.6 m).....	53
Figure 4-18: Maximum air speed profiles in the vertical longitudinal plane for the two diffusers tested	55
Figure 4-19: Minimum temperature profile in the vertical longitudinal plan for the two diffusers tested (measurement uncertainty of 0.5°C).....	56
Figure 4-20: Vertical profiles of air speed at 0.05 m in front of the diffuser for the five supply temperatures studied	58
Figure 4-21 : Vertical profiles of air temperature at 0.05 m in front of the diffuser for the five supply temperatures studied	59
Figure 4-22 : Vertical profiles of normalized air temperature at 0.05 m in front of the diffuser for the five supply temperatures studied	59
Figure 4-23 : Longitudinal profiles of maximal air speed for the five supply temperatures studied	61
Figure 4-24: Longitudinal profiles of minimal air temperature for the five supply temperatures studied	62
Figure 4-25: Vertical profiles of air speed at the end of primary zone for the five supply temperatures studied	64
Figure 4-26: Transversal profiles of air speed at the end of primary zone at the height of maximal air speed for the five supply temperatures studied.....	65
Figure 4-27 : Transversal profiles of air temperature at the end of primary zone at the height of maximal air speed for the five supply temperatures studied	65

Figure 5-1: Measured and correlated air speed decay for an under-temperature of 2.4°C..... 70

Figure 5-2: Measured versus correlated air speed for the Nordtest model for the five supply conditions tested 72

Figure 5-3: Control volume and control surfaces in the primary zone 74

Figure 5-4: DV jet assuming entrainment 82

Figure 5-5: Maximum air speed profiles in experimental data (not normalized) 91

Figure 5-6: Normalized maximum air speed from experimental data 93

Figure 5-7: Normalized maximum velocities and proposed correlation-based model 94

Figure 5-8: Measured and correlated maximum air speed in the secondary zone for the five supply conditions studied 97

Figure 5-9: Vertical profile of air speed at different distances from the diffuser DF1W (0.6m x 0.6m) for $\Delta T=5.0^{\circ}\text{C}$ 101

Figure 5-10: Normalized vertical profiles in the secondary zone 103

Figure 5-11: Comparison between the normalized air speed profiles in the secondary zone and the theoretical profile..... 106

Figure 5-12: Comparison between the proposed vertical profile, the profile from the literature and experimental data..... 108

Figure 5-13: Thickness of the jet versus distance from the diffuser for the four cases studied 110

Figure 5-14: Thickness of the jet versus the distance from the diffuser for the first diffuser and $\Delta T=5.0^{\circ}\text{C}$, separated into three zones 111

Figure 5-15: Thickness of the jet versus the distance from the diffuser based on Nielsen (2000) 113

Figure 5-16: Minimal thickness in the jet versus modified Archimedes number..... 117

Figure 5-17: Thickness of the jet versus the normalized local under-temperature for the four cases studied (dotted-lines for eye-guiding)..... 119

Figure 5-18: Thickness of the jet as a function of normalized local under-temperature in the secondary zone (Axial?) and regression model 121

Figure 5-19: Predicted versus measured thickness in the secondary zone 122

Figure 5-20: Thickness in the jet versus distance from the longitudinal axis, at a distance 2.16 m from the diffuser 124

Figure 5-21: Thickness of the jet as a function of local under-temperature in the secondary zone (Transversal) 126

Figure 5-22: Dimensionless transversal air speed profiles in the vertical transversal plane 129

Figure 5-23: Dimensionless transversal air speed profiles in the horizontal plane..... 131

Figure 5-24: Spread coefficients in the secondary zone at different distances from the diffuser 132

Figure 5-25: Longitudinal profile of minimal temperature in the jet for different cases 137

Figure 5-26: Normalized profiles of minimal temperature in the secondary zone for different cases 137

Figure 5-27: Correlation for the normalized under-temperature profile in the secondary zone and results from different cases. 139

Figure 5-28: Measured versus correlated air minimum temperature in the jet at different distances from the diffuser 140

Figure 5-29: Vertical profiles of air temperature in the secondary zone for DF1W diffuser of size 0.6 m x 0.6 m for a supply under-temperature of 5.0°C..... 143

Figure 5-30: Longitudinal profiles of air temperature at heights of 0.02 m and 0.10 m (left axis) and floor temperature (right axis) for DF1W diffuser of size 0.6 m x 0.6 m for a supply under-temperature of 5.0°C..... 143

List of tables

Table 3-1: Location of the thermocouples and RTDs.....	25
Table 3-2: Testing conditions for experimental work.....	27
Table 3-3: Testing conditions for the additional measurements	31
Table 4-1: Supply air conditions and thermal stratification for the two experimental cases.....	33
Table 4-2: Supply conditions for experimental work for the two diffusers	54
Table 4-3: Length of primary zone and height of maximum air speed at the end of the primary zone for various supply under-temperatures	63
Table 5-1: K_N coefficient for various supply under-temperatures.....	69
Table 5-2: Experimental conditions for the validation data.....	87
Table 5-3: Parameters of Equation 5-39 from measurements.....	88
Table 5-4: Estimated and measured maximum velocities	89
Table 5-5: Experimental data used for normalization	90
Table 5-6: Parameters used in Equation 5-43	97
Table 5-7: Diffuser and supply conditions in experimental data.....	100
Table 5-8: R^2 and air thicknesses for the vertical air speed profiles.....	104
Table 5-9: Diffuser information and minimum air jet thickness	115
Table 5-10: β and R^2 coefficients in the transversal vertical plane for different heights	128
Table 5-11: β and R^2 coefficients at different distances from the diffuser in the horizontal plane	130
Table 7-1: Air speed measured at 0.05 m from the diffuser for the 0.6 m x 0.6 m diffuser for a supply under-temperature of 2.4°C [m/s].....	164
Table 7-2: Temperature measured at 0.05 m from the diffuser for the 0.6 m x 0.6 m diffuser for a supply under-temperature of 2.4°C [°C].....	165
Table 7-3: Air speed measured in the longitudinal plane for the 0.6 m x 0.6 m diffuser for a supply under-temperature of 2.4°C [m/s].....	165

Table 7-4: Air temperature measured in the longitudinal plane for the 0.6 m x 0.6 m diffuser for a supply under-temperature of 2.4°C [°C].....	166
Table 7-5: Air speed measured in the transversal plane for the 0.6 m x 0.6 m diffuser for a supply under-temperature of 2.4°C [m/s].....	167
Table 7-6: Air temperature measured in the transversal plane for the 0.6 m x 0.6 m diffuser for a supply under-temperature of 2.4°C [°C].....	168
Table 7-7: Air speed measured in the horizontal plane at a height of 0.05 m for the 0.6 m x 0.6 m diffuser for a supply under-temperature of 2.4°C [m/s]	168
Table 7-8: Air temperature measured in the horizontal plane at a height of 0.05 m for the 0.6 m x 0.6 m diffuser for a supply under-temperature of 2.4°C [°C]	169
Table 7-9: Air speed measured at 0.05 m from the diffuser for the 0.6 m x 0.6 m diffuser for a supply under-temperature of 5.0°C [m/s].....	170
Table 7-10: Temperature measured at 0.05 m from the diffuser for the 0.6 m x 0.6 m diffuser for a supply under-temperature of 5.0°C [°C]	171
Table 7-11: Air speed measured in the longitudinal plane for the 0.6 m x 0.6 m diffuser for a supply under-temperature of 5.0°C [m/s].....	172
Table 7-12: Air temperature measured in the longitudinal plane for the 0.6 m x 0.6 m diffuser for a supply under-temperature of 5.0°C [°C]	172
Table 7-13: Air speed measured in the transversal plane for the 0.6 m x 0.6 m diffuser for a supply under-temperature of 5.0°C [m/s].....	173
Table 7-14: Air temperature measured in the transversal plane for the 0.6 m x 0.6 m diffuser for a supply under-temperature of 5.0°C [°C]	174
Table 7-15: Air speed measured in the horizontal plane at a height of 0.05 m for the 0.6 m x 0.6 m diffuser for a supply under-temperature of 5.0°C [m/s]	175
Table 7-16: Air temperature measured in the horizontal plane at a height of 0.05 m for the 0.6 m x 0.6 m diffuser for a supply under-temperature of 5.0°C [°C]	175
Table 7-17: Air speed and temperature measured at 0.05 m from the diffuser on a vertical axis passing through the center of the diffuser for the 0.6 m x 0.6 m diffuser for several supply under-temperature.....	176
Table 7-18: Maximum air speed and minimum temperature measured in the longitudinal plane for the 0.6 m x 0.6 m diffuser for several supply under-temperature.....	177

Table 7-19: Table 7-20: Air speed and temperature at different heights at the end of the primary zone for the 0.6 m x 0.6 m diffuser for several supply under-temperature	178
Table 7-21: Air speed and temperature measured on the transversal axis at height of maximum air speed at the end of the primary zone for the 0.6 m x 0.6 m diffuser for several supply under-temperature	179
Table 7-22: Air speed measured at 0.05 m from the diffuser for the 1.2 m x 0.6 m diffuser for a supply under-temperature of 2.5°C [m/s].....	179
Table 7-23: Air temperature measured at 0.05 m from the diffuser for the 1.2 m x 0.6 m diffuser for a supply under-temperature of 2.5°C [°C]	181
Table 7-24: Air speed measured in the longitudinal plane for the 1.2 m x 0.6 m diffuser for a supply under-temperature of 2.5°C [m/s].....	182
Table 7-25: Air temperature measured in the longitudinal plane for the 1.2 m x 0.6 m diffuser for a supply under-temperature of 2.5°C [°C]	183
Table 7-26: Air speed measured in the transversal plane for the 1.2 m x 0.6 m diffuser for a supply under-temperature of 2.5°C [m/s].....	184
Table 7-27: Air temperature measured in the transversal plane for the 1.2 m x 0.6 m diffuser for a supply under-temperature of 2.5°C [°C]	184
Table 7-28: Air speed measured in the horizontal plane at a height of 0.05 m for the 1.2 m x 0.6 m diffuser for a supply under-temperature of 2.5°C [m/s]	185
Table 7-29: Air temperature measured in the horizontal plane at a height of 0.05 m for the 1.2 m x 0.6 m diffuser for a supply under-temperature of 2.5°C [°C]	186
Table 7-30: Air speed measured at 0.05 m from the diffuser for the 1.2 m x 0.6 m diffuser for a supply under-temperature of 5.5°C [m/s].....	187
Table 7-31: Air temperature measured at 0.05 m from the diffuser for the 1.2 m x 0.6 m diffuser for a supply under-temperature of 5.5°C [°C]	188
Table 7-32: Air speed measured in the longitudinal plane for the 1.2 m x 0.6 m diffuser for a supply under-temperature of 5.5°C [m/s].....	189
Table 7-33: Air temperature measured in the longitudinal plane for the 1.2 m x 0.6 m diffuser for a supply under-temperature of 5.5°C [°C]	190
Table 7-34: Air speed measured in the transversal plane for the 1.2 m x 0.6 m diffuser for a supply under-temperature of 5.5°C [m/s].....	191

Table 7-35: Air temperature measured in the transversal plane for the 1.2 m x 0.6 m diffuser for a supply under-temperature of 5.5°C [°C] 191

Table 7-36: Air speed measured in the horizontal plane at a height of 0.05 m for the 1.2 m x 0.6 m diffuser for a supply under-temperature of 5.5°C [m/s] 192

Table 7-37: Air temperature measured in the horizontal plane at a height of 0.05 m for the 1.2 m x 0.6 m diffuser for a supply under-temperature of 5.5°C [°C] 193

List of Symbols

Ar	Archimedes number [-]
A_f	floor area [m^2]
B_F	buoyancy flux in Nordtest model [m/s]
c_p	specific heat of air [J/kg K]
$Ep_{0.05}$	rate of potential energy at 0.05 m from the diffuser [$kg \cdot m^2/s^3$]
$Ep_{0.05 \text{ avg}}$	weighted average of the potential energy at 0.05 m from the diffuser [m^2/s^2]
Ep_{EPZ}	rate of potential energy at the end of the primary zone [m^2/s^2]
erf	error function
g	acceleration of gravity [m^2/s^2]
g'	apparent acceleration of gravity caused by buoyancy forces [m^2/s^2]
H_{diff}	diffuser height [m]
$k_{1,\phi}$	constant used in Nordtest model [m/s]
$k_{2,\phi}$	constant used in Nordtest model [-]
$k_{3,\phi}$	constant used in Nordtest model [-]
$K_{0.05}$	rate of kinetic energy at 0.05 m from the diffuser [$kg \cdot m^2/s^3$]
K_{EPZ}	rate of kinetic energy at the end of the primary zone [$kg \cdot m^2/s^3$]
K_N	constant used in Nielsen's model [-]
L_{PZ}	length of the primary zone [-]
$m_{0.05}$	mass flow rate at 0.05 m from the diffuser [$kg \cdot m^3/s$]
m_{EPZ}	mass flow rate at the end of the primary zone [$kg \cdot m^3/s$]
P	air pressure [Pa]

q_s	supply flow rate [m^3/s]
T_{occ}	temperature in the occupied zone [K or $^{\circ}\text{C}$]
T_{return}	return air temperature [K or $^{\circ}\text{C}$]
T_{room}	room air temperature [K];
T_{supply}	supply air temperature [K or $^{\circ}\text{C}$]
$T_{1.1 m}$	temperature in the middle of the room at a height of 1.1 m [K]
$T_{0.05}$	temperature at 0.05 m from the diffuser [K]
$T_{0.05 wavg}$	the weighted average air temperature at 0.05 m from the diffuser [K]
ΔT_{norm}	normalized under-temperature in the secondary zone [-]
V_f	supply face velocity [m/s]
V_{EPZ}	maximum air speed at the end of the primary zone [m/s]
V_{normY}	normalized air speed for transversal profile [-]
V_{normZ}	normalized air speed for vertical profile [-]
V_{scd}	normalized air speed for the secondary zone model [-]
$V_{0.05 wavg}$	weighted average of the square air speed air velocity at 0.05 m from the diffuser [m^2/s^2]
X	longitudinal distance from the diffuser [m]
Y	distance from the longitudinal axis [m]
Z	height from the floor [m]
α_{cf}	convection heat transfer coefficient for the floor surface [$\text{W}/\text{m}^2\text{K}$]
α_r	radiation heat transfer coefficient for the floor surface [$\text{W}/\text{m}^2\text{K}$]
γ	ratio of air entrainment in the jet [-]
δ_{XY}	thickness of the jet at a distance X from the diffuser and a distance Y from the axis [m]
δ_{min}	minimum thickness in the jet for a given diffuser and supply condition [m]

η	normalized height [-]
θ	dimensionless temperature [-]
ξ	normalized distance from the primary zone [m]
ρ	air density [kg/m ³]

CHAPTER 1: INTRODUCTION

1.1 Problem statement

Ventilation and air conditioning are generally required in modern buildings to provide adequate thermal comfort and air quality. They are also critical components in terms of building energy consumption. Several novel air delivery strategies, such as mixing ventilation, displacement ventilation, or personalized ventilation, have been developed over the years. Displacement Ventilation (DV) has recently attracted growing interest in North America as a way to save energy and increase Indoor Air Quality (IAQ). The basic mechanism of displacement ventilation is the supply of fresh air at low velocity at floor level, at a temperature slightly lower than room temperature (typically between 17°C and 20°C (Skistad et al, 2002)). The occupants and other heat sources inside the room then act as plume convectors, the resulting air movement is known to lead to temperature and contaminant vertical stratification in the room (Figure 1-1). The advantage of displacement ventilation over mixing ventilation is that the air brought at breathing level is not or only slightly mixed with the indoor air, leading to an increased perceived indoor air quality. In addition, all the positively buoyant contaminants such as human-related odours are brought in the upper part of the room, outside of the breathing zone, due to the plume effect. This mechanism results in a very good Indoor Air Quality (IAQ) in the room (Skistad et al. 2002). Various studies have proven that the contaminant removal efficiency and the overall IAQ is in most cases higher in rooms equipped with displacement ventilation than in rooms equipped with mixing systems (Chen and Glicksman, 2003).

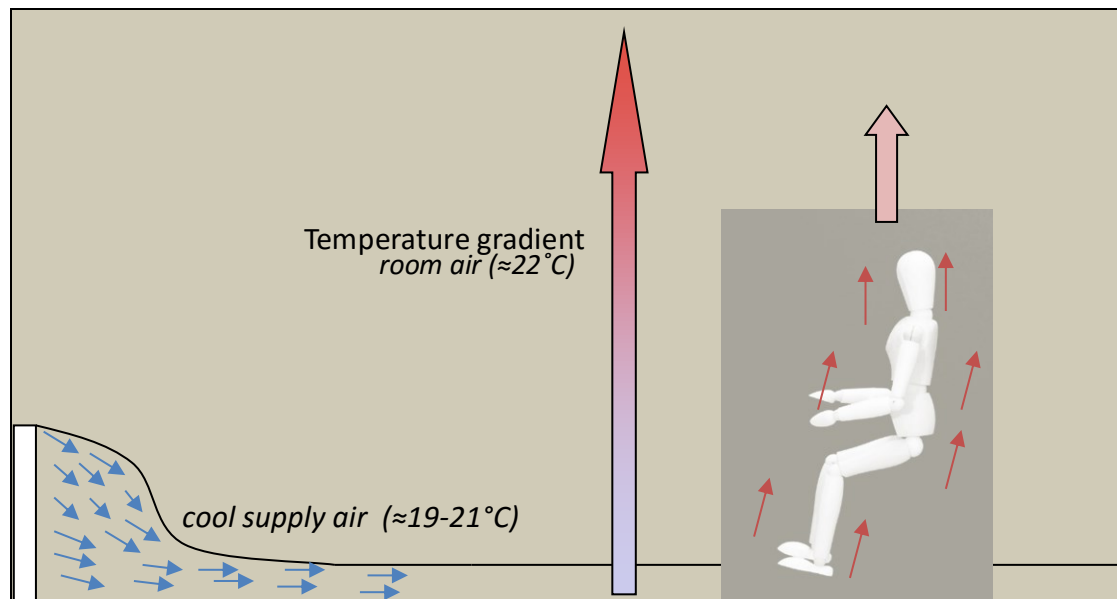


Figure 1-1: Illustration of Displacement Ventilation

In terms of energy use, the action of the thermal plumes also creates vertical temperature stratification in the room. This stratification enables to cool only the occupied portion of a room, while leaving the higher portion at a higher temperature. As a result, the supply air flow rate required to make the room thermally comfortable is smaller. Overall the higher supply air temperature and lower supply air flow rate lead to lower loads on the cooling coils of the air handling units, and lower electricity use for mechanical refrigeration as well as for supply fans. The higher supply temperature, compared to mixing ventilation, also enables a more frequent use of free cooling over the year, leading to further energy savings (Chen and Glicksman, 2003).

Despite these advantages, the use of displacement ventilation is still limited. A problem frequently associated with DV is indeed local discomfort. Due to the cold air moving at the foot level, the risk of draft discomfort is higher in DV systems. A survey of 227 workers in 10 office buildings equipped with displacement ventilation showed that as much as 24% of the occupants experienced discomfort at the lower leg level (Melikov et al. 2005). The temperature stratification can also lead to an excessive temperature difference between the head and the ankle, and therefore discomfort. The issue of local comfort, closely related to the velocity and

temperature distribution within the DV jet, needs to be addressed before DV is used at a greater scale.

1.2 Objectives of this thesis

Despite its great potential in terms of energy saving and indoor air quality, the use of DV is still limited due to concerns regarding local thermal comfort. The first main objective of this thesis is to acquire an in-depth understanding of the physics of a DV jet and of the distributions of velocity and temperatures inside the jet. The second objective is that, based on this knowledge, correlation models be developed to describe the variations of air speed and temperature in the secondary zone of a DV jet, as such descriptions are needed to better design and operate DV systems.

In order to achieve these objectives, this thesis aims to:

- Perform extensive measurements in the DV jet using a fine three-dimensional grid, in order to create a database of velocity and temperature distributions within the jet.
- Quantify the variations of velocity and temperature within the DV jet, and analyze their impact on local comfort and local comfort assessment.
- Based on the measured data, validate existing models and develop new mathematical models for the profile of maximum air speed in a DV jet.
- Study in depth the vertical profile of air speed in the jet and develop new correlations.
- Analyze the thickness of the jet and its variation with distance from the diffuser.
- Analyze and develop new mathematical models for the distribution of air temperature in a DV jet.

In order to achieve these objectives, a literature review of the existing experimental data is performed, as well as a review of the existing tools available to model the DV jet (Chapter 2). Based on the literature review, an experimental protocol is developed (Chapter 3). The experimental results are presented in Chapter 4. Based on the data, several correlation-based models are developed for the distributions of air speed and air temperature in the DV jet (Chapter 5). Finally, the contributions of this thesis are highlighted and future work is suggested (Chapter 6).

CHAPTER 2: LITERATURE REVIEW

This chapter first presents a literature review of studies related to the velocity and temperature distributions within a DV jet. Only displacement ventilation non-isothermal air jet in cooling mode is discussed in this review. Displacement ventilation is indeed not recommended nor generally used for heating purpose, due to its poor performance in that use (Skistad et al. 2002). It is also noteworthy that the review presented in this chapter only focuses on the displacement ventilation jet coming from a wall-diffuser, installed close to the floor. Diffusers installed higher in the room (confluent jets) or inside the floor (underfloor air distribution) are out of the scope of this literature review.

2.1 Introduction

This section first presents an overview of the DV jet and some basics of theoretical analysis. A discussion regarding the thermal comfort aspects and issues in regard of displacement ventilation follows.

2.1.1 Overview of a displacement ventilation jet

The DV jet can be separated into two distinct zones (Figure 2-1). The first zone, or primary zone, is a zone where the air jet falls onto the floor due to the action of buoyancy forces. As a consequence, the thickness of the air jet decreases and the air velocity increases significantly. The limit of the primary zone is the point where the velocity in the jet has reached its maximum. This limit is in the order of one meter, depending on the supply characteristics (Etheridge and Sandberg, 1996). The air velocity in the jet at that point is generally several times greater than the face velocity of the diffuser. The secondary zone is characterized by a decrease of the horizontal velocity, with relatively small variations in the thickness of the air layer. The

secondary zone is of primary interest to designers since it generally corresponds to the occupied zone.

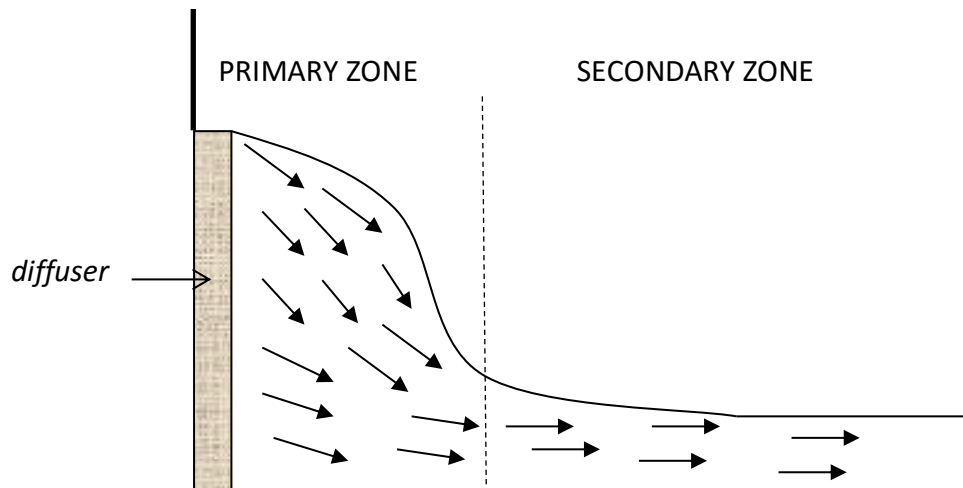


Figure 2-1: Schematic view of the two flow regions in a DV jet

The proper physical way to describe the flow of a DV diffuser is low-velocity negatively buoyant horizontal wall-jet. As discussed by Nielsen (1994), DV flow can be considered using different theories such as the ones of wall-jets, confluent jets, or gravity currents. The wall-jet theory is for instance very valuable to understand the vertical velocity profile of the DV flow. However, it is incompatible with some major parameters of DV flow such as the variation in thickness of the air layer or the horizontal velocity decay. The gravity current theory (Turner, 1973), in turn, might be useful to understand the flow behaviour in the primary zone. The information in the gravity current literature is however of little practical interest in the secondary zone.

2.1.2 Thermal comfort

Thermal comfort is a crucial parameter to be considered when designing a ventilation system. In the case of DV system, both global thermal comfort (PMV, PPD (ASHRAE 55, 2010)) and local thermal comfort need to be considered. While the former is relatively easy to satisfy, the latter is more complex and caused several DV-system related complaints in the past (Melikov et al.

2005). In terms of local thermal comfort, two parameters are particularly problematic in DV: temperature stratification and air movement at foot level.

Draft discomfort is a problem commonly associated with displacement ventilation (Skistad et al. 2002), due to the movement of cold air at foot level. The risk of draft is generally assessed based on the air velocity measured at floor level. Several velocity limits can be found in the literature: in some standards the air velocity limit is 0.20 m/s (CEN, 1998; ISO, 2005); in other standards, the limit is set at 0.25 m/s (ASHRAE 55, 1992; Nordtest VVS083, 1990); finally, in the ASHRAE 55 2010 standard, the velocity limit is set either at 0.15 m/s or 0.80 m/s depending on the operative temperature. Studies show that the draft discomfort is nonetheless dependent not only on the air velocity but also on the turbulence intensity and air temperature. A metric used to assess the number of person dissatisfied due to draft is the Draft Rate (DR), defined by Equation 2-1 (ISO, 2005). In ISO 7730 (2005), the DR limit is between 10% and 30% depending on the comfort category. In the 2004 version of ASHRAE 55 (ASHRAE, 2004) the limit for draft discomfort was 20%. It should be noted that in the newest version of ASHRAE 55 (ASHRAE, 2010), the equation of the Draft Rate has been removed; a limit of 20% of occupants affected by draft discomfort is however still present.

$$DR = (34 - T) \cdot (V - 0,05)^{0,62} \cdot (0,37 \cdot TI \cdot V) + 3.14)$$

Equation 2-1

where:

- *DR* is the draft rate;
- *T* is the air temperature [°C];
- *TI* is the local turbulence intensity [%], and;
- *V* is the local air velocity [m/s];

For practical purpose, a velocity limit of 0.20 m/s is generally retained in the industry (E.H. Price, 2009; Flaktwood, 2010) and in REHVA's and ASHRAE's guidelines (Skistad et al. 2002; Chen and Glicksman, 2003). An information missing in thermal comfort standards is the height at which the draft discomfort should be evaluated. In principle, there is not limitation regarding where it

could be evaluated and the maximum DR should be considered. On one hand, many field studies (Love, 2010) focus on the standardized ankle height of 0.1 m from ASHRAE 113 (ASHRAE, 2009) and ASHRAE 55 (ASHRAE, 2004; ASHRAE 2010). While this height of 0.10 m might however not correspond to the height of maximum velocity in the jet. On the other hand, one can wonder if a draft rate occurring at 0.03 m from the floor could cause any discomfort for an occupant wearing shoes.

In terms of temperature stratification, ASHRAE 55 (2004) states that the Vertical Air Temperature Difference (VATD) between the head and the ankle should be lower than 3°C to ensure comfortable conditions, i.e. resulting in less than 10% of the occupants dissatisfied. The VATD is calculated using the local air temperature at 0.1 m from the floor (ankle level) and at a height of 1.1 m for a seated person, or 1.7 m for a standing person (head level). In ISO 7730 (2005), the VATD limit is between 2°C and 4°C depending on comfort category. While a DV system should take advantage of stratification to reduce the cooling load, the temperature gradient in the room should nevertheless be controlled to prevent discomfort. A thorough understanding of temperature stratification in the room and of temperature distribution in the vicinity of the floor is thus required in order to properly design a DV system. This point is discussed further in section 3 of this chapter.

2.2 Velocity distribution in the DV jet

Velocity is an important parameter affecting the feeling of draft. Experimental data and models regarding the velocity distribution in the DV jet are discussed in this section.

2.2.1 Velocity increase in the primary zone

As discussed previously, the DV jet is separated in two zones. The velocity increase in the primary zone is an important parameter since it determines the maximum velocity reached in the jet and the distance from the diffuser at which this velocity is reached. In terms of

experimental data, focus is generally found on the secondary zone, where the occupant is installed. Some data can however be found in some laboratory study such as Li et al. (2003) or in experiments performed for CFD validation purposes such as Cehlin et al. (2010). These studies confirm the decrease of jet thickness in the primary zone, as well as the increase of velocity. No model or correlation has however been developed in these studies. A conclusion that can be drawn from these studies is that, after about half a meter distance from the diffuser, the DV jet appears to follow a wall-jet-like vertical velocity profile (Rajaratnam, 1976), regardless of the air distribution profile at the diffuser exit.

Only a limited number of models are found in the literature for the velocity field in the primary zone of a DV jet. Sandberg and Blomqvist (1989) proposed a formula to determine the maximum velocity reached at the end of the primary zone, based on the conservation of kinetic and potential energy. While interesting, their theoretical analysis was limited as energy loss through turbulence, entrainment of room air, or spreading of the jet was not considered. Later, Etheridge and Sandberg (1996) proposed a formula to predict the length of the primary zone for a radial gravity current. According to the authors, the equation fits well with experiments for a round wall-diffuser. Measurements in this study were however never verified or mentioned outside of the original study and might not be applicable to rectangular diffuser. A second formula available in the literature is from the Nordtest model, as described in the NT VSS 083 (Nordtest, 2009). In this standard, a two-coefficient correlation is proposed to evaluate the maximum velocity reached at the end of the primary zone. The formula is based on the Archimedes number and on the buoyancy flux from the diffuser, and on coefficients specific to the diffuser. According to the authors of the model, the coefficients used are independent of the supply conditions. No published validation of this model could however be found in the literature.

2.2.2 Velocity decay in the secondary zone

Several velocity decay models have been developed in the last decades (Nielsen, 2000; Nordtest, 2009; Skåret, 2000; Sandberg and Blomqvist, 1989). The more complete models are described in this section.

Nielsen model

The first model developed specifically for the velocity decay in a DV diffuser has been proposed by Nielsen in 1994. This model was developed based on both a theoretical analysis and a series of experimental measurements. Nielsen proposed that the velocity decay in the secondary zone of a DV jet, for a wall diffuser with a radial distribution and along the central axis, can be described by the following equation:

$$\frac{V(x)}{V_f} = K_{dr} \frac{H_{diff}}{x} \quad \text{Equation 2-2}$$

where

- $V(x)$ is the maximum velocity at a distance x from the diffuser [m/s];
- V_f is the face velocity of the diffuser [m/s];
- K_{dr} is an experimentally determined constant [-];
- H_{diff} is the height of the diffuser [m];
- x is the distance from the diffuser [m];

Nielsen used his model to correlate the velocity decay measured in experiments performed on various DV wall diffusers at various supply conditions. The correlations are in good agreement with the experimental data once the appropriate K_{dr} constant is experimentally determined. Nielsen's model is the most accepted velocity model in the literature and has shown a reasonably good agreement with various experimental data (Skistad, 1994, for instance). It is also referenced in major design guidelines such as the REHVA's guidebook (Skistad et al. 2002) and ASHRAE's design guidelines (Chen and Glicksman, 2003). It is noteworthy that several

versions of Nielsen model exist. An early version of the model for instance used a power factor associated with the distance from the diffuser, as well as a correction factor to account for a virtual origin of the diffuser.

The use of the K_{dr} constant in Nielsen's model is intended to characterize the flow from a diffuser using a single value, as it is the case with classical high-velocity free jets. In the case of displacement ventilation however, K_{dr} value is valid only for a specific diffuser, with a specific outlet size and aspect ratio, and a specific under-temperature. While some theoretical formulations of K_{dr} were proposed (Nielsen, 1994; Skistad, 1994), these formulations are generally of little practical use since the parameters they used are difficult to quantify (entrainment, virtual origin etc). Nielsen (2000) also proposed a linear relation between K_{dr} and the root of the Archimedes number (Ar). This approximation however appears to be mostly qualitative. As a conclusion, no satisfactory relationship could be found in the literature to relate the K_{dr} constant with the diffuser characteristics or the supply temperature. Therefore, for each diffuser, K_{dr} needs to be determined through laboratory measurements, for all the sizes and under-temperatures of interest.

Nordtest model

The Nordtest model, as described in the NT VSS 083 (Nordtest, 2009), is a recent correlation-based model for the velocity decay in a DV jet. This model was developed based on laboratory measurements and on the work of Skåret (1998) and Schild et al. (2003a, 2003b). According to this model, the maximum air velocity at a radius R from the diffuser (i.e. the distance between the point of interest and the center of the diffuser) and an angle ϕ from the longitudinal axis can be described by Equation 2-3.

$$V(R, \phi) = k_{1,\phi} \cdot Ar_N^{k_{2,\phi}} \cdot B_f \cdot \left(\frac{R}{L}\right)^{k_{3,\phi}} \quad \text{Equation 2-3}$$

where:

- $V(R,\phi)$ is the maximum velocity at a radius R from the diffuser and an angle ϕ from the longitudinal axis [m/s];
- Ar_N is the Archimedes number as defined in Nordtest (2009) [-];
- B_f is the buoyancy flux defined in Nordtest (2009) [m/s] ;
- L is the horizontal perimeter of the diffuser [m], and;
- $k_{1,\phi}$, $k_{2,\phi}$ and $k_{3,\phi}$ are experimentally determined coefficients.

The Nordtest model presents several advantages compared to Nielsen's model. First, it can model the velocity distribution both in the centerline and outside the centerline (once empirical coefficients are known). Another significant asset of the Nordtest model is that, according to the authors, the correlation coefficients are independent of the supply conditions. Moreover, the coefficients are claimed to be constant for a given aspect ratio of a diffuser. Once the three correlation coefficients are determined, the Nordtest model is therefore able to handle more situations than Nielsen's model.

A limitation of the Nordtest model is that it requires three correlation coefficients, determined based on experimental data for several supply conditions. The investment, in terms of experimental work, required to use this model is therefore significant. In addition, the correlation coefficients are also dependent on the angle ϕ from the centerline; for each new angle, three new correlation coefficients need to be experimentally determined. Finally, no validation of the Nordtest model could be found in the literature.

Sandberg and Blomqvist theoretical model

The only theoretical model found in the literature, specifically aimed at the displacement ventilation jet, is from Sandberg and Blomqvist (1989). The approach developed by these authors was to analyze the flow by studying the conservation of energy and conservation of mass. In terms of flow field in the secondary zone, Sandberg and Blomqvist proposed a velocity

decay in the form of a negative exponential term. Although interesting, the air speed model is based on assumptions such as a constant temperature difference between the air in the jet and the ambient air, and a constant jet thickness. These assumptions are however disproved by experiments. Indeed, the air temperature difference between the jet and the ambient air was found in several experimental studies to vary with the distance from the diffuser (Kegel and Schulz, 1989; for instance). The jet thickness, in turn, was also found to vary with the distance from the diffuser (Nielsen, 2000). Overall, Sandberg and Blomqvist's model, while interesting as the only attempt to analyze the DV jet from a theoretical point of view, suffers from oversimplifying assumptions. This model has also never been validated by experimental data.

Discussion

While several velocity decay models have been developed over the last decades, there is still a lack for a validated model with coefficients independent of supply conditions. For instance, Nielsen's model is limited by the case-specificity of coefficient K_{dr} . The Nordtest model, in turn, is independent of the supply conditions, but a significant amount of experimental data is required to determine its three correlation coefficients. This model is also very recent and has not been validated in the literature. Studying the different models in the literature, it is also noteworthy that there is no strong agreement in the literature regarding how to relate the velocity with the distance from the diffuser. In Nielsen model, a simple inverse function is used, in Nordtest model, a case specific power function is used, and finally, in the theoretical model of Sandberg and Blomqvist (1989), a negative exponential function is used. Another important issue is that all the models developed in the literature focus only on the maximal velocity at a given distance from the diffuser. However, as it will be described in the next section, the air velocity shows significant vertical variation within the jet. The maximum velocity, in turn, might not occur at ankle level (0.10 m) and may therefore not be representative of draft discomfort. Hence the velocity models described in this section cannot be directly used for comfort assessment without further knowledge regarding the vertical velocity profile in the DV jet.

2.2.3 Vertical velocity profile in the secondary zone

The vertical velocity profile occurring in the vicinity of the floor in the secondary zone of a DV jet is generally described using the wall jet theory. The dimensionless vertical velocity profile can then be expressed by Equation 2-4 (see also Figure 2-2) (Rajaratnam, 1976).

$$\frac{V(x,y,z)}{\max_z V(x,y,z)} = 1.48 \cdot \left(\frac{z}{\delta}\right)^{\frac{1}{7}} \cdot \left[1 - \operatorname{erf}\left(0.68 \cdot \left(\frac{z}{\delta}\right)\right)\right] \quad \text{Equation 2-4}$$

where:

- $V(x,y,z)$ is the velocity at a distance x from the diffuser, y from the central axis, and at height z ;
- $\frac{V(x,y,z)}{\max_z V(x,y,z)}$ is the normalized air speed at a distance x from the diffuser, y from the central axis, and at height z ;
- δ is the thickness of the air jet, defined as the distance from the floor to the height where the velocity has decreased to half of the maximum velocity;
- $\frac{z}{\delta}$ is the normalized height, and;
- erf is the error function.

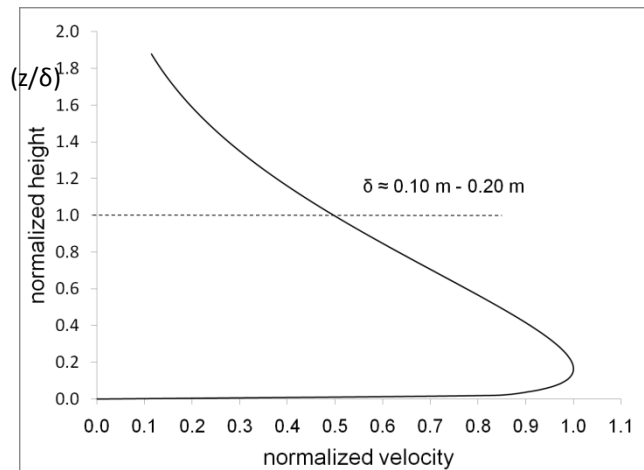


Figure 2-2: Theoretical vertical velocity profile in a DV jet (based on Rajaratnam, 1976)

This theoretical profile has shown good agreement with several laboratory and field measurements, using either wall-mounted DV diffusers (Cho et al. 2008; Lau and Chen. 2007) or quarter-corner DV diffusers (Nielsen, 2000; Zhang et al. 2009). This profile has however be found valid only in the secondary zone of the DV jet (Cho et al. 2008). As can be seen in Figure 2-2, the velocity within the jet varies significantly with height. The vertical velocity profile should thus be considered for thermal comfort assessment. Some laboratory or field studies (Kegel and Schulz, 1989; Lau and Chen, 2007) presented the air velocity solely at the height of 0.1 m, corresponding to the occupant's ankle in ASHRAE 55 (2004). While the use of measurements at 0.1 m height is useful for comfort assessment, it provides only limited information on the whole flow.

A major parameter of Equation 2-4 is the thickness δ of the jet. According to literature, the air thickness of the flow in the secondary zone generally lies between 10 and 20 centimetres, the maximal velocity occuring between 2 and 5 centimetres (Li et al., 1993; Nielsen, 2000; Nordtest, 2009). There is however no agreement in the literature regarding which parameters influence the thickness of the DV jet and no model to predict this thickness. The only study in the literature discussing the variation of the jet thickness is Nielsen (2000). In this study, Nielsen found that the thickness of the flow decreases with the Archimedes number (based on three supply conditions tested). Nielsen also found that the flow thickness may slightly increase with the distance from the diffuser (order of centimetres for a 4 m distance). According to his results, the rate of thickness increase appears to be dependent on the Archimedes number. No quantitative correlation was however proposed regarding the increase of thickness with the distance from the diffuser, or with decreasing Archimedes number. It is also unclear in this study whether the increase of thickness is actually related to the Archimedes number, to a change in supply temperature or to a different stratification inside the room. Finally, no information is given regarding the variations of flow thickness outside the longitudinal axis.

2.2.4 Transversal velocity profiles

Most of the data regarding the velocity variation is focused on the longitudinal axis of the diffuser (Li et al. 1993; Nielsen, 2000). The velocity measurements performed outside of this axis (Kegel and Schulz, 1989; Zhang et al. 2009) generally use a limited number of sampling locations (generally less than 10). The conclusions of such studies are then limited in terms of understanding the jet spreading. It can nonetheless be noted in the literature that the air velocity in the DV jet may vary significantly over the floor area. According to the wall-jet theory, the transversal velocity profile in a DV jet should follow a Gaussian distribution (Rajaratnam, 1976). The only measured transversal data for a DV jet found in the literature are two transversal profiles from Nielsen (1988), measured at a single distance from the diffuser, for two different diffusers. No information could be found in literature regarding transversal profiles measured at different distances from the diffuser for a same diffuser and different supply conditions.

Due to the lack of reliable experimental data, the air velocity variation away from the longitudinal axis is not included in current velocity models. In the recent Nordtest model (2009), the velocity outside the longitudinal axis is simply modelled using the same formulas as the one used on the axis, changing the three correlation coefficients. There is however no indication on how the coefficients for locations away from the axis could be estimated using as base the coefficients identified to model the velocity on the axis. It is also noteworthy that while most theoretical models (Nielsen, 1994; Sandberg and Blomqvist, 1989) are based on an assumption of radial distribution for the flow from the diffuser, such assumption has never been thoroughly verified (Nielsen, 1989). Regarding the radial assumption, it should also be noted that, in practical situations, a radial DV flow will always eventually be affected by the room walls. This issue has however never been discussed, except very briefly in Nielsen (1989).

2.3 Temperature distribution

In displacement ventilation, a vertical temperature gradient appears in the room due to the cold air supplied at floor level and the convective plumes resulting from the presence of heat sources such as occupants. The air temperature in the room is generally considered to linearly increase with height (Chen et al. 2003). As written in section 2.1.2, the temperature stratification can significantly impact thermal comfort in a room. A major parameter in evaluating the temperature stratification is the air temperature at floor level.

2.3.1 Temperature at floor level

The temperature at floor level is influenced by various parameters. The supply flow rate is recognized as one of the most influencing parameters and is a predominant parameter in Mundt's model (Mundt, 1996). The types and location of heat sources inside the room can also have a significant impact on the air temperature at floor level. The "kappa model" (Brohus and Ryberg, 1999), for instance, determines the air temperature at floor level based solely on the type and distribution of the heat sources inside the room. In literature, the floor surface temperature is found to be an influential parameter, especially in case of solar radiation heating the floor (Kegel and Schulz 1989). The height of the room is also important, as high-ceiling spaces behave differently than low-ceiling spaces in terms of stratification (Skistad et al. 2002). Finally, Li et al. (1993) demonstrated that heat transfer by radiation in the room can have a significant impact on the temperature at floor level.

The method most widely used in literature to determine air temperature at floor level is the so-called 50% rule (Skistad et al. 2001; Chen et al. 2003). This rule of thumb states that the dimensionless temperature, θ_f , at 0.1 m from the floor is halfway between supply temperature (T_{supply}) and exhaust temperature (T_{return}) (Equation 2-5). As described in the previous paragraph though, many parameters affect the air temperature close to the floor. The 50% rule can then only be used as a first approximation. Indeed, according to literature, the dimensionless

temperature at floor level θ_f can vary from 0.2 to 0.65 (Skistad et al. 2002, Mundt 1996). Several field measurements studies also report a θ_f generally closer to 40% (Sandberg and Blomqvist, 1989; Love, 2009). Experimental data also suggest that the 50% rule should be changed to a 33% rule in rooms with high ceilings (Skistad et al. 2002).

$$\theta_f = \frac{T_{0.1} - T_{\text{supply}}}{T_{\text{return}} - T_{\text{supply}}} = 0.5 \quad \text{Equation 2-5}$$

A more detailed model to evaluate the temperature at floor level was developed by Mundt (1996). This model is based on a theoretical analysis of heat transfer inside a room and validated with numerous experimental data. This model suggests that the air temperature at floor level is primarily influenced by the flow rate, the floor area and the convection heat transfer coefficient between the floor and the airflow. Mundt's model has been validated using data from eleven different experimental studies, each presenting different room dimensions, heat sources and supply conditions (Mundt, 1996). Results show good agreement with measured data, even for high-ceiling rooms, with errors generally less than 0.1 when estimating θ_f . A more advanced model has been proposed recently by Mateus and Carrilho da Graça (2014), which further improves the overall prediction of temperature stratification in the room, including the average temperature at floor level.

Despite good agreement between these models and experimental data, a major limitation is the consideration of a single temperature for the whole floor area. Variations of temperature inside the DV jet are not considered. A new model therefore needs to be developed to take that aspect into account.

2.3.2 Temperature variation inside the DV jet

In a room equipped with displacement ventilation, it is reasonable to assume that the air temperature in the room does not vary significantly horizontally, for heights higher than 0.5 m

(Kegel and Schulz, 1989; Li et al. 1993). At the height of 0.1 m though, i.e. within the DV jet, this assumption is not valid anymore. According to experimental data, differences of temperature as high as 1.5°C can appear between different locations in a room for measurements performed at 0.10 m from the floor (Kegel and Schulz 1989; Ming, 2001). Such temperature variations at different locations can then lead to variations in the VATD. Since existing thermal stratification models assume temperature uniformity at floor level, they fail to predict such temperature differences.

The study of the air temperature variations within the DV jet suffers from the same limitations as the study of velocity variations. Most experimental data use coarse measuring meshes, with less than 10 measuring locations over the floor area (Kegel and Schulz, 1989; Lau and Chen, 2007). The temperature in the DV jet is also generally measured solely at the standard ankle height of 0.10 m (ASHRAE 55, 2004). The vertical variation of temperature within the jet is seldom reported (Li et al. 1993). Nonetheless, based on the data available in the literature, quantitative conclusions can be drawn. First, the air temperature at floor level generally increases with the distance from the diffuser (Li et al. 1993). In an experimental study of a DV jet over a heated floor, Novoselac et al. (2006) found that both the floor surface temperature and the temperature of the air at 0.1 m from the floor can increase by as much as 4°C between 0 m and 4 m from the diffuser. According to experiments performed on a gravity current induced by a cold wall (Heiselberg, 1994), a flow relatively similar to a DV jet, the minimum temperature in the jet increases linearly with the distance from the source.

Regarding the vertical profile of temperature inside the jet, laboratory studies show that vertical temperature differences up to 1°C can appear within the jet (Li et al. 1993). According to the wall jet theory, the vertical temperature profile in a non-isothermal wall jet could be expressed by Equation 2-6. In a discussion in Chen (2001) however, this equation is found not applicable by Amiri et al. (1996). Chen (2001) concluded that Equation 2-6 is not valid for displacement ventilation jets. Regarding the transversal variations of temperature within the jet, the data found in the literature were found too limited to draw any clear conclusions.

$$\frac{T - T_{room}}{T_{min} - T_{room}} = \sqrt{\frac{V}{V_M}} \quad \text{Equation 2-6}$$

where the variables are defined in Chen (2001) as:

- T is the air temperature at a given location in the jet [K];
- T_{room} is the air temperature in the room [K];
- T_{min} is the minimum air temperature in a given cross-section of the jet [K];
- V is the air velocity at a given location in the jet [m/s], and;
- V_M is the maximum air velocity in a given cross-section of the jet [m/s].

2.4 Summary of the literature

Most of the experimental data on DV jet in the literature focus on the air speed decay in the longitudinal plane. Significantly less data is available regarding the variation of air speed in the transversal and vertical directions. In terms of temperature, the data available in the literature are very scarce, even along the longitudinal axis. A more systematic experimental study of the distributions of air speed and temperature is therefore required, in the three directions of relevance, namely longitudinal, transversal, and vertical. As for models in literature, some models exist for the velocity decay in the secondary zone, but are limited by case-specific parameters. For temperature, current models only focus on the average temperature at floor level, neglecting the variations of temperature at different distances from the diffuser. New models therefore need to be developed.

CHAPTER 3: EXPERIMENTAL PROTOCOL

The experimental work is aimed at overcoming the current lack of data regarding the velocity and temperature distributions in the DV jet. An environmental chamber is set up to reproduce a small room where a DV diffuser is installed and measurements of velocity and temperature are performed using a very fine mesh, with a focus on heights between 0.02 m and 0.20 m. Measurements in the non-isothermal DV jets are performed in three perpendicular planes to acquire a three-dimensional dataset. The data gathered through experiments can then be used to evaluate the velocity and temperature variations in the three dimensions of space, as well as their effects on thermal comfort.

3.1 Testing facility and instrument

This section describes the facility, instruments and measuring protocol used for the experimental work (Magnier et al. 2012).

3.1.1 Testing facility

The environmental chamber used in our experiments is depicted in Figure 3-1a. Its inside dimensions are 3.56 m (length) by 2.32 m (width) by 2.17 m (height). The DV diffuser (described in a next paragraph) is denoted by (1) on Figure 3-1a. The diffuser is installed inside a partition wall, with its lowest point located at 0.1 m from the floor, as recommended by the manufacturer. The diffuser is connected to the ventilation system of the chamber for control of

the supply air flow rate and temperature. The air leaves the chamber through a 3.6 m by 0.3 m gap on the top of one of the chamber sidewalls, denoted by (2) on Figure 3-1a. Figure 3-1b shows the details of the exhaust system: the exhaust air comes from the top of the wall (2.1), to the bottom of the wall (2.2), then passes through the cooling coils (2.3) and is then redistributed into the main duct to the diffuser (2.4). The main duct is insulated using 50 mm of fibreglass insulation. In order to balance the loads during experiments, two types of heat source are used. The first heat source is eight fluorescent lamps of 40 W each distributed over the ceiling area. Second, to balance the loads with more accuracy, an adjustable low-temperature heating panel (0-750W) is also used. This heating panel is installed on the wall opposed to the diffuser (denoted by (3) on Figure 1).

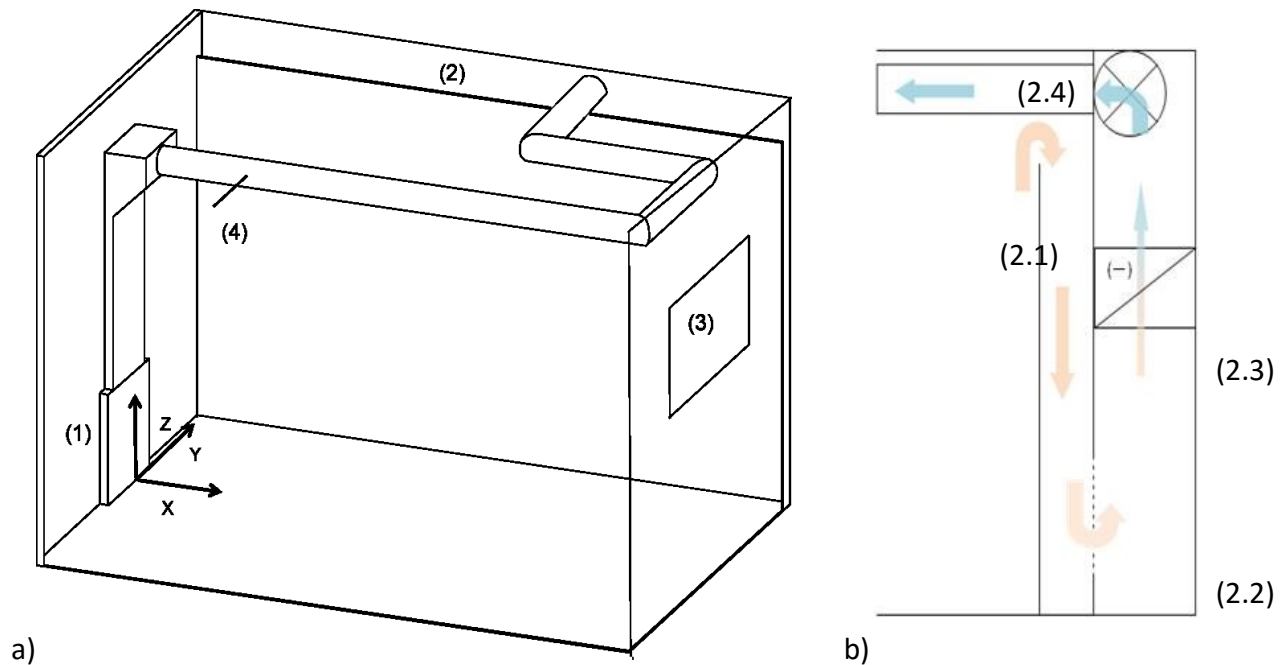


Figure 3-1: Schematic view a) of the environmental chamber; b) of the exhaust system

3.1.2 Measuring instruments

The air speed is measured by an omnidirectional low-velocity anemometer (ThermoAir 6/64 from Schiltknecht), with a standard error of 0.01 m/s for velocities between 0.01 m/s and 1.00 m/s. This anemometer was calibrated in a wind tunnel at the Indoor air research laboratory of the National research council of Canada in Ottawa. The air temperature in the DV jet, the floor surface temperature and the air temperature in the duct are measured using T-type thermocouples with a standard error of 0.5°C. These thermocouples were all calibrated in a thermal bath at Concordia. The air temperature at different heights in the chamber is measured by Resistance Temperature Detectors (RTDs) having a standard error of 0.1°C. These RTDs were also calibrated in a thermal bath in Concordia. Finally, in order to calculate the supply flow rate, a Pitot-tube is used (denoted by (4) in Figure 3-1a) while the pressure differential is read by a 2110F Smart Flow Gauge manometer from Meriam Instrument. This Pitot tube was calibrated for flow rates ranging from 1 L/s to 200 L/s by a side-by-side comparison with a high-accuracy Laminar Flow Elements (50MC2 from Meriam Instrument).

In order to be able to perform numerous measurements inside the jet with a minimum disturbance of the flow, a motorized rail is used to control remotely the displacement of measuring instruments inside the chamber. Figure 3-2 shows the moving support, where the anemometer and two thermocouples are installed. The displacement of the support is automated using SI Programmer, of Applied Motion Products. Finally, all measuring instruments are connected to a data acquisition system, Agilent 34970. This data acquisition system enables real-time reading of all the measured values; the results are then saved in Excel files for further analysis. The data acquisition system is also connected to the rail control system, which enable to keep track of the rail support displacement inside the chamber.

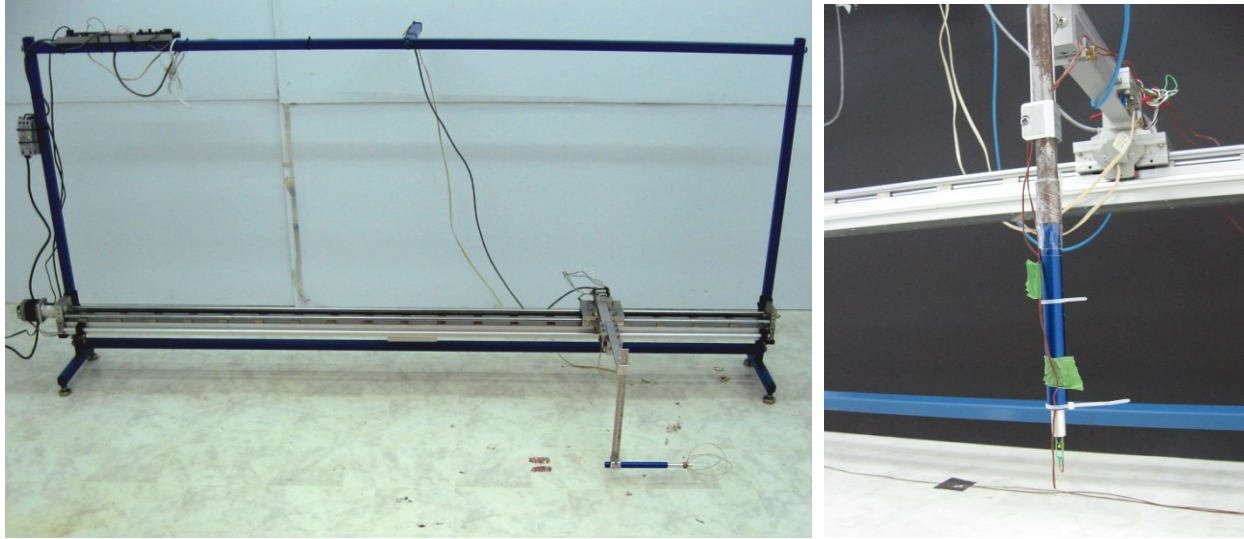


Figure 3-2: Motorized rail and anemometer used for measurements inside the jet

3.1.3 Testing conditions

All measurements are performed once steady state conditions are attained inside the room. Steady state is defined as the state when all measured temperatures (supply temperature, air temperature in the room, surface temperature) do not vary by more than 0.1°C over the full period of measurement. Measurements inside the jet are recorded every 10 seconds, for a total measuring time of 3 minutes, at each location (as recommended by ASHRAE 113, 2009). The average and standard deviation are then calculated for each sampling point. Measurements are taken after a minimum settling time of 60 seconds following any rail movement (ASHRAE 113, 2009 and Nordtest, 2009), and of 10 minutes after the experimenter leaves the chamber. Measurements outside of the jet (surface temperatures mostly) are recorded every 10 seconds for the whole measuring period.

3.1.4 Measurements outside the jet

Although the main focus of the experimental work is the air speed and temperature fields inside the jet, several additional temperature measurements are performed for further analysis, and

eventually simulation purpose. The locations of these additional measurements are summarized in Table 3-1.

The air temperature in the chamber is measured on three columns inside the room, at the heights of 0.6 m, 1.1 m, and 1.7 m, as recommended by ASHRAE 113 (2009) and ASHRAE 55 (2004). These measurements are performed by three RTDs (for the middle column) and six thermocouples (for the columns at 1/4 and 3/4 of the room length). These measurements serve two purposes. First, they are used to evaluate the thermal stratification inside the room. Second, measurements at 1.1 m and 1.7 m are used to evaluate the VATD in the room.

Table 3-1: Location of the thermocouples and RTDs

	X (Length) [m]	Y (Width) [m]	Z (Height) [m]		X (Length) [m]	Y (Width) [m]	Z (Height) [m]	
Floor (Thermo- couples)	0.71	-0.58	0.00	Side wall 2 (Thermo- couples)	0.77	-1.16	0.80	
	1.42	-0.58	0.00		0.77	-1.16	1.60	
	2.13	-0.58	0.00		2.59	-1.16	0.80	
	2.84	-0.58	0.00		2.59	-1.16	1.60	
	0.71	0.00	0.00	Opposite wall (Thermo- couples)	3.56	0.00	0.80	
	1.42	0.00	0.00		3.56	-0.60	1.60	
	2.13	0.00	0.00	Ceiling (Thermo- couples)	1.20	0.60	2.17	
	2.84	0.00	0.00		2.40	0.60	2.17	
	0.71	0.58	0.00	Stratification (RTDs)	1.78	0.00	0.60	
	1.42	0.58	0.00		1.78	0.00	1.10	
	2.13	0.58	0.00		1.78	0.00	1.70	
	2.84	0.58	0.00					
Diffuser's wall (Thermo- couples)	0.00	-0.60	1.60	Stratification (Thermo- couples)	0.89	0.00	0.60	
	0.00	0.00	1.08		0.89	0.00	1.10	
	0.00	0.60	0.80		0.89	0.00	1.70	
	0.00	0.60	1.60		2.67	0.00	0.60	
Side wall 1 (Thermo- couples)	1.20	1.16	0.80		2.67	0.00	1.10	
	1.20	1.16	1.60		2.67	0.00	1.70	
					Exhaust	1.20	1.16	1.95

	2.40	1.16	0.80	(Thermo- couples)	2.40	1.16	1.95
	2.40	1.16	1.60				

The surface temperatures in the chamber are also recorded, since they could be used as boundary conditions for potential CFD models. Thermocouples are used to measure the surface temperature of all walls, at several locations and heights, as shown in Table 3-1. For the floor surface, a total of 12 thermocouples (3 rows of 4 thermocouples) are installed, in order to study the variations of the floor temperature at different distances from the diffuser.

Finally, the air temperature is measured at several locations in the HVAC system. The supply air temperature is measured using thermocouples at two locations: right after the fan, and right before the diffuser. In the remaining of this work, the temperature referred to as “supply temperature” is the one measured right before the diffuser. For the exhaust air temperature, two thermocouples are placed in the middle of the exhaust gap (see Table 3-1 for details). The average of the two measured values is considered as the exhaust temperature.

3.2 Measurements locations in a DV jet for the two diffusers

3.2.1 Diffusers studied and supply conditions

The type of diffuser used in our experiment is the DF1W diffuser from HVAC manufacturer E.H. Price (E.H. Price, 2006). This diffuser is a standard wall-mounted DV diffuser, commonly used for displacement ventilation. Two sizes of this diffuser are tested in our measurements. First, a diffuser with 0.6 m by 0.6 m (height by width) outlet size is tested. This size was chosen as it is the size the most likely to be used in small rooms such as the environmental chamber. Then, a second diffuser with outlet size (1.2 m by 0.6 m (height by width)) is tested, in order to study the influence of the diffuser’s height on the DV jet.

For each diffuser, measurements are performed for two supply under-temperatures ΔT_s , where the under-temperature is defined as the difference between the supply air temperature before the diffuser and the air temperature in the center of the room at 1.1 m height. The supply under-temperatures used (see Table 3-2) are based on Nordtest VVS083, which is a standard specifically designed for displacement ventilation (Nordtest, 2009). Such supply conditions are also representative of the range commonly used in displacement ventilation. Regarding the supply flow rate, the measurements are performed for a flow rate of around 35 L/s (70 CFM), which corresponds to approximately seven Air Change per Hour.

Table 3-2: Testing conditions for experimental work

	Flow rate [m ³ /s]	Under- temperature ΔT_s [°C]	Supply temperature [°C]	Temperature at 1.1 m from the floor [°C]
Diffuser 0.6 m x 0.6 m	0.035	2.4	19.4	21.8
		5.0	16.9	21.9
Diffuser 1.2 m x 0.6 m	0.032	2.5	19.4	21.9
		5.5	16.8	22.3

3.2.2 Measurements in front of the diffuser

The first series of measurements to be performed are measurements in front of the diffuser. These measurements are useful for correlation purposes, as well as for potential boundary conditions in CFD simulations. Also, the measured values allow characterizing the jet leaving the diffuser, and identifying possible non-uniformities of air speed and temperature. Measurements in front of the diffuser are performed for the three supply conditions (isothermal, $\Delta T_s = 2.4^\circ\text{C}$, $\Delta T_s = 5.0^\circ\text{C}$) by measuring the air speed and the air temperature in a plane 0.05 m from the diffuser, along the vertical and horizontal axes passing through the centre of the diffuser (see

Figure 3-3), with a step of 0.05 m. In addition to this, measurements are also performed over the whole area of the diffuser for an under-temperature of 5.0°C, with a step of 0.5 m. These measurements are performed for both sizes of diffuser. Measurements locations are schematized in Figure 3-3 for diffuser DF1W with an outlet size of 0.6 m by 0.6 m.

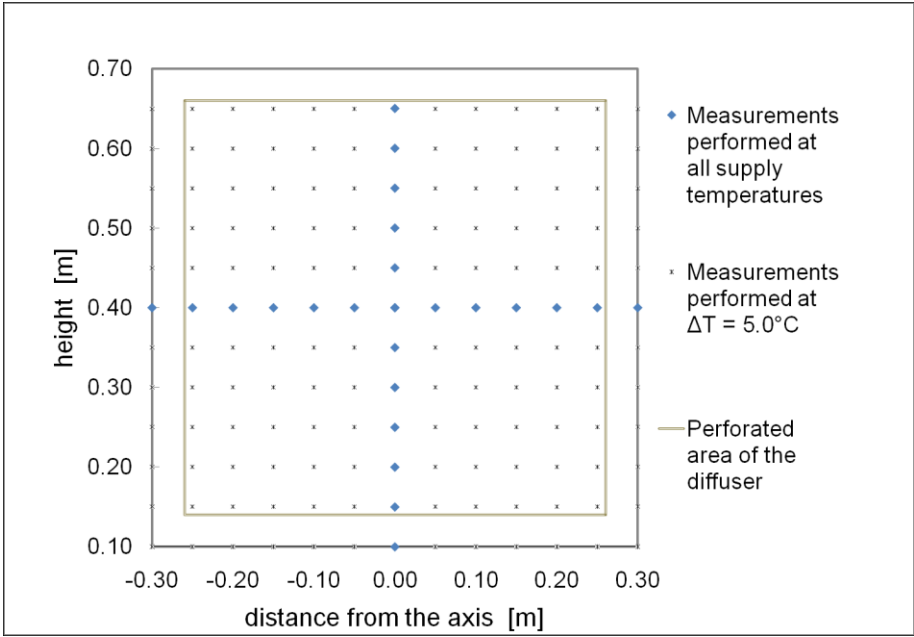


Figure 3-3: Schematic view of the axes of measurements for the DF1W 0.6 m x 0.6 m diffuser

3.2.3 Measurements in the DV jet for non-isothermal supply conditions

Air speed and temperature measurements in the jet for non-isothermal supply conditions are performed in three perpendicular planes in the room, as shown in Figure 3-4, to acquire a three dimensional dataset.

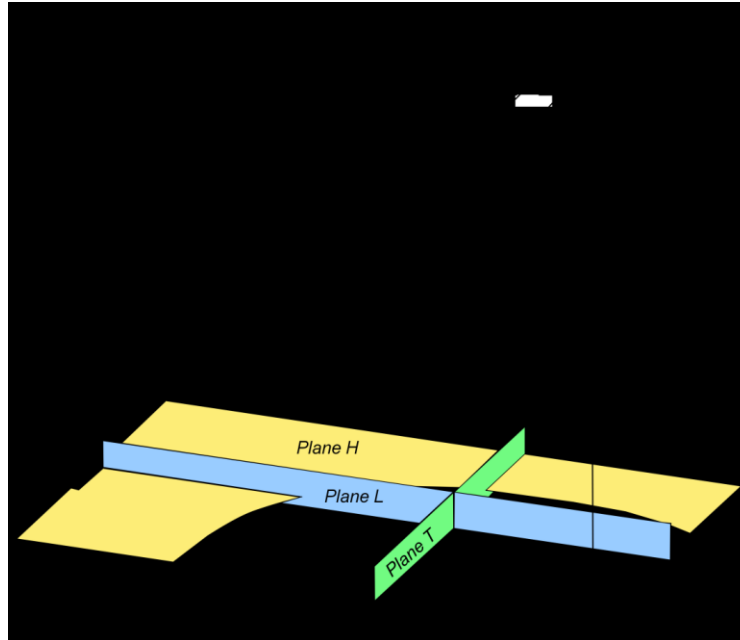


Figure 3-4: Measurement planes for non-isothermal jet measurements

The first plane of measurement, Plane L, is the vertical plane passing through the Longitudinal axis of the air jet, in the center of the room (plane $Y=0$). In this plane, the air speed and temperature are measured at distances from the diffuser of 0.16 m to 3.16 m, with steps of 0.2 m, and at the 10 heights of 0.02 m, 0.03 m, 0.04 m, 0.05 m, 0.06 m, 0.07 m, 0.08 m, 0.10 m, 0.20 m, and 0.26 m for a total of 160 measurement points (see Figure 3-5).

The second plane of measurement, Plane T, is the vertical Transversal plane at 2.16 m from the diffuser (plane $X=2.16$ m). The air speed and temperature are measured in this plane at nine heights, specifically 0.02 m, 0.03 m, 0.04 m, 0.05 m, 0.06 m, 0.07 m, 0.08 m, 0.10 m, and 0.20 m, at distances from the central axis of 0.1 m to 0.9 m, thus with 5 locations spaced at 0.2 m (8 in), on each side of the axis, for a total of 90 measurement points (see Figure 3-5).

Finally, the air speed and temperature are measured in Plane H, which is the Horizontal plane at 0.05 m above the floor (plane $Z=0.05$). In this plane, measurements are performed at distances from the diffuser from 0.16 m to 2.76 m, with steps of 0.4 m until 1.76 m, and steps of 0.2 m afterwards, thus a total of 10 locations, and for distances from the central axis varying from 0.1

m to 0.9 m, thus 5 steps of 0.2 m on each side of the axis, for a total of 100 measurement points (see Figure 3-5).

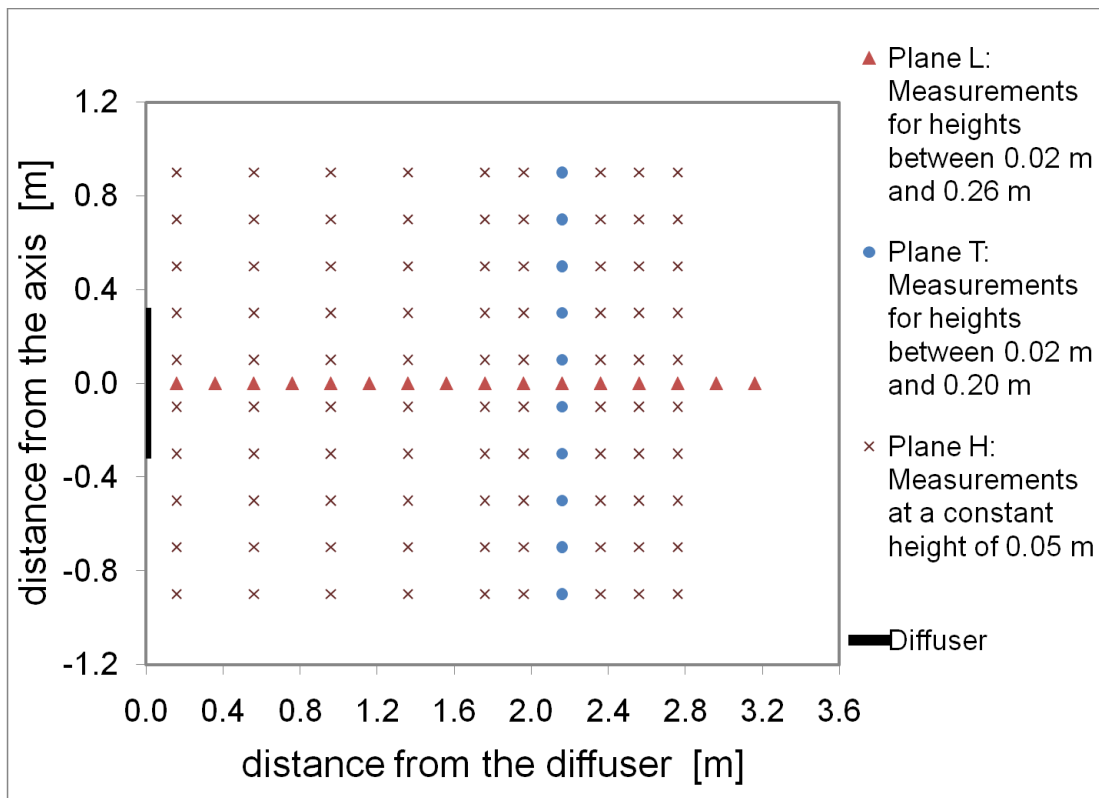


Figure 3-5: Measurement locations for non-isothermal jet measurements (Top view)

3.3 Additional measurement for the 0.6 m x 0.6 m diffuser

An additional series of measurements are performed on the DF1W 0.6 m x 0.6 m diffuser. These measurements are aimed at studying more specifically the effect of the supply under-temperature on the longitudinal profiles of maximum air speed and minimum temperature. In addition, these measurements provide experimental data regarding the DV jet characteristics at diffuser exit and at the transition between the primary and secondary zones of the jet. These

data are useful for modeling purpose. Overall, five supply conditions are measured, as summarized in Table 3-3

Table 3-3: Testing conditions for the additional measurements

	Flow rate [m ³ /s]	Under- temperature ΔT_s [°C]	Supply temperature [°C]	Temperature at 1.1 m from the floor [°C]
Diffuser 0.6 m x 0.6 m	0.035	1.5	20.6	22.0
		2.4	19.4	21.8
		3.7	18.8	22.5
		5.0	16.9	21.9
		6.3	15.4	21.7

The measurements locations can be summarized as follows, for each set of supply conditions tested:

At the diffuser exit: First, the air speed and temperature are measured in the jet at 0.05 m from the diffuser, on a vertical axis passing through the center of the diffuser, for heights from 0.10 m to 0.70 m, with a step of 0.05 m.

In the vertical longitudinal plane: Then, the air speed and temperature are measured in the longitudinal plane, for several heights from 0.02 m to 0.10 m, and for distances from the diffuser from 0.66 m to 2.36 m, with a step of 0.10 m. These measurements enable to determine the longitudinal profiles of maximum air speed and minimum temperature in the DV jet. Using the maximum air speed profile, the length of the primary zone can be determined.

At the transition between the primary and secondary zones: The extent of the primary zone is defined as the distance from the diffuser at which the maximum air speed is reached, for each

set of supply conditions. At this distance from the diffuser, the air speed and temperature are measured, on the longitudinal axis, for the heights of 0.02 m, 0.03 m, 0.04 m, 0.05 m, 0.06 m, 0.08m, 0.10 m, and 0.20 m. At the height corresponding to the maximum air speed, the air speed and temperature are also measured in the transversal direction. These measurements are performed for distances from the longitudinal between 0.1 m and 0.9 m, with a step of 0.2 m, on both sides of the longitudinal axis.

CHAPTER 4: EXPERIMENTAL RESULTS

This chapter presents the results from experimental measurements. Experimental results from section 4.1 have been published (see Magnier et al. 2011, Magnier et al. 2012). First are presented the results using the diffuser DF1W of size 0.6 m x 0.6 m for the two main supply conditions. Then, results for the second diffuser size (diffuser DF1W size 1.2 m x 0.6 m) are presented, and compared with the first diffuser. Finally are presented the additional measurements focusing on the transition between first and secondary zones and on the profiles of maximal air speed and minimal temperature.

4.1 Experimental results for the diffuser of size 0.6 m x 0.6 m for under-temperatures of 2.4°C and 5.0°C

This section presents the experimental results for the measurements performed on diffuser DF1W of outlet size 0.6 m x 0.6 m (E.H. Price, 2007), for the supply conditions and indoor temperatures given in Table 4-1. We present first the results of the measurements taken at the diffuser. Then, we present and discuss the results for each of the three planes investigated in this study to capture the behaviour of the air jet.

Table 4-1: Supply air conditions and thermal stratification for the two experimental cases

ΔT_s [°C]	Supply flow rate [m ³ /s]	Supply air temperature [°C]	Air temperature at 0.6 m [°C]	Air temperature at 1.1 m [°C]	Air temperature at 1.7 m [°C]
2.4	0.035	19.4 ± 0.2	21.3	21.8	22.5
5.0	0.035	16.9 ± 0.1	20.8	21.9	23.0

4.1.1 Measurements in front of the diffuser

Figure 4-1a and Figure 4-1b present the air speed and temperature distributions measured in front of the diffuser for an under-temperature of 5.0°C. The dashed square on this figure shows the limits of the perforated area of the diffuser (0.52 m by 0.52 m); the dots on the figures indicate the locations where air speed and temperature are measured. As shown in Figure 4-1a, the air speed from the diffuser is not uniform throughout the diffuser area. The air speed gradually increases in the lower half of the diffuser and reaches its maximum at the bottom corners of the diffuser. The maximum speed measured is 0.48 m/s, which is more than twice than the average air speed of 0.18 m/s. Figure 4-1b shows that the temperature of the air coming from the diffuser is relatively uniform over the diffuser area, with slightly higher values in the upper half of the diffuser, where the flow rate is lower. The air temperature increases on the perimeter of the diffuser by up to 2°C above the supply temperature in the diffuser centre, due to mixing with the surrounding warmer indoor air that is induced by the jet.

Figure 4-1c to Figure 4-1f show, for the two supply conditions studied, the air speed and temperature distributions measured on the central vertical and horizontal axes. The air speed profiles measured for both supply under-temperatures are similar. The only significant difference is the amplitude of the air speed peaks appearing at the border of the diffuser. In all likelihood, this difference is caused by the inability of the measuring grid to capture the conditions in the mixing layer. In the case of air temperature distribution, for the two supply under-temperatures, within an area of 0.4 m x 0.4 m at the center of the diffuser, the air temperature is very close to the supply temperature. The air temperature gets higher at the border of the diffuser, where mixing occurs. It is noteworthy that the fluctuations of temperature for heights between 0.2 m and 0.6 m in Figure 4-1d, for the under-temperature of 2.4°C, are due to fluctuations of the supplied air temperature and to the measuring device uncertainty. This last point was verified by comparison with the supply temperature measured during the same period.

Overall, the air speed and temperature distributions at the diffuser seem to be independent of the supply under-temperature. Additional measurements performed with isothermal supply conditions lead to air speed profiles very similar to the ones displayed in Figure 4-1c and Figure 4-1e, supporting the conclusion that the air speed distribution at the diffuser outlet is not significantly influenced by the supply temperature. Finally, for the diffuser and supply conditions studied, the supply air turbulence intensity is negligible (lower than 2%), except within the mixing layer around the diffuser (with values over 40%).

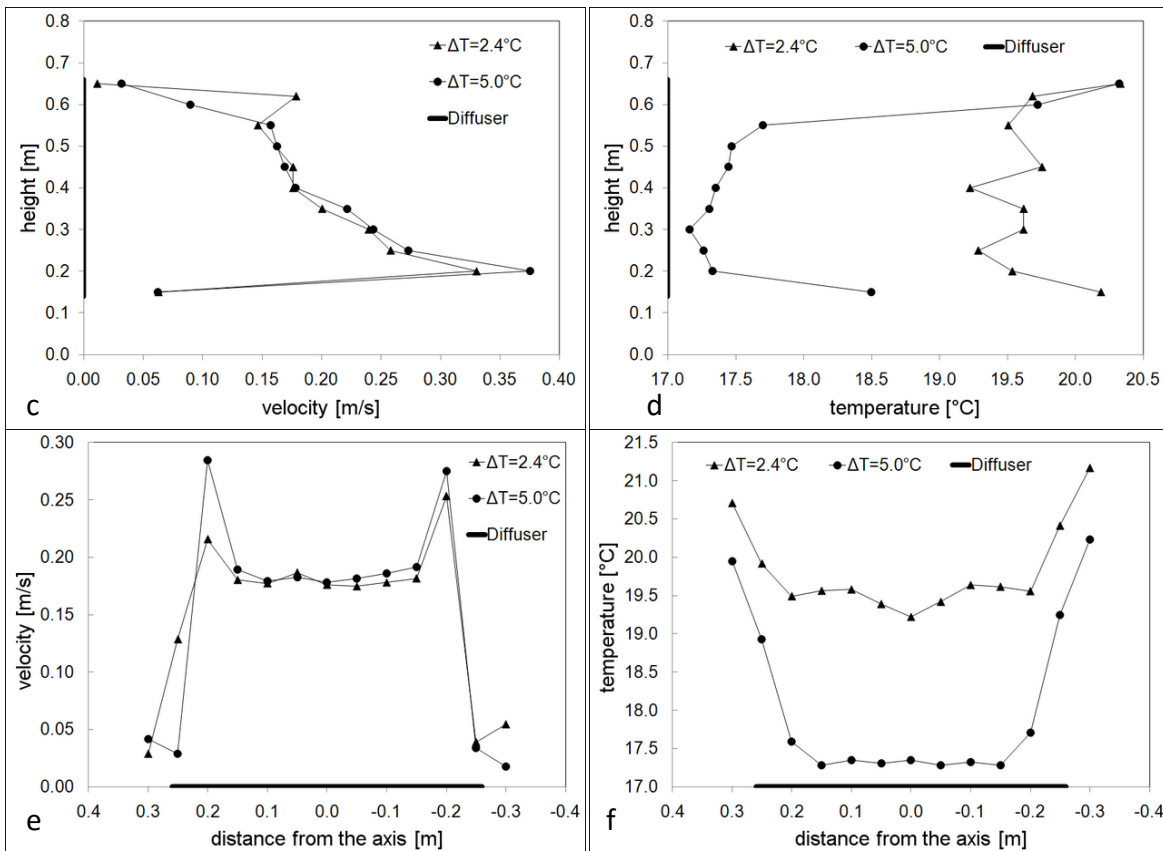
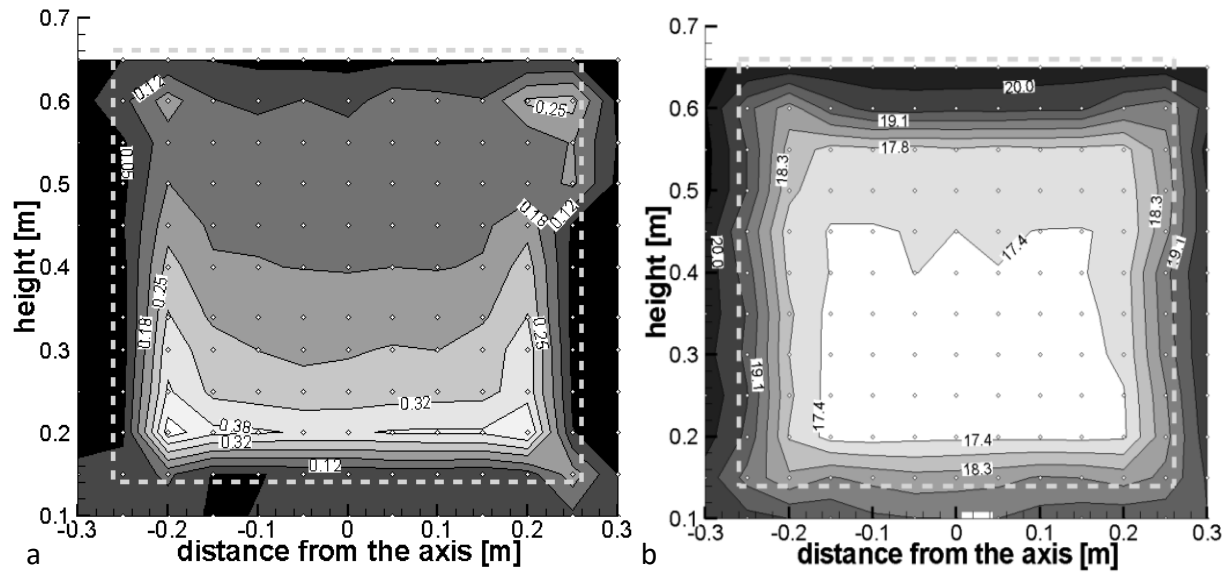


Figure 4-1: Air speed (left) and temperature (right) measurements at 0.05 m from the diffuser (a, b) on the complete grid for $\Delta T=5.0^\circ\text{C}$; (c, d) on a vertical axis passing by the center of the diffuser for both supply conditions; (e, f) on the horizontal axis passing by the center of the diffuser for both supply conditions

4.1.2 Measurements in the longitudinal vertical plane, Plane L

Air speed

Figure 4-2 shows the air speed distributions measured in Plane L for the two supply conditions studied. As mentioned above, in the literature reviewed for this study, a DV jet is often described by having two zones: the primary zone, close to the diffuser, where the flow drops to the floor and the air speed increases due to the action of the buoyancy forces; and the secondary zone, where the air speed decreases. These two zones appear clearly on Figure 4-2, where the jet leaves the diffuser, decreases in thickness as it touches the floor, and then maintains a rather constant thickness in the secondary zone. The separation frontier between primary and secondary zones, defined as the distance from the diffuser to the point of maximum air speed, is represented as a vertical white line in Figure 4-2. This distance is equal to about 1.2 m for the under-temperature of 5.0°C, while it is about 1.4 m for the under-temperature of 2.4°C. This difference is attributed to the stronger buoyancy forces in the former case, making the flow drop faster to floor level. The stronger buoyancy forces also explain the higher air speed of 0.42 m/s reached with an under-temperature of 5.0°C compared to the maximum air speed of 0.36 m/s reached with an under-temperature of 2.4°C. It should finally be noted that, close to the diffuser, the DV jet is not yet in contact with the floor. The measurement points below 0.10 m close to the diffuser are therefore not within jet, but under the jet.

Figure 4-3 plots the longitudinal air speed profiles measured at different heights for the two supply conditions. This figure highlights the increase of air speed in the primary zone, and its decrease in the secondary zone. The decrease of thickness of the flow in the primary zone (as noticed in Figure 4-2) combined with the increase of air speed, explains that the air speed profiles at different heights do not reach their maximum value at the same distance from the diffuser (Figure 4-3). In our measurements, the rate of air speed decay in the secondary zone is somewhat higher for measurements performed with an under-temperature of 5.0°C than for

2.4°C. However, after 2 m from the diffuser the velocities are slightly higher for the case with an under-temperature of 2.4°C than for the case with an under-temperature of 5.0°C.

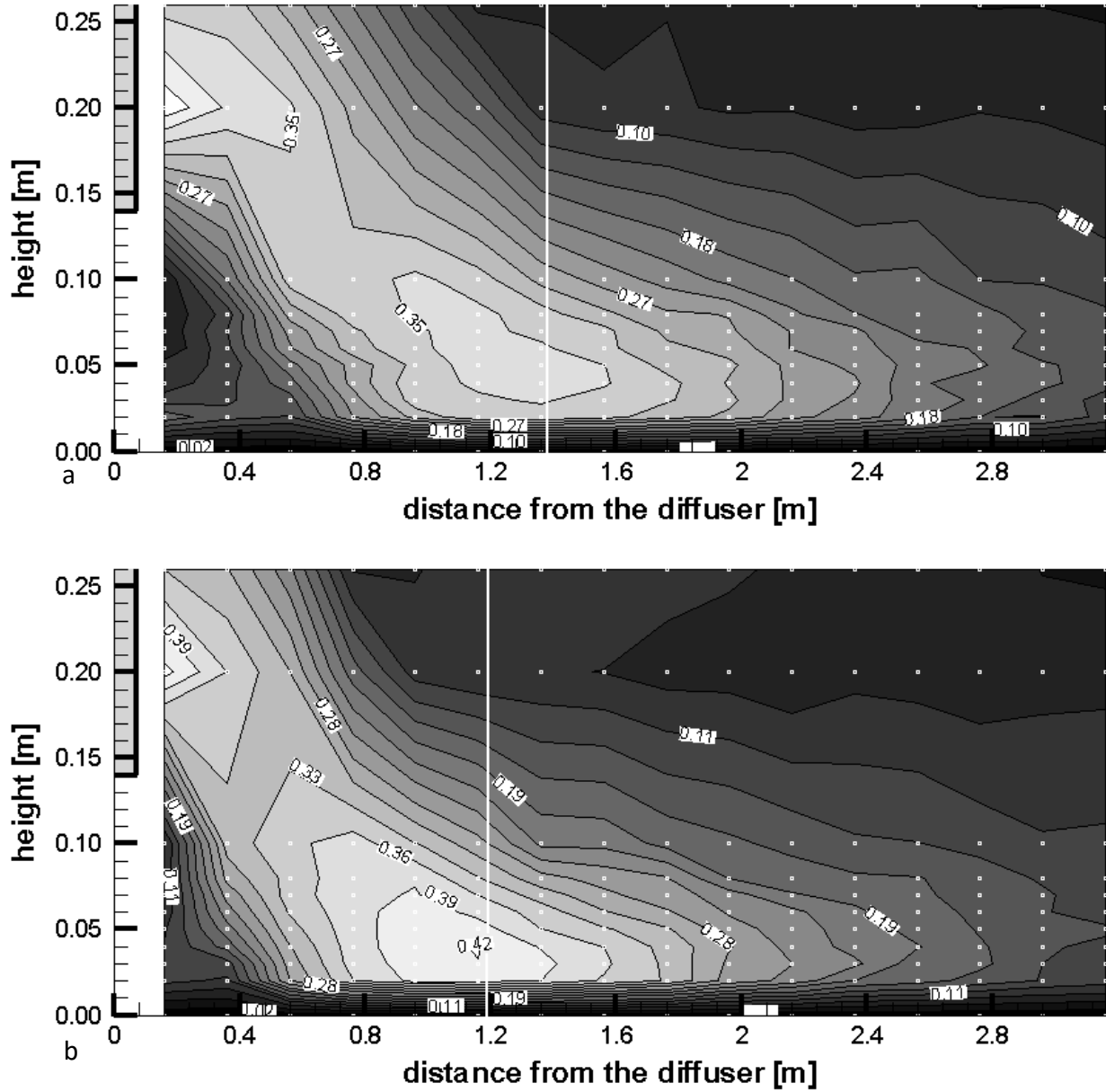


Figure 4-2: Air speed distribution in Plane L for $\Delta T = 2.4^\circ\text{C}$ (a) and $\Delta T = 5.0^\circ\text{C}$ (b), the vertical white line refers to the maximum air speed attained.

Figure 4-4 plots the vertical air speed profiles measured at different distances from the diffuser in the secondary zone. The vertical profiles measured are consistent with profiles found in isothermal wall jets (Rajaratnam1 1976). The air speed measured at a height of 0.10 m (the height of ankle in ASHRAE 55 (2004)) was generally found 30% lower than the maximum air speed in the jet at the same distance from the diffuser. The maximum air speed typically occurs at heights ranging between 0.03 m and 0.05 m. This result is consistent with literature (Skistad, 1994; Nordtest, 2009). The maximum air speed seems to happen slightly lower for measurements with the highest under-temperature. This difference in height is however very small and should be confirmed with a larger range of supply conditions. Figure 4-4 shows also that the height of maximal air speed does not vary significantly with increasing distance from the diffuser. These findings are consistent with Nielsen's measurements (2000).

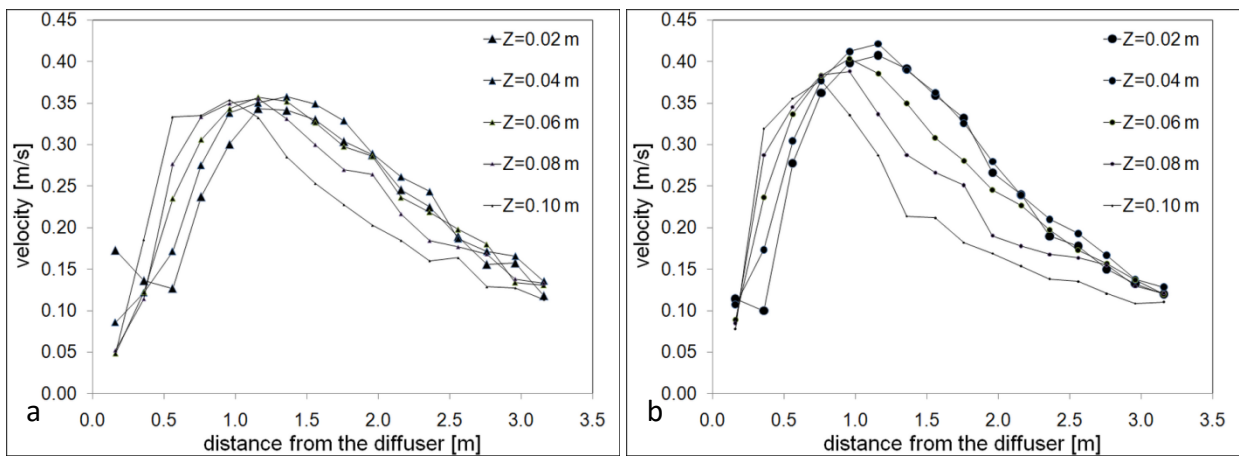


Figure 4-3: Air speed profiles at different heights in plane L for $\Delta T = 2.4^\circ\text{C}$ (a) and $\Delta T = 5.0^\circ\text{C}$ (b)

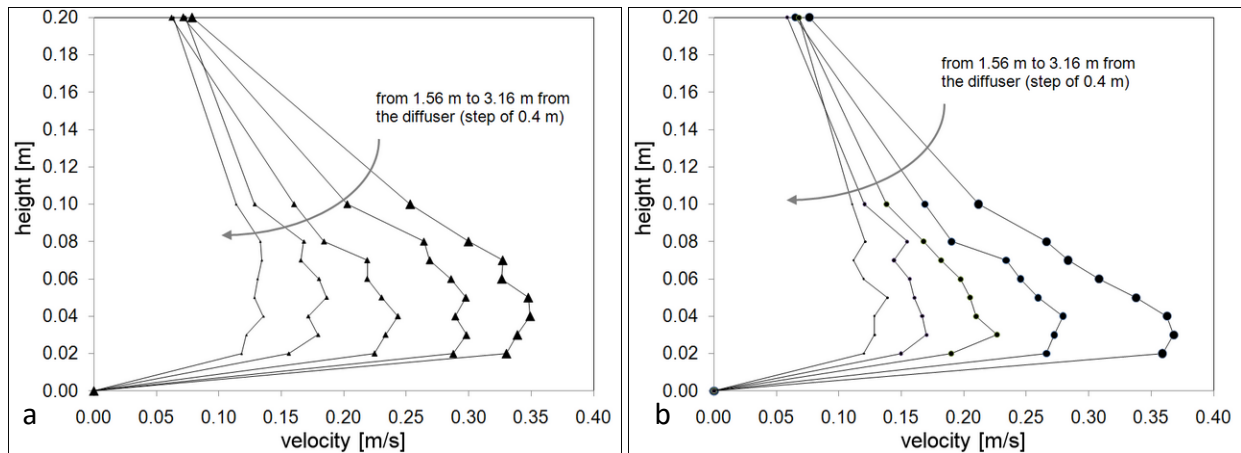


Figure 4-4: Vertical air speed profiles in the primary and secondary zones for $\Delta T = 2.4^\circ\text{C}$ (a) and $\Delta T = 5.0^\circ\text{C}$ (b)

Air temperature

Figure 4-5a and Figure 4-5b show the temperature distribution measured in Plane L for supply under-temperatures of 2.4°C and 5.0°C , respectively. Measurements show that the air temperature within the jet varies significantly with the distance from the diffuser. For instance, the difference between the coolest and warmest points in the vicinity of the floor (heights lower or equal to 0.10 m) is 1.2°C for an under-temperature of 2.4°C , and reaches 2.3°C for an under-temperature of 5.0°C . This temperature non-uniformity, not handled by current temperature models, is significant and can impact local thermal comfort. Figure 4-6 shows the longitudinal temperature profiles measured at different heights for the two supply conditions studied. The floor temperature, measured at different distances from the diffuser, is also indicated on this figure. Figure 4-6 shows that, for most of the primary zone, the air temperature for heights between 0.02 m and 0.10 m decreases with the distance from the diffuser. This decrease should not be confused with a temperature decrease inside the DV jet. For heights below 0.10 m, the measurement points the closest to the diffuser are under the DV jet and, therefore, are not directly affected by the air jet temperature. As the distance from the diffuser increases, the measurement points enter the boundary layer of the colder air jet and then the jet itself, causing the apparent decrease in temperature. Figure 4-6 also shows that the temperature in the secondary zone increases linearly with increasing distance from the diffuser, due to heat

transfer with the floor and room air. Measurements of the floor surface temperature also revealed that the floor temperature is not constant, but increases with increasing distance from the diffuser. The rate of temperature increase of the floor surface temperature is similar to the rate of increase of air temperature inside the jet. This result is consistent with measurement performed by Novoselac et al. (2006) on a DV jet over a heated floor.

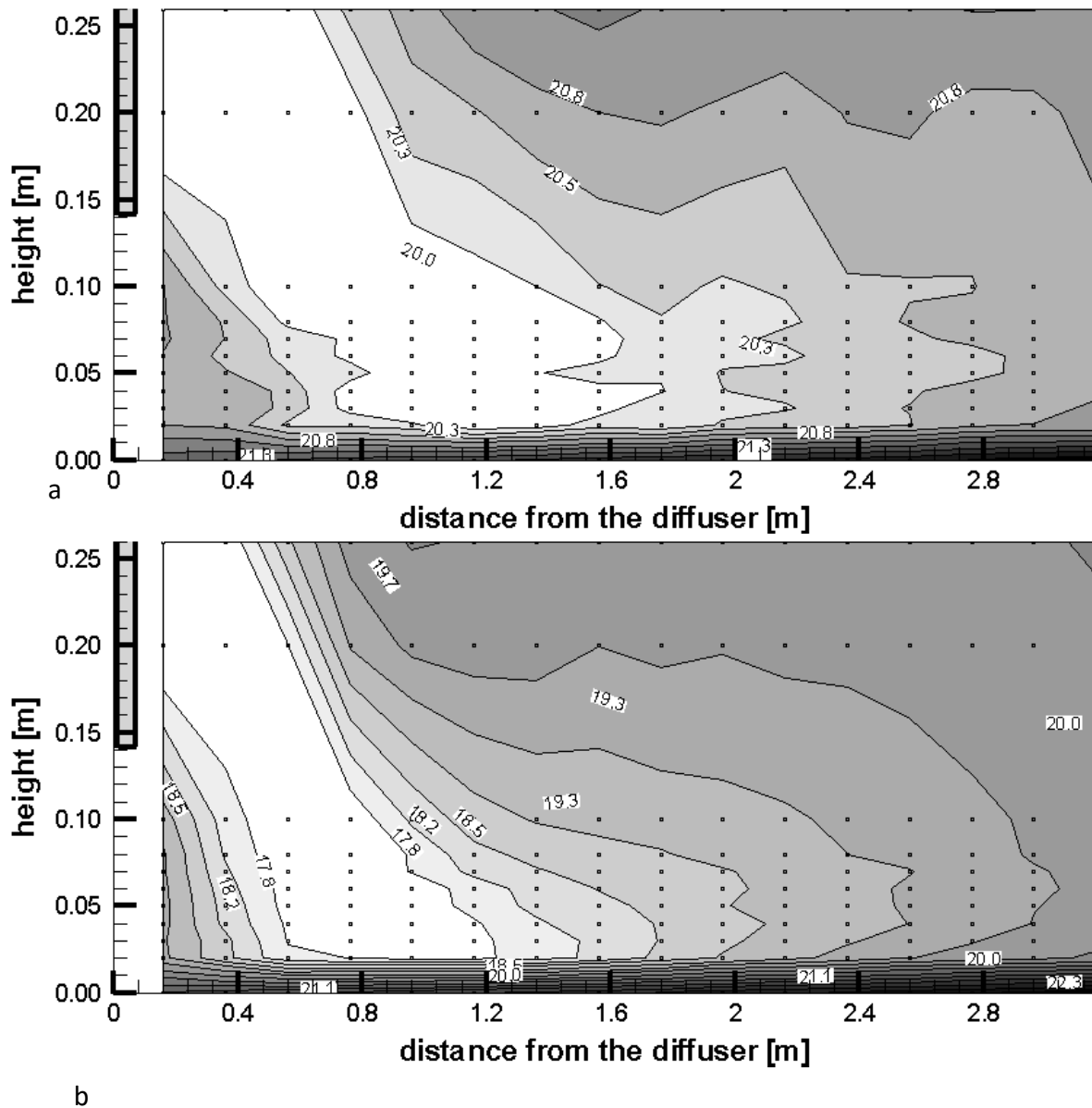


Figure 4-5: Temperature distribution in Plane L for $\Delta T=2.4^{\circ}\text{C}$ (a) and $\Delta T=5.0^{\circ}\text{C}$ (b)

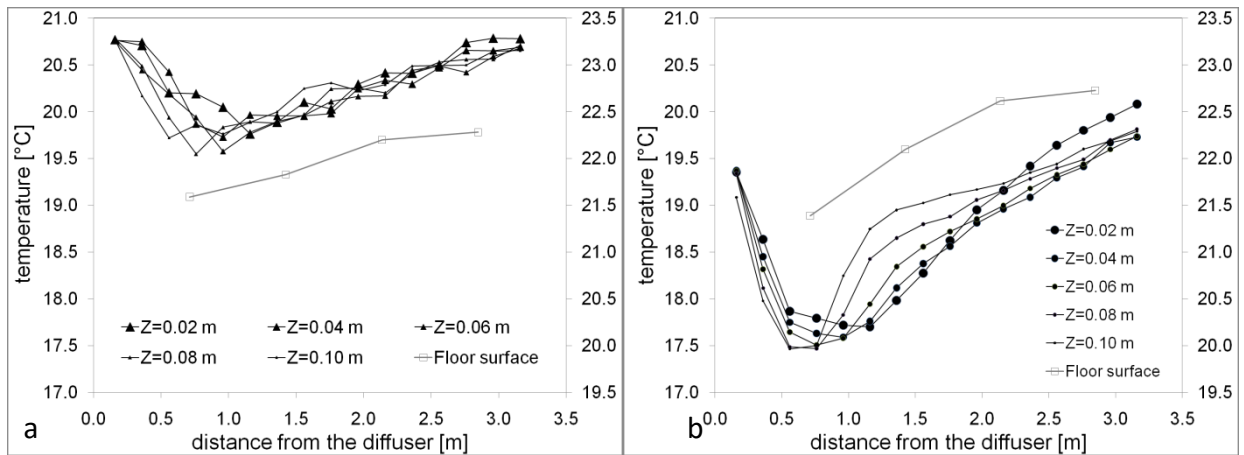


Figure 4-6: Air temperature profiles at different heights (left axis) and floor surface temperature (right axis) in Plane L for $\Delta T = 2.4^\circ\text{C}$ (a) and $\Delta T = 5.0^\circ\text{C}$ (b)

Figure 4-7 shows the vertical temperature profiles measured at different distances from the diffuser in the secondary zone. The difference in measured temperature between the heights of 0.02 m and 0.10 m is generally small (lower than 0.3°C), and falls under the thermocouple accuracy. The only location where the temperature difference is significantly high is at the very beginning of the secondary zone, at 1.36 m distance from diffuser, for the under-temperature of 5.0°C . The vertical variation of air temperature in the secondary zone is of much less magnitude that the change of temperature with increasing distances from the diffuser.

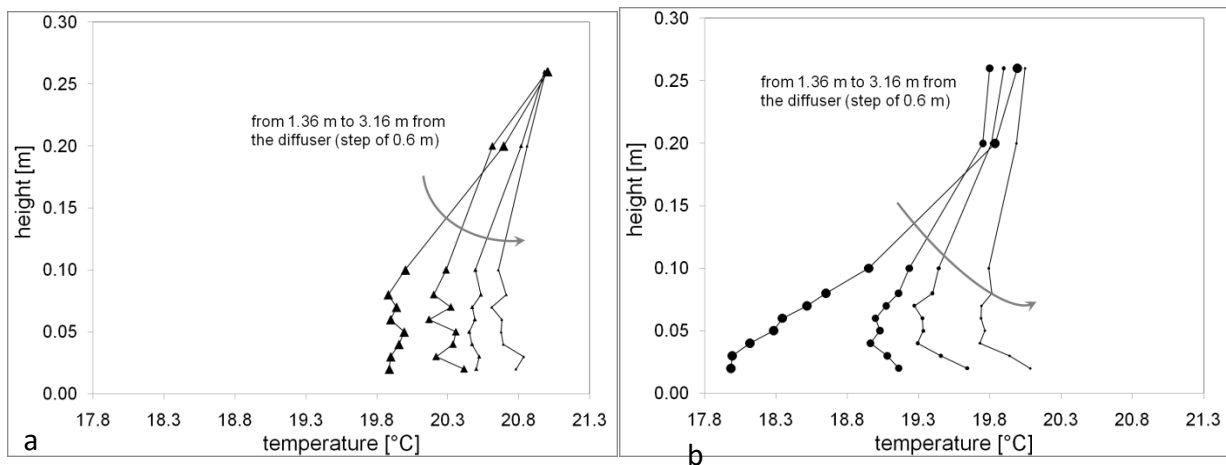


Figure 4-7: Vertical temperature profiles at different distances from the diffuser for $\Delta T = 2.4^\circ\text{C}$ (a) and $\Delta T = 5.0^\circ\text{C}$ (b)

4.1.3 Measurements in the transversal vertical plane, Plane T

Figure 4-8 shows the air speed and temperature distributions measured in Plane T for the two supply temperatures studied. For measurements performed with an under-temperature of 2.4°C (Figure 4-8a and Figure 4-8b), measurements show that, for all heights, the maximum air speed and the minimal air temperature occur on the central axis of the diffuser. Away from the centerline, the air velocities decrease and the air temperature increases. For example, the air speed measured at 0.9 m from the longitudinal axis and at heights below 0.1m are generally between 0.05 m/s to 0.10 m/s lower than the velocities measured on the central axis. Similarly, the difference between the air temperature measured at 0.9 m from the longitudinal axis and the air temperature measured on the axis can be as high as 0.5°C. For the second supply temperature studied, (Figure 4-8c and Figure 4-8d), the same conclusions can be drawn; in this latter case though, the flow is shifted toward one of the lateral wall of the chamber. It is assumed that this shift is due to the exhaust installed on the lateral wall. Finally, in terms of turbulence, the turbulence intensity for both supply conditions is between 5% and 25% for heights lower or equal to 0.10 m. The transversal profiles of air speed and temperature for measurement performed at a height of 0.05 m are shown in Figure 4-9. The transversal profiles of air speed appear to follow a Gaussian distribution. This result is consistent with some early measurements by Nielsen (1998). The height at which the maximum air speed occurs appeared to be unaffected by the distance from the longitudinal axis.

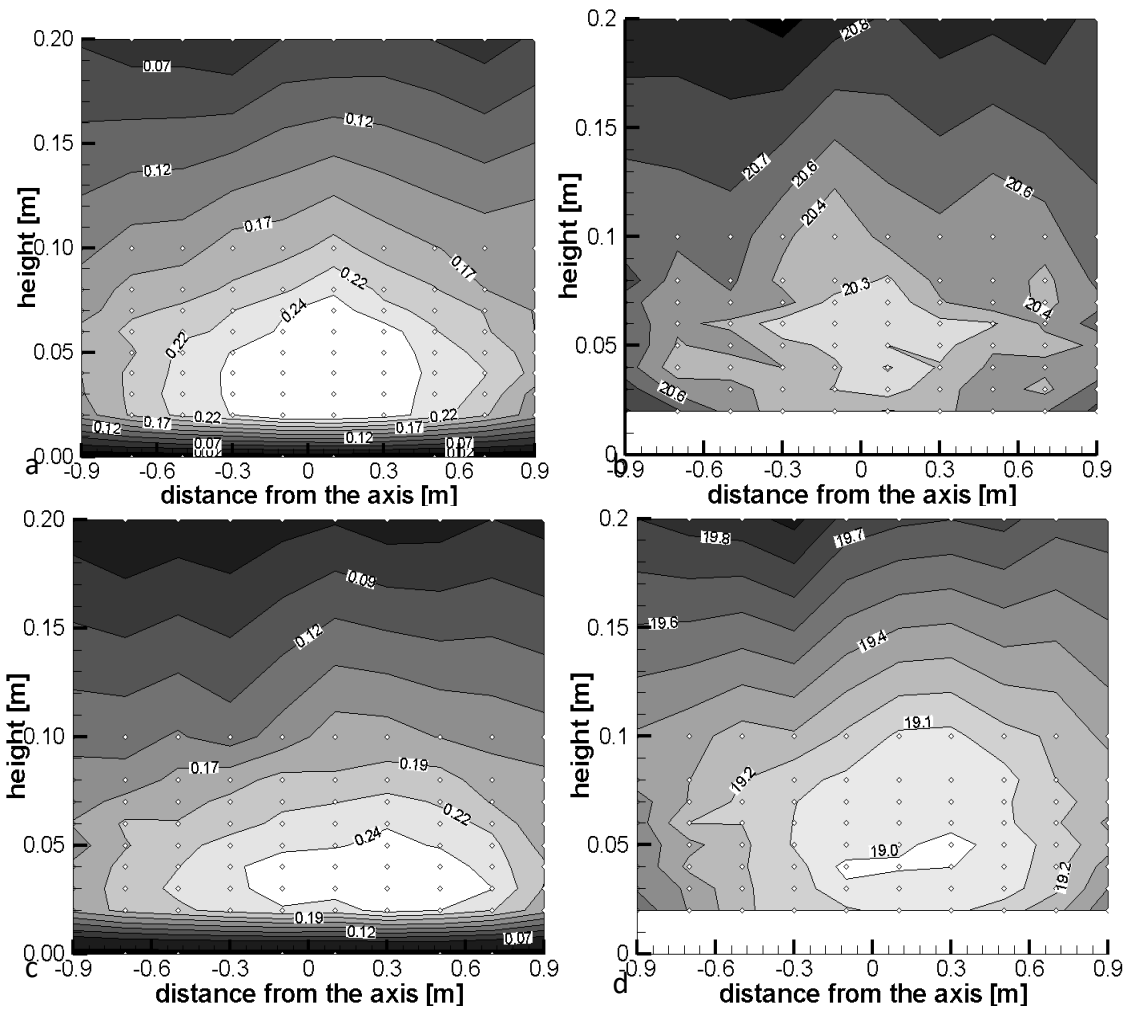


Figure 4-8: Air speed (left) and temperature (right) distributions in Plane T for $\Delta T = 2.4^\circ\text{C}$ (a, b) and $\Delta T = 5.0^\circ\text{C}$ (c, d)

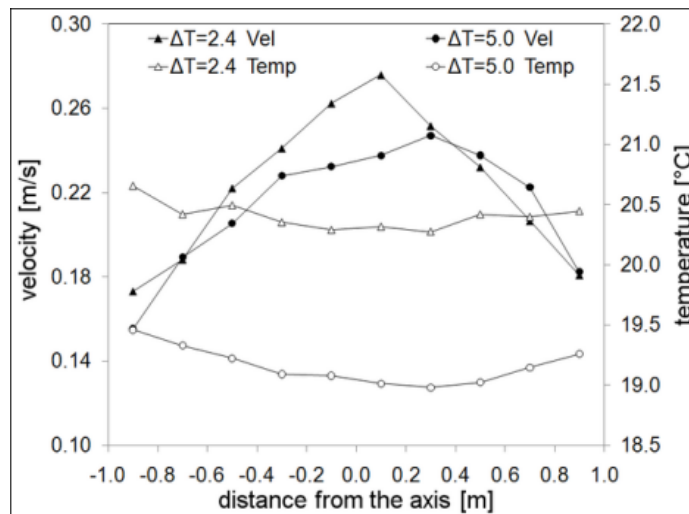


Figure 4-9: Air speed and temperature profiles at 2.16 m from the diffuser and at 0.05 m from the floor for both supply conditions

4.1.4 Measurements in a horizontal plane, plane H

Figure 4-10 shows the air speed and temperature distributions measured in Plane H, located at a height of 0.05 m above the floor, for the two supply temperatures studied. One can again notice the primary zone, where the air speed increases, and the secondary zone, where the air speed decreases. The interesting point highlighted by measurements in Plane H is the large non-uniformity of air speed and temperature over the floor area, caused by the progressive lateral expansion of the flow. In the literature, the DV jet is generally studied under an assumption of radial distribution from the diffuser (Nielsen, 2000). For the diffuser studied though, preliminary measurements (not detailed here) have shown no lateral spreading of the jet for isothermal supply, even at 2 m from the diffuser. The lateral expansion of the jet is however found significant when the supply temperature is lower than the room temperature.

Figure 4-11a shows the transversal air speed profile measured at different distances from the diffuser for an under-temperature of 2.4°C. The transversal profile of the jet is relatively sharp in the primary zone (solid lines), and smoothens as the distance from the diffuser increases in the secondary zone (dashed lines). At 0.96 m from the diffuser, there is a difference of 0.15 m/s between the air speed measured on the longitudinal axis and that measured at 0.9 m lateral from the axis, at 0.05 m from the floor. At 2.56 m from the diffuser, the difference is still present but is reduced to 0.05 m/s.

Figure 4-11b shows the transversal air speed profiles measured at 0.96 m and 2.16 m from the diffuser, at 0.05 m from the floor, for the two supply temperatures studied. At 2.16 m from the diffuser, the transversal air speed profiles are similar for the two supply conditions. At 0.96 m from the diffuser though, the shapes of the lateral profiles are different for the two supply conditions, with the profile for the lowest under-temperature (2.4°C) being sharper than the profile for the highest under-temperature (5.0°C). This result tends to confirm that the lateral expansion of the jet in the primary zone is caused by the buoyancy forces, with faster lateral expansion for higher under-temperatures. The same conclusions are found for the transversal temperature profiles measured at different distances from the diffuser at a height of 0.05 m.

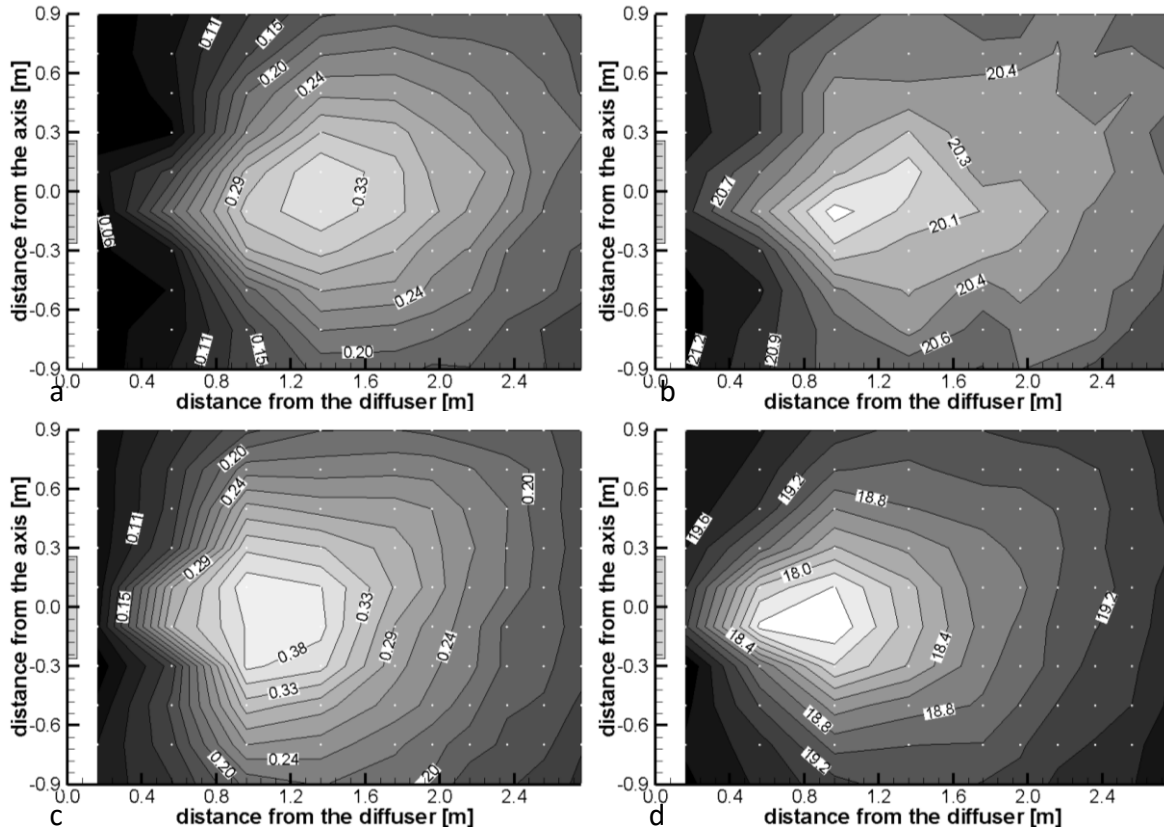


Figure 4-10: Air speed (left) and temperature (right) distributions at 0.05 m from the floor for $\Delta T=2.4^\circ\text{C}$ (a, b) and $\Delta T=5.0^\circ\text{C}$ (c, d)

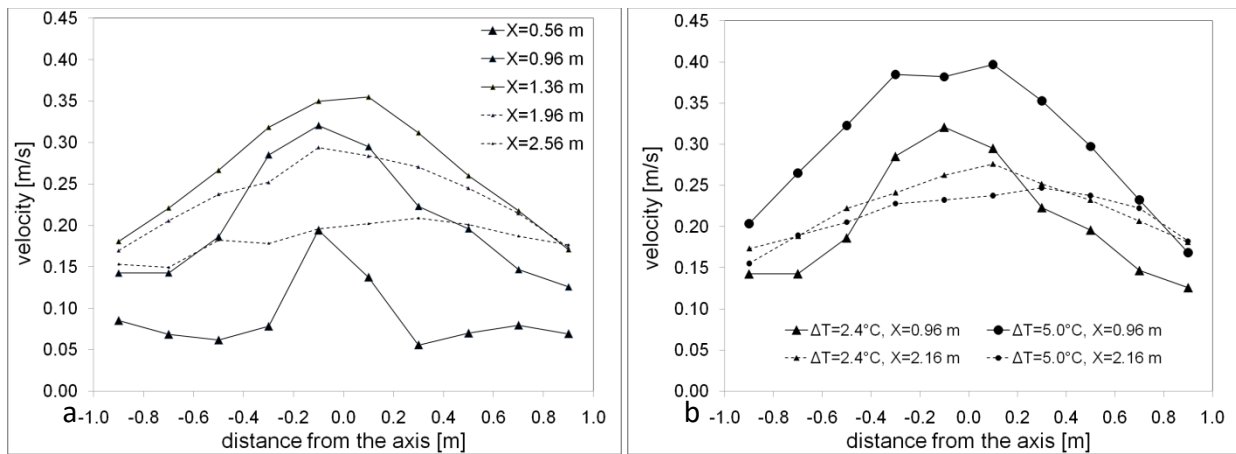


Figure 4-11: Transverse air speed profiles measured at a height of 0.05 m a) at different distances from the diffuser for $\Delta T=2.4^\circ\text{C}$; b) at 0.96 m and 2.16 m from the diffuser for both supply conditions

4.1.5 Additional discussion

This section discusses additional measurements and puts the experimental results in perspective of thermal comfort.

Vortices

Air speed measurements (Figure 4-3) suggested the presence of vortices close to the diffuser. In order to visualize the flow pattern close to the diffuser, smoke was injected below the jet, close to the diffuser. These smoke tests permitted to visualize two significant vortices in the space bounded by the wall, the floor and the DV jet. It is reasonable to assume that these vortices have a significant impact on the distance required for the DV jet to drop to the floor surface. The acknowledgment of such vortices is also important for CFD, as the turbulence models used for simulations should be able to handle such flow behaviours.

Turbulence intensity

Turbulence intensity was assessed in this thesis by studying the variations of air speed compared to the average air speed at a given location. The Turbulence Intensity (TI) results are not discussed in details as the variations of air speed from turbulence are within the experimental error (0.03 m/s). Nonetheless, it can be noted that the turbulence intensities in the jet were evaluated to be around 20%, which is consistent with the literature.

Particle Image Velocimetry (PIV)

In order to study further the air velocity field, some PIV measurements were performed. Despite numerous attempts, the quality of the PIV results was however too low to be published

in this thesis. The main problem encountered was with the seeding, i.e. the particles used to track the jet with PIV. Experiments with soap bubbles were performed, but the bubbles were found to be too large to go through the diffuser grille. Later, a smoke generator was used for seeding, but the optimal quantity of smoke to use was extremely difficult to find, especially since the introduction of smoke significantly affected the temperature and flowrate of the supplied air. Finding an appropriate seeding technique appears to be necessary before PIV measurements of good quality can be performed on displacement ventilation jet.

Draft rate

The results presented in section 3 can all be translated into local comfort indices. As an example, the comfort indices related to the measurements performed in the vertical longitudinal plane are presented in this section. Figure 4-12 plots the Draft Rate (DR), calculated as in ASHRAE 55 (2004), using the local air temperature, air speed and turbulence, for both supply conditions studied. The DR plotted at each distance from the diffuser corresponds to the maximum DR from measurements taken in the 0-0.20 m height range. For distances lower than 2 m, Figure 4-12 shows that the DR is higher for $\Delta T=5.0^{\circ}\text{C}$ than for $\Delta T=2.4^{\circ}\text{C}$, due to the higher buoyancy forces. For distances from the diffuser higher than 2 m though, there is no significant difference between the DR values obtained for both under-temperatures. Measurements show that the room is not comfortable (DR higher than 20%) for the first 2.5 m from the diffuser, based on the maximum DR typically occurring at a height of 0.04 m in the secondary zone. It is noteworthy that considering only measurements at a height of 0.10 m would underestimate this draft zone by almost one meter.

Vertical Air Temperature Difference

Figure 4-12 also plots the Vertical Air Temperature Difference (VATD) for a seated person. VATD is calculated based on the air temperature measured at 0.10 m from the floor at several distances from the diffuser, and on the air temperature measured at the height of 1.1 m in the

middle of the room. According to our measurements, the air temperature at the height of 1.1 m does not vary by more than 0.1°C for distances from the diffuser between 0.36 m and 2.16 m. Consequently, the Vertical Air Temperature Difference variations are solely due to the variations of air temperature at 0.10 m from the floor. Figure 4-12 shows that all VATD values are acceptable (below 3°C) when the under-temperature is 2.4°C, regardless of the distance from diffuser. However, in the case of under-temperature of 5.0°C locations at less than about 1.5 m from the diffuser are uncomfortable (VATD above 3°C), while for greater distances the conditions are comfortable. These results suggest that the local comfort/discomfort at the ankle level should be estimated using the temperature in the air jet, measured at different distances from the diffuser, rather than using one single value such as recommended by the 50% rule.

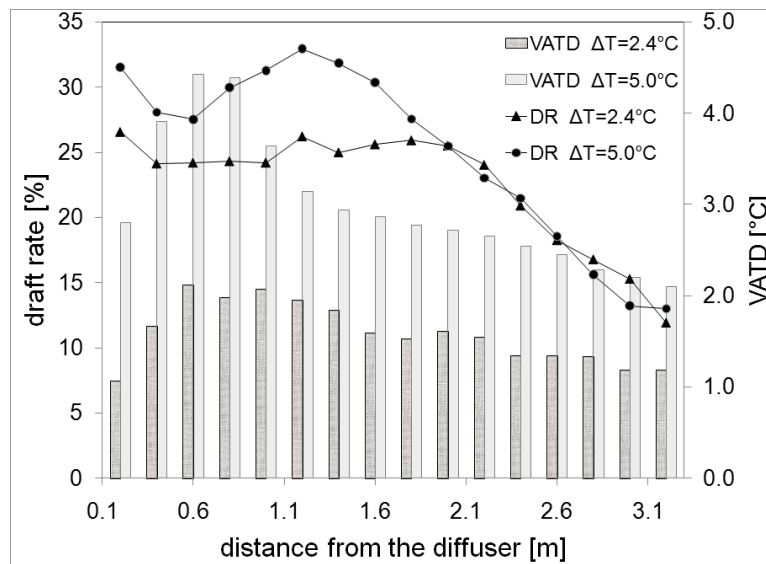


Figure 4-12 : VATD and maximum Draft Rate at floor level for both supply conditions

4.2 Experimental measurements on the large diffuser (1.2 m x 0.6m)

The air speed and temperature distribution in the DV jet with the second diffuser are similar, qualitatively speaking, to the distributions found with the first diffuser. The discussion in this section is then shorter than the one in the previous section. Complete tabulated data for

measurements with the second diffuser are available in appendix. The second part of this section focuses on comparing the temperature and air speed distributions with the two diffusers.



Figure 4-13 : Diffuseur DF1W 1.2m x 0.6 m

4.2.1 Air speed measurements in the vertical longitudinal plane

Figure 4-14 and Figure 4-15 show the air speed distribution measured in the vertical longitudinal plan for two supply conditions studied. Similarly to measurements with the smaller diffuser, the jet displays a primary zone, where the jet falls onto the floor while increasing the air speed, and the secondary zone, where the thickness of the jet is mostly constant and the air speed decreases. The length of the primary zone (0.76 m) is smaller than the one of the first diffuser studied (1.16m-1.36 m).

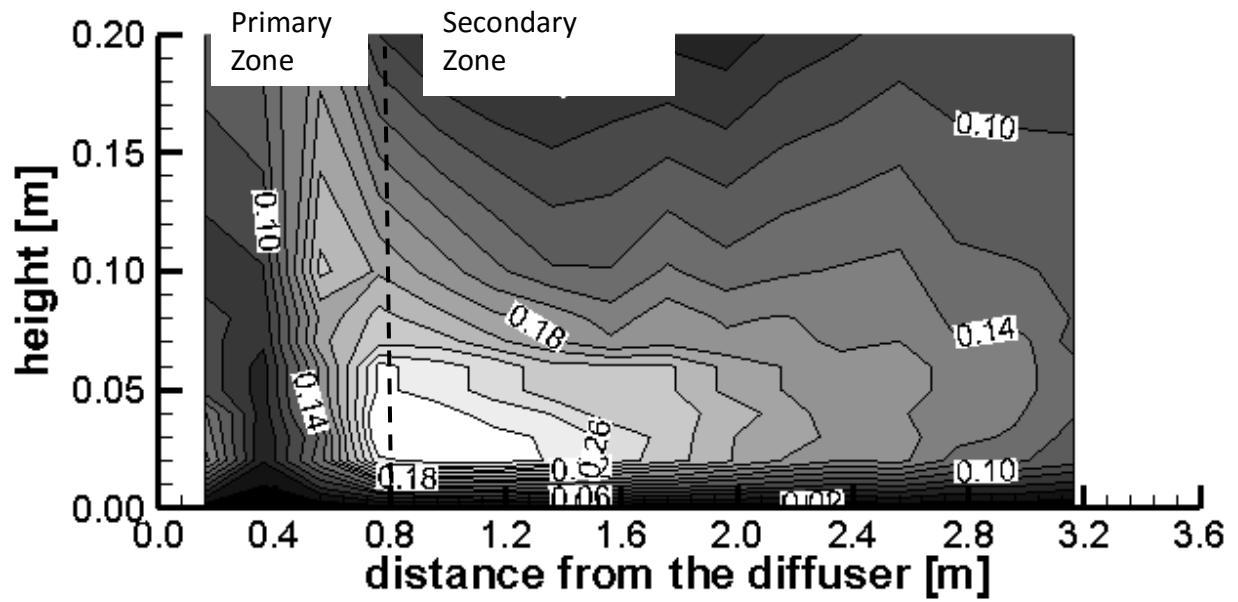


Figure 4-14: Air speed distribution in the vertical longitudinal plane for an under-temperature of 2.5°C (diffuser 1.2 m x 0.6 m)

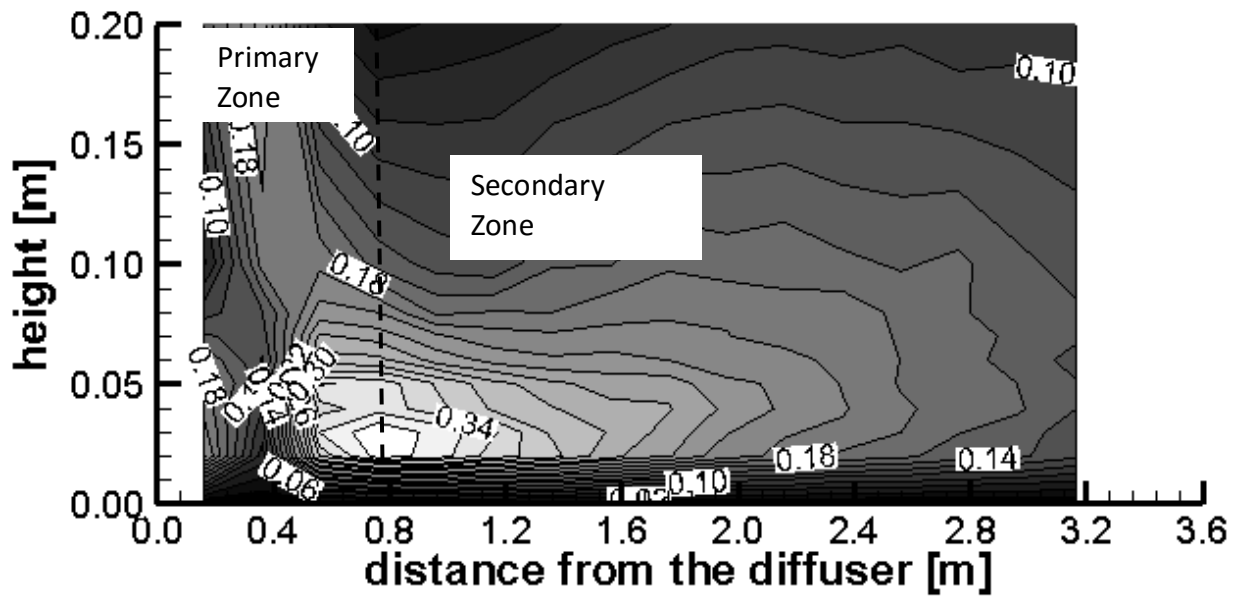


Figure 4-15: Air speed distribution in the vertical longitudinal plane for an under-temperature of 5.5°C (diffuser 1.2 m x 0.6 m)

4.2.2 Temperature distribution in the horizontal plane at 0.05 m from the floor

Figure 4-16 and Figure 4-17 shows the temperature distribution in the horizontal plane at 0.05m from the floor for the two supply conditions studied. As for previous measurement, the air temperature increases as the distance from the diffuser increases, due to heat transfer with the floor and mixing with indoor air. This confirms the fact that the air temperature at floor level varies significantly, and should be taken into account accordingly when assessing local thermal comfort.

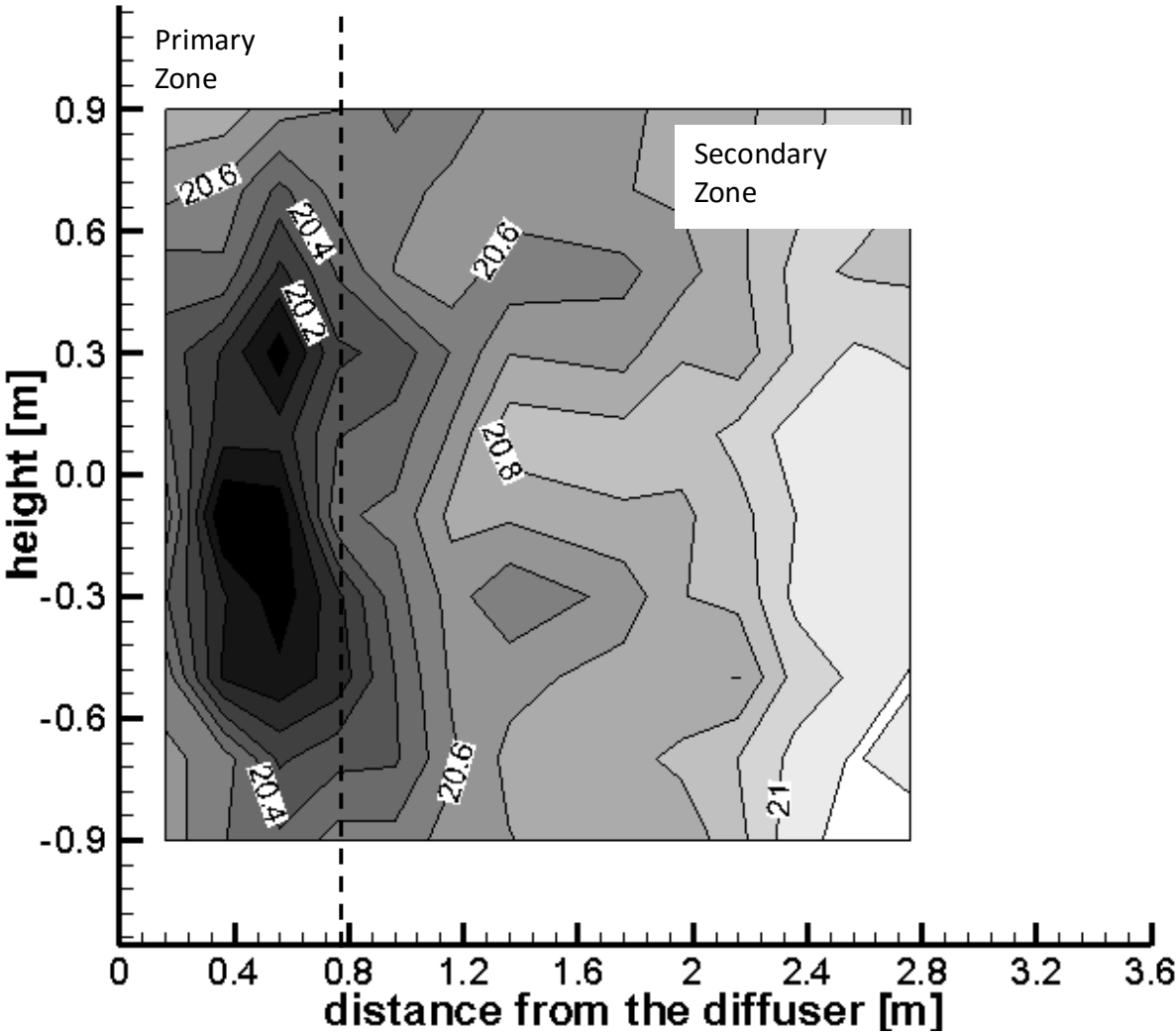


Figure 4-16: Temperature distribution in the horizontal plane at a height of 0.05 m for an under-temperature of 2.5°C (diffuser 1.2 m x 0.6 m)

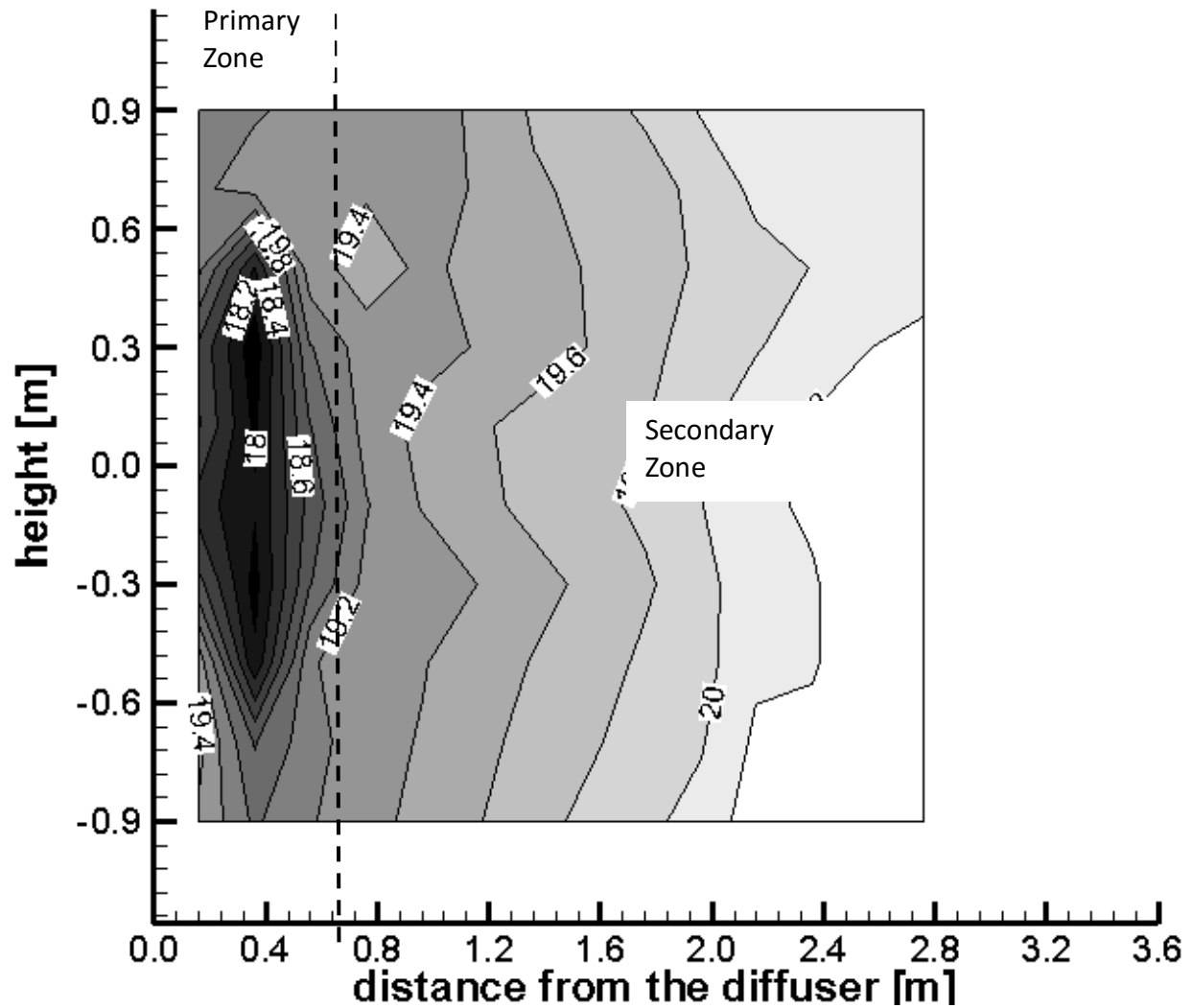


Figure 4-17: Temperature distribution in the horizontal plane at a height of 0.05 m for an under-temperature of 5.5°C (diffuser 1.2 m x 0.6 m)

4.2.3 Comparison of the two diffusers tested

In this thesis, two wall diffusers designed for displacement ventilation were studied: a diffuser DF1W of size 0.6 m x 0.6 m (HxW), and a diffuser DF1W of size 1.2 m x 0.6 m (HxW). Measurements were performed for both diffusers under similar supply conditions (Table 4-2). The variations in temperature and air speed profiles in the experimental data are therefore due to the change of height of the diffuser and the specific air speed profile at the diffuser exit.

Table 4-2: Supply conditions for experimental work for the two diffusers

	Flowrate [m ³ /s]	Under- temperature ΔT_s [°C]	Supply- temperature [°C]	Temperature at a height of 1.1 m [°C]
Diffuser 0.6 m x 0.6 m	0.035	2.4	19.4	21.8
		5.0	16.9	21.9
Diffuser 1.2 m x 0.6 m	0.032	2.5	19.4	21.9
		5.5	16.8	22.3

Figure 4-18 shows the maximum air speed profiles measured in the vertical longitudinal plane for each supply conditions for the two diffusers studied. Figure shows that, for a same supply under-temperature, the maximum air speed reached in the jet is smaller for the largest diffuser than for the smaller one. This result can be explained by the smaller exhaust velocity in the longer diffuser. Figure 4-18 also shows that the length of the primary zone is smaller for the longer diffuser than for the smaller one. For the diffuser and supply conditions tested, the length of the primary zone seems therefore to increase primarily with increasing exhaust air velocity and, to a lower extent, with increasing supply under-temperature.

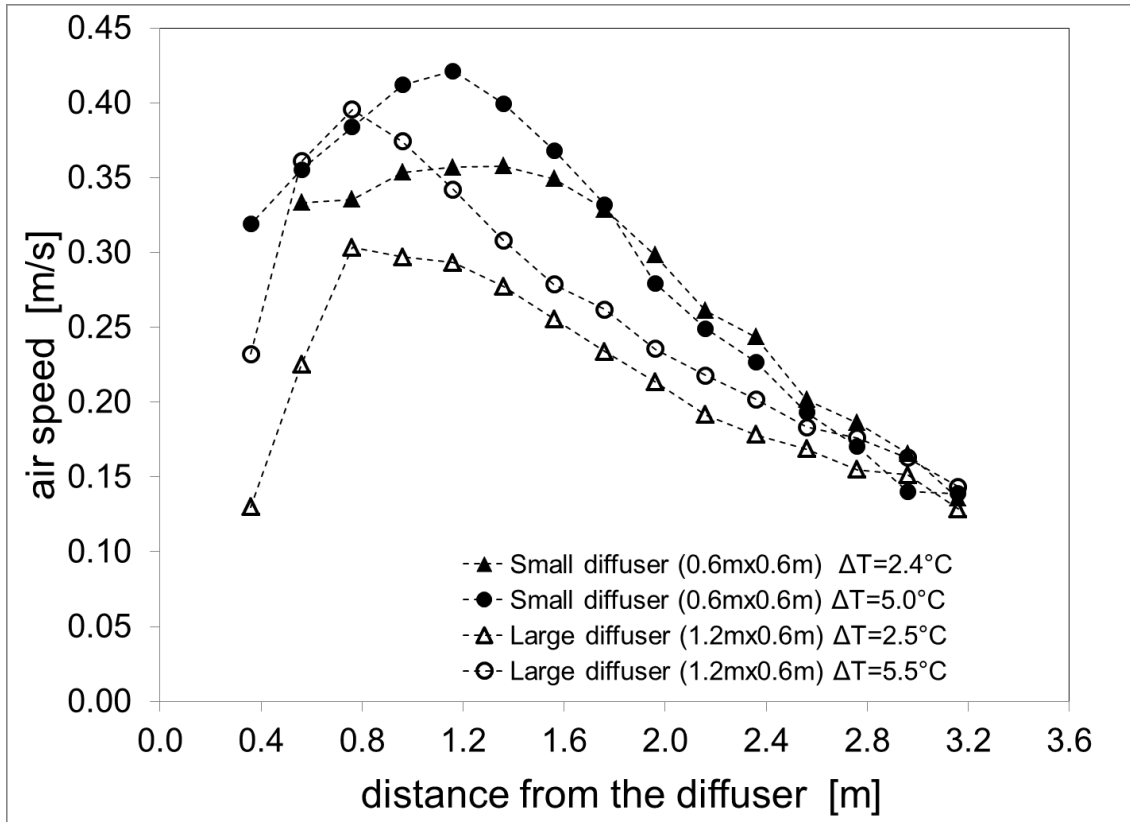


Figure 4-18: Maximum air speed profiles in the vertical longitudinal plane for the two diffusers tested

Figure 4-19 shows the longitudinal profiles of minimum temperature in the jet for each supply condition for the two sizes of diffuser. The temperature profiles show that, for a same supply under-temperature, the air temperature is higher with the longer diffuser than with the smaller one. This result might be explained by more air entrainment in the jet with the longer diffuser, due to its largest surface area and its lower exhaust velocity. More air entrainment is also consistent with the lower air speed noted in Figure 4-18.

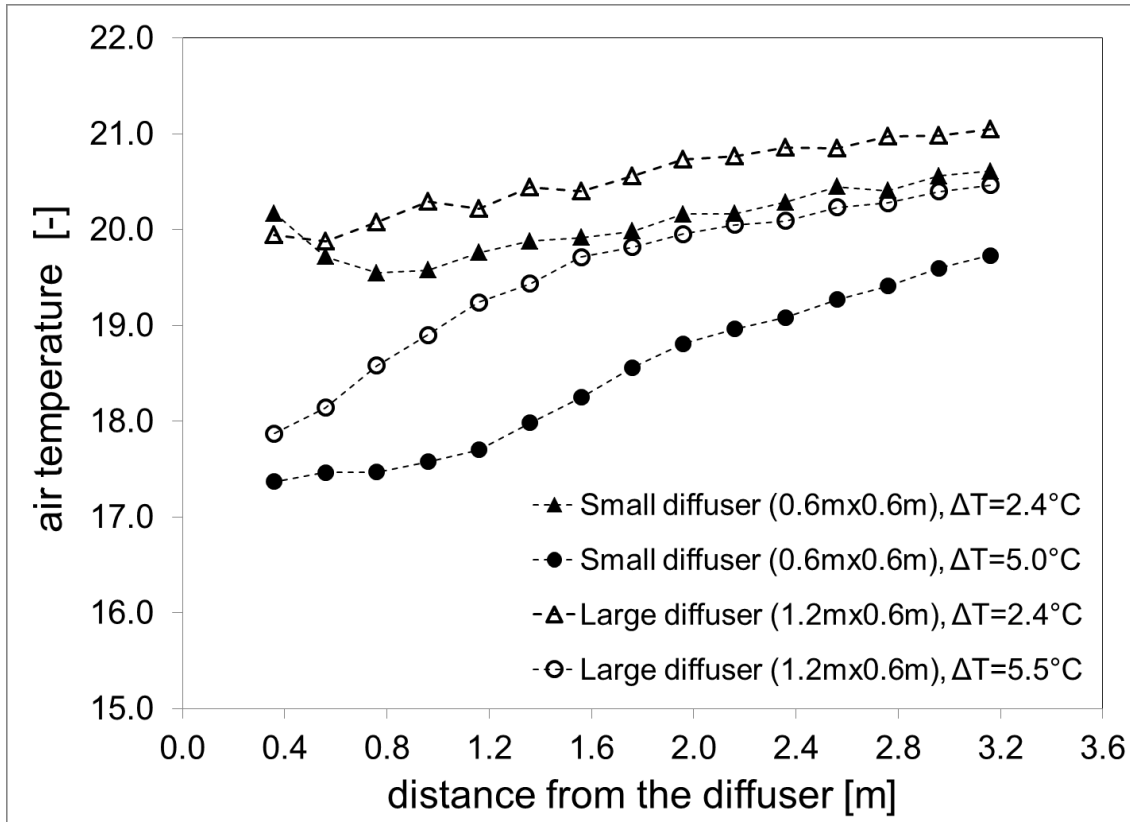


Figure 4-19: Minimum temperature profile in the vertical longitudinal plan for the two diffusers tested (measurement uncertainty of 0.5°C)

Our results indicate that, for the diffusers and supply conditions tested, using a longer diffuser is better in terms of local thermal comfort. Indeed, with the longer diffuser, the maximum air speed in the jet is reduced, leading to lower draft discomfort. The primary zone, where no occupants should be located, is also reduced with the higher diffuser. In addition, using a higher diffuser increases the air temperature in the jet, leading to a lower head-to-ankle temperature difference, hence a better local comfort. The changes of temperature and air speed in the jet are due to higher air entrainment. For the experimental conditions studied, the higher air entrainment did not show any negative effect in terms of temperature stratification.

4.3 Additional measurements on the 0.6 m x 0.6 m diffuser

This section summarizes the results of the series of measurements described in section 3.3, focusing on the effect of different supply under-temperature on the DV jet and on the characteristics of the jet at the end of the primary zone. All the experimental data is tabulated and available in Appendix.

4.3.1 Measurements at 0.05 m in front of the diffuser

Figure 4-20 shows the air speed measured at 0.05 m in front of the diffuser on a vertical axis passing through the center of the diffuser, for the five supply conditions studied. The vertical profile of air speed in Figure 4-20 display the same characteristics as discussed in section 4.1. Figure 4-20 shows that the air speed profile is not significantly affected by the supply under-temperature for the supply conditions tested. This result indicates that the air speed profile at the diffuser exit is not affected by the supply under-temperature, even for the relatively low flow rate used in the measurements ($0.035 \text{ m}^3/\text{s}$).

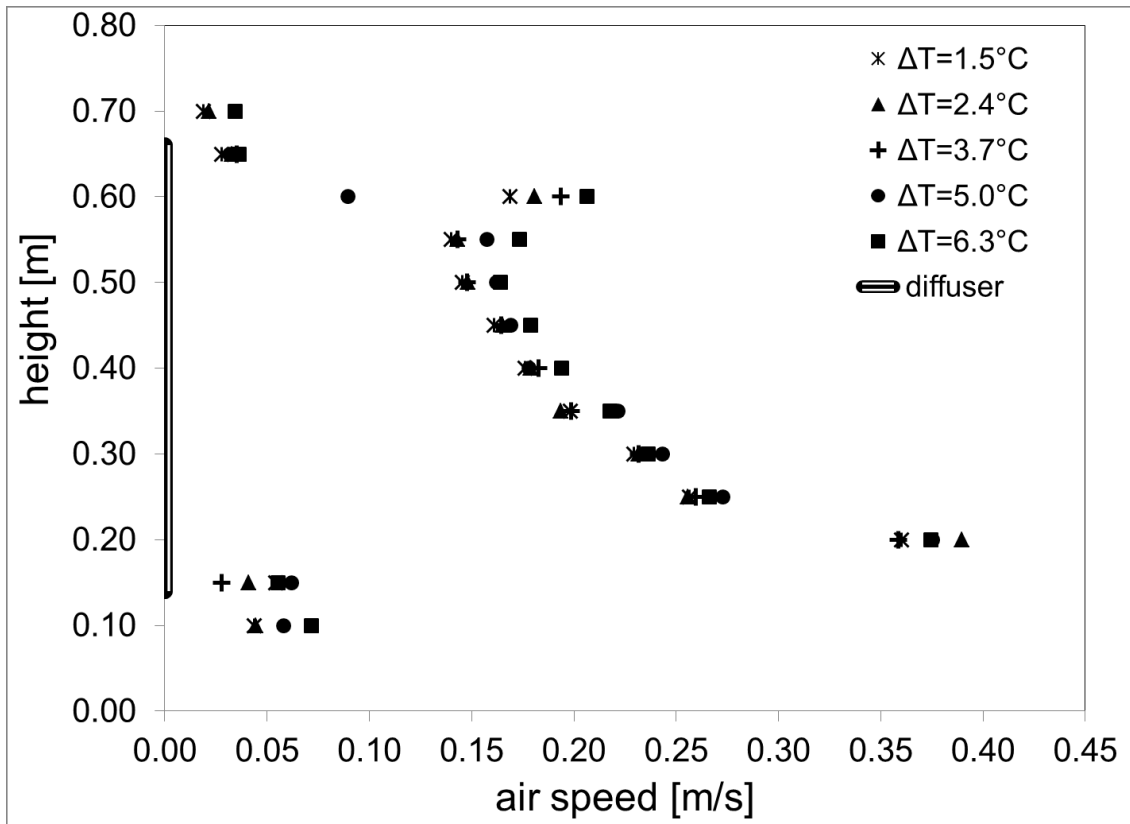


Figure 4-20: Vertical profiles of air speed at 0.05 m in front of the diffuser for the five supply temperatures studied

Figure 4-21 shows the air temperature measured at 0.05 m in front of the diffuser on a vertical axis passing through the center of the diffuser, for the supply conditions studied. The temperature is then normalized according to the supply air temperature and the air temperature in the middle of the room at a height of 1.1 m. Figure 4-22 shows that the profile of normalized temperature in front of the diffuser is not significantly affected by the supply under-temperature for the supply conditions tested. The greater discrepancies appear for low supply under-temperature; these discrepancies are however explained by the experimental measurements error (0.5°C), which becomes significant once normalized.

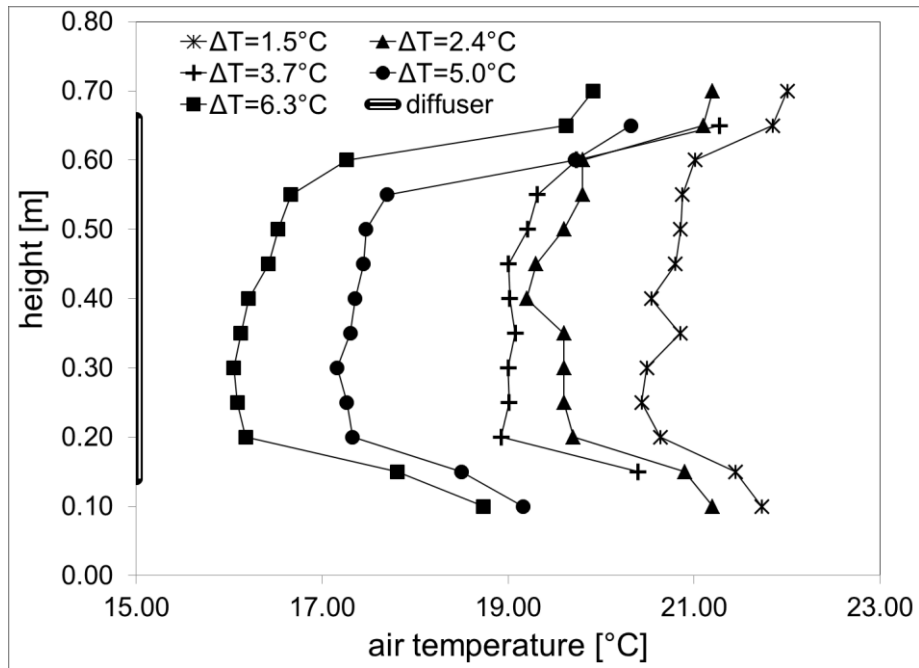


Figure 4-21 : Vertical profiles of air temperature at 0.05 m in front of the diffuser for the five supply temperatures studied

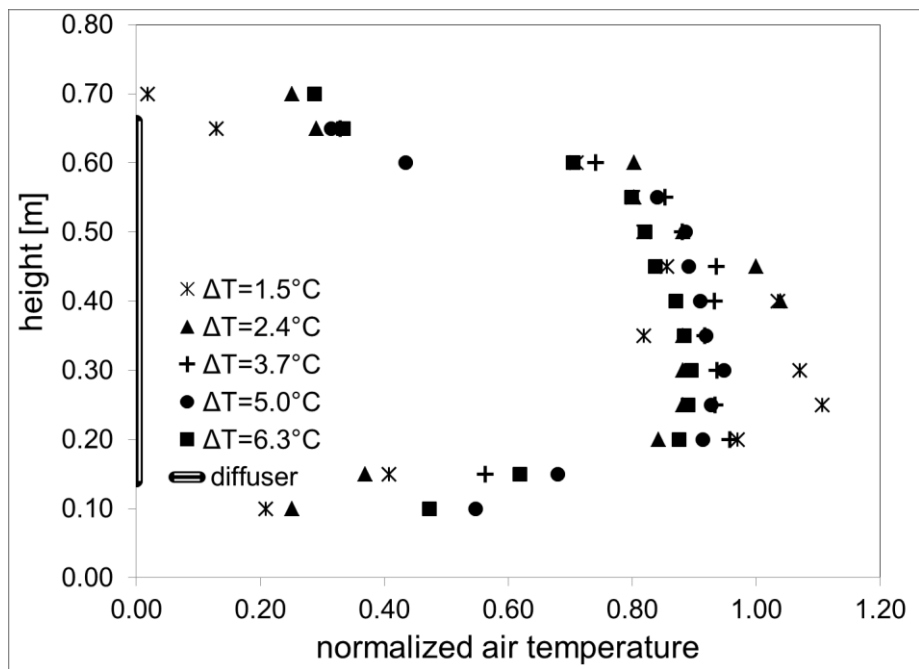


Figure 4-22 : Vertical profiles of normalized air temperature at 0.05 m in front of the diffuser for the five supply temperatures studied

As a conclusion, our results indicate that the vertical profiles of air speed and normalized temperature in front of the diffuser are not significantly affected by the supply under-temperatures for the diffuser and supply flow-rate tested. As the flow rate used in our measurements was relatively low ($0.035 \text{ m}^3/\text{s}$), it is reasonable to assume that, for higher flow rates, the effect of supply temperature would have an even smaller effect, because the ratio of gravity to kinetic forces would be even smaller.

4.3.2 Air speed and temperature profiles in the vertical longitudinal plane

Figure 4-23 shows the profiles of maximum air speed in the vertical longitudinal plane for the supply under-temperatures tested. The general shape of the air speed profile is similar to the one described in section 4.1, with an increase of air speed in the first part of the jet (primary zone) and a decrease of air speed in the second part of the jet. The maximum air speed reached at the end of the primary zone is different for each supply conditions tested, and generally increases with increasing under-temperature. This is explained by the higher buoyancy forces acting on the jet at higher supply under-temperatures.

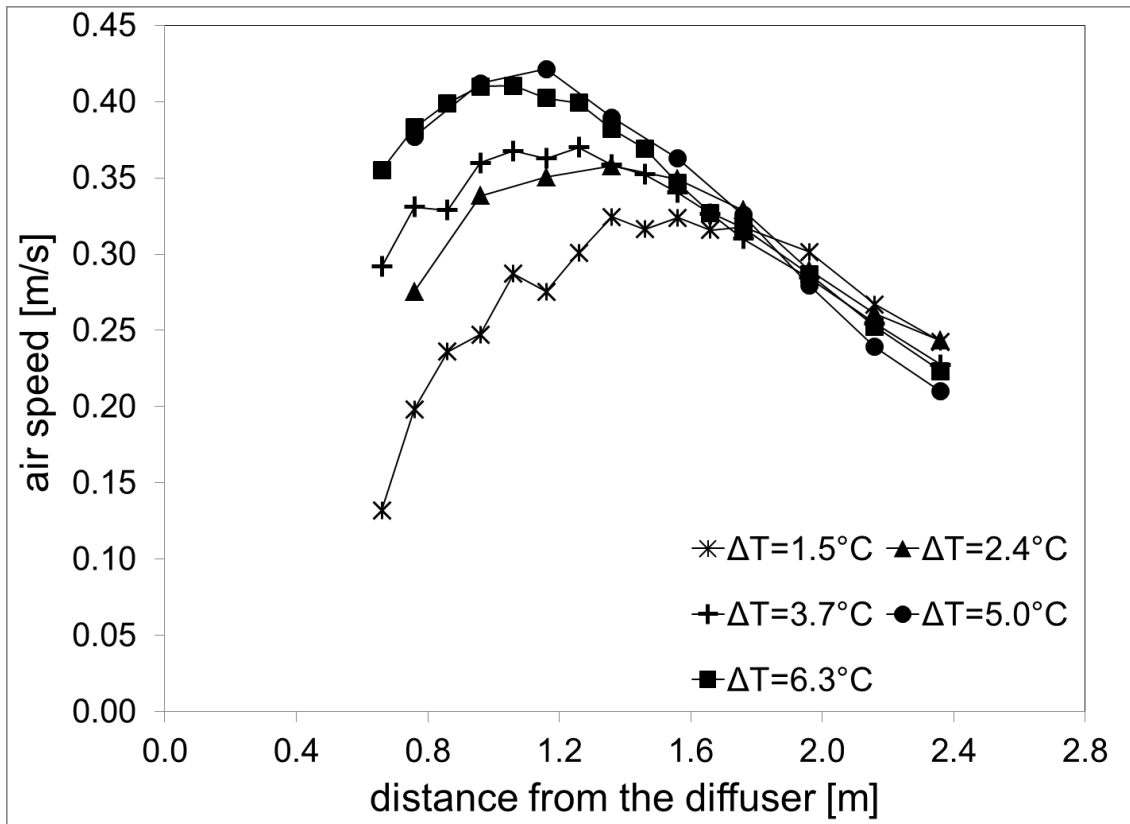


Figure 4-23 : Longitudinal profiles of maximal air speed for the five supply temperatures studied

Figure 4-24 shows the profiles of minimum temperature in the vertical longitudinal plane for the supply under-temperatures tested. The general shape of the air temperature profile is similar to the one described in section 4.1, with the temperature increasing as the distance from the diffuser increases. The extent of the increase is different for each supply temperature, with the air temperature rising significantly for an under-temperature of 6.3°C and the temperature being almost constant for the under-temperature of 1.5°C .

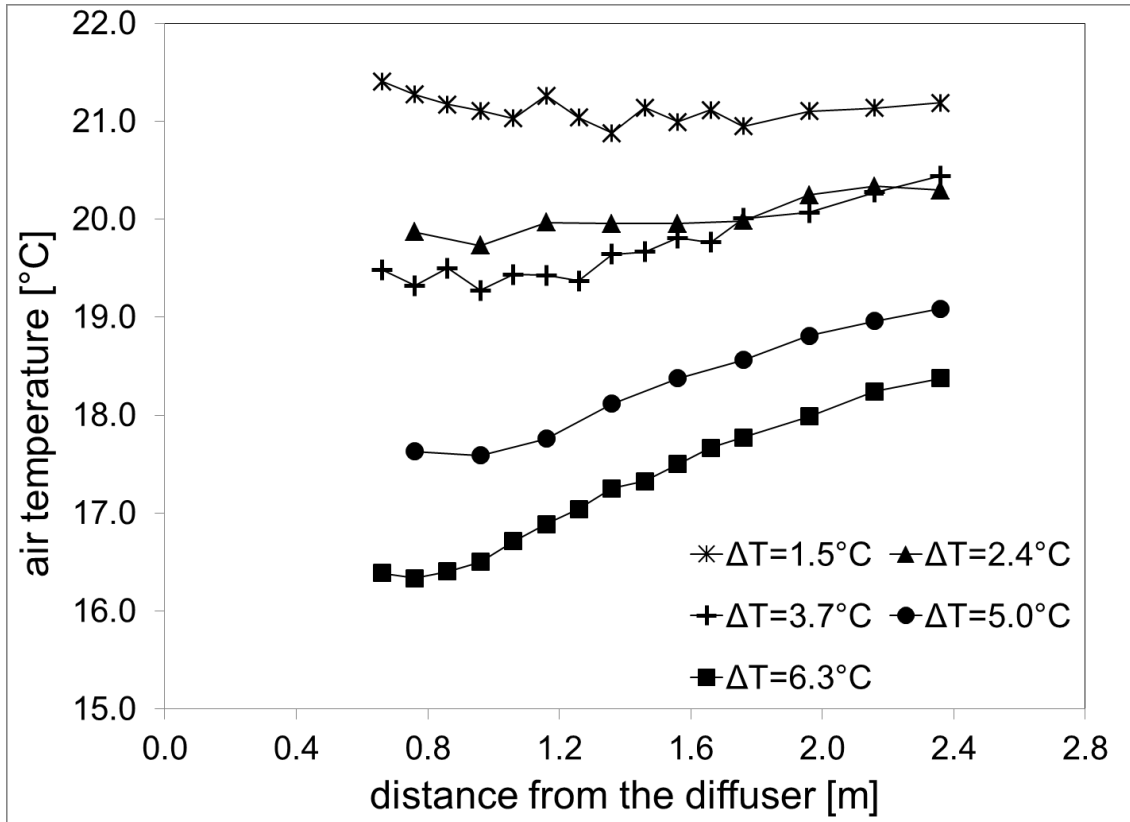


Figure 4-24: Longitudinal profiles of minimal air temperature for the five supply temperatures studied

4.3.4 Characteristics of the DV jet at the end of the primary zone

Thanks to the maximum air speed profile, the length of primary zone was determined. This distance corresponds to the distance from the diffuser at which the air speed reaches its maximum, for each supply condition. The lengths of the primary zone for each supply conditions are summarized in Table 4-3. The length of the primary zone decreases with increasing under-temperature. This result is consistent with previous results in the literature (Etheridge and Sandberg, 1996). The existing models to predict the length of the primary zone (Etheridge and Sandberg, 1996; Nordtest, 2009) were not found applicable for our data.

Table 4-3: Length of primary zone and height of maximum air speed at the end of the primary zone for various supply under-temperatures

	Flow rate [m ³ /s]	Under-temperature ΔT_s [°C]	Estimated length of the primary zone [m]	Height of maximum air speed [m]
Diffuseur 0.6 m x 0.6 m	0.035	1.5	1.46	0.05
		2.4	1.36	0.04
		3.7	1.26	0.04
		5.0	1.16	0.04
		6.3	1.06	0.03

Figure 4-25 shows the vertical profile of air speed at the end of the primary zone for the five supply conditions studied. This figure shows that, at the transition between the primary and secondary zone, the vertical profile of air speed seems to follow the classical wall-jet profile. The height of maximum air speed is slightly different for each supply under-temperature studied. This thickness generally decreases as the supply under-temperature increases. This is most likely due to the stronger buoyancy forces for higher supply under-temperatures.

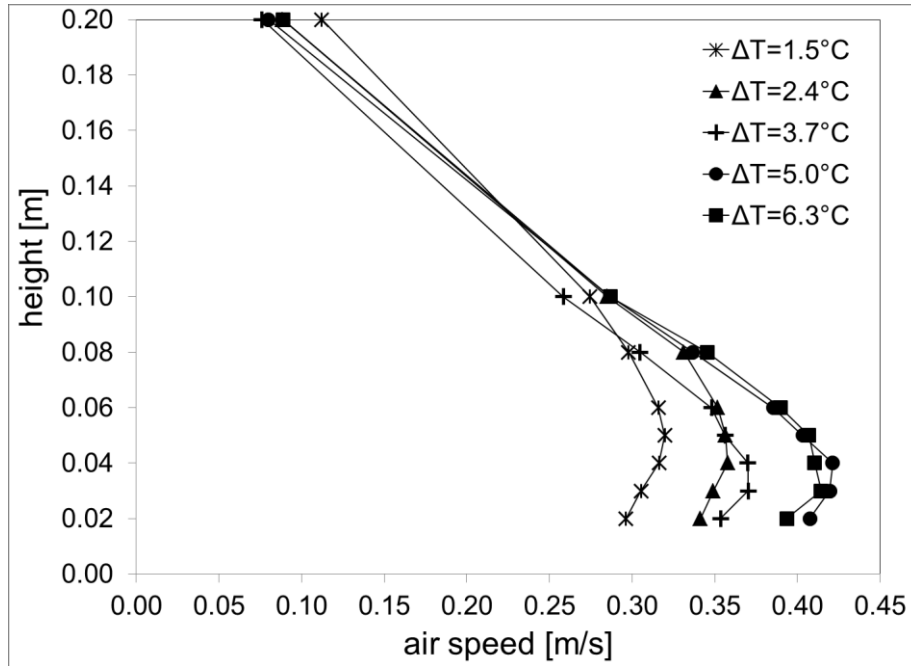


Figure 4-25: Vertical profiles of air speed at the end of primary zone for the five supply temperatures studied

Figure 4-26 and Figure 4-27 show respectively the air speed and air temperature measured at the end of the primary zone, at the height of maximum air speed, for different supply temperatures. Figure 4-26 shows that the spreading of the jet in terms of air speed is mostly similar for the different supply under-temperature. This could indicate that the transversal profile of air speed is primarily influence by the diffuser characteristics. As for air temperature, Figure 4-27 shows that the air temperature profile is more uniform for lower supply under-temperatures.

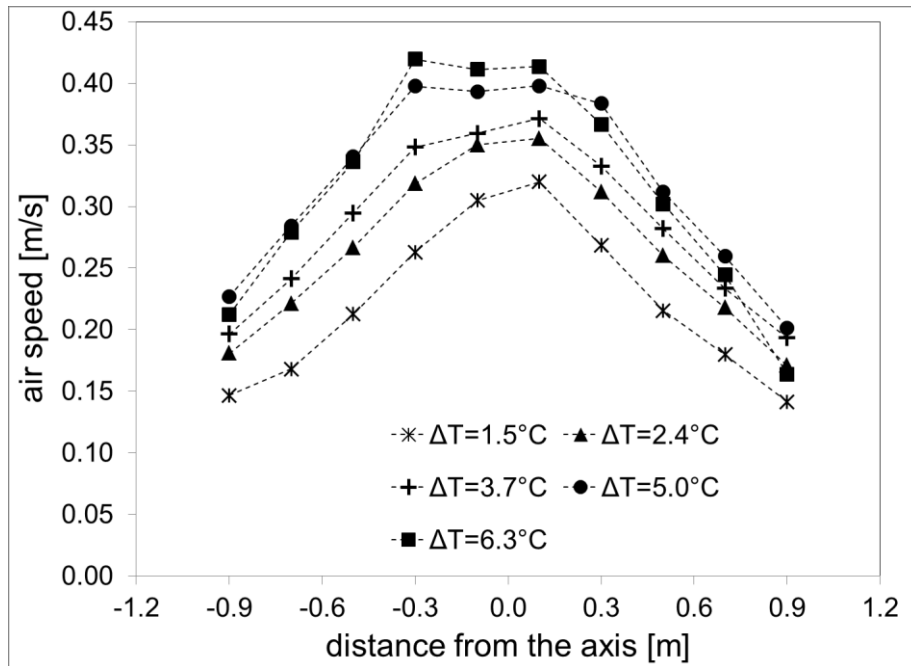


Figure 4-26: Transversal profiles of air speed at the end of primary zone at the height of maximal air speed for the five supply temperatures studied

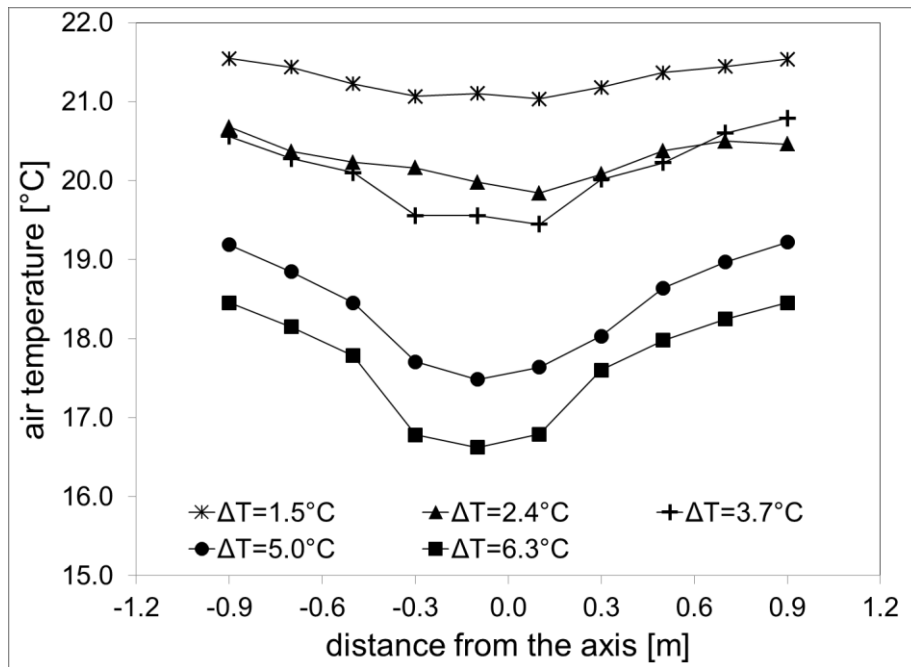


Figure 4-27 : Transversal profiles of air temperature at the end of primary zone at the height of maximal air speed for the five supply temperatures studied

4.4 Summary

This chapter presented the experimental results of measurements performed on a very fine mesh in the DV jet, covering the longitudinal, transversal, and vertical directions. These measurements were performed on two diffusers, for several under-temperatures. The conclusions of these measurements can be summarized as follows:

Regarding the variation of air speed in the DV jet:

- Measurements confirm the clear separation of the jet between a primary zone and a secondary zone
- The air speed varies significantly with the distance from the diffuser, and also varies with the distance from the longitudinal axis and with height.

Regarding the variation of air temperature in the DV jet:

- The air temperature varies significantly in the DV jet, and cannot be represented with a single value as suggested by previous studies.
- In the secondary zone, the air temperature varies primarily with the distance from the diffuser, and to a lesser extent with the distance from the longitudinal axis and with height.

Regarding the air distribution at the diffuser exit:

- Both the air speed and temperature vary significantly over the diffuser area. These variations appear to be important enough to be considered in further models.

- Some vortices seem to appear under the diffuser studied. Proper representation of these vortices might be important in Computational Fluids Dynamics (CFD) modeling of a DV jet.

Regarding the transition between the primary zone and the secondary zone:

- The transition between the primary zone and the secondary zone occurs at different distances from the diffuser for each diffuser and supply condition studied
- The maximal air speed reached at the end of the primary zone is different for each diffuser and supply condition studied
- The height at which the maximal air speed is reached is different for each supply condition studied

The next chapter focuses on further analysis of the experimental results using appropriate normalizations, and on the development of models to represent the variations of air speed and temperature in the DV jet.

CHAPTER 5: DATA ANALYSIS AND CORRELATIONS

This chapter presents the analysis of the experimental data and the models developed. After an analysis using existing models in the literature (section 5.1), a new correlation-based model is presented for the air speed decay in a DV jet. This model is elaborated as a two-step process, first studying the primary zone (section 5.2), then focusing on the secondary zone (5.3). In the second part of this chapter, the air speed in the jet is studied according to its variation in the vertical and transversal planes (section 5.5 and 5.7). A deep study of the variation of the jet thickness is also proposed (section 5.6). Finally, the variations of air temperature in the jet are studied (section 5.8).

5.1 Analysis of existing models for air speed decay in a DV jet

Several models exist in the literature to represent the air speed decay in a DV jet. This section discusses these models and how they perform with the experimental data.

Nielsen's model

Nielsen's model (Nielsen, 1991) represents the air speed decay using a single correlation parameter K_N , as described in Equation 2-2. In this section, this model was applied with the maximum air speed measured on the longitudinal axis, in the secondary zone, for each supply condition tested for the diffuser DF1W of size 0.6 m x 0.6 m (see Chapter 4, section 3). Table 5-1

shows the coefficient of determination R^2 , computed to minimize the sum of squared error between the measured and correlated air speeds. Table 5-1 summarizes the results for each supply condition tested.

Table 5-1: K_N coefficient for various supply under-temperatures

Under-temperature ΔT_s [°C]	K_N	R^2
1.5	7.1	0.67
2.4	6.8	0.77
3.7	6.7	0.83
5.0	6.8	0.93
6.3	6.7	0.76

The K_N constants have values between 6.7 and 7.1 for the test conditions. Table 5-1 shows that the accuracy of Nielsen’s model is generally acceptable, with R^2 values higher ranging from 0.67 to 0.93. The accuracy gets lower as the under-temperature decreases. The literature mentions that the correlation coefficients are dependent on supply conditions. In this study, the coefficients however seem mostly independent of the supply under-temperature. Figure 5-1 shows the experimental data for the under-temperature of 2.4°C, as well as the correlation from Nielsen’s model. This figure shows that Nielsen’s model has difficulties capturing the air speed decay as the distance from the diffuser increases. The same effect is observed for the other supply temperatures tested.

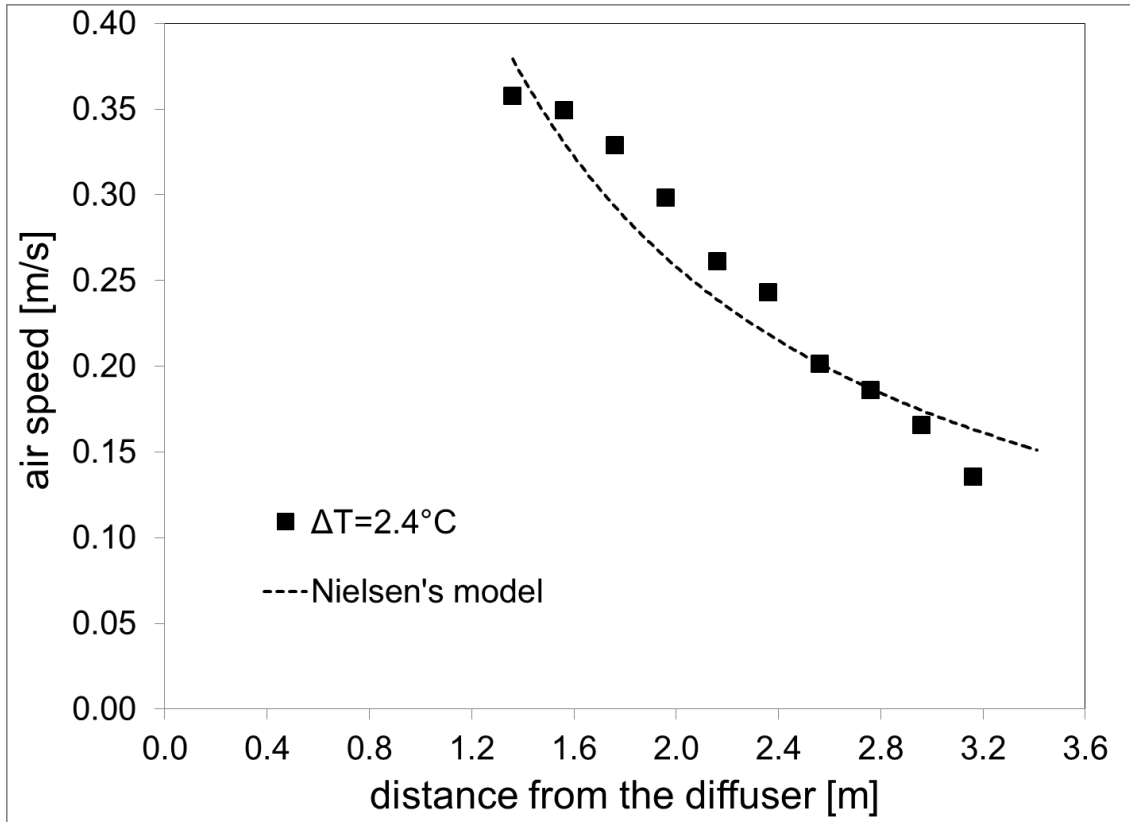


Figure 5-1: Measured and correlated air speed decay for an under-temperature of 2.4°C

Nordtest model

A more recent model for the air speed decay in a DV jet is the model mentioned in Nordtest VVS 083 (Nordtest, 2009). This model uses three correlation coefficients, as described in Equation 5-1. The particularity of this model is that the coefficients are independent of supply conditions.

$$V(X) = k_1 \cdot Ar_N^{k_2} \cdot B_f \cdot \left(\frac{X}{L}\right)^{k_3} \quad \text{Equation 5-1}$$

where:

- $V(X)$ is the maximum air speed at a distance X from the diffuser from the longitudinal axis [m/s];
- Ar_N is the Archimedes number as defined in Nordtest (2009) [-];
- B_f is the buoyancy flux defined in Nordtest (2009) [m/s];
- L is the horizontal perimeter of the diffuser [m], and;
- k_1 , k_2 and k_3 are experimentally determined coefficients.

For this analysis, the air speed data on the longitudinal axis for the five supply conditions on diffuser DF1W (0.6 m x 0.6 m) were combined. Equation 5-1 was then applied, with the correlation coefficients (k_1 , k_2 , k_3) found through an iterative process to maximize the coefficient of determination R^2 . The final equation including the optimal correlation coefficients is displayed in Equation 5-2.

$$V(X) = 14.9 \cdot Ar_N^{-0.35} \cdot B_f \cdot \left(\frac{X}{L}\right)^{-0.95} \quad \text{Equation 5-2}$$

The Nordtest model performs very well with our experimental data, with an overall coefficient R^2 of 0.91. The agreement between measured and correlated data is good, as shown in Figure 5-2. However, this model uses 3 different correlation coefficients, which makes it quite complex. Also, the physical meaning of those correlation coefficients is unclear. For instance, in this case, the air speed in the jet is inversely correlated with the Archimedes term (exponent -0.35), which seems opposite to the physical sense. An increased Archimedes number means increased buoyancy forces, which should increase the air speed; the exponent should therefore be positive. It is unclear if this negative exponent is due to overfitting or is representative of a deeper physical phenomenon.

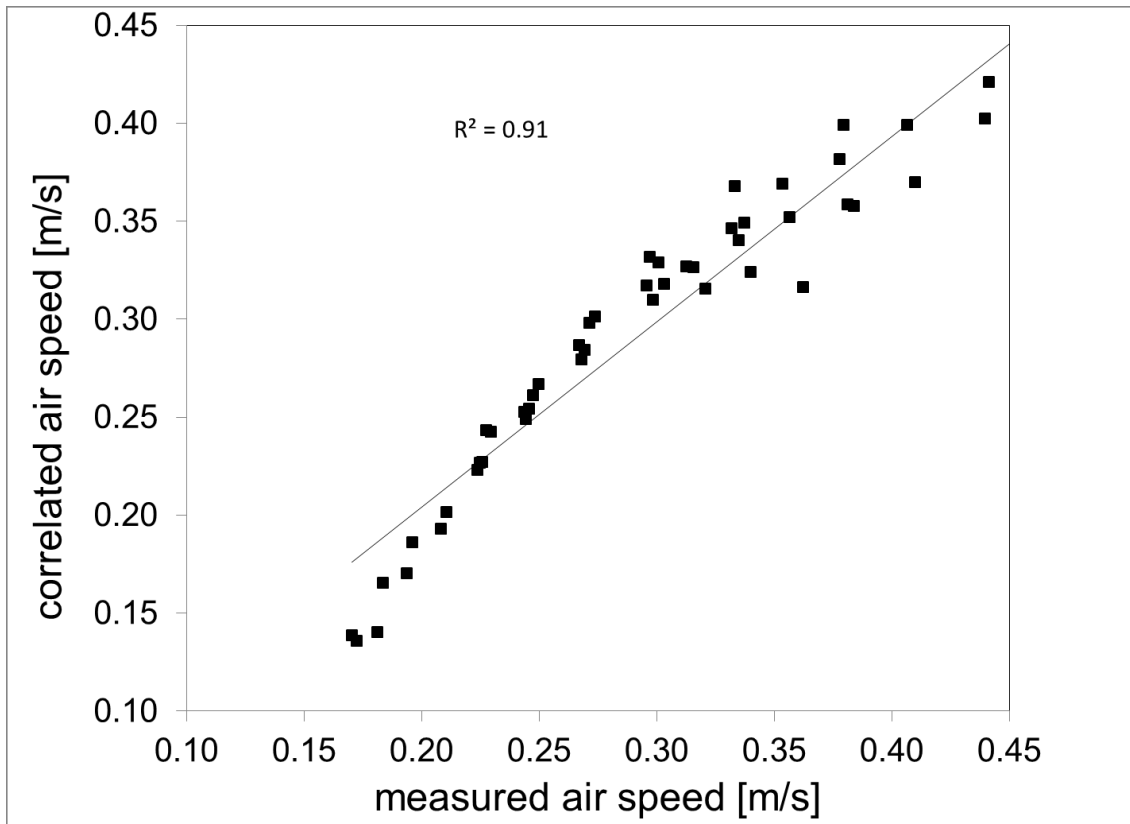


Figure 5-2: Measured versus correlated air speed for the Nordtest model for the five supply conditions tested

Conclusion

As a conclusion of this section, the models available in the literature are somewhat limited in correlating the air speed decay in a DV jet. Nielsen's model is simple, but its accuracy is sometimes low and the coefficients are generally dependent on a specific case. The Nordtest model is a significant improvement as it is applicable for several supply conditions simultaneously, but this model relies on 3 different correlation parameters, which makes it complex to use or to interpret the physical meaning of those coefficients. A further limitation of existing models is that they focus only on the secondary zone of the DV jet. The primary and secondary zones of a DV jet are however two very different physical phenomena, which deserve

each a specific analysis. In order to study the air speed distribution in a DV jet, the author therefore proposes a new methodology, separating the analysis of the DV jet into its two distinct zones, to follow the physical phenomenon of the jet.

5.2 Determination of the maximal air speed at the end of the primary zone

In the analysis performed in this section, only the terminal maximum air speed at the end of the primary zone is studied. Determining the precise variations of velocity in the primary zone is indeed of little value for designers, as no occupants should be placed in this zone given that the high air speeds and low temperatures in this zone are generally deemed unsuitable for comfort (Skistad et al. 2002). The maximum air speed at the end of the primary zone, however, is important both in terms of comfort and in the analysis of the secondary zone. In this section, the analysis focuses on the terminal maximal air speed, neglecting voluntarily the analysis of complex phenomena occurring between the diffuser and the end of the zone. In order to do so, three parts are presented: 1) the development of a mathematical model of the jet assuming no air entrainment, 2) a correction of the mathematical model to account for air entrainment, and 3) the validation of the mathematical model using experimental data.

5.2.1 Determination of the maximal air speed in a DV jet without air entrainment

In order to determine the maximal air speed at the end of the primary zone, the principle of conservation of energy is applied on the primary zone of the DV jet. In this study, the principle of conservation of energy is applied between 0.05 m from the diffuser (diffuser exit) and the end of primary zone (Figure 5-3). Starting the analysis at 0.05 m from the diffuser ensures that the specific air speed distribution from the diffuser is taken into account.

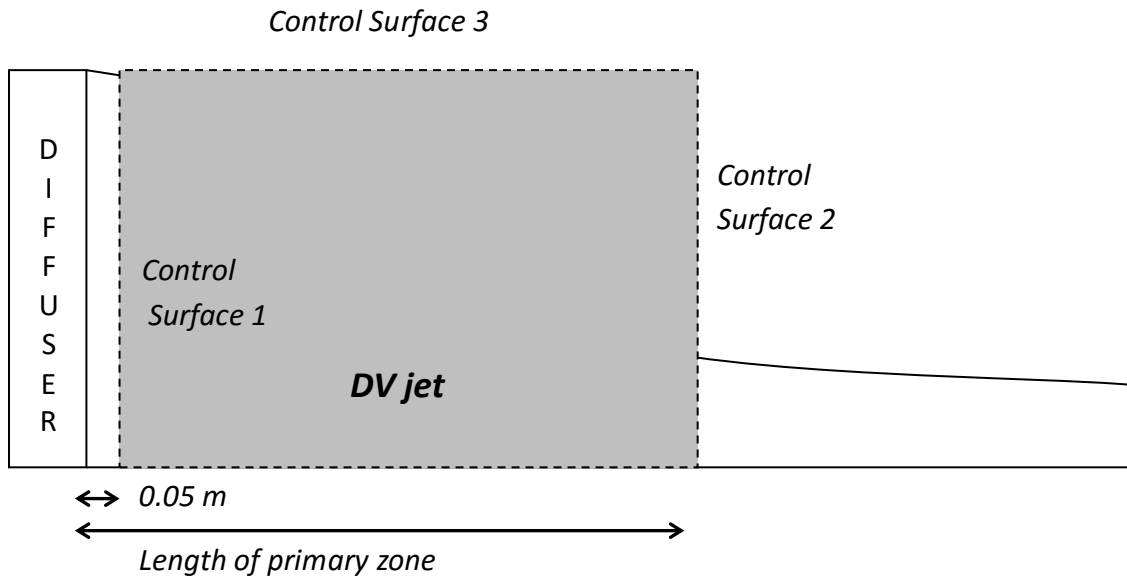


Figure 5-3: Control volume and control surfaces in the primary zone

Conservation of energy in the primary zone

The principle of conservation of energy states the sum of kinetic, potential, and internal energy should be conserved throughout the primary zone. In this thesis, the potential energy will refer to the *apparent* potential energy, caused by the buoyancy forces acting on the jet. Since no entrainment is considered, and since the heat transfer between the jet and the floor is neglected, the internal energy of the jet can be considered as constant. Only the kinetic and potential energies are then of interest in analyzing the jet, as pointed out by Sandberg and Blomqvist (1989). The conservation of energy in the primary zone can therefore be written as follows:

$$K_{0.05} + Ep_{0.05} = K_{EPZ} + Ep_{EPZ} \quad \text{Equation 5-3}$$

Where:

- $K_{0.05}$ is the rate of kinetic energy flowing through the control surface at 0.05 m from the diffuser [$\text{kg}\cdot\text{m}^2/\text{s}^3$];
- $Ep_{0.05}$ is the rate of potential energy flowing through the control surface at 0.05 m from the diffuser [$\text{kg}\cdot\text{m}^2/\text{s}^3$];
- K_{EPZ} is the rate of kinetic energy flowing through the control surface at the end of the primary zone [$\text{kg}\cdot\text{m}^2/\text{s}^3$], and;
- Ep_{EPZ} is the rate of potential energy flowing through the control surface at the end of the primary zone [$\text{kg}\cdot\text{m}^2/\text{s}^3$].

Kinetic and potential energies at 0.05 m from the diffuser

The kinetic and potential energy in the DV jet at 0.05 m from the diffuser can be determined from measured data. They can be expressed as shown in Equation 5-4 and Equation 5-5. All the variables in this equation can be measured and finally tabulated in the manufacturer's catalogue.

$$K_{0.05} = \frac{1}{2} \cdot \iint_{diffuser} \rho \cdot (V_{0.05}(Z))^3 \cdot dY \cdot dZ \quad \text{Equation 5-4}$$

$$Ep_{0.05} = \iint_{diffuser} \rho \cdot \frac{g \cdot (T_{room} - T_{0.05}(Z))}{T_{room}} \cdot Z \cdot V_{0.05}(Z) \cdot dY \cdot dZ \quad \text{Equation 5-5}$$

Where:

- $V_{0.05}$ is the velocity in the jet at 0.05 m from the diffuser at a distance Y from the longitudinal axis and at a height Z [m/s];
- Y is the distance from the longitudinal axis [m];
- Z is the height from the floor [m];
- g is the acceleration of gravity [m/s^2];
- T_{room} is the room temperature, taken as the temperature measured in the middle of the room at a height of 1.1 m [K], and;
- $T_{0.05}$ is the air temperature in the jet at 0.05 m from the diffuser at a distance Y from the longitudinal axis and at a height Z [K].

Rearranging the equations, and introducing the variables $V_{0.05\ avg}^2$ and $[g'Z]_{0.05\ avg}$, Equation 5-4 and Equation 5-5 can be rewritten as Equation 5-6 and Equation 5-7. These notations are used to simplify the further readability. In this analysis, it is assumed that the air speed does not vary significantly over the width of the diffuser, and that the variations in air density are negligible.

$$K_{0.05} = \frac{1}{2} \cdot \dot{m}_{0.05} \cdot V_{0.05\ avg}^2 \quad \text{Equation 5-6}$$

$$Ep_{0.05} = \dot{m}_{0.05} \cdot Ep_{0.05\ avg} \quad \text{Equation 5-7}$$

Where:

- $\dot{m}_{0.05}$ is the mass flow rate in the DV jet at 0.05 m from the diffuser [m^3/s];

- $V_{0.05 \text{ wavg}}^2$ is a weighted average of the square air speed at 0.05 m from the diffuser [m²/s²], calculated as $V_{0.05 \text{ wavg}}^2 = \frac{1}{H_{diff} \cdot \bar{V}_{0.05}} \cdot \int_{H_{diff}} (V_{0.05}(Z))^3 \cdot dZ$ and;
- $Ep_{0.05 \text{ wavg}}$ is a weighted average of the potential energy per kg/s at 0.05 m from the diffuser [m²/s²], calculated as $[g' \cdot Z]_{0.05 \text{ wavg}} = \frac{1}{H_{diff} \cdot \bar{V}_{0.05}} \cdot \int_{H_{diff}} \frac{g \cdot (T_{room} - T_{0.05}(Z))}{T_{room}} \cdot Z \cdot V_{0.05}(Z) \cdot dZ$

Kinetic and potential energies of the DV jet at the end of the primary zone

The kinetic and potential energies at the end of the primary zone can be calculated from the air speed distribution in the jet at that point. Experimental data from this study (see Chapter 3) show that, at the end of the primary zone, the air speed in the jet follows a wall-jet-like vertical profile (Equation 5-9) and a Gaussian transversal profile (Equation 5-10). This result is in agreement with previous research (Skistad et al. 2002). The air speed at the end of the primary zone can then be written as:

$$V(X_{EPZ}, Y, Z) = f\left(\frac{Z}{\delta_{EPZ}}\right) \cdot g\left(\frac{Y}{b_{EPZ}}\right) \cdot \max_{Y,Z} V(X_{EPZ}, Y, Z) \quad \text{Equation 5-8}$$

Where the wall-jet profile function f is defined as (Rajaratnam, 1976):

$$f\left(\frac{Z}{\delta_{EPZ}}\right) = 1.48 \cdot \left(\frac{Z}{\delta_{EPZ}}\right)^{\frac{1}{7}} \cdot \left[1 - \text{erf}\left(0.68 \cdot \left(\frac{Z}{\delta_{EPZ}}\right)\right)\right] \quad \text{Equation 5-9}$$

And where the Gaussian transversal profile function g is defined as:

$$g\left(\frac{Y}{b_{EPZ}}\right) = \exp\left(-\left(\frac{Y}{b_{EPZ}}\right)^2\right) \quad \text{Equation 5-10}$$

Using Equation 5-8, the kinetic energy at the end of the primary zone (Equation 5-11) can be computed. Equation 5-11 is rearranged and numerically integrated as shown in Equation 5-12 to Equation 5-19. The kinetic energy at the end of the primary zone, assuming no entrainment, can then be expressed as Equation 5-20.

$$K_{EPZ} = \iiint \frac{V^2}{2} \rho V \cdot n dA \quad \text{Equation 5-11}$$

$$K_{EPZ} = \rho_{EPZ} \cdot \int_{Y=-\infty}^{Y=+\infty} \int_{Z=0}^{Z=\delta_{EPZ}} \frac{V_{EPZ}(Y,Z)^3}{2} \cdot dZ \cdot dY \quad \text{Equation 5-12}$$

$$K_{EPZ} = \frac{\rho_{EPZ}}{2} \cdot \int_{Y=-\infty}^{Y=+\infty} \int_{Z=0}^{Z=\delta_{EPZ}} V_{\max EPZ}^3 \cdot \left(f\left(\frac{Z}{\delta_{EPZ}}\right) \right)^3 \left(g\left(\frac{Y}{b_{EPZ}}\right) \right)^3 \cdot dZ \cdot dY \quad \text{Equation 5-13}$$

$$K_{EPZ} = \frac{\rho_{EPZ}}{2} \cdot V_{\max EPZ}^3 \cdot \delta_{EPZ} \cdot b_{EPZ} \cdot \int_{Y=-\infty}^{Y=+\infty} \int_{Z=0}^{Z=\delta_{EPZ}} \left(f\left(\frac{Z}{\delta_{EPZ}}\right) \right)^3 \left(g\left(\frac{Y}{b_{EPZ}}\right) \right)^3 \cdot d\frac{Z}{\delta_{EPZ}} \cdot d\frac{Y}{b_{EPZ}} \quad \text{Equation 5-14}$$

In order to simplify Equation 5-14, we need to introduce the mass flow-rate (Equation 5-15). After rearrangement (Equation 5-16) and numerical integration, Equation 5-15 leads to Equation 5-17.

$$\dot{m}_{EPZ} = \rho_{EPZ} \cdot \int_{Y=-\infty}^{Y=+\infty} \int_{Z=0}^{Z=\delta_{EPZ}} V_{\max EPZ} \cdot f\left(\frac{Z}{\delta_{EPZ}}\right) \cdot g\left(\frac{Y}{b_{EPZ}}\right) \cdot dZ \cdot dY \quad \text{Equation 5-15}$$

$$\begin{aligned} \dot{m}_{EPZ} &= \rho_{EPZ} \cdot V_{\max EPZ} \cdot \delta_{EPZ} \cdot b_{EPZ} \\ &\cdot \int_{Y=-\infty}^{Y=+\infty} \int_{Z=0}^{Z=\delta_{EPZ}} f\left(\frac{Z}{\delta_{EPZ}}\right) \cdot g\left(\frac{Y}{b_{EPZ}}\right) \cdot d\frac{Z}{\delta_{EPZ}} \cdot d\frac{Y}{b_{EPZ}} \end{aligned} \quad \text{Equation 5-16}$$

$$\dot{m}_{EPZ} = 1.380 \cdot \rho_{EPZ} \cdot V_{\max EPZ} \cdot \delta_{EPZ} \cdot b_{EPZ} \quad \text{Equation 5-17}$$

Rearranging Equation 5-14 with help of Equation 5-17, we get:

$$\begin{aligned} K_{EPZ} &= \frac{1}{2 \cdot 1.380} \cdot \dot{m}_{EPZ} \cdot V_{\max EPZ}^2 \cdot \int_{Y=-\infty}^{Y=+\infty} \left(g\left(\frac{Y}{b_{EPZ}}\right)\right)^3 \cdot d\frac{Y}{b_{EPZ}} \\ &\cdot \int_{Z=0}^{Z=\delta_{EPZ}} \left(f\left(\frac{Z}{\delta_{EPZ}}\right)\right)^3 \cdot d\frac{Z}{\delta_{EPZ}} \end{aligned} \quad \text{Equation 5-18}$$

Numerical integrations lead to:

$$K_{EPZ} = \frac{1}{2 \cdot 1.380} \cdot 1.023 \cdot 0.578 \cdot \dot{m}_{EPZ} \cdot V_{\max EPZ}^2 \quad \text{Equation 5-19}$$

$$K_{EPZ} = 0.429 \cdot \dot{m}_{EPZ} \cdot \frac{V_{\max EPZ}^2}{2} \quad \text{Equation 5-20}$$

The potential energy in the jet at the end of the primary zone (Equation 5-21) can also be computed using Equation 5-8. Equation 5-21 is rearranged and numerically integrated as shown in Equation 5-22 to Equation 5-25. After numerical integration and rearranging, the potential energy at the end of the primary zone can be expressed as Equation 5-26.

$$E_{p_{EPZ}} = \iiint \rho \cdot g' \cdot Z \cdot V \cdot ndA \quad \text{Equation 5-21}$$

$$E_{p_{EPZ}} = \rho_{EPZ} \cdot g' \cdot \int_{Y=-\infty}^{Y=+\infty} \int_{Z=0}^{Z=\delta_{EPZ}} V_{\max EPZ} \cdot f\left(\frac{Z}{\delta_{EPZ}}\right) \cdot g\left(\frac{Y}{b_{EPZ}}\right) \cdot Z \cdot dZ \cdot dY \quad \text{Equation 5-22}$$

$$E_{p_{EPZ}} = g' \cdot \rho_{EPZ} \cdot V_{\max EPZ} \cdot \delta_{EPZ}^2 \cdot b_{EPZ} \cdot \int_{Y=-\infty}^{Y=+\infty} g\left(\frac{Y}{b_{EPZ}}\right) \cdot d\frac{Y}{b_{EPZ}} \cdot \int_{Z=0}^{Z=\delta_{EPZ}} f\left(\frac{Z}{\delta_{EPZ}}\right) \cdot \frac{Z}{\delta_{EPZ}} \cdot d\frac{Z}{\delta_{EPZ}} \quad \text{Equation 5-23}$$

Using Equation 5-17, we get:

$$E_{p_{EPZ}} = \frac{1}{1.380} \cdot \dot{m}_{EPZ} \cdot g' \cdot \delta_{EPZ} \cdot \int_{Y=-\infty}^{Y=+\infty} g\left(\frac{Y}{b_{EPZ}}\right) \cdot d\frac{Y}{b_{EPZ}} \cdot \int_{Z=0}^{Z=\delta_{EPZ}} f\left(\frac{Z}{\delta_{EPZ}}\right) \cdot \frac{Z}{\delta_{EPZ}} \cdot d\frac{Z}{\delta_{EPZ}} \quad \text{Equation 5-24}$$

Numerical calculations lead to:

$$Ep_{EPZ} = \frac{1}{1.380} \cdot 1.716 \cdot 0.360 \cdot \dot{m}_{EPZ} \cdot g' \cdot \delta_{EPZ} \quad \text{Equation 5-25}$$

$$Ep_{EPZ} = 0.449 \cdot \dot{m}_{EPZ} \cdot g' \cdot \delta_{EPZ} \quad \text{Equation 5-26}$$

Maximum air speed at the end of the primary zone assuming no entrainment

Replacing Equation 5-6, Equation 5-7, Equation 5-20 and Equation 5-26, into Equation 5-3, the conservation of energy in the primary zone of a DV jet, assuming no entrainment, can be expressed as:

$$\begin{aligned} & \dot{m}_{0.05} \cdot \left(\frac{V_{0.05 \text{ avg}}^2}{2} + Ep_{0.05 \text{ avg}} \right) \\ & = \dot{m}_{EPZ} \cdot \left(0.429 \cdot V_{\max \text{ jet EPZ}}^2 + 0.449 \cdot \frac{g \cdot (T_{\text{room}} - T_{0.05 \text{ avg}})}{T_{\text{room}}} \cdot \delta_{\text{jet EPZ}} \right) \end{aligned} \quad \begin{array}{l} \text{Equation} \\ \text{5-27} \end{array}$$

Rearranging Equation 5-27, the maximal air speed at the end of the primary zone can be expressed as a function of the jet properties at 0.05 m from the diffuser. In addition, since it is assumed there is no entrainment, the mass flow rate at the end of the primary zone (\dot{m}_{EPZ}) is the same as the mass flow rate at 0.05 m from the diffuser ($\dot{m}_{0.05}$). The maximum air speed at the end of the primary for a DV jet without entrainment can then be expressed as:

$$\begin{aligned} V_{\max \text{ jet EPZ-no entrainment}} & = \alpha_1 \\ & \cdot \sqrt{\left(V_{0.05 \text{ avg}}^2 + 2 \cdot \left(Ep_{0.05 \text{ avg}} - \alpha_2 \cdot \frac{g \cdot (T_{\text{room}} - T_{0.05 \text{ avg}})}{T_{\text{room}}} \cdot \delta_{\text{jet EPZ}} \right) \right)} \end{aligned} \quad \begin{array}{l} \text{Equation} \\ \text{5-28} \end{array}$$

Where:

- α_1 and α_2 are numerical constants respectively equal to 1.707 and 0.663.

5.2.2 Correction for the entrainment of room air

In the previous section, a formulation for the maximum air speed in the jet at the end of the primary is developed assuming no entrainment of room air in the DV jet. Meanwhile, measurements performed by the author show that a non-negligible quantity of indoor air is entrained in the DV jet (see Chapter 4). Equation 5-28 therefore needs to be corrected in order to take into account this entrained air (Figure 5-4).

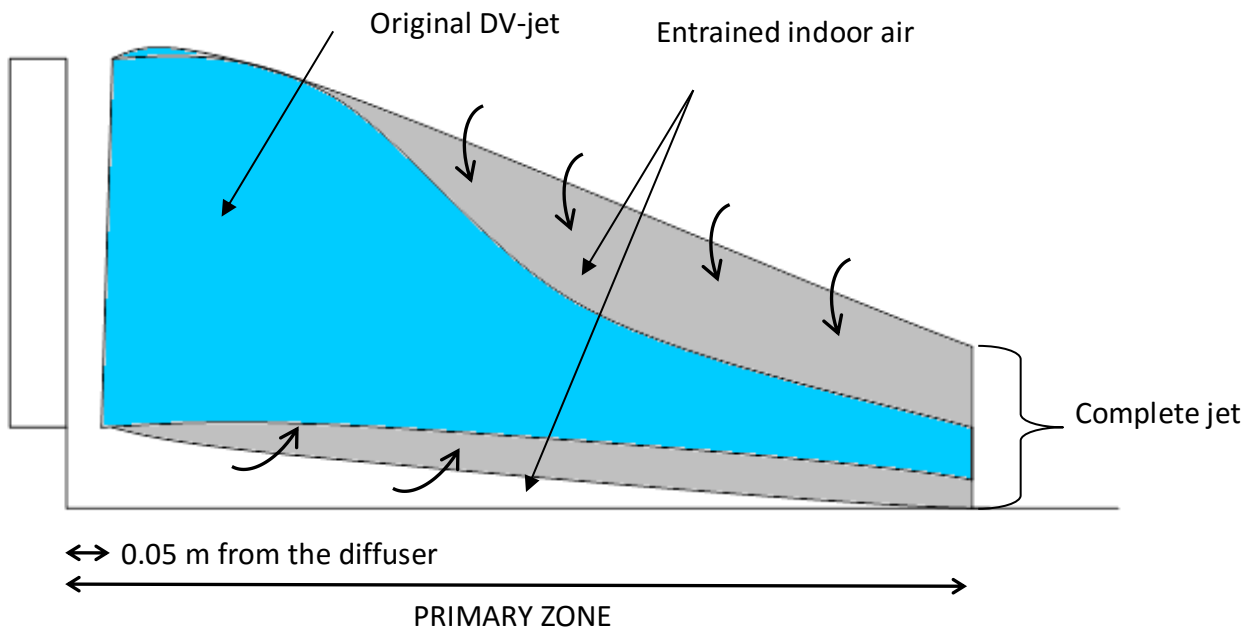


Figure 5-4: DV jet assuming entrainment

Conservation of momentum in the jet

At the end of the primary zone, the DV jet is composed of both air from the original unmixed jet, and of entrained room air. At the end of the primary zone, the momentum in the complete jet, i.e. including entrained air, is equal to the sum of the momentum from the jet without entrainment and of the momentum of the entrained air (Equation 5-29).

$$\dot{M}om_{jet \text{ with entrainment}} = \dot{M}om_{jet \text{ without entrainment}} + \dot{M}om_{jentrainment \text{ air}} \quad \text{Equation 5-29}$$

Where:

- $\dot{M}om_{jet \text{ with entrainment}}$ is the momentum flowrate in the jet with entrainment [kg.m/s²];
- $\dot{M}om_{jet \text{ without entrainment}}$ is the momentum flowrate in the jet without entrainment [kg.m/s²], and;
- $\dot{M}om_{jentrainment \text{ air}}$ is the momentum flowrate of the entrained air [kg.m/s²].

Outside of the DV jet, the room air is mostly still, with air speeds in the order of 0.01-0.05 m/s, as measured by the author. The momentum input from the entrained indoor air can therefore be considered as negligible. The conservation of momentum can then be reduced to Equation 5-30.

$$\dot{M}om_{jet \text{ with entrainment}} = \dot{M}om_{jet \text{ without entrainment}} \quad \text{Equation 5-30}$$

Calculation of the momentum terms

The momentum terms in Equation 5-30 can be calculated by using the vertical and transversal air speed profiles at the end of the primary zone (Equation 5-8). The momentum term without entrainment is given as an example (Equation 5-31). After rearrangement and numerical integrations (Equation 5-32 to Equation 5-35), the momentum term can be reduced to Equation 5-36. Similarly, the momentum term including entrainment can be reduced to Equation 5-37. The momentum terms are then written as a function of the mass flow rate times the maximal air speed.

$\dot{M}om_{jet \text{ without entrainment}}$

Equation 5-31

$$= \oiint \mathbf{V}_{\text{without entrainment}} \rho \mathbf{V}_{\text{without entrainment}} \cdot \mathbf{n} dA$$

$\dot{M}om_{jet \text{ without entrainment}}$

Equation 5-32

$$= \rho_{EPZ} \cdot \int_{Y=-\infty}^{Y=+\infty} \int_{Z=0}^{Z=\delta_{EPZ}} V_{EPZ \text{ without entrainment}}(Y, Z)^2 \cdot dZ \cdot dY$$

$\dot{M}om_{jet \text{ without entrainment}}$

Equation 5-33

$$= \rho_{EPZ} \cdot \int_{Y=-\infty}^{Y=+\infty} \int_{Z=0}^{Z=\delta_{EPZ}} V_{\max EPZ \text{ without entrainment}}^2 \cdot \left(f\left(\frac{Z}{\delta_{EPZ}}\right) \right)^2 \left(g\left(\frac{Y}{b_{EPZ}}\right) \right)^2 \cdot dZ \cdot dY$$

$\dot{M}om_{jet \text{ without entrainment}}$

Equation 5-34

$$= \rho_{EPZ} \cdot V_{\max EPZ \text{ without entrainment}}^2 \cdot \delta_{EPZ} \cdot b_{EPZ} \cdot \int_{Y=-\infty}^{Y=+\infty} \int_{Z=0}^{Z=\delta_{EPZ}} \left(f\left(\frac{Z}{\delta_{EPZ}}\right) \right)^2 \left(g\left(\frac{Y}{b_{EPZ}}\right) \right)^2 \cdot d\frac{Z}{\delta_{EPZ}} \cdot d\frac{Y}{b_{EPZ}}$$

Using Equation 5-17, we get:

$\dot{M}om_{jet \text{ without entrainment}}$

Equation 5-35

$$= \frac{\dot{m}_{jet \text{ without entrainment}}}{1.380} \cdot V_{\max EPZ \text{ without entrainment}}^2 \cdot \int_{Y=-\infty}^{Y=+\infty} \int_{Z=0}^{Z=\delta_{EPZ}} \left(f\left(\frac{Z}{\delta_{EPZ}}\right) \right)^2 \left(g\left(\frac{Y}{b_{EPZ}}\right) \right)^2 \cdot d\frac{Z}{\delta_{EPZ}} \cdot d\frac{Y}{b_{EPZ}}$$

After numerical integration, we get:

$\dot{M}om_{jet \text{ without entrainment}}$

Equation

$$= 0.488 \cdot \dot{m}_{jet \text{ without entrainment}} \cdot V_{\max EPZ \text{ without entrainment}}$$

5-36

Similarly, for the momentum with entrainment, we get:

$$\dot{M}om_{jet \text{ with entrainment}} = 0.488 \cdot \dot{m}_{jet \text{ with entrainment}} \cdot V_{\max EPZ \text{ with entrainment}}$$

Equation

5-37

Using Equation 5-36, Equation 5-37 and Equation 5-30, the maximum air speed at the end of the primary zone in the complete DV jet (including air entrainment) can be written as the maximal air speed in the DV jet calculated without entrainment multiplied by the ratio of the jet initial mass flow-rate divided by the jet total mass flow-rate at the end of the primary zone.

$$V_{\max EPZ \text{ jet with entrainment}} = \gamma \cdot V_{\max EPZ \text{ jet without entrainment}}$$

Equation

5-38

Where:

- γ is defined as the ratio between the mass flow-rate at 0.05 m from the diffuser and the mass flow-rate at the end of the primary ($\frac{\dot{m}_{0.05}}{\dot{m}_{\text{complete jet}}}$), $(1 - \gamma)$ represents the entrainment of room air in the DV jet in the primary zone [-].

Final equation for the maximum air speed at the end of the primary zone of a DV jet

Combining Equation 5-38 and Equation 5-28, the maximal air speed at the end of the primary zone of a DV jet can be expressed as Equation 5-39.

$$V_{max EPZ} = \alpha_1 \gamma \cdot \sqrt{\left(V_{0.05 wavg}^2 + 2 \cdot \left(E_{p0.05 wavg} - \alpha_2 \cdot \frac{g \cdot (T_{room} - T_{0.05 wavg})}{T_{room}} \cdot \delta_{jet EPZ} \right) \right)}$$

Equation 5-39

factor
accounting
for
entrained
room air

initial
kinetic
energy

initial
potential
energy

remaining potential
energy at the end of
the primary zone

Equation 5-39 is composed of four elements. First, there is a multiplying factor in front of the square root; this factor accounts for the entrainment of room air in the DV jet. Then, there are three terms inside the square root representing respectively: the initial kinetic energy of the jet exiting the diffuser (considered here at 0.05 m from the diffuser), the initial potential energy of the jet exiting the diffuser, and the potential energy remaining in the jet at the end of the primary zone. It should also be noted that the two initial energy terms take into account the height, width and specific face velocity distribution of the diffuser. These factors can be measured and catalogued by manufacturers and provided to engineers or building operators.

5.2.3 Validation with experimental data

Validation of the theoretical model is performed using the measurements discussed in Section 4 of Chapter 4. The data used for analysis is composed of a series of measurements performed on

the diffuser of size 0.6 m x 0.6, for five different under-temperatures, at a given flow-rate (see Table 5-2).

Table 5-2: Experimental conditions for the validation data

Supply flow-rate [m ³ /s]	0.035				
Under-temperature [°C]	1.5	2.4	3.7	5	6.3
Supply air temperature [°C]	20.6	19.4	18.8	16.9	15.4
Room air temperature at 1.1 m [°C]	22.0	21.8	22.5	21.9	21.7

Identification of variables used in Equation 5-39

Five variables need to be determined to enable the use of Equation 5-39. These variables are calculated based on the experimental data and are reported in Table 5-3. The following conclusions can be made regarding these parameters for the diffuser and experimental conditions studied:

- The parameters $V_{0.05 \text{ avg}}^2$, $Ep_{0.05 \text{ avg}}$, and $T_{0.05 \text{ avg}}$ are sensitive to the specific face velocity profile from the diffuser. These factors can however be quite easily tabulated by HVAC manufacturers. Also, as mentioned in section 3.4, the air speed profile at 0.05 m from the diffuser does not change for the range of under-temperature studied for the diffuser tested. Therefore, the parameter $V_{0.05 \text{ avg}}^2$ is also relatively unchanged for the under-temperatures and the diffuser studied. An average value can therefore be used in calculations.
- The thickness of the jet at the end of the primary zone, $\delta_{\text{jet EPZ}}$, varies with the supply under-temperature. This variation is however relatively small (between 0.14 m and 0.18 m for the range of under-temperature studied). An average thickness value can therefore be used in

calculation.

- Finally, the parameter γ , accounting for the entrainment of room air can be considered as mostly constant for the range of under-temperature studied. An average value can therefore be used in calculations.

Table 5-3: Parameters of Equation 5-39 from measurements

Under-temperature [°C]	$V_{0.05 \text{ wavg}}^2$	$Ep_{\text{wavg}}^{0.05}$	$T_{0.05 \text{ wavg}}$	$\delta_{\text{jet EPZ}}$	γ
1.5	0.054	0.008	20.7	0.18	0.68
2.4	0.060	0.015	19.6	0.16	0.72
3.7	0.056	0.021	19.2	0.15	0.69
5.0	0.060	0.028	17.5	0.14	0.64
6.3	0.060	0.033	16.4	0.14	0.68
Average (if relevant)	0.058	N.A.	N.A.	0.15	0.68

Comparison with experimental data

Using Equation 5-39 and the parameters from Table 5-3, the maximum air speed in the DV jet at the end of the primary zone can be evaluated for each supply condition studied. Results are shown in Table 5-4, with calculations made first using the parameters calculated for each supply under-temperature and then using averaged parameters. The maximum air speed from experiments is also shown for comparison.

Table 5-4: Estimated and measured maximum velocities

Under-temperature [°C]	1.5	2.4	3.7	5.0	6.3
Measured maximum air speed [m/s]	0.32	0.36	0.37	0.42	0.41
Maximum air speed calculated using specific parameters [m/s]	0.29	0.36	0.37	0.38	0.42
Error [m/s]	-0.03	0.00	0.00	-0.04	0.01
Maximum air speed calculated using averaged parameters [m/s]	0.30	0.34	0.37	0.40	0.42
Error [m/s]	-0.02	-0.02	0.00	-0.02	0.00

Table 5-4 shows that the model predicts the maximal air speed with good accuracy in both cases. Using averaged values actually improves the prediction and gives errors that are lower than the measurement uncertainty (0.03 m/s). This is probably due to the fact that using averaged values lowers the impact of individual measurements errors. Since the errors are lower than the measurement uncertainty, the model can be considered as validated for the set of experimental data of this study.

5.3 Normalization and correlation for the air speed in the secondary zone

In addition to maximal air speed at the end of the primary zone, the whole air speed distribution is required to design a DV system. This section focuses on the study of the variation of maximal air speed with the distance from the diffuser, in the secondary zone of the DV jet, using a normalization developed by the author and validated with published data.

5.3.1 Data used for the study of the secondary zone

In order to analyze the air speed profile in the secondary zone, data from this study and from other available DV measurements are analyzed. The details and sources for the experimental data used are summarized in Table 5-5. This figure is not limited to the secondary zone; it includes also the primary zone. The analysis is based on the study of a total of 13 maximum air speed profiles in the secondary zone of a DV jet, from seven different diffusers. The profiles or maximum air speed of the different DV jets are plotted in Figure 5-5.

Table 5-5: Experimental data used for normalization

Case number	Diffuser	Supply flow rate [m ³ /s]	Supply under-temperature [°C]	Reference
1	Flat wall-mounted diffuser of size 0.6m x 0.6m (H x W)	0.035	1.5	Magnier et al. 2012
2		0.035	2.4	
3		0.035	3.7	
4		0.035	5.0	
5		0.035	6.3	
6	Flat wall-mounted diffuser of size 1.2m x 0.6m (H x W)	0.032	2.5	
7		0.032	5.6	
8	Radial diffuser of diameter 0.25 m	0.037	4.4	Schild et al. 2003
9	Flat wall diffuser of size of perforated area of 0.159 m ²	0.026	6.0	Nielsen, 2000
10	Flat wall-mounted diffuser of perforated area of 0.306 m ²	0.028	6.0	
11		0.028	3.0	

12	Half cylinder diffuser with a perforated area of 0.188 m ²	0.029	6.0
13	Flat wall-mounted diffuser of perforated area of 0.437 m ²	0.028	Not given in the original study.

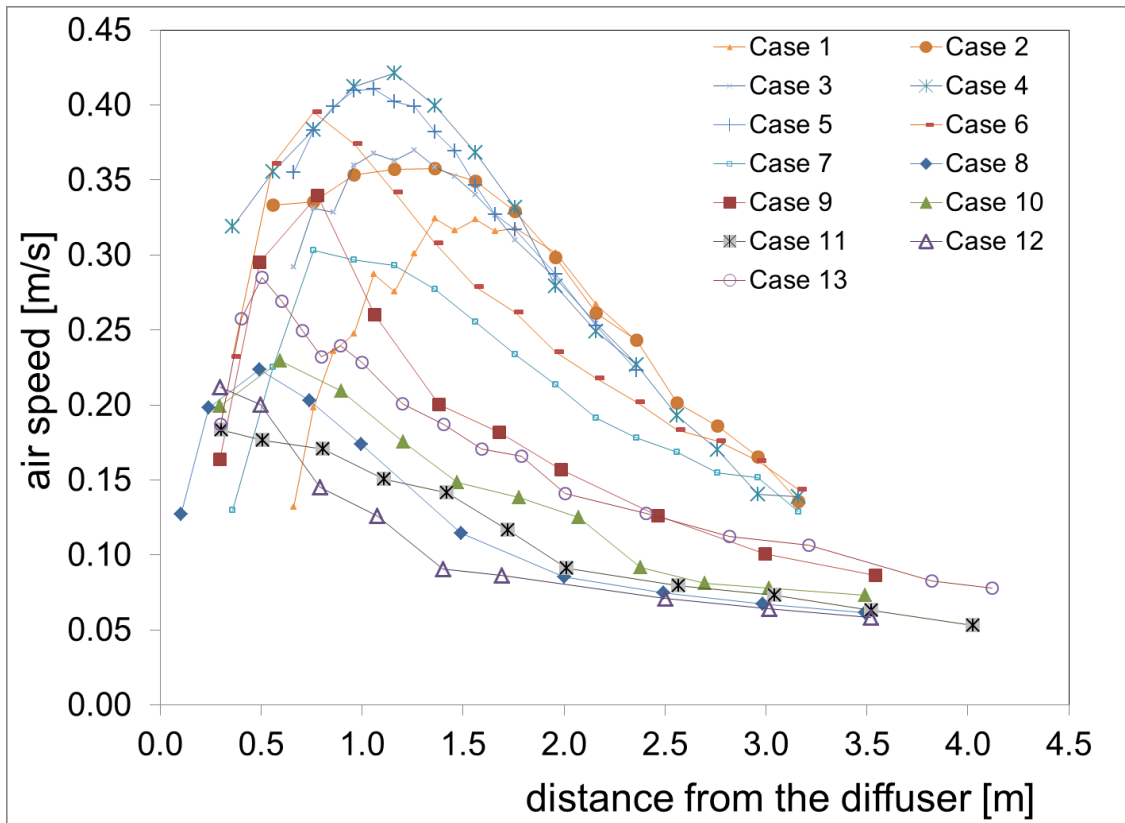


Figure 5-5: Maximum air speed profiles in experimental data (not normalized)

5.3.2 Normalization of air speed in the secondary zone

Figure 5-5 shows that the air speed profiles from the various diffusers and supply conditions are very different, with different amplitudes and different air speed decay in each case. For instance, in Case 4, the maximum speed is about 0.42 m/s at the end of primary zone (1.2 m). Figure 5-5 shows also the end of primary zone which varies in terms of diffusers' type and supplying conditions. This wide variety of trends illustrates clearly the difficulty in creating a

general correlation for the air speed profile in a DV jet. In order to better analyze the DV jet in the secondary zone, the author developed a normalization model. The underlying idea of this model is to consider the secondary zone of the DV jet as an actual new zone, from which the jet can be analyzed independently of the jet behavior in the primary zone. The normalization model is therefore based on a normalization of the air speed according to the terminal speed at the end of the primary zone, and on a re-initialization of the distance from the beginning of the secondary zone. The normalization air speed model can therefore be described as Equation 5-40:

$$V_{scd}(\xi) = \frac{V_M(\xi)}{V_{EPZ}} \quad \text{Equation 5-40}$$

where:

- V_{scd} is the normalized air speed at a distance ξ from the end of the primary zone [-];
- V_M is the maximum air speed at a distance ξ from the end of the primary zone [m/s];
- V_{EPZ} is the maximum air speed reached at the end of the primary zone [m/s] and;
- ξ is the distance from the end of the primary zone [m], defined as $\xi = (X - L_{PZ})$ where X is the distance from the diffuser [m] and L_{PZ} is the length of the primary zone [m].

5.3.3 Graphical representation of the normalization model

The air speed profiles from Figure 5-5 are normalized using Equation 5-40 and the normalized air speed profiles are plotted in Figure 5-6. Figure 5-7 shows that, after normalization, the air speed profiles from all sources display a rather similar pattern, both in terms of amplitude and decay. The proposed normalization is therefore effective in producing a generalized profile for

air speed in the secondary zone of a DV jet, independent of the diffuser types and supply conditions.

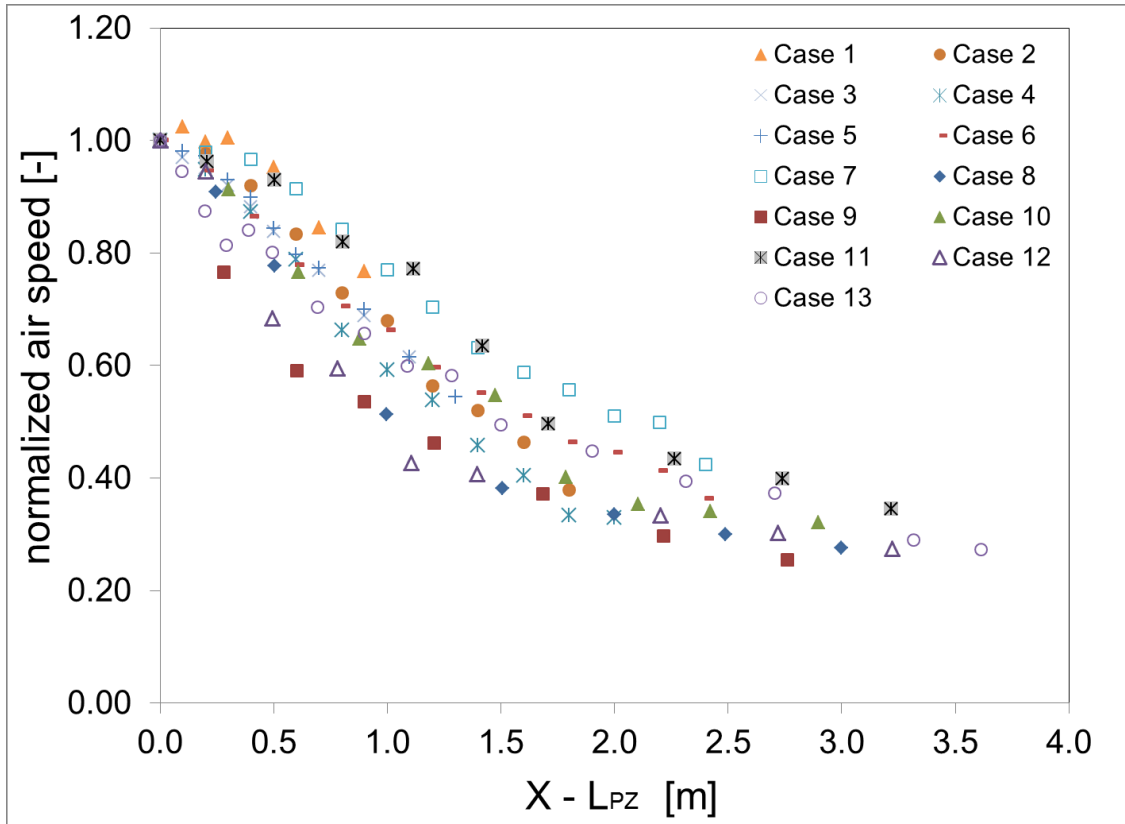


Figure 5-6: Normalized maximum air speed from experimental data

5.3.4 Regression for the normalized air speed profile

Based on the normalized air speeds shown in Figure 5-6, a correlation-based model is developed for the longitudinal profile of normalized air speed in the secondary zone of a DV jet (Equation 5-43 and Figure 5-7). The coefficient of determination R^2 is 0.94, showing a good correlation between the results of regression model (Equation 5-43) and the normalized experimental data. Therefore, Equation 5-41 accurately describes the decay of normalized air speed in the secondary zone for all the diffusers and supply conditions tested.

$$V_{\text{scd}}(\xi) = \frac{1}{\sqrt{1 + 1.5 \cdot \xi^2}}$$

Equation 5-41

where:

- V_{scd} is the normalized air speed in the secondary zone [-], and;
- ξ is the distance from the end of the primary zone [m].

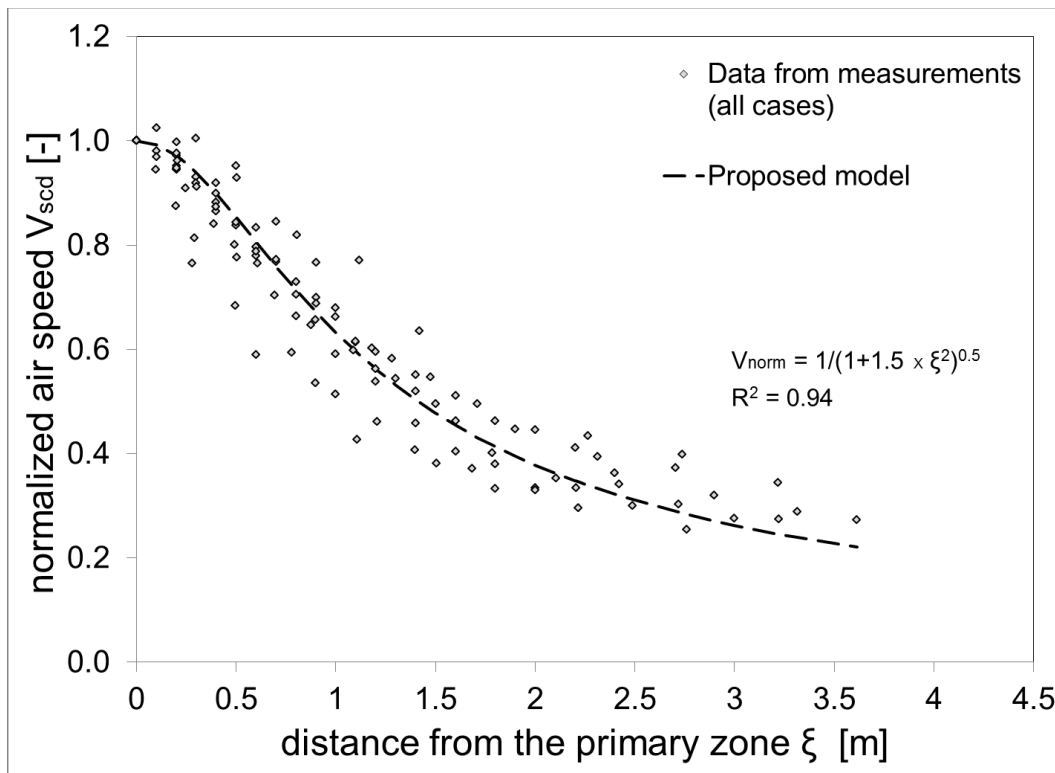


Figure 5-7: Normalized maximum velocities and proposed correlation-based model

5.3.5 Conclusion and discussion

Combining Equation 5-40 and Equation 5-41, the maximum air speed in the secondary zone can be expressed as:

$$V_{\max}(X \geq L_{PZ}) = V_{EPZ} \cdot \frac{1}{\sqrt{1 + 1.5 \cdot (X - L_{PZ})^2}}$$

Equation 5-42

where :

- $V_M(X)$ is the maximum air speed at a distance X from the diffuser [m/s];
- V_{EPZ} is the maximum air speed reached at the end of the primary zone [m/s];
- X is the distance from the diffuser [m] and;
- L_{PZ} is the length of the primary zone [m].

This equation has been found valid for all the diffusers and supply conditions tested. Thanks to the new approach considering the secondary zone as an entirely new zone, the author developed a normalization model applicable to all experimental cases studied. A general regression equation was also created to represent the normalized air speed profile. This regression displayed good agreement with experimental data. Also, it can also be noted that, as the distance from the diffuser increases, the regression equation (Equation 5-41) becomes similar to the classical air speed decay equation in a DV jet (i.e. inversely proportional to the distance from the diffuser (Nielsen, 1994)). This equation is therefore still in agreement with previous studies on the non-normalized air speed decay in the secondary zone of a DV jet.

5.4 Combination of the primary zone and secondary zone models

5.4.1 Maximum air speed in the secondary zone

Combining the formula developed in the first section for the maximum air speed at the end of the primary zone (Equation 5-39) with the normalized air speed profile in the secondary zone (Equation 5-41), the maximum air speed in a DV jet at any distance from the diffuser in the secondary zone can be expressed as :

$$V_{\max}(X \geq L_{PZ}) = \frac{\alpha_1 \cdot \gamma}{\sqrt{1 + 1.5 \cdot (X - L_{PZ})^2}} \cdot \sqrt{\left(V_{0.05 \text{ wavg}}^2 + 2 \cdot \left(Ep_{0.05 \text{ wavg}} - \alpha_2 \cdot \frac{g \cdot (T_{\text{room}} - T_{0.05 \text{ wavg}})}{T_{\text{room}}} \cdot \delta_{\text{jet EPZ}} \right) \right)}$$

Equation 5-43

5.4.2 Validation of the maximum air speed profile equation

Equation 5-43 is tested against the author's experimental data for the diffuser of size 0.6 m x 0.6 m for the five supply conditions previously mentioned (see Table 5-2 in section 4.1.4). The maximum air speed in the jet is calculated and compared with the measurements in the secondary zone. The parameters used in calculation are summarized in Table 5-6. The air speeds measured and calculated using Equation 5-43 are plotted on Figure 5-8.

Table 5-6: Parameters used in Equation 5-43

Under-temperature [°C]	1.5	2.4	3.7	5	6.3
$V_{0.05 \text{ wavg}}^2$	0.058				
$\delta_{\text{jet EPZ}}$	0.15				
γ	0.68				
$[g_{0.05'}Z]_{\text{wavg}}$	0.060	0.015	19.6	0.16	0.72
$T_{0.05 \text{ wavg}}$	0.056	0.021	19.2	0.15	0.69
$L_{\text{PZ}} [\text{m}]$	1.46	1.36	1.26	1.16	1.06

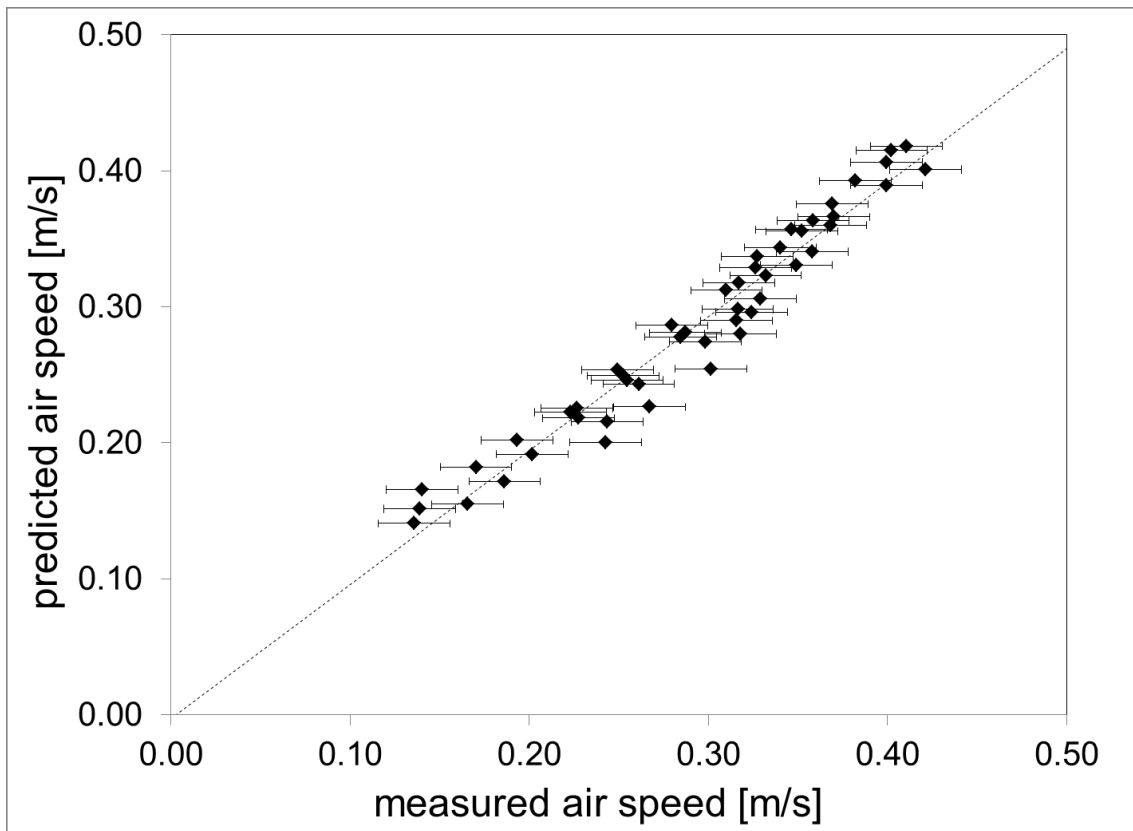


Figure 5-8: Measured and correlated maximum air speed in the secondary zone for the five supply conditions studied

Figure 5-8 shows that the agreement between the measured and correlated data is very good, with a coefficient of determination R^2 between the two sets of data is 0.96. The average absolute error between the measured and correlated data is 0.01 m/s. This error is acceptable as it is lower than the experimental error in measurements (0.02-0.03 m/s). In addition, the error between predicted and measured air speeds is lower than the experimental error except for a few locations. The complete model for the maximum air speed in the secondary zone is therefore validated.

5.4.3. Discussion

The combination of the theoretical study of the primary zone and normalization in the secondary zone enabled to develop a general model to determine the variation of maximal air speed throughout the secondary zone. This model is based mostly on parameters that can be tabulated by manufacturers and supplied to designers and HVAC engineers. The agreement between predicted and measured data is very good and the error is in most cases within the range of experimental error. The model takes into account various important parameters such as the supply under-temperature, the supply flow rate, the entrainment, the height of the diffuser, the width of the diffuser and the specific face velocity distribution from the diffuser. Once the proper parameters are known, the model could be used to study the impact of supply conditions on the maximum air air speed profile. Knowing the profile of maximum air speed in the secondary zone will help designers predicting discomfort and operating the DV system accordingly.

Despite these qualities, some limitations remain in the model. More experimental data – especially data from different diffusers and different flow-rates – should be used to further validate the model to determine the maximum air speed in the primary zone. A limitation of the model is also that there is currently no easy way to determine the entrainment of room air in

the jet. It should nonetheless be noted that the entrainment was independent of the supply temperature in the experimental data and would only have to be determined once per flow rate. Another issue of the current model is that it requires knowing the length of the primary zone. Despite some tentative studies (Etheridge and Sandberg, 1996), there is currently no validated formula to predict this length. A possible experimental way to determine it would be to perform smoke measurements and note the length at which the jet thickness stops decreasing significantly. Additional work is required on those parameters to make the model fully functional.

5.5 Analysis of the vertical air speed profile

The vertical profile of air speed and thickness of a DV jet are essential yet seldom discussed parameters in assessing thermal comfort for displacement ventilation. On one hand, air speed models for DV jets in the literature only study the maximum air speed in the jet at different distances from the diffuser. On the other hand, standards such as ASHRAE 113 (2009) evaluate the thermal comfort at fixed reference heights, such as 0.10 m for the ankle level. As shown by experimental results, the air speed at 0.10 m is however different from the maximum air speed in the jet. According to the experimental data, the air speed at 0.10 m height varies between 55% and 85% of the maximum air speed, depending on the jet thickness. An accurate knowledge of the vertical air speed profile and of the thickness of the DV jet is hence essential to accurately assess local thermal comfort. This section studies the vertical profile of air speed in the DV jet; the next section studies the variations in jet thickness.

5.5.1 Normalization of experimental data

The main data used in this section is the experimental data described in Chapter 3, section 2 and 3. As a reminder, the data includes air speed measurements performed in the vertical longitudinal plane (0.16 m to 3.16 m from the diffuser) and in a vertical transversal plane at 2.16 m from the diffuser (up to 0.9 m on both sides of the longitudinal axis), for two flat wall-mounted DV diffusers, with two supply under-temperature tested for each (Table 5-7). At each location in both planes, the air speed was measured at 9 different heights in the jet: 0.02 m, 0.03 m, 0.04 m, 0.05 m, 0.06 m, 0.07 m, 0.08 m, 0.10 m, and 0.20 m. An example of the vertical profiles of air speed found at different distances from the diffuser is shown in Figure 5-9.

Table 5-7: Diffuser and supply conditions in experimental data

Diffuser	Supply flow rate [m ³ /s]	Supply under- temperature [°C]
Flat wall-mounted diffuser of size 0.6m x 0.6m (H x W)	0.035	2.4
	0.035	5.0
Flat wall-mounted diffuser of size 1.2m x 0.6m (H x W)	0.032	2.5
	0.032	5.5

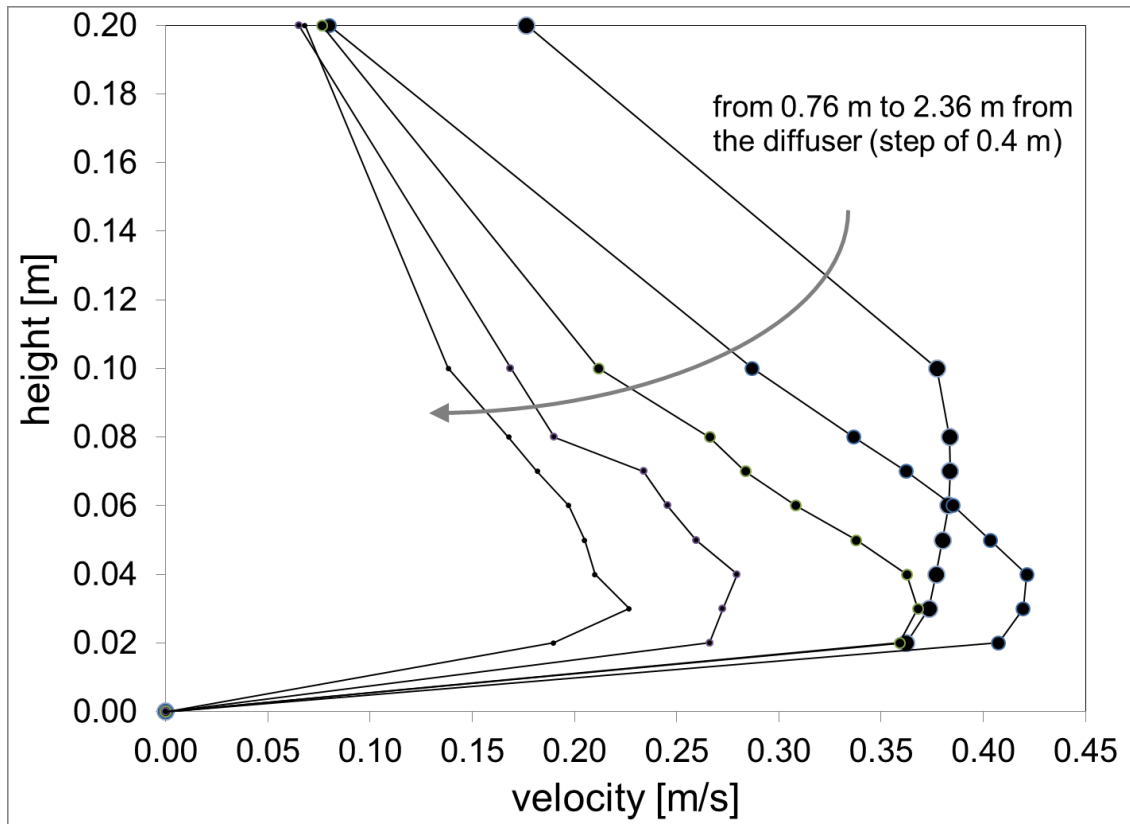


Figure 5-9: Vertical profile of air speed at different distances from the diffuser DF1W (0.6m x 0.6m) for $\Delta T=5.0^{\circ}\text{C}$

Figure 5-9 shows that a general pattern appears in the vertical profile of air speed. In order to study these profiles, two normalizations have to be performed:

- an air speed normalization (Equation 5-44), with respect to the maximum air speed in the jet at a location (distance X from the diffuser and distance Y from the longitudinal axis) where the vertical profile is measured:

$$V_{norm_z}(X, Y, Z) = \frac{V(X, Y, Z)}{\max_z V(X, Y, Z)} \quad \text{Equation 5-44}$$

- a height normalization (Equation 5-45), with respect to thickness of the jet at a location (distance X from the diffuser and distance Y from the longitudinal axis) where the vertical profile is measured:

$$\eta = \frac{Z}{\delta_{XY}} \quad \text{Equation 5-45}$$

These normalizations, commonly used in the literature (Rajaratnam, 1976), are the basis of next analysis. Figure 5-10 shows the same profiles of Figure 5-9 after performing the two normalizations. This figure shows that a consistent vertical profile emerges. The next subsections are aimed at characterizing this profile.

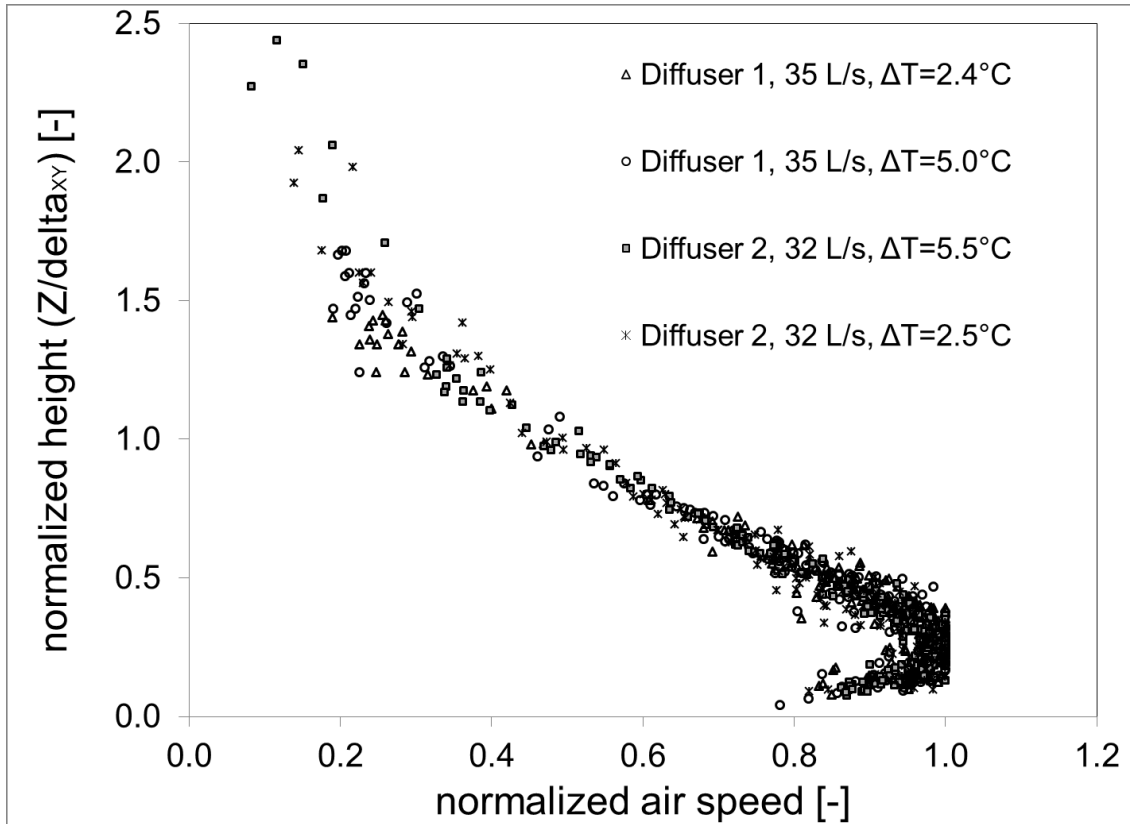


Figure 5-10: Normalized vertical profiles in the secondary zone

5.5.2 Wall-jet vertical profile

The vertical profile of air speed in a DV jet is generally described in the literature to follow the universal wall-jet profile shown in Equation 5-46 (Rajaratnam, 1976). This profile was found to agree well with experimental data in previous studies (Skaret, 1998, Nielsen 2000, Nielsen 2004). It is therefore used as a reference model in the current work to analyze the vertical air speed profile from experimental data.

$$F(\eta) = 1.48 \cdot (\eta)^{0.413} \cdot [1 - \text{erf}(0.68 \cdot (\eta))] \quad \text{Equation 5-46}$$

where :

- F is the function representing the vertical profile of normalized air speed in a DV jet;
- H is the normalized height [-], and;
- erf is the error function.

Equation 5-46 is compared with the normalized experimental data. In order to be able to apply Equation 5-46 though, one has first to determine the appropriate thickness of the jet δ_{xy} , for each location. In this study, the thickness δ_{xy} was computed for each location to minimize the sum of square errors between the profile of normalized air speed (V_{normz}) and the theoretical profile F . The resulting δ_{xy} for each location are summarized in Table 5-8. Table 5-8 also includes the R^2 values between the experimental profile and the normalized experimental data for each location.

Table 5-8: R^2 and air thicknesses for the vertical air speed profiles

Distance from the diffuser [m]	Distance from the diffuser [m]	Diffuser 1, 35 L/s, $\Delta T=2.4^\circ C$		Diffuser 1, 35 L/s, $\Delta T=5.0^\circ C$		Diffuser 2, 32 L/s, $\Delta T=2.5^\circ C$		Diffuser 2, 32 L/s, $\Delta T=5.5^\circ C$	
		R^2	δ_{xy} [m]						
X=0.56 m	Y=0.0 m	N.A.	N.A.	N.A.	N.A.	N.A.	N.A.	0.97	0.107
X=0.76 m		N.A.	N.A.	0.88	0.219	0.96	0.134	0.99	0.088
X=0.96 m		0.74	0.263	0.92	0.162	0.99	0.119	0.98	0.082
X=1.16 m		0.92	0.209	0.99	0.136	0.99	0.104	0.97	0.085
X=1.36 m		0.94	0.162	0.98	0.119	0.98	0.098	0.97	0.098
X=1.56 m		0.96	0.150	0.99	0.120	0.94	0.102	0.96	0.118
X=1.76 m		0.98	0.141	0.99	0.121	0.97	0.128	0.95	0.136
X=1.96 m		0.96	0.148	0.97	0.125	0.97	0.125	0.92	0.159
X=2.16 m		0.98	0.149	0.98	0.125	0.98	0.158	0.94	0.177
X=2.36 m		0.97	0.138	0.89	0.130	0.92	0.176	0.92	0.192
X=2.56 m		0.94	0.162	0.95	0.153	0.98	0.211	0.94	0.214
X=2.76 m		0.86	0.166	0.94	0.157	0.82	0.206	0.85	0.209
X=2.96m		0.83	0.168	0.94	0.195	0.68	0.215	0.91	0.223
X=3.16 m		0.85	0.203	0.70	0.180	N.A.	N.A.	0.72	0.266

X=2.16 m	Y= -0.9 m	0.91	0.169	0.98	0.156	0.99	0.201	0.94	0.224
	Y= -0.7 m	0.96	0.162	0.98	0.137	0.97	0.160	0.95	0.168
	Y= -0.5 m	0.99	0.140	0.99	0.133	0.97	0.156	0.98	0.160
	Y= -0.3 m	0.98	0.139	0.97	0.127	0.95	0.148	0.95	0.161
	Y= -0.1 m	0.99	0.140	0.98	0.128	0.97	0.137	0.92	0.181
	Y= 0.1 m	0.97	0.149	0.97	0.141	0.97	0.125	0.97	0.176
	Y= 0.3 m	0.98	0.144	0.99	0.139	0.99	0.139	0.94	0.171
	Y= 0.5 m	0.99	0.153	0.99	0.132	0.96	0.153	0.97	0.154
	Y= 0.7 m	0.96	0.144	0.96	0.133	0.94	0.140	0.93	0.203
	Y= 0.9 m	0.75	0.177	0.95	0.158	0.93	0.153	0.91	0.235

Table 5-8 shows that, once the appropriate δ_{xy} is found, the wall-jet profile fits well with the measured data in the secondary zone, with R^2 values higher than 0.90 in almost all cases. This conclusion is in agreement with previous analysis of DV jets in the literature (Nielsen 1994, Skistad et al. 2002). Close to the diffuser, in the primary zone, the wall-jet profile does not appear appropriate. This result is probably due to the fact that, close to the diffuser, the DV jet is not yet fully developed. Also the jet at these locations has a relatively large thickness and is not necessarily in contact with the floor, hence it might fall outside of the grid of measurements. The air speed profiles in the transversal plane are not discussed in the literature. In this study, the wall-jet profile is also found applicable for the profiles in the transversal plane, with R^2 values higher than 0.90 in almost all cases. Figure 5-11 plots the vertical profiles of normalized air speed in the secondary zone for the four cases studied, with data from both the longitudinal and the transversal planes. The theoretical profile from Equation 5-46 is also shown in this figure. Figure 5-11 shows that the theoretical profile fits reasonably well with the experimental data; the profile differs from the experimental data for normalized heights lower than 0.3.

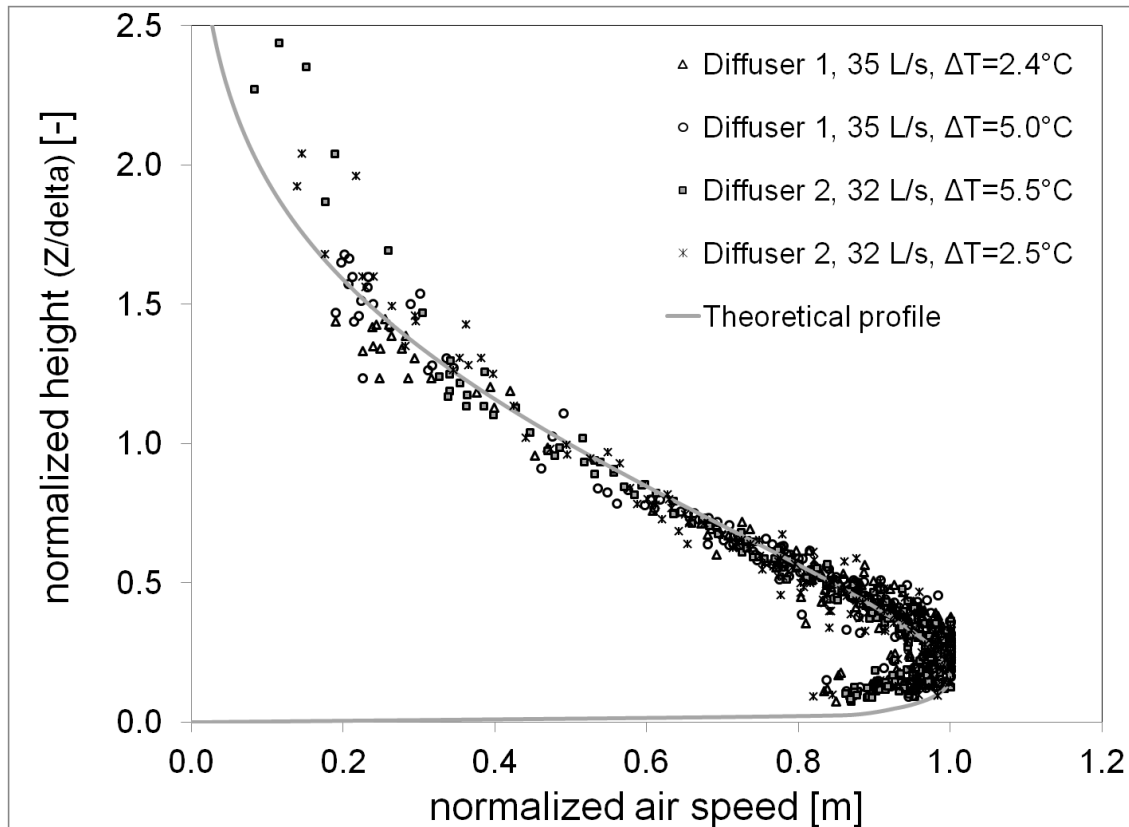


Figure 5-11: Comparison between the normalized air speed profiles in the secondary zone and the theoretical profile

5.5.3 A new proposed vertical profile specific to displacement ventilation jets

In order to further study the vertical air speed profile specifically in the case of a displacement ventilation jet, a new profile is developed in this section. The proposed profile keeps the same form as the classical wall jet profile (see Equation 5-47) but the coefficients β_i used in the general equation are determined specifically, based on the experimental data from a DV jet. The data used for this analysis is the same data as in the previous section excluding the primary zone, i.e. measurements taken in the secondary zones for two sizes of the DF1W diffusers and four supply conditions, as described in Chapter 3 section 2 and 3. The formula represents the vertical profile of normalized air speed and is therefore independent of the distance from the diffuser (X) or the distance from the longitudinal axis (Y), in the secondary zone a of a DV jet.

$$G(\eta) = \beta_1 \cdot \eta^{\beta_2} \cdot [1 - \text{erf}(\beta_3 \cdot \eta)] \quad \text{Equation 5-47}$$

where :

- G is the proposed vertical profile for normalized air speed in a DV jet, [-];
- η is the normalized dimensionless height [-];
- erf is the error function, and;
- β_1 , β_2 , and β_3 are constant to be determined [-].

The coefficients β_i in Equation 5-47 have been determined in order to minimize the sum of squared-errors between the normalized data from experiments (normalized heights and velocities) and the proposed vertical profile. The coefficients providing the best agreement between the correlated profile and the normalized data are shown in Equation 5-48. The profile created using these coefficients is plotted in Figure 5-12, along with the classical wall-jet profile.

$$G(\eta) = 1.687 \cdot \eta^{0.226} \cdot [1 - \text{erf}(0.752 \cdot \eta)] \quad \text{Equation 5-48}$$

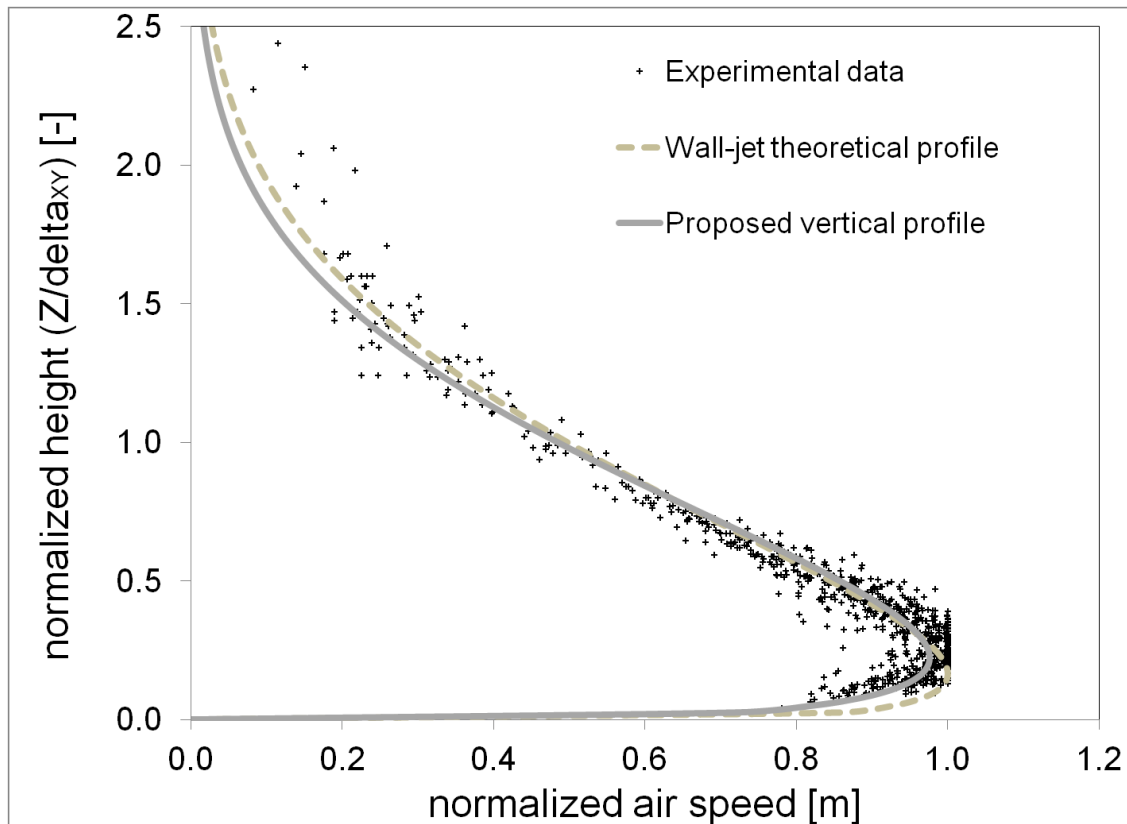


Figure 5-12: Comparison between the proposed vertical profile, the profile from the literature and experimental data

Figure 5-12 shows that the proposed profile fits well with the experimental data in the secondary zone, with an average R^2 coefficient of 0.97 (versus 0.96 for the classical profile). Figure 5-12 also shows that the proposed profile is better than the classical profile at representing the cluster around the height of maximum air speed. The height of maximum air speed in the proposed profile is also more representative of the actual height of maximal air speed than the height of maximum air speed in the classical wall-jet profile. Indeed, in the experimental data (Chapter 4) the dimensionless height of maximal air speed is around 0.25; and the dimensionless height of maximal air speed is 0.22 in the proposed profile, while it is 0.175 in the classical profile. It can be noted that the proposed profile is slightly less accurate than the classical profile for dimensionless heights over 1.5. The air speeds at these heights

however correspond to the boundary mixing layer of the DV jet, and are of little practical interest for design or comfort assessment. It is also noteworthy that the proposed profile does not reach the normalized air speed of 1, although its maximum value is very close (0.98). Overall, the improvement of the proposed profile in terms of pure R^2 coefficient is small (0.97 versus 0.96), but it offers an improvement in terms of general shape, especially around the height of maximal air speed, which is of prime interest when studying a DV jet.

5.6 Thickness variations in a DV jet

A major limitation of the normalized vertical profile, either the classical wall-jet profile or the proposed profile, is the necessity to know the local thickness of the jet δ_{xy} to be able to use it. As pointed out in the literature review (Chapter 2), a measurement at a given height (0.10 m for instance) does not provide any information regarding the maximal air speed unless both the vertical profile and the jet thickness are known. No model however exists in the literature to evaluate the thickness in a DV jet. Furthermore, according to the results presented in Table 5-8, the thickness of jet appears to vary with the supply conditions, with the diffuser used, with the distance from the diffuser and with the distance from the axis. Studies regarding the thickness of a tri-dimensional DV jet are very limited in the literature. Published DV studies, measurement standards or reference books simply state that the jet thickness is generally between 0.10 m and 0.20 m, and the maximum air speed occurs between 0.025 and 0.05 m (Nordtest, 2009; Skistad et al. 2002). The thickness variation of a tri-dimensional DV jet with the distance from the diffuser has seldom been studied in the past. The overall conclusion of those studies is that the thickness of the jet decreases in the primary zone, and then increases slightly in the secondary zone (Skaret, 1998; Nielsen 2001). No relation is however proposed in those studies to link the variations in jet thickness with other flow parameters. Those studies do not explain either why some DV jets show a significant increase of thickness with the distance from the diffuser, whereas for others DV jets the thickness is almost constant in the secondary zone. In

addition, no study could be found regarding the variation in DV jet thickness apart from along the longitudinal axis. The next sections are dedicated to further study the variation in jet thickness with the diffuser and supply conditions studied, and with location within the room.

5.6.1 Variation of the jet thickness with the distance from the diffuser

Figure 5-13 plots the local jet thickness δ_{xy} found in the section 5.4 (Table 5-8) at different distances from the diffuser on the longitudinal axis, for the four cases studied. This figure shows that the jet thickness varies significantly both with the distance from the diffuser and with the supply conditions. Values of jet thickness range from 0.08 m to almost 0.27 m depending on the case and distance to the diffuser.

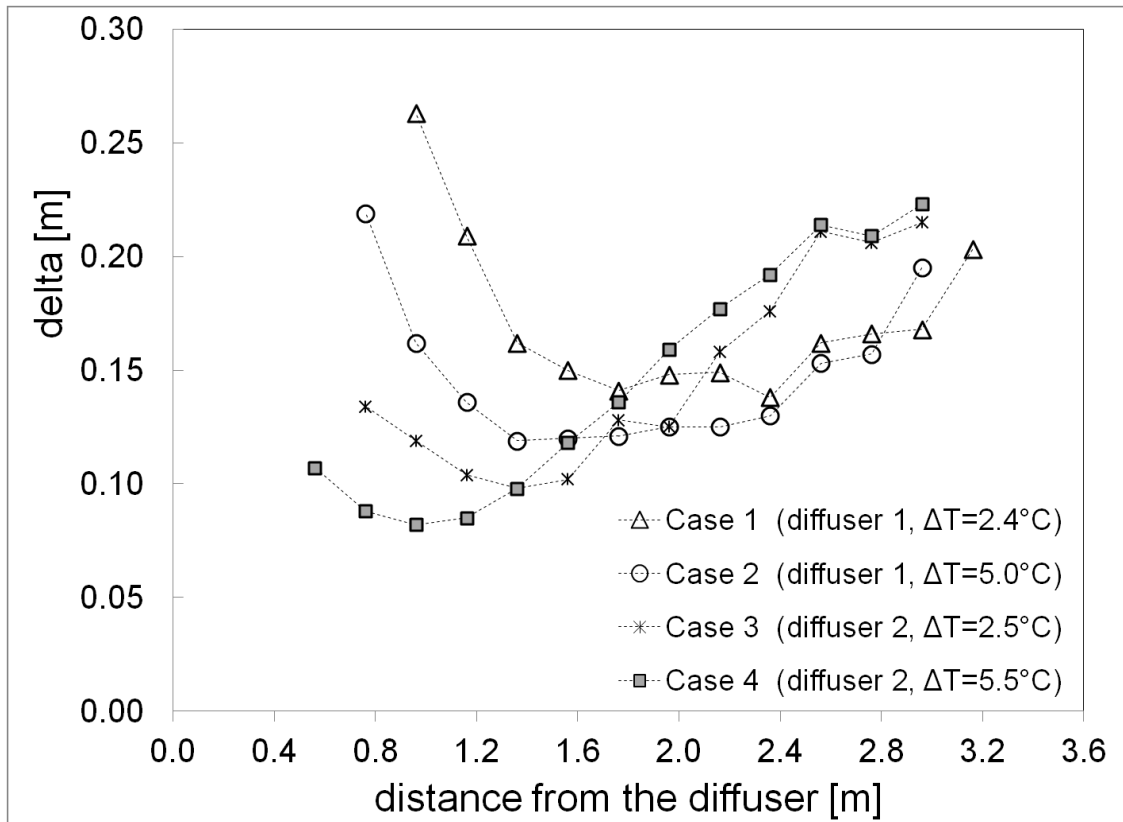


Figure 5-13: Thickness of the jet versus distance from the diffuser for the four cases studied

No immediate relation appears to link the local thickness with the supply parameters or with the distance from the diffuser. A higher under-temperature or a higher diffuser generally leads to a lower jet thickness, which seems logical considering the buoyancy forces of the jet, but this is not always the case. For instance, at 2.96 m from the diffuser, the lowest jet thickness amongst the four cases occurs for the smallest diffuser with the smallest under-temperature. The variation of thickness with the distance from the diffuser can be divided into three parts. Figure 5-14 illustrates this point by plotting the variation of jet thickness with the distance from the diffuser for measurements on the small diffuser with a supply under-temperature of 5.0°C.

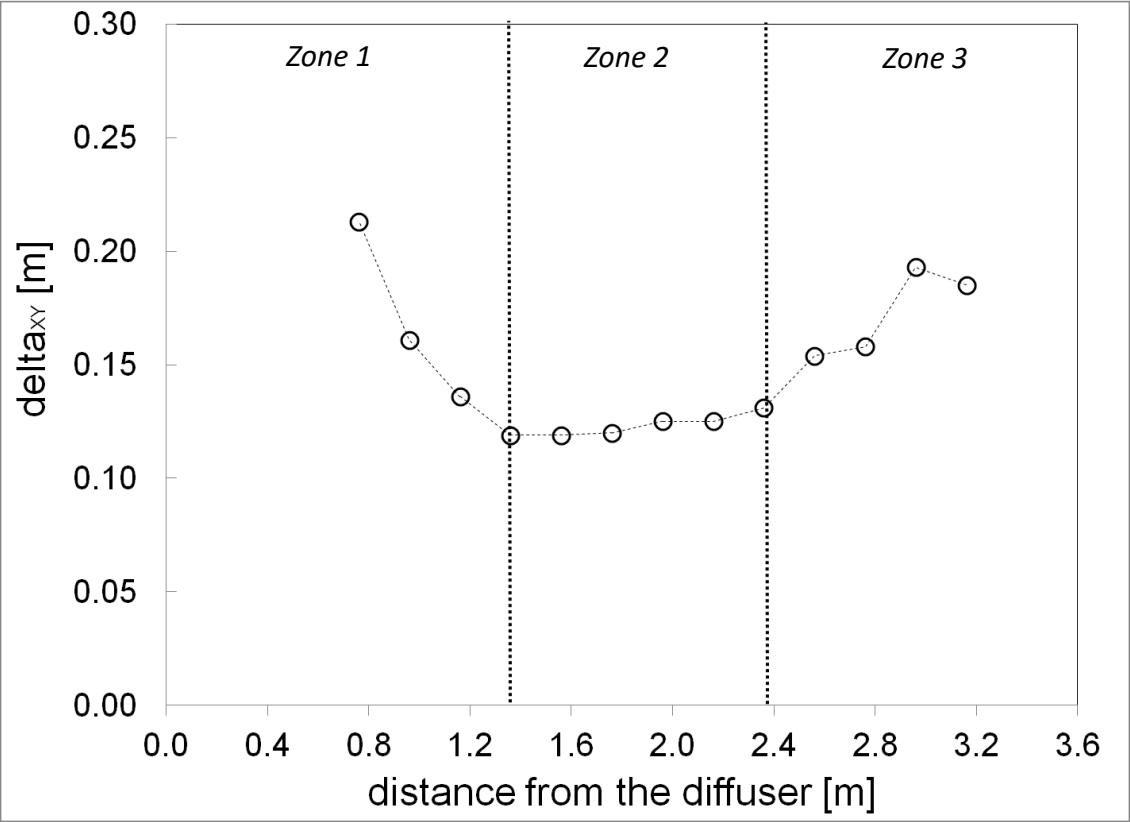


Figure 5-14: Thickness of the jet versus the distance from the diffuser for the first diffuser and $\Delta T=5.0^\circ\text{C}$, separated into three zones

Figure 5-14 highlights three distinct zones which can be described as follows:

- In the first part of the jet, the thickness of the jet decreases rapidly, due to the action of the gravity forces. This part corresponds to the primary zone of the jet.
- As for the second part of the jet, this part corresponds to part of the jet where the jet shows very limited variations of thickness, in the order of one or two centimeters. This part occurs at different distances from the diffuser for each case studied. It is also noteworthy that the thickness reached in this part is different for all the cases studied, ranging from 0.08 m to 0.14 m.
- Finally, in the last part of the jet, the thickness of the jet starts to increase significantly. As for the second part, the third part occurs at different distances from the diffuser for each case studied. For instance, it starts at 1.4 m from the diffuser for case 4, whereas it starts at almost 3.0 m from the diffuser for case 1.

This division of the jet in three parts corresponds well for the four cases studied, as all of them display such division. The division in three parts can also be found in published data in the literature, such as in Nielsen (2000) (see Figure 5-15). For other DV jets in the literature with a very high Archimedes number though, the third part seems to be absent (Nielsen, 2000). In addition, Figure 5-13 above shows that the transitions between the three parts occur at different distances from the diffuser for each case studied. The extent of each part also varies. The next section proposes an analysis of the jet thickness.

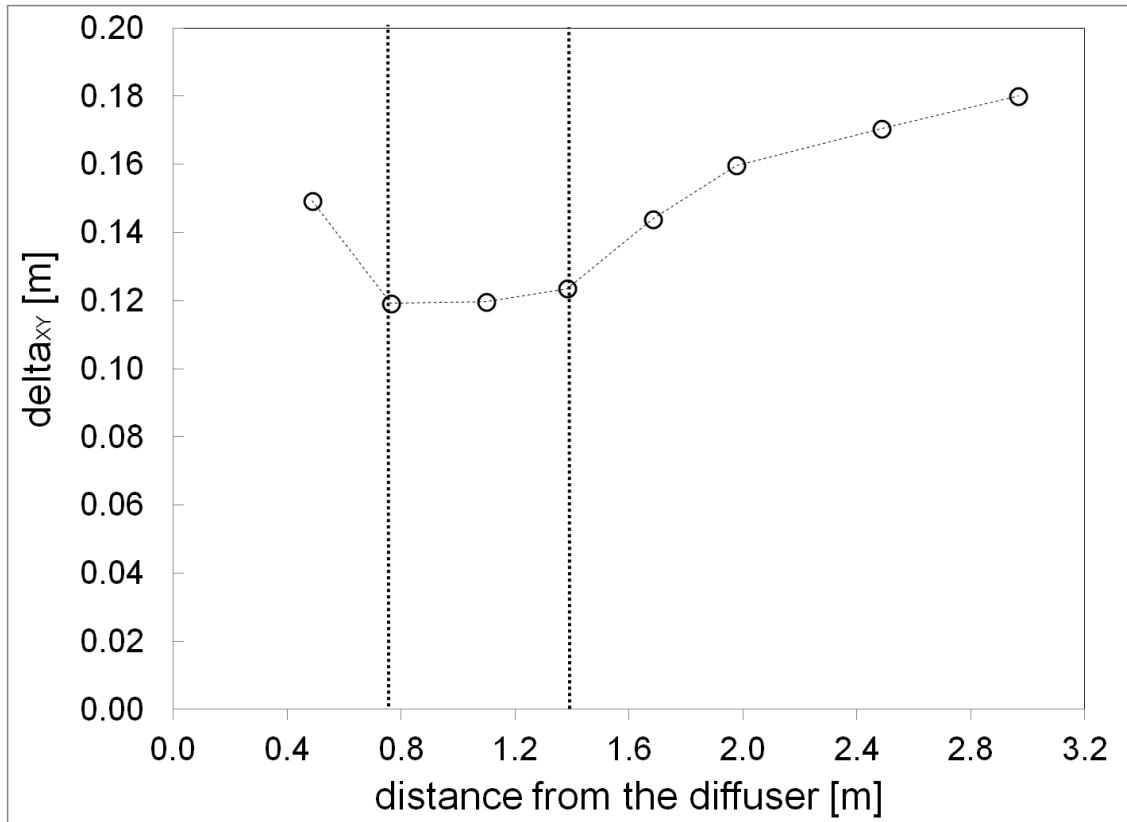


Figure 5-15: Thickness of the jet versus the distance from the diffuser based on Nielsen (2000)

5.6.3 Proposed correlation for the jet thickness along the longitudinal axis

Intuitively, one would assume that the thickness of a DV jet is related to the buoyancy forces acting on the jet. Some researchers such as Nielsen (2000) have already explored this idea and found that the thickness of DV jet varies with the Archimedes number calculated at the diffuser. A higher Archimedes number, hence higher buoyancy forces, is found by Nielsen to lead to a lower thickness of the jet. No formula is however proposed to link the thickness of the jet with the Archimedes. The study does not explore further whether the thickness variation in the jet is affected only by the supply under-temperature, only by the supply flow rate or both. REHVA's guidebook on displacement ventilation (Skistad et al. 2002), in turn, mentions that the thickness

of the jet varies with the Archimedes number or with the ratio of the supply under-temperature and the squared supply flow-rate. Unfortunately, no reference study or validation is provided for this statement. Finally, as discussed previously, no correlation is proposed in the literature for the variation of jet thickness with the distance from the diffuser or with the distance from the axis.

Based on the experimental data presented in Chapter 3, the author is able to study the variation in jet thickness against several flow parameters (air speed, temperature, Archimedes number, etc.). In this study, only the jet thickness in the secondary zone is studied, as it is the most important for thermal comfort assessment. Based on the discussion in the previous section, the analysis is divided as follows. First a correlation-based model is proposed for the minimum thickness reached in the jet. Then, the variation in jet thickness from this minimum thickness is studied and correlated. Finally, an overall model is proposed and compared with experimental data.

Minimum thickness in the DV jet

Data used for the analysis

As discussed before, very few data are available in the literature regarding the thickness of a DV jet. The data used for this analysis come from the author's measurements for the four cases described in section 2.1 and for an additional case on the smaller diffuser (0.6 m x 0.6 m) with a supply under-temperature of 6.5°C and a supply flow rate of 35 L/s. In addition to the author's data, data from an experimental study performed by Nielsen (2000) is also included. In this latter study, the diffuser was a semi-cylindrical DV diffuser of height 0.56 m, with a perforated area of 0.188 m². Table 5-9 summarizes the information regarding the experimental data used. The minimum thicknesses regarding the author's own experimental data come from the analysis discussed in section 5.4 (Table 5-8).

Table 5-9: Diffuser information and minimum air jet thickness

Diffuser type	Semi-cylindrical (Nielsen, 2001)			Flat wall-mounted diffuser (Magnier et al., 2012)				
	Height [m]	0.56			0.7		1.3	
Supply flow rate [m ³ /s]	Not specified			0.035		0.032		
Perforated area [m ²]	0.188			0.054		0.116		
Supply under-temperature [°C]	Not specified			2.4	5.0	6.5	2.5	5.5
Archimedes number at supply	1.5	4.6	8.4	5.3	11.1	14.4	12.3	27.0
Minimum thickness in the jet [m]	0.12	0.11	0.08	0.14	0.12	0.11	0.10	0.08

Correlation and discussion

Preliminary analysis of the minimal thickness leads to the conclusion that the minimum thickness is not directly related to the supply temperature, classical Archimedes number, supply flow rate or height of the diffuser. Experiments with a same Archimedes number or experiments with the same supply temperature can indeed lead to different minimal thicknesses. A deeper analysis of the data however shows that the minimum thickness in the jet can be related to a modified version of the Archimedes number, Ar_Q . This modified Archimedes number is a function of the supply under-temperature, of the height of the diffuser and the supply flow-rate, as described in Equation 5-49. Figure 5-16 plots the minimum thickness in the jet versus the modified Archimedes number Ar_Q for both the author’s and Nielsen’s data.

$$Ar_q = \frac{g \cdot \beta \cdot H_{\text{diff}} \cdot (T_{\text{room}} - T_{\text{supply}})}{Q_{\text{supply}}^2}$$

Equation 5-49

where:

- g is the acceleration of gravity [m/s^2];
- β is the thermal expansion coefficient of air [K^{-1}];
- H_{diff} is the height of the diffuser [m];
- T_{room} is the air temperature in the room, taken in this study as the temperature in the middle of the room at a height of 1.1 m [K];
- T_{supply} is the supply air temperature [K] and;
- Q_{supply} is the supply flow-rate [m^3/s].

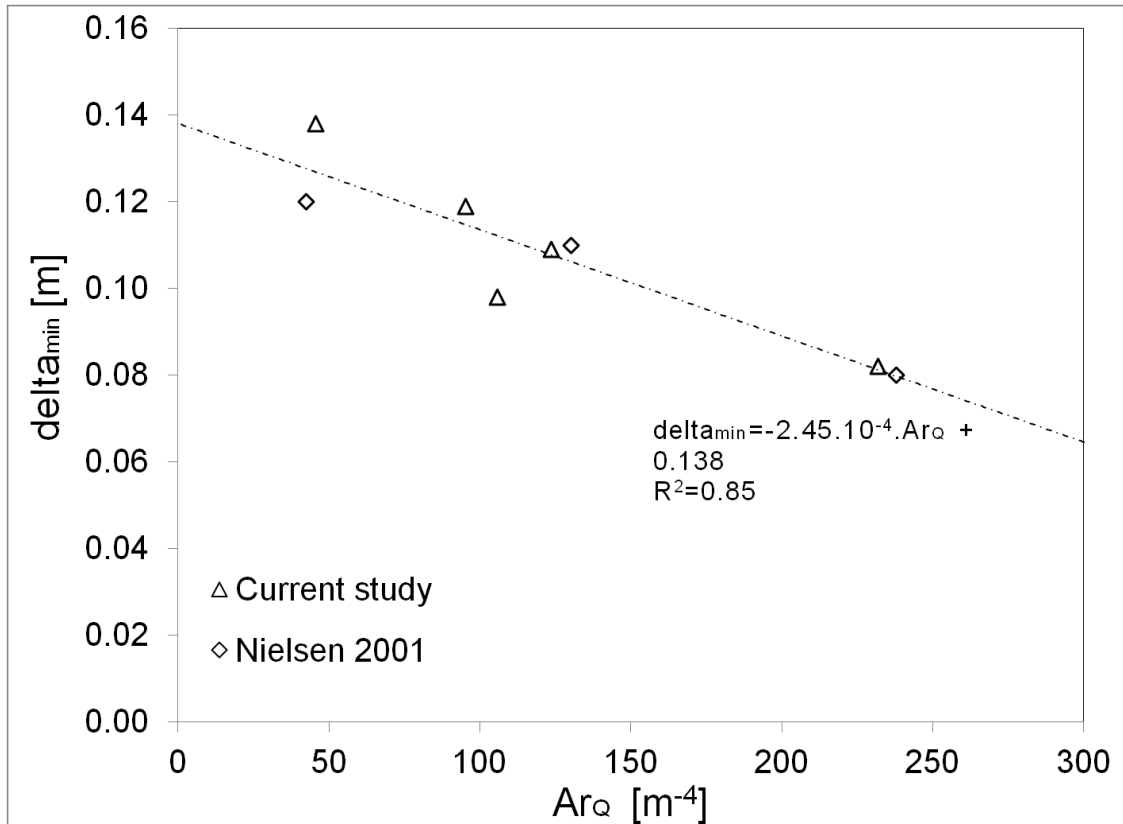


Figure 5-16: Minimal thickness in the jet versus modified Archimedes number

Figure 5-16 shows that the use of the modified Archimedes number Ar_Q enables to get a similar trend for both Nielsen's and the author's results. The minimum thickness also appears to vary linearly with the modified Archimedes number Ar_Q , for the supply conditions and diffuser studied. The minimum thickness in the DV jet can therefore be written as in Equation 5-50. This equation agrees reasonably well with experimental data, with a R^2 value of 0.85 for the three different diffusers and the eight supply conditions studied.

$$\delta_{\min} = -2.45 \cdot 10^{-4} \cdot Ar_q + 0.138 \quad [\text{m}]$$

Equation 5-50

Variation in jet thickness from the minimum thickness δ_{min}

Data used and normalization

The variation in jet thickness has been studied using the author's data described in section 5.4. In order to represent the variation in jet thickness, the author proposes to use the local normalized under-temperature in the jet (Equation 5-51). From a physical point of view, the local normalized under-temperature in the jet is representative of the local buoyancy forces acting on the jet. Figure 5-17 plots the variation of the jet thickness, in the axial plane, for all cases studied against the local normalized under-temperature (see Table 5-8), defined as follows:

$$\Delta T_{norm}(X, Y) = \frac{T_{1.1\text{ m}} - T_{min}(X, Y)}{T_{1.1\text{ m}} - T_{supply}}$$

Equation 5-51

where:

- $\Delta T_{norm}(X, Y)$ is the local normalized under-temperature, at a distance X from the diffuser and a distance Y from the axis of the diffuser [-];
- $T_{min}(X, Y)$ is the minimum air temperature in the jet at a distance X from the diffuser and a distance Y from the axis of the diffuser [K];
- $T_{1.1\text{ m}}$ is the air temperature measured in the center of the room at a height of 1.1 m [K], and;
- T_{supply} is the supply air temperature [K].

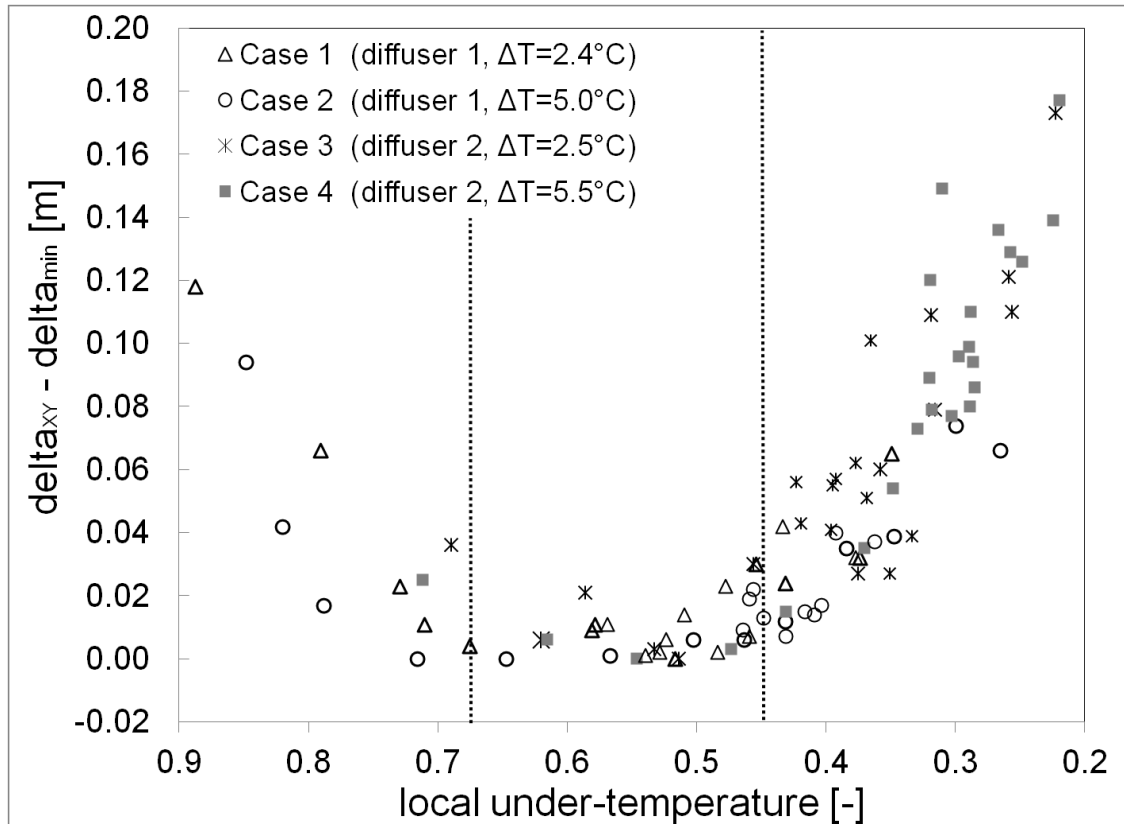


Figure 5-17: Thickness of the jet versus the normalized local under-temperature for the four cases studied (dotted-lines for eye-guiding)

In Figure 5-17, the three regions of thickness variation already mentioned can be noticed. The advantage of the representation in terms of normalized local under-temperature is that the extents of the three regions now mostly coincide for the four cases studied and that the division of the thickness variation in three regions can now be explained in physical terms. The first region, for high local under-temperatures, corresponds to the primary zone of the DV jet. In this region, the buoyancy forces acting on the jet are strong, which leads to a fast decrease in the jet thickness. The second and third regions correspond to the secondary zone of the DV jet, and show respectively a stagnation and an increase in jet thickness.

This division of the jet variation in the secondary zone in two regions may appear unintuitive, as one would rather expect a monotonic behavior for the increase of the jet thickness, as it is the case for isothermal wall-jets. A possible explanation for this phenomenon, based on the

buoyancy forces on the jet, could be as follows. At the beginning of the secondary zone of a DV jet, the under-temperatures in the jet are still high, indicating relatively strong buoyancy forces acting on the flow. Those buoyancy forces are not strong enough to further reduce the thickness of the flow, but are nonetheless strong enough to prevent its thickening. When the local under-temperature reaches 0.45, the density difference between the jet and the air layer just above of the jet gets sufficiently small so that mixing and entrainment occurs. This entrainment leads to an increase in the jet thickness; this is region 3 in Figure 5-17.

Correlation

Based on the experimental data, a correlation can be developed for the jet thickness variation along the longitudinal axis in the secondary zone of a DV jet. The correlation developed is described in Equation 5-52 and illustrated in Figure 5-18. The correlation is found using the least square errors method, with a resulting coefficient of determination R^2 of 0.89. The correlation therefore shows good agreement with the experimental data and can explain the variation in jet thickness in the longitudinal vertical plane.

$$\delta_{XY} = \begin{cases} \delta_{\min} + 0.011 & \text{if } \Delta T_{\text{norm}}(X, Y) \geq 0.44 \\ \delta_{\min} + 0.011 + 0.68 \cdot (0.44 - \Delta T_{\text{norm}}(X, Y)) & \text{if } \Delta T_{\text{norm}}(X, Y) \leq 0.44 \end{cases} \quad \text{Equation 5-52}$$

where:

- δ_{XY} is the jet thickness at a distance X from the diffuser and a distance Y from the axis of the diffuser [m];
- δ_{\min} is the minimum thickness reached in the jet for a given diffuser and supply conditions [m], and;

- $\Delta T_{\text{norm}}(X,Y)$ is the under-temperature at a distance X from the diffuser and a distance Y from the axis of the diffuser [-].

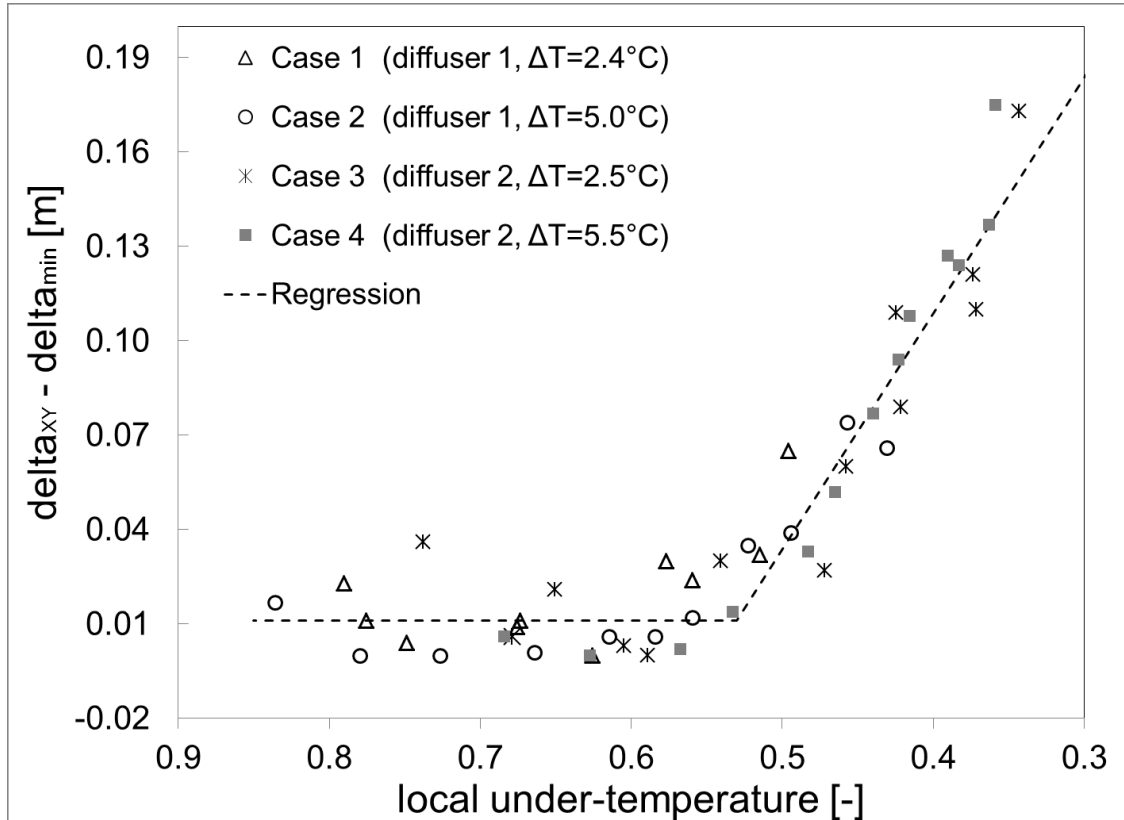


Figure 5-18: Thickness of the jet as a function of normalized local under-temperature in the secondary zone (Axial?) and regression model

General model of the thickness in the secondary zone of a DV jet

Combining the model presented in Equation 5-50 and Equation 5-52, a complete model for the thickness of a DV jet in the secondary zone on the longitudinal axis can be found (Equation 5-53). Figure 5-19 plots the jet thickness calculated using Equation 5-53 versus the jet thickness from experimental data, in the longitudinal planes in the secondary zone, for the four cases studied.

$$\delta_{XY} = \begin{cases} -2.45 \cdot 10^{-4} \cdot Ar_q + 0.011 & \text{if } \Delta T_{norm}(X, Y) \geq 0.44 \\ (-2.45 \cdot 10^{-4} \cdot Ar_q + 0.011) + 0.68 \cdot (0.44 - \Delta T_{norm}(X, Y)) & \text{if } \Delta T_{norm}(X, Y) \leq 0.44 \end{cases} \quad \text{Equation 5-53}$$

where:

- δ_{XY} is the jet thickness at a distance X from the diffuser and a distance Y from the axis of the diffuser [m];
- AR_Q is the modified Archimedes number defined in Equation 5-49 [$m^{-4}s^{-2}$], and;
- $\Delta T_{norm}(X, Y)$ is the under-temperature at a distance X from the diffuser and a distance Y from the axis of the diffuser (Equation 5-51) [-].

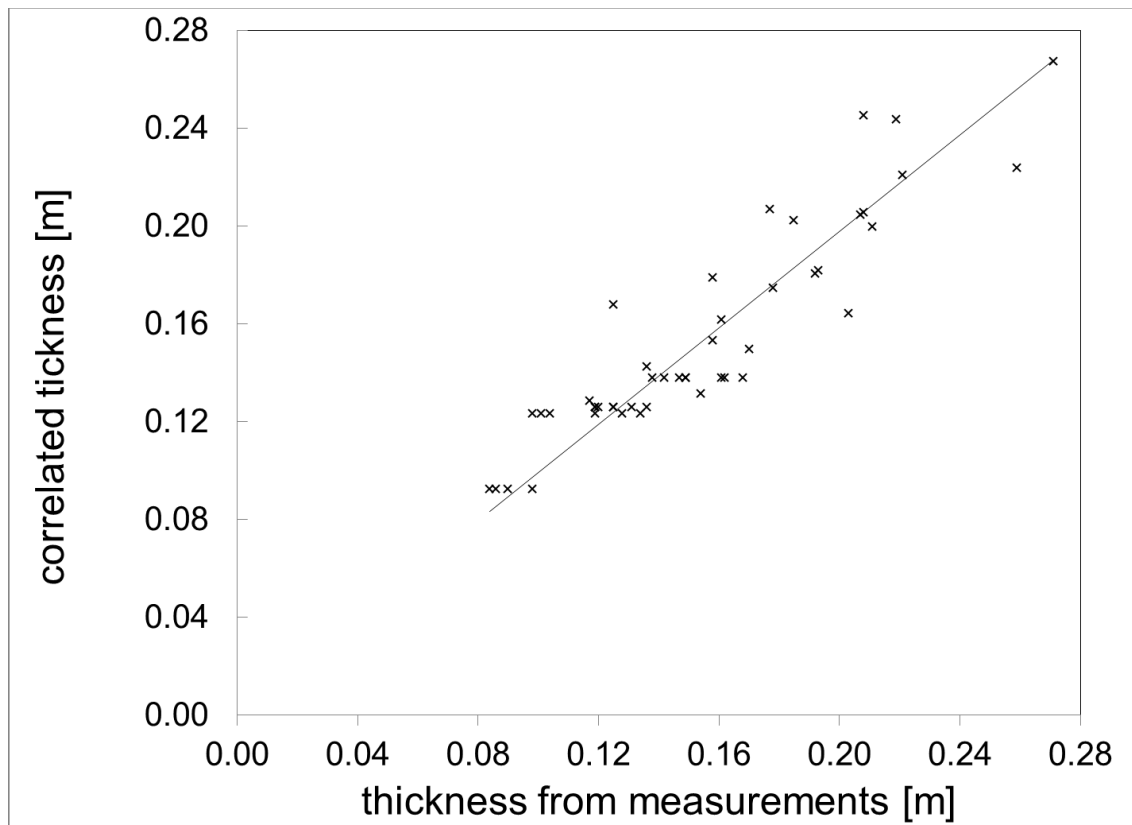


Figure 5-19: Predicted versus measured thickness in the secondary zone

As shown in this figure, the agreement with the experimental data is relatively good, with errors in estimated thickness being generally lower than 0.02 m. These errors are considered to be acceptable, especially considering the different errors introduced in the analysis by normalizations and measurement uncertainties. Equation 5-53 is able to predict the minimum thickness in the jet based on the supply and diffuser characteristics and to predict the thickness variation in the secondary zone based on the minimum temperature profile, for any location on the longitudinal axis in the secondary zone.

Discussion

The developed correlation enables predicting the thickness of a DV jet in the secondary zone. Combined with the results of section 5.4, the maximal air speed in the jet –predominant for thermal comfort and predicted by air speed model – can be used to evaluate the air speed at a height of 0.10 m – used in air comfort standards and in many field studies, or vice versa,

The reference temperature used to calculate the under-temperature might be a source of error. The reference temperature has to be close enough to the jet to represent the actual buoyancy forces acting on the jet, while being far enough for the jet not to be affected by it. Choosing the appropriate height for the reference temperature is therefore complex. For instance, preliminary calculations showed that using a reference temperature measured at a height of 0.6 m leads to slightly better correlations than using a reference temperature at a height of 1.1 m. In this study, the reference height of 1.1 m is nonetheless kept for practicality as it is a standard height to assess the room temperature in a room equipped with DV system.

The study of the jet thickness as a function of the under-temperature provides an explanation of the variation of thickness in the longitudinal plane. The division of the secondary zone in two regions based on the normalized local under-temperature also explains why the last region is absent in some DV jets (as in Nielsen, 2000). In some cases, the local under-temperature in the

jet might never be smaller than 0.44 for a range of distances from the diffuser and, therefore, the steep increase of the third region does not occur, leading to an almost constant jet thickness in the secondary zone. It should finally be noted that the developed correlation implies that the local air speed in the jet does not influence the thickness variation. This result is in agreement with isothermal turbulent wall-jet where the local air velocity is not an influential parameter for the jet thickness increase (Rajaratnam, 1976).

5.6.2 Thickness of a DV jet in the transversal plane

Variation in jet thickness over the transversal axis

The thickness of a DV jet outside the longitudinal axis has never been studied in the literature. Figure 5-20 plots the jet thickness at different distances from the longitudinal axis for each case studied.

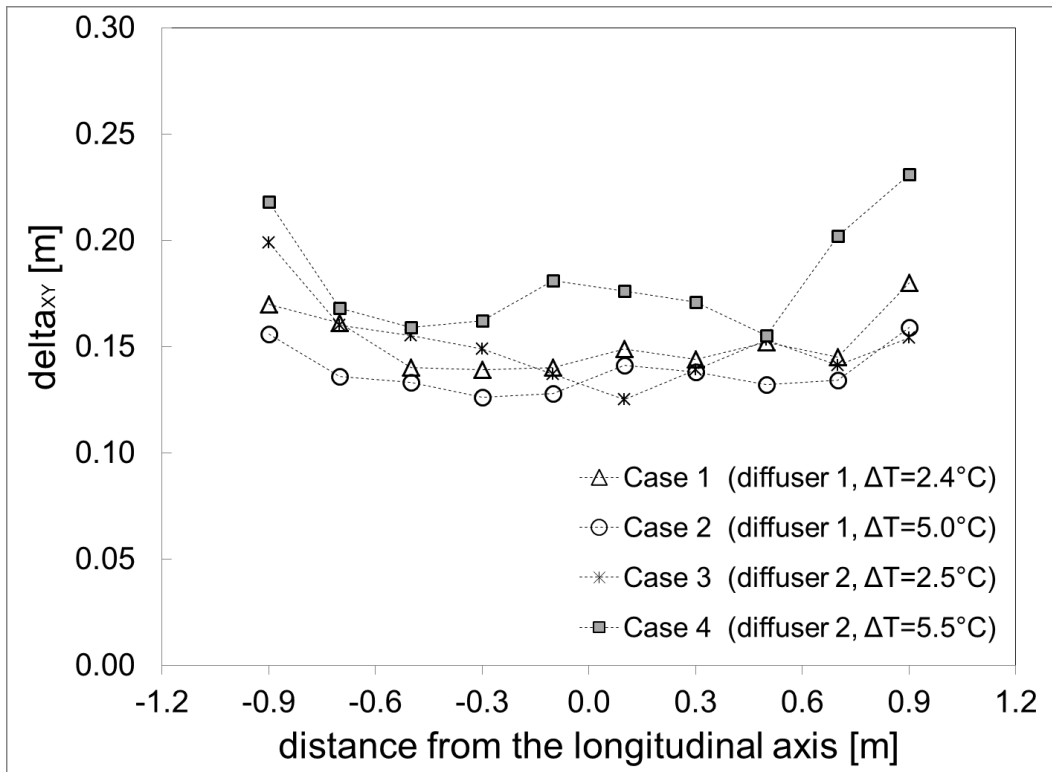


Figure 5-20: Thickness in the jet versus distance from the longitudinal axis, at a distance 2.16 m from the diffuser

Figure 5-20 shows that the thickness of the jet is not constant on the transversal axis, but rather increases with increasing distances from the longitudinal axis. The extent of this increase is different for each case studied and is relatively small (order of a few centimeters). A careful reminder is however that the analysis presented here is based on vertical profiles measured up to 0.9 m from the axis. Further distances from the longitudinal axis should be studied to determine how the jet thickness varies far from the axis. Also, our experimental data is based on measurements at 2.16 m from the diffuser, hence relatively far in the secondary zone, where the transversal profiles of air speeds and temperature are relatively uniform. Closer to the diffuser, greater variations in jet thickness might appear. Further measurements and analysis should be performed to study this point.

Correlation for the jet thickness in the transversal plane

As for the correlation developed in the previous section (Equation 5-53), Figure 5-21 shows that the correlation still stands for the variation of thickness over the transversal axis. The agreement is however slightly lower, especially for relatively high distances from the longitudinal axis (more than 0.7 m from the axis). Using data from both the transversal and longitudinal vertical planes, the R^2 coefficient associated with Equation 5-53 is 0.76, which is still acceptable. Overall, Equation 5-53 is considered as valid for the jet thickness of a DV jet in all the secondary zone of a DV jet.

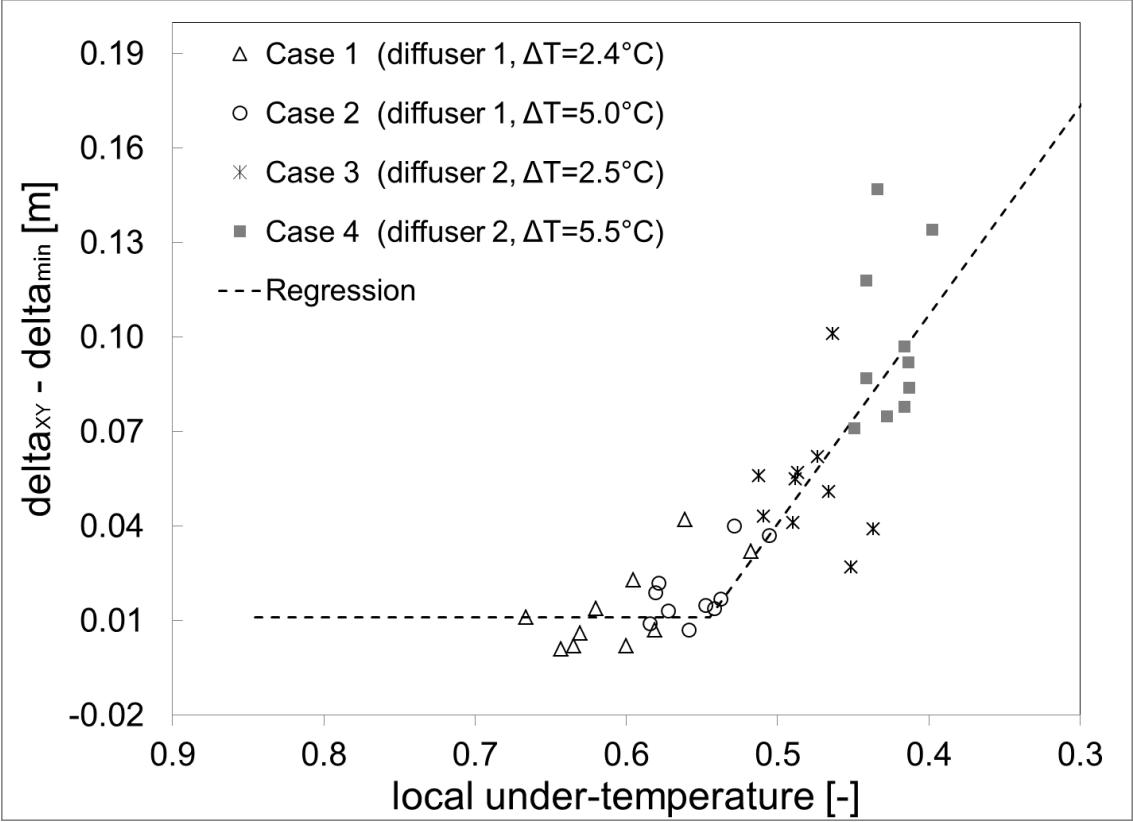


Figure 5-21: Thickness of the jet as a function of local under-temperature in the secondary zone (Transversal)

5.7 Analysis of the transversal air speed profile

5.7.1 Experimental data used and normalization

In order to properly assess thermal comfort, the analysis of the DV jet needs to be performed both along the longitudinal axis and apart from the longitudinal axis. The study of the transversal profiles of air speed in the DV jet is based on measurements performed in two planes (see Chapter 3 for details). As a reminder, the first plane studied is the transversal vertical plane located at 2.16 m from the diffuser, in the secondary zone of the DV jet. Measurements in this plane were performed at several heights from 0.02 m to 0.20 m, at several distances from the longitudinal axis (up to 0.9 m). The other plane studied is the horizontal plane at a height of 0.05 m. In this plane, measurements were performed at several distances from the diffuser and at several distances from the longitudinal axis (up to 0.9 m).

In order to study the air speed profile, the air speed is first normalized as shown in Equation 5-54. Then, the hypothesis of a Gaussian profile states that the normalized air speed should follow Equation 5-55. The inner parenthesis in Equation 5-55 is the dimensionless distance from the diffuser. In Equation 5-55, a parameter b is added to account for the shifting of the flow from the longitudinal axis encountered in the experimental data (see Chapter 3 section 3 for details). The parameter β_{xz} is representative of the width of the jet and corresponds to the distance from the longitudinal axis at which the air speed is equal to 36% of the air speed on the longitudinal axis. This parameter is the parameter of interest in the next subsections.

$$V_{norm_y}(X, Y, Z) = \frac{V(X, Y, Z)}{\max_Y V(X, Y, Z)} \quad \begin{array}{l} \text{Equation} \\ 5-54 \end{array}$$

$$V_{norm_y}(X, Y, Z) = \exp\left(-\left(\frac{Y - b}{\beta_{XZ}}\right)^2\right) \quad \text{Equation 5-55}$$

Where

- Y is the distance from the longitudinal axis [m];
- b is a correction coefficient to account for shifting of the jet [m], and;
- β_{XZ} is the spread parameter at a height Z and a distance X from the diffuser [m].

5.7.2 Vertical transversal plane

Table 5-10 shows the β parameters at different heights in the vertical transversal plane, along with the R^2 coefficients associated with the correlations. This table shows that the Gaussian profile is generally appropriate for the transversal air speed profile, with R^2 coefficient generally higher than 0.75. Figure 5-22 plots the normalized air speed from measurements against the dimensionless distance from the axis for all profiles studied. The theoretical Gaussian profile is also plotted on this figure. As can be seen, the agreement between experimental data and the theoretical Gaussian profile is acceptable.

Table 5-10: β and R^2 coefficients in the transversal vertical plane for different heights

		0.02 m	0.03 m	0.04 m	0.05 m	0.06 m	0.07 m	0.08 m	0.10 m	Average
Diffuser 0.6mx0.6 m $\Delta T=2.4$ °C	β_{XZ}	1.22	1.25	1.27	1.26	1.25	1.26	1.25	1.50	1.25
	R^2	0.99	0.98	0.94	0.91	0.74	0.82	0.69	0.54	0.95
Diffuser 0.6mx0.6 m $\Delta T=5.0$ °C	β_{XZ}	1.54	1.64	1.59	1.52	1.57	1.54	1.82	1.76	1.57
	R^2	0.83	0.91	0.96	0.95	0.77	0.85	0.88	0.29	0.91

Diffuser 1.2mx0.6 m $\Delta T=2.5\text{ }^{\circ}\text{C}$	β_{xz}	1.77	1.86	1.77	1.76	1.81	2.00	2.04	1.70	1.79
	R^2	0.84	0.94	0.88	0.51	0.54	0.76	0.64	0.79	0.80
Diffuser 1.2mx0.6 m $\Delta T=5.5\text{ }^{\circ}\text{C}$	β_{xz}	1.44	1.59	1.48	1.48	1.44	1.54	1.55	1.67	1.50
	R^2	0.80	0.82	0.85	0.84	0.61	0.75	0.71	0.69	0.82

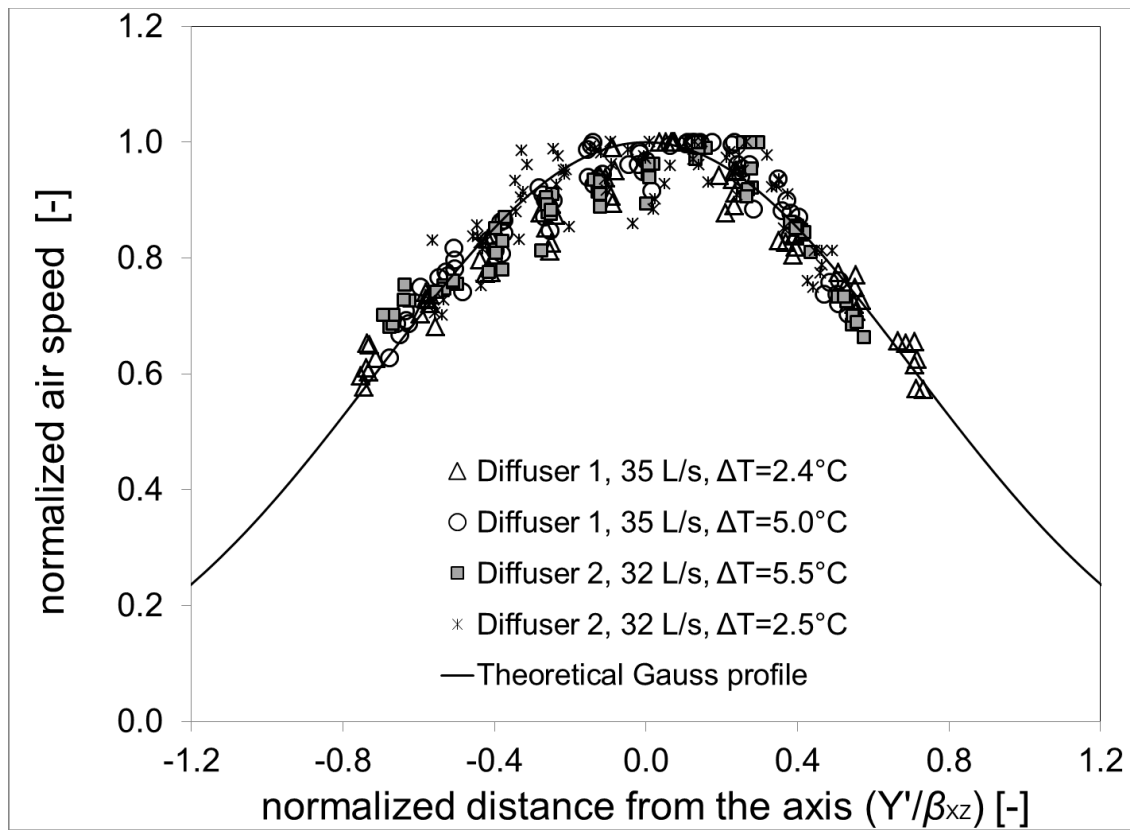


Figure 5-22: Dimensionless transversal air speed profiles in the vertical transversal plane

Analysis of Table 5-10 shows that, for a given supply condition and at a given longitudinal distance from the diffuser, the β parameters are similar for all heights. An average β coefficient can then be used, as shown in the last column of Table 5-10. The coefficients of determination R^2 associated with using an average coefficient are higher or equal to 0.8, indicating a relatively

good agreement with experimental data. Thus, the transversal profile of normalized air speed in a DV jet, at a given distance from the diffuser in the secondary zone, can be considered as independent of height, for height lower than or equal to 0.10 m. In practical terms, this means that one height of measurement (0.10 m for instance) is sufficient to assess the lateral spreading of the jet at a given distance from the diffuser.

5.7.3 Transversal profiles of air speed in the horizontal plane

The analysis described in the previous section has been repeated for the measurements performed in the horizontal plane at a height of 0.05 m. Table 5-11 shows the β coefficients found for each case at different distances from the diffuser, along with the R^2 coefficients associated with the correlations. Figure 5-23 plots the normalized air speed from measurements against the dimensionless distance from the axis for all the profiles studied.

Table 5-11: β and R^2 coefficients at different distances from the diffuser in the horizontal plane

		0.16 m	0.56 m	0.96 m	1.36 m	1.76 m	1.96 m	2.16 m	2.36 m	2.56 m	2.76 m
Diffuser 0.6m x 0.6 m $\Delta T = 2.4$ °C	β_{xz}	N.A	N.A	0.82	1.02	1.17	1.20	1.27	1.30	1.75	1.43
	R^2	N.A	N.A	0.82	0.97	0.98	0.96	0.91	0.61	0.83	0.86
Diffuser 0.6m x 0.6 m $\Delta T = 5.0$ °C	β_{xz}	N.A	N.A	1.03	1.06	1.33	1.44	1.52	1.76	2.20	2.08
	R^2	N.A	N.A	0.99	0.95	0.93	0.87	0.95	0.82	0.87	0.92
Diffuser 1.2m x 0.6 m $\Delta T = 2.5$ °C	β_{xz}	N.A	1.15	1.18	1.31	1.43	1.69	1.76	2.11	1.75	2.24
	R^2	N.A	0.93	0.91	0.84	0.95	0.94	0.51	0.57	0.40	0.33
Diffuser 1.2m x 0.6 m $\Delta T = 5.5$ °C	β_{xz}	N.A	0.87	1.04	1.21	1.32	1.49	1.48	1.96	1.84	1.87
	R^2	N.A	0.96	0.94	0.96	0.96	0.86	0.84	0.65	0.61	0.74

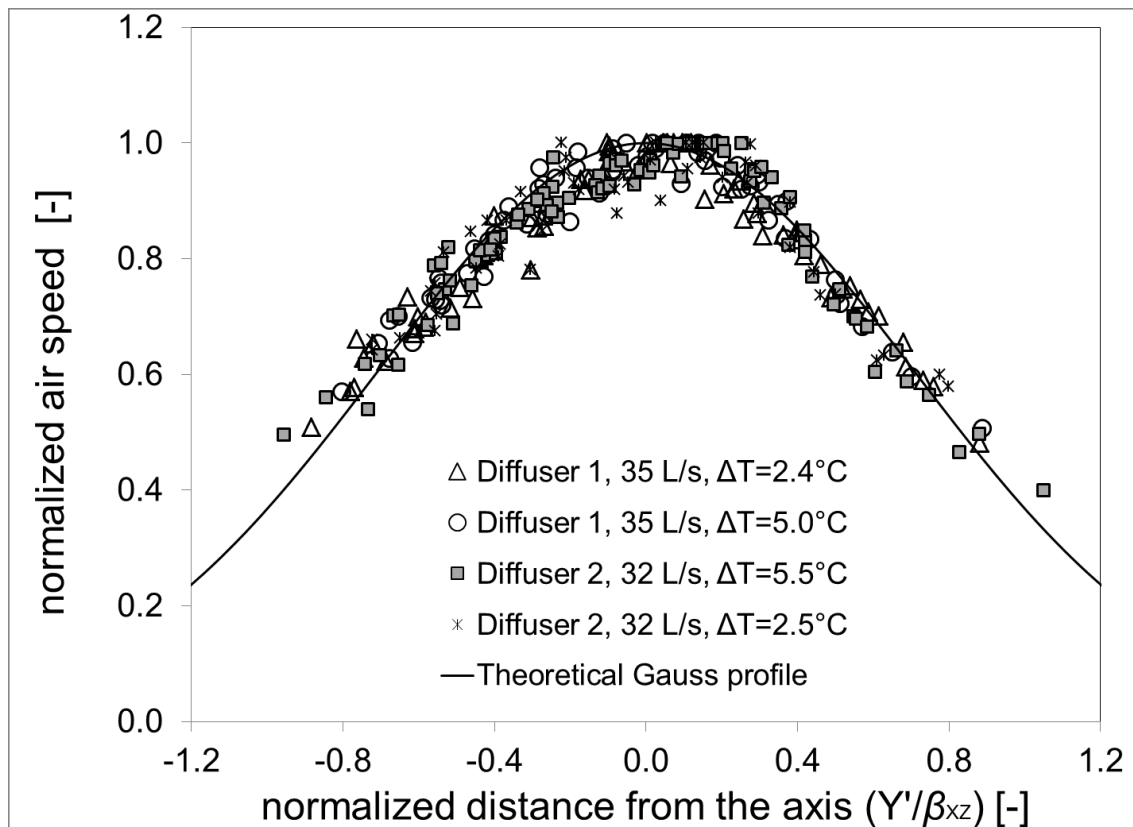


Figure 5-23: Dimensionless transversal air speed profiles in the horizontal plane

Figure 5-24 and Figure 5-23 show that the Gaussian profile describes well the transversal profile of air speed in a DV jet, except very close to the diffuser and far from the diffuser. The profile is not applicable close to the diffuser due, probably, to the height of measurement (0.05 m). Close to the diffuser, the jet is not yet in contact with the floor and therefore measurements at 0.05 m are not representative of the jet (see Chapter 3 for details). As for greater distances from the diffuser, Table 5-11 shows that the β coefficients increase with distance from the diffuser. This indicates that the transversal profile of air speed becomes more and more uniform away from the diffuser. Far from the diffuser, the variations of air speed compared to the air speed measured along the longitudinal axis are relatively small. Eventually, these variations fall within

the measurements uncertainty, which explains the small R^2 coefficients. Overall, the Gaussian profile is nonetheless found applicable to represent the transversal variation of air speed in a DV jet.

As for the β coefficients, Table 5-11 shows that the coefficients are different for each supply conditions studied and each distance from the diffuser. One general conclusion is that, for a specific of diffuser and under-temperature, the β coefficients increase with the distance from the diffuser. Further analysis shows that this increase is linear with the distance from the diffuser (Figure 5-24). The rate of increase is however different for each supply condition or diffuser. No relation with other flow parameters (air speed, thickness, temperature, etc.) or dimensionless numbers could be found to predict the slopes.

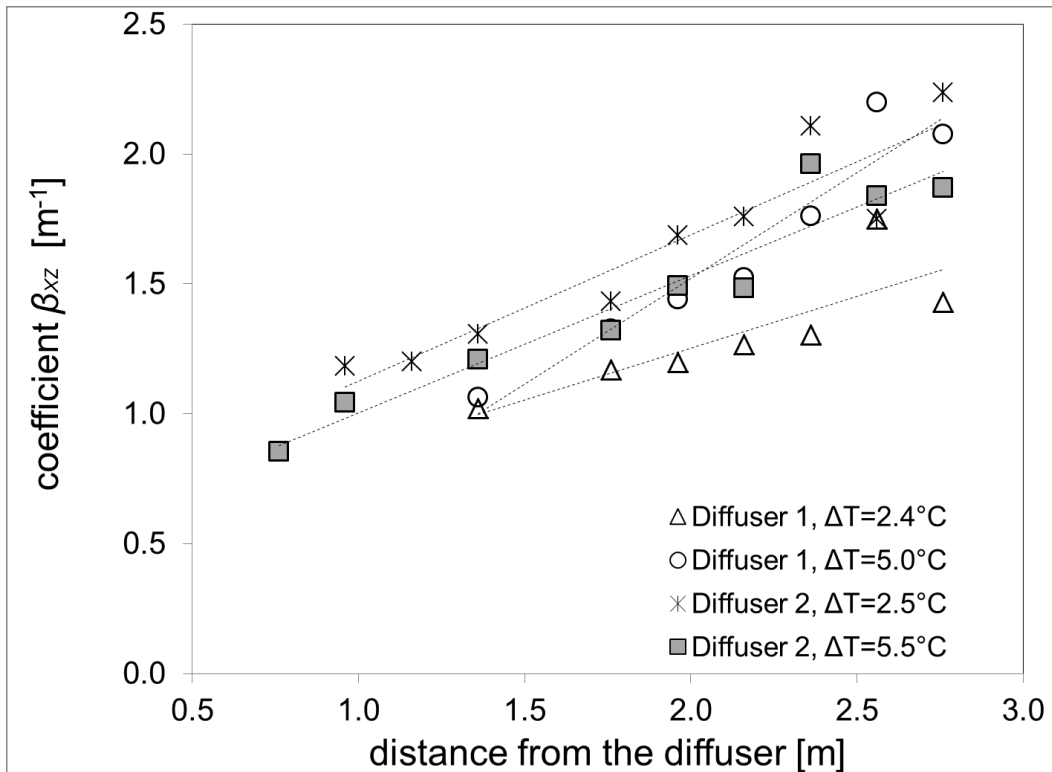


Figure 5-24: Spread coefficients in the secondary zone at different distances from the diffuser

Additional discussion

The study of the transversal profiles of air speed in the vertical transversal plane and the horizontal plane shows that the Gaussian profile can relatively well represent the transversal profile of air speed in the secondary zone of the DV jet. Our analysis also shows that the transversal profile of normalized air speed is independent of height for height within the 0.02 m to 0.10 m range. As the distance from the diffuser increases in the secondary zone, the transversal profile of air speed becomes more and more uniform. The β coefficients appear to increase linearly with the distance from the diffuser in the secondary zone. More studies are required to relate this increase with other flow parameters. In terms of comfort, the analysis shows that the transversal profile of air speed is to be taken into account at the beginning of the secondary zone. Indeed, experimental data shows that, at the beginning of the primary zone, the air speed on the longitudinal axis can be significantly different from the air speed at 0.9 m from the longitudinal axis. Further in the secondary zone, the flow becomes more uniform and the air speed away from the longitudinal axis can be taken as equal to the air speed measured on the longitudinal air speed, as a first approximation for comfort assessment.

A noteworthy comment is that, in the experimental set-up used for this study and despite careful settings, the jet slightly shifts from the longitudinal axis as the distance from the diffuser increases. This calls for an increased attention in further measurements to make sure the jet is perfectly central, in order to accurately study the longitudinal profile of air speed. In the measurements, due to the fact that the jet was not perfectly centered, the maximum air speed in the jet (see section 4.3) was slightly underestimated. An analysis performed by the author however shows that the results developed in the section 4.3 are still valid, as the underestimation of the maximum air speed is in the order of 0.01 m/s, i.e. below the experimental error.

5.8 Analysis of the temperature distribution in the DV jet

The temperature distribution in the DV jet has attracted less interest in the literature than the study of the air speed distribution. Significantly less data is available and correlation models are rare. Current correlation models such as Mundt's model (1996) only focus on the average temperature in the jet. On the other hand, experimental results show that the temperature in the jet varies significantly with the distance from the diffuser and to lesser extent with the distance from the longitudinal axis and the height. This in turn affects significantly comfort metrics such as the temperature difference between the head and ankles. The purpose of this section is to discuss the temperature distribution in the DV jet based on the experimental data presented in Chapter 4.

5.8.1 Variation of temperature along the longitudinal axis

Variation of temperature in the primary zone

The temperature change in the primary zone is a complex phenomenon. In the primary zone, the jet temperature changes mainly due to mixing and entrainment of indoor air. As mentioned above, there is currently no formula to predict the entrainment of room air. Another difficulty comes from that the temperature of the mixing air is also unknown. Indeed, the temperature of the air in the room changes with height due to thermal stratification. As shown in the measurements (see section 3.3), the temperature of the air directly above the jet also varies with distance from the diffuser. Finally, for the diffusers tested, mixing occurs both on the upper layer of the jet and in the space between the lower layer of the jet and the floor, at the diffuser exit. Determining which temperature to take into account for entrainment is therefore extremely difficult in this case. Thus, the full understanding of the temperature field in the primary zone of a V jet is left outside the scope of this thesis and the study of the temperature

distribution is focused on the secondary zone. In terms of thermal comfort, the secondary zone is also the only important zone to study, as the air speed in the primary zone is already outside of comfort range.

Normalization of the minimal air temperature in the secondary zone

This section focuses on the minimal temperature measured at a given longitudinal distance from the diffuser (T_{min}). The study of the temperature field in the secondary zone follows the same concept as the one used in the study of air speed distribution, in saying that the secondary zone can be considered independently from the primary zone. The following normalization is proposed. First, the distance from the diffuser is reinitiated using the same formula as in section 5.4 (Equation 5-56). It can be noted that the length of the primary L_{pz} remains defined in terms of maximal air speed, and not temperature. Then, the under-temperature in the jet is normalized with respect to the minimal temperature reached at the end of the primary zone, as shown in Equation 5-57. From a physical standpoint, the normalized under-temperature as described in Equation 5-57 is representative of the buoyancy forces acting from the room on the jet. The normalized under-temperature written in Equation 5-57 takes its maximum (1) when the air temperature in the jet is equal to the air temperature at the end of the primary zone and becomes null when the air temperature in the jet reaches the room air temperature, where no buoyancy force is present.

$$\xi = X - L_{pz}$$

Equation 5-56

Where:

- X is the distance from the diffuser [m] and;
- L_{pz} is the length of the primary zone [m].

$$\Delta T_{norm}(\xi) = \frac{T_{1.1\text{ m}} - T_{min}(\xi)}{T_{1.1\text{ m}} - T_{EPZ}} \quad \text{Equation 5-57}$$

where:

- $\Delta T_{norm}(\xi)$ is the normalized under-temperature at a distance ξ from the diffuser [-];
- $T_{min}(\xi)$ is the minimum air temperature in the jet at a distance ξ from the diffuser [°C];
- $T_{1.1\text{ m}}$ is the air temperature measured in the center of the room at a height of 1.1 m [°C], and;
- T_{EPZ} is the minimum air temperature in the jet at the end of the primary zone [°C].

Figure 5-25 and Figure 5-26 show the longitudinal profile of minimum temperature in the secondary zone, respectively before and after normalization. As shown in Figure 5-25, before normalization, large differences of temperature amplitudes and variations appear between the different cases. Figure 5-26 shows that, after normalization, the normalized profiles of air temperature become very similar. This demonstrates that the normalization proposed is efficient for the data studied.

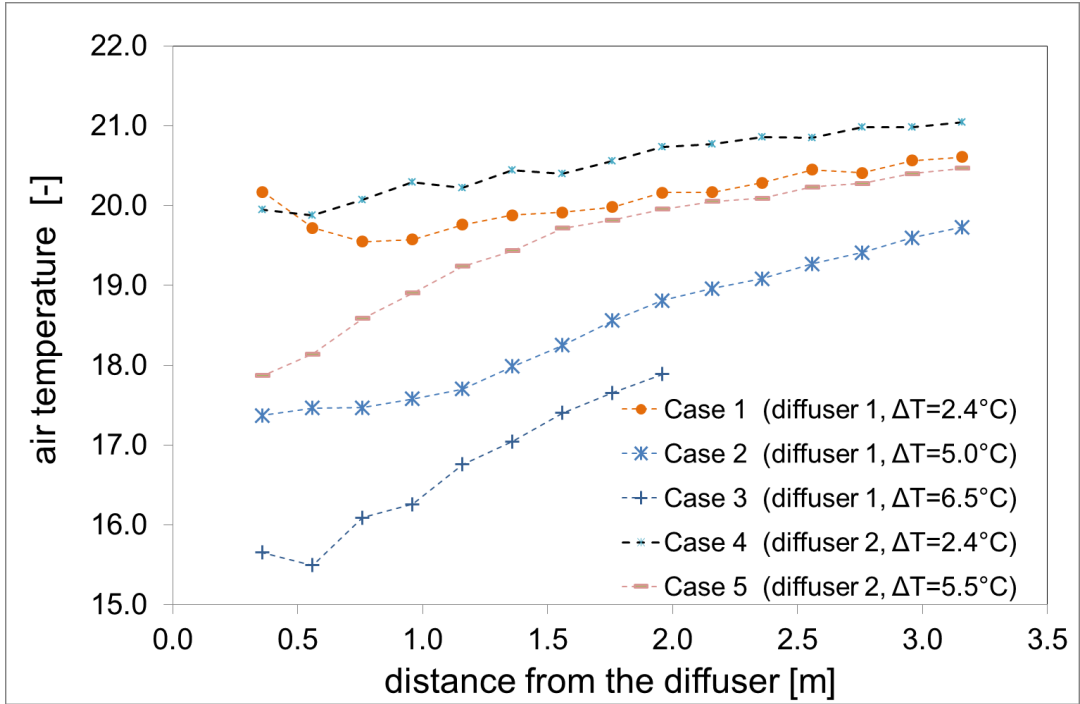


Figure 5-25: Longitudinal profile of minimal temperature in the jet for different cases

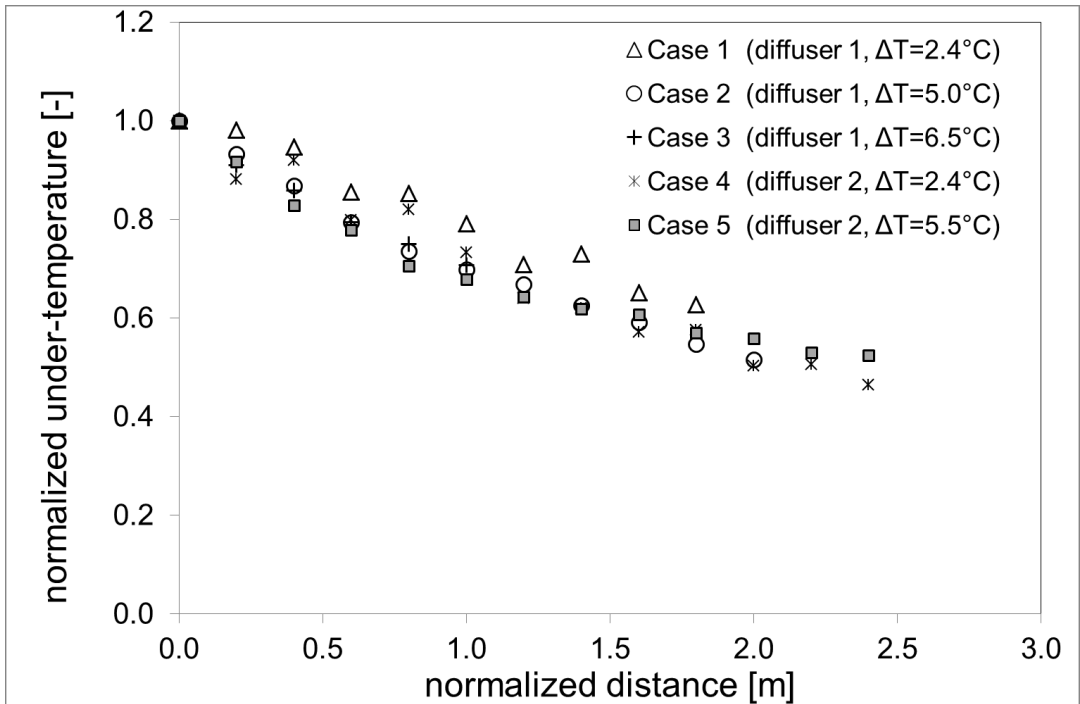


Figure 5-26: Normalized profiles of minimal temperature in the secondary zone for different cases

Regression on the normalized profile of temperature

Based on the normalized under-temperature data, a correlation analysis can be performed. Regression analysis shows that the normalized profile of temperature can be described by Equation 5-58. The coefficient of determination R^2 associated with this regression is 0.94, showing a good agreement with experimental data. The under-temperatures from measurements and correlated using Equation 5-58 are plotted on Figure 5-27.

$$\Delta T_{norm}(\xi) = \frac{1}{1 + 0.393 \cdot \xi} \quad \text{Equation 5-58}$$

where:

- ΔT_{norm} is the normalized under-temperature at a distance ξ [-], and;
- ξ is the distance from the end of the primary zone [m].

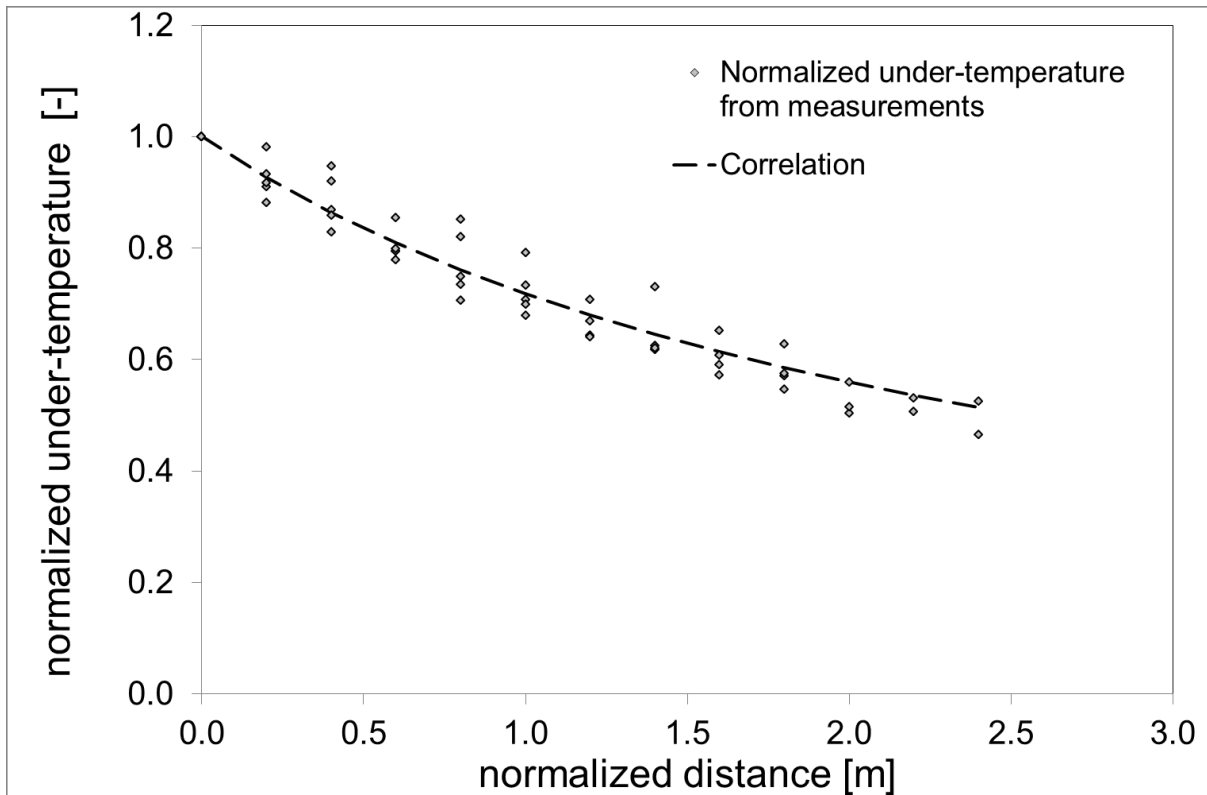


Figure 5-27: Correlation for the normalized under-temperature profile in the secondary zone and results from different cases.

Final formulation for the longitudinal profile of minimum air temperature in the secondary zone of a DV jet

Combining Equation 5-57 and Equation 5-58, the minimum air temperature in the jet at different distances from the diffuser can be predicted using into Equation 5-59. Equation 5-59 has been found applicable for the two diffusers and the five supply conditions tested in this study. Figure 5-28 shows the comparison between the minimum air temperature measured in the jet for the different cases and the air temperature calculated using Equation 5-59. The R^2 coefficient between the measured and correlated data is 0.99, showing an excellent agreement between measurements and correlation. The average error is 0.1°C , inferior to the uncertainty of measurements (0.5°C).

$$T_{min}(X) = T_{1.1m} - \frac{T_{1.1m} - T_{EPZ}}{1 + 0.393 \cdot (X - L_{PZ})}$$

Equation 5-59

Where:

- $T_{min}(X)$ is the minimum air temperature at a distance X from the diffuser [°C];
- $T_{1.1m}$ is the air temperature measured in the center of the room at a height of 1.1 m [°C];
- T_{EPZ} is the minimum air temperature in the jet at the end of the primary zone [°C], and;
- L_{PZ} is the length of the primary zone [m].

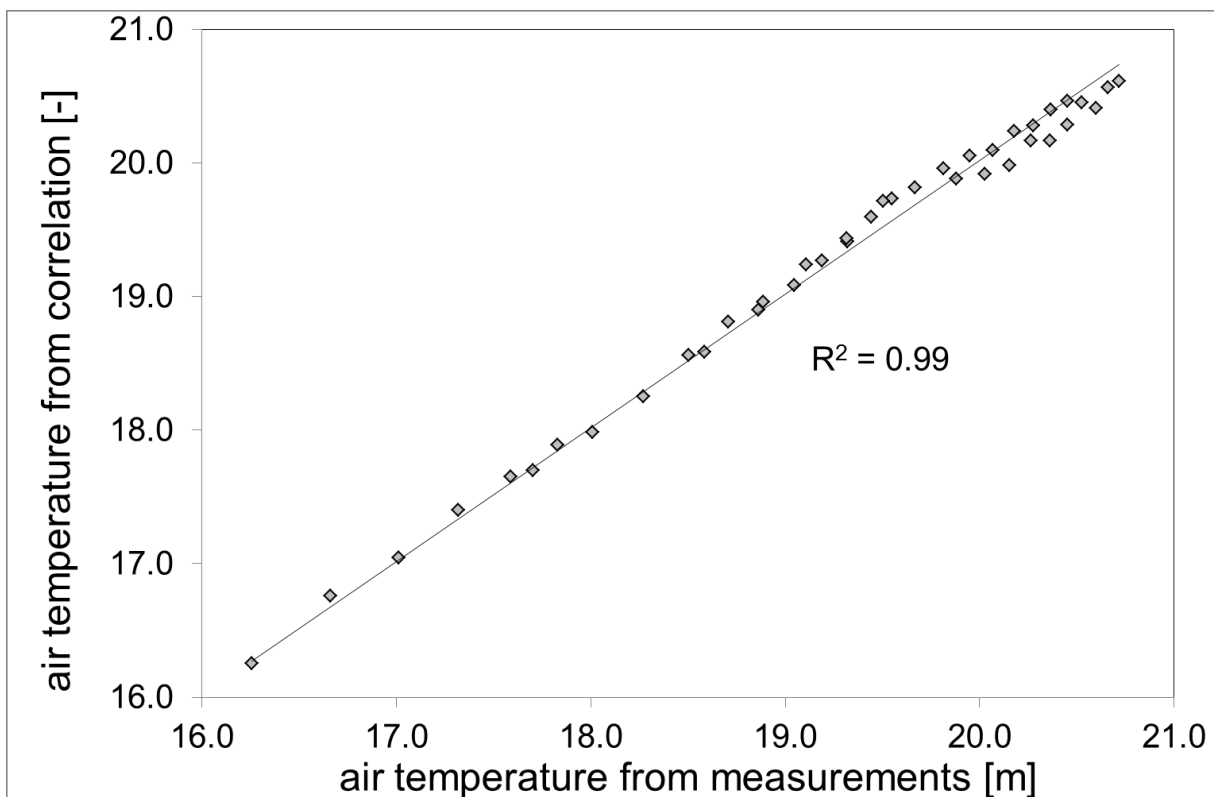


Figure 5-28: Measured versus correlated air minimum temperature in the jet at different distances from the diffuser

5.8.2 Discussion on the transversal and vertical profiles of temperature in the jet

The vertical and transversal profiles of temperature in the secondary zone of a DV jet have seldom been studied in the literature. Some correlations can be found in literature for the vertical profiles of temperature in non-isothermal jets (Chen 2001; Amiri et al. 1996). These correlations were however not applicable for the profiles measured in this study. A major problem found by the author in the study of the temperature profiles is that a normalizing equation is required to be able to analyze together the profiles at different positions in the room. None of the normalization proposed in the literature were however found valid for the specific case of a DV jet. Despite numerous attempts, the author could either not develop a satisfying normalization equation. The main problem for proposing a normalizing equation is to determine the appropriate reference temperature. In classical non-isothermal wall-jet analysis (Chen 2001), a stable reference temperature can be used, as all surroundings are at a uniform temperature. In the specific case of a DV jet, the temperature distribution in the jet is influenced both by the surrounding air and by the floor surface temperature. As for the room air, its temperature varies with height, due to thermal stratification. In addition, at low heights outside the jet (0.26 m or 0.6 m for instance), the air temperature is also dependent on the distance from the diffuser. The surface temperature of the floor, in turn, is also dependent on the position in the room. Further, a significant difference appears between the floor temperature and the air temperature at 0.26 m. Since the temperature of the surroundings of the jet is not constant, it was impossible for the author to find a reference temperature. No normalization could therefore be developed to analyze together the profiles at different position in the room and, therefore, no correlations could be developed. Numerous attempts were also made to relate the vertical or transversal profiles to local flow parameters or dimensionless numbers, without noteworthy results.

Based on the experimental data gathered through this thesis, general trends can however be formulated. In terms of transversal profiles of temperature, the temperature is minimal on the longitudinal axis and increases as the distance from the axis increases. The extent of this

increase, measured to be 0.9 m span on both sides of this axis, is found to be lower than or equal to 1°C in the secondary zone. As the distance from the diffuser increases, the jet spreads and the difference between the centerline temperature and the outer temperature gets lower. In terms of comfort assessment, the temperature on the centerline is lower than that outside the axis and, hence, the discomfort due to temperature difference between head and ankles is higher. The temperature predicted by Equation 5-59, therefore, represents the safest, worst case scenario.

In terms of vertical profile of temperature, the profile is found to change shape with the distance from the diffuser (see Figure 5-29). This change of shape is assumed to be due to the impact of both exchange with room air and heat gain from the floor. Figure 5-30 shows that the air temperatures at 0.02 m from the floor and at 0.10 m from the floor increase at different rates. The air temperature at a height of 0.10 m increases due to mixing with indoor air. On the other hand, the air temperature at a height of 0.02m increases with the distance from the diffuser, due to heat exchange with the floor. As shown in Figure 5-30, the increase in floor temperature follows closely the increase of the air temperature flowing on it. Eventually, the air temperature at 0.02 m from the floor becomes higher than the air temperature at 0.10 m from the floor, changing significantly the vertical temperature profile.

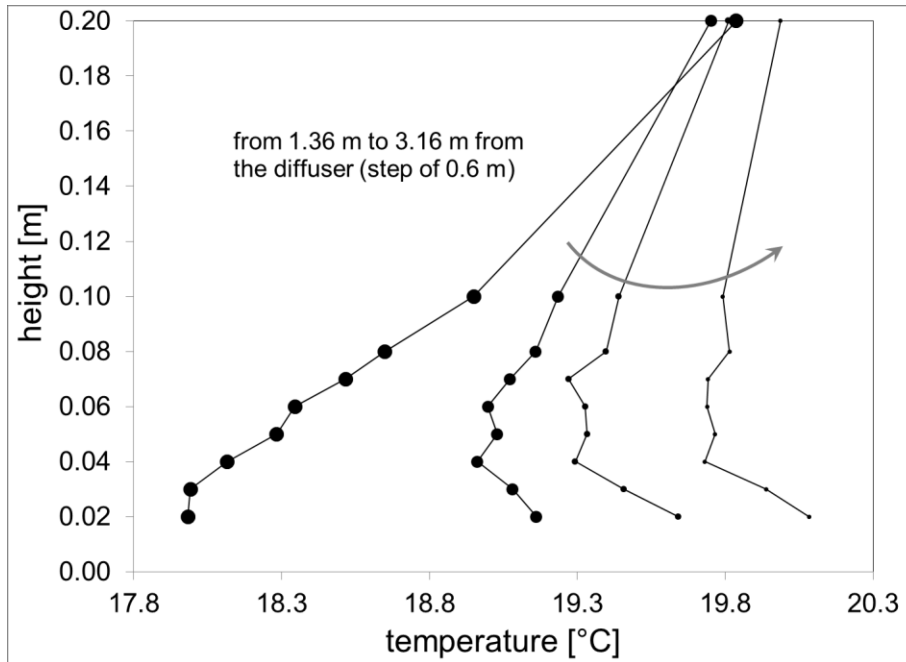


Figure 5-29: Vertical profiles of air temperature in the secondary zone for DF1W diffuser of size 0.6 m x 0.6 m for a supply under-temperature of 5.0°C

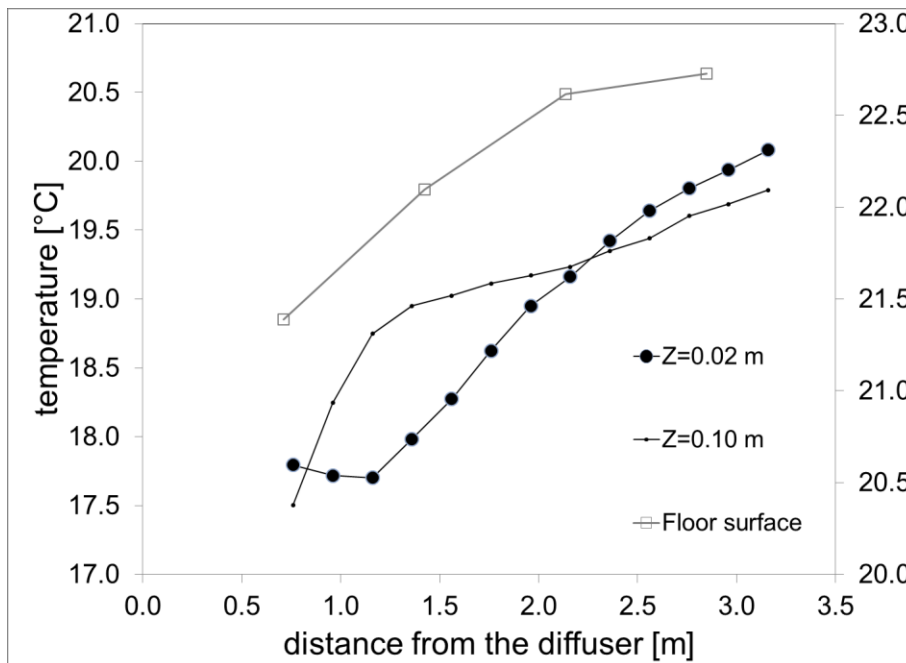


Figure 5-30: Longitudinal profiles of air temperature at heights of 0.02 m and 0.10 m (left axis) and floor temperature (right axis) for DF1W diffuser of size 0.6 m x 0.6 m for a supply under-temperature of 5.0°C

In practical terms, it is nonetheless noteworthy that the temperature difference between heights of 0.02m and 0.10m is relatively small. For the supply conditions and the diffusers studied, the difference between the minimum temperature in the jet and the temperature measured at a height of 0.10 m, for a same distance from the diffuser, is found to be always lower than 0.5°C for distance from the diffuser greater than 1.56 m. This difference of 0.5°C is equal to the experimental error associated with the thermocouples used in experiments. Based on experimental results, for distances from the diffuser greater than 1.56 m, the air temperature at a height of 0.10 m on the longitudinal axis can be approximated, for practical purpose, by Equation 5-59. At a given distance from the diffuser, Equation 5-59 will underestimate the air temperature at a height of 0.10 m, by at most 0.5°C, representing once again the safest worst-case scenario.

5.9 Conclusion

Based on the correlations developed in the previous sections, general equations for the air speed and air temperature in the secondary zone of a DV jet can be formulated.

5.9.1 Final equation for the air speed in the secondary zone of a DV jet

The air speed in the secondary zone of a DV jet can be expressed by the following three-dimensional model (as of X, Y, Z):

$$V(X \geq L_{PZ}, Y, Z) = \frac{2.88 \cdot \gamma}{\sqrt{1 + 1.5 \cdot (X - L_{PZ})^2}} \cdot \sqrt{\left(V_{0.05 \text{ wavg}}^2 + 2 \cdot \left(E_{P0.05 \text{ wavg}} - 0.663 \cdot \frac{g \cdot (T_{\text{room}} - T_{0.05 \text{ wavg}})}{T_{\text{room}}} \cdot \delta_{\text{min}}^* \right) \right)} \cdot \exp\left(-\left(\frac{Y}{\beta_X^*}\right)^2\right) \cdot \left(\frac{Z}{\delta_{XY}^*}\right)^{0.226} \cdot \left[1 - \text{erf}\left(0.752 \cdot \left(\frac{Z}{\delta_{XY}^*}\right)\right)\right] \quad \text{Equation 5-60}$$

Where:

- L_{PZ} is the length of the primary zone [m];
- γ is a factor representing the entrainment of room air in the jet, as defined in section 5.2;
- $V_{0.05 \text{ wavg}}^2$ is a weighted average of the square velocity at 0.05 m from the diffuser [m^2/s^2], as defined in section 5.2;

- $E_{P\ 0.05\ wavg}$ is a weighted average of the potential energy of the DV jet at 0.05 m from the diffuser [m^2/s^2], defined in section 5.2;
- $T_{0.05\ wavg}$ is the weighted average air temperature at 0.05 m from the diffuser [K], as defined in section 5.2;
- δ_{min} is the minimum thickness at the end of the primary zone [m], which can be expressed as in Equation 5-53;
- β_x is a coefficient representing the spreading of the jet, independent of Z, and which increases linearly with the distance from the diffuser [m^{-1}];
- δ_{xy} is the thickness of the jet [m] which can be expressed as in Equation 5-53;
- g is the acceleration of gravity [m/s^2] and;
- T_{room} is the room temperature, taken as the temperature measured in the middle of the room at a height of 1.1 m [K];

Equation 5-60 is found applicable to all the experimental conditions tested, for data from the literature and data from the experimental measurements (Chapter 3). This equation includes: 1. a novel formulation for the air speed decay, independent of the supply temperature, 2. a novel formulation for the vertical air speed profile, specific to DV jets, and 3. additional information regarding the lateral spreading of the jet. Some parameters such as γ or L_{PZ} should be further studied to improve Equation 5-60.

5.9.2 Final equation for the air temperature in the secondary zone of a DV jet

The air temperature in the secondary zone of a DV jet can be expressed by the following three-dimensional model (as of X, Y, Z):

$$T(X \geq L_{PZ}, Y, Z) = \left[T_{1.1\text{ m}} - \frac{T_{1.1\text{ m}} - T_{EPZ}}{1 + 0.393 \cdot (X - L_{PZ})} \right] \cdot F(Y) \cdot F'(Z) \quad \text{Equation 5-61}$$

Where:

- $T(X, Y, Z)$ is the air temperature at a longitudinal distance X from the diffuser, at distance Y from the longitudinal axis and a height Z [°C];
- $T_{1.1\text{ m}}$ is the air temperature measured in the center of the room at a height of 1.1 m [°C];
- T_{EPZ} is the minimum air temperature in the jet at the end of the primary zone [°C];
- L_{PZ} is the length of the primary zone [m];
- $F(Y)$ is a function yet to be determined, reaching its minimum on the longitudinal axis [-] and;
- $F'(Z)$ is a function yet to be determined, however, which can be considered as unity as a first approximation for heights inferior or equal to 0.10 m and sufficiently far from the diffuser (1.56 m in the experimental data used for this analysis) [-].

Equation 5-61 has been found applicable to all the experimental conditions tested. More studies are required to be able to fully understand the interaction between the air temperature in the jet and the floor and room air temperature, in order to be able to further develop Equation 5-61. Despite its limitations, Equation 5-61 can nevertheless be used, omitting functions F and F', to predict the minimal temperature in the jet on the longitudinal axis. This temperature is of primary importance to assess local thermal comfort and temperature difference between head

and ankles. As noted before, the minimal temperature on the longitudinal axis represents the safest worst case scenario. Equation 5-61 can then be used to ensure thermal comfort while designing a DV system. Considering that the air temperature models in the literature consider only the DV jet temperature as an average value, Equation 5-61 represents a significant contribution and a step towards a more complete model.

CHAPTER 6: CONTRIBUTIONS AND FUTURE WORK

In this chapter, a summary of the results and contributions is presented. Future work to expand on this thesis is also proposed.

6.1 Summary and contributions

- The first major contribution of this thesis is the experimental data collected, using a very fine mesh (order of centimeter) and covering the full extent of the jet. All the experimental data from this study is available in the appendix of this thesis, for all the conditions and locations tested. This data can be used by researchers for further analysis and to create or to validate airflow models. The fine mesh data in the jet, including measurements in front of the diffuser, is also very useful to validate CFD models. Throughout the course of this thesis, some new studies have published some new data on DV jets (Rees and Haves, 2013; Fatemi et al. 2013), but never to the extent of the data provided here.
- The experimental data provides a better understanding of the distribution of air speed in a DV jet in three dimensions. The variations of air speed along the longitudinal, transversal and vertical directions are studied in depth in the secondary zone of the jet. A better understanding of the variation of the jet thickness jet is also gathered. In terms of air temperature, experimental data highlights that the air temperature in a DV jet varies primarily with the distance from the diffuser, and to a lesser extent with height and distance from the longitudinal axis. The interaction between the floor surface temperature and the air temperature in the jet is also highlighted.

- Thanks to the experimental data, a three-dimensional correlation model has been developed for the air speed in the secondary zone of a DV jet. This model integrates the variations of air speed along the longitudinal, transversal and vertical directions. This model proposes a new way to analyze the DV jet by dividing the analysis, studying first the primary zone and, then, using a dimensionless representation in the secondary zone. The primary zone model is based on conservation of energy in the jet, from the diffuser exit to the end of the primary zone, in order to predict the maximum air speed reached in the jet. This model has been validated using experimental data from this thesis. The dimensionless model developed for the secondary zone is tested and found valid for various sets of experimental data from both this thesis and the literature. A generalized equation for the air speed decay in the secondary zone is also developed. This equation is independent of the diffuser type or of the supply condition. This represents a significant improvement compared to previous models which had to use a specific constant for each diffuser and each supply condition.
- In the secondary zone, an in-depth analysis has also been performed to develop a new correlation for the vertical profile of air speed, specifically for DV jets. The variation of jet thickness has also been studied in depths and gives rise to a new correlation to evaluate the increase in jet thickness with the distance from the diffuser increases. Finally, the transversal profiles of air speed have been studied for several heights in the jet and at several distances from the diffuser in the secondary zone.
- In terms of air temperature in the jet, a dimensionless model has also been developed for the variation of minimal air temperature in the jet with increasing distance from the diffuser. A general equation is developed for the increase of minimal temperature in the secondary zone; this equation is validated using experimental data. No correlations could be found for the variations of temperature in the jet in the transversal and vertical directions. Those variations have nonetheless been discussed quantitatively.
- In terms of design and operation, the experimental data has shown the importance of the variation of air speed in the jet in the three dimensions, and the variation of air

temperature in the jet primarily with the distance from the diffuser. Using a single value for the air temperature at floor level has been found inappropriate to ensure local thermal comfort. In order to provide acceptable local comfort, the variation of air temperature in the jet needs to be taken into account. In order to avoid an excessive temperature difference between head and ankles, designers should either set parameters for worst case scenario (minimal temperature in the jet) or set a minimal distance from the diffuser for occupants based on the model developed. In terms of design, the primary zone model developed in this thesis can also help study the impact of diffuser characteristics (velocity profile and entrainment) on the maximal air speed in the jet and, eventually, give rise to more adequate or novel DV diffusers.

- In term of measurements standards, current standards ,such as ASHRAE 113 (ASHRAE, 2005), should be updated to take into account the variations of air speed and temperature in the jet. Using only a few locations in the room might not be sufficient to ensure thermal comfort. The height of measurement for air speed is also a parameter to study be discussed. The current standard ankle level in ASHRAE 113 is 0.10 m; this height however does not correspond to the height of maximal air speed in a DV jet. There is therefore a gap between the data from model (maximal air speed at any height) and data used for comfort assessment (air speed measured at a specific height of 0.10 m). Thanks to the progress in terms of vertical profile and jet thickness correlations in the thesis, this gap can now be reduced and comfort can be studied more thoroughly.

6.2 Future work

This thesis improves on current knowledge in terms of both experimental data and modelling. Nonetheless, some future work is needed to consolidate the findings and expand the analysis.

- Regarding experimental data, only one flow rate was tested in this study, due to limited size of the experimental facility. Additional measurements with different flow-rates would be useful to expand the analysis of air speed and temperature in the jet and to further validate the correlation models. The impact of occupancy on the jet should also be studied. Preliminary data using a cylindrical heated “occupant” showed no impact of the occupant on the flow, apart from mere obstruction on the airflow. Further study with a more elaborate mannequin might however be useful in assessing its impact on the flow, especially regarding a possible upward plume disturbing the air speed distribution. Fine-mesh experimental data in the primary zone would also be useful to gather a better understanding of the impact of diffuser’s exhaust profile on the DV jet. Such data would lead to better DV diffuser design by being able to understand the mixing occurring in the primary zone.
- In terms of air temperature in the jet, it would be interesting to further study the interaction between the air temperature in the jet and the floor surface temperature. A promising area of study would be to study the interaction between displacement ventilation and a heated floor. Such measurements could be done using the same facility, protocol and analysis method as those described in this thesis. A model for the transversal and vertical profiles of air temperature in the jet also remains to be found. Finally, the impact of floor temperature on the jet thickness should be studied.
- As far as the air speed correlation model is concerned, an important parameter to study is the entrainment of indoor air in the jet. Further work is needed to estimate this parameter and study its variation for different diffusers or supply conditions. An obvious tool for some complex study would be computational fluids dynamics (CFD) simulations. The model should also be improved regarding the transversal profile correlations. Additional data regarding jet thickness should also be gathered to further validate the model on that aspect. Finally, the overall air speed model developed could be used to design better DV diffuser or optimize design conditions for improved thermal comfort.

References

Amiri, S., Sandberg, M., Moshfegh, B., 1996, Effects of cooling loads on warm plane air jet, Proc. of ROOMVENT '96, 1, pp. 407-414.

Anderson R., Hassani V., Kirkpartick, A., 1991, Visualizing the airflow from cold air ceiling jets, ASHRAE journal 33(5), pp. 30-35.

ANSYS Inc., 2010, Documentation, version 13.0, Pennsylvania, United States of America.

ASHRAE, ASHRAE Standard 55, 1992, Thermal Environmental Conditions for Human Occupancy, American Society of Heating, Refrigerating and Air-Conditioning Engineers, Atlanta, GA, USA.

ASHRAE, ASHRAE Standard 55, 2004, Thermal Environmental Conditions for Human Occupancy, American Society of Heating, Refrigerating and Air-Conditioning Engineers, Atlanta, GA, USA.

ASHRAE, ASHRAE Standard 55, 2010, Thermal Environmental Conditions for Human Occupancy, American Society of Heating, Refrigerating and Air-Conditioning Engineers, Atlanta, GA, USA.

ASHRAE, 1991, ANSI/ASHRAE 70: Method of Testing the Performance of Air Outlets and Air Inlets, Atlanta, GA, USA.

ASHRAE 2005, ANSI/ASHRAE 113: Method of Testing for Room Air Diffusion, Atlanta, GA, USA.

Béghein, C., Jiang Y., Chen Q., 2005, Using large eddy simulation to study particle motions in a room, Indoor Air 15 (4), pp. 281–290.

Bérubé Dufour M., Derome D., Tardif M., Zmeureanu R., 2008, Measurement of air temperature using infrared thermography in rooms equipped with UFAD systems in cold climate, Proceedings of the 8th Nordic Symposium on Building Physics, Copenhagen, Denmark.

Bérubé Dufour M., Derome D. Zmeureanu R., 2009, Analysis of thermograms for the estimation of dimensions of cracks in building envelope, *Infrared Physics Technology* 52 (2–3), pp. 70–78.

Bosbach, J., Pennecot J., Wagner C., Raffel M., Lerche T., Repp. S., 2006, Experimental and numerical simulations of turbulent ventilation in aircraft cabins. The Second ASME-ZSIS International Thermal Science Seminar (ITSS II) 31(5), pp. 694-705.

Brohus, H., Ryberg, H., 1999, Beskrivelse af "Kappa-modellen" - en simpel model for tilnærmet bestemmelse af vertikal temperaturfordeling i rum. (Description of the "Kappa Model" - a Simplified Model for an Approximate Determination of the Vertical Temperature Distribution in Rooms), Institutet for Bygningsteknik, Aalborg Universitet.

Cao G., Sivukari M., Kurnitski J., Ruponen M., Seppanen O., 2010, Particle Image Velocimetry (PIV) application in the measurement of indoor air distribution by an active chilled beam, *Building and Environment* 45(9), pp. 1932-1940.

Cehlin, M. 2006. Visualization of airflow temperature and concentration indoors whole-field measuring methods and CFD. PhD thesis, KTH, Stockholm.

Cehlin M. Moshfegh B., 2010, Numerical modeling of a complex diffuser in a room with displacement ventilation, *Building and Environment* 45(10), pp. 2240-2252.

CEN, 1998, Technical Report CR 1752, Ventilation for Buildings: Design Criteria for the Indoor Environment, Brussels: European Committee for Standardization.

Cenedese A., Doglia G., Romano G.P., De Michele G., Tanzini G., 1994a, LDA and PIV velocity measurements in free jets, *Experimental Thermal and Fluid Science* 9(2), pp. 125-134.

Cenedese A., Doglia G., Romano G.P., De Michele G., Tanzini G., 1994b, LDA and PIV velocity measurements in free jets, *Experimental Thermal and Fluid Science* 9(2), pp. 125-134.

Chen Q. Moser A., 1991, Simulation of a multiple nozzle diffuser. In: *Proceedings of the Twelfth AIVC Conference, Ottawa, Canada, Vol. 2*, pp. 1-14.

Chen Q. Srebric J., 2001, Simplified diffuser boundary conditions for numerical room airflow models. ASHRAE RP-1009, American Society of Heating, Refrigerating and Air-conditioning Engineers, Atlanta.

Chen Q, Suter P, Moser A., 1991, A database for assessing indoor air flow, air quality and draught risk, *ASHRAE Transactions* 97(2), pp. 150-163.

Chen Q., Xu W., 1998, A zero-equation turbulence model for indoor airflow simulation. *Energy and Buildings* 28(2), pp. 137-144.

Chen Q. Glicksman L., 2003, *System Performance Evaluation Design Guidelines for Displacement Ventilation*. ASHRAE Atlanta, GA, USA.

Cho Y., Awbi H. B., Karimipannah T., 2008, Theoretical and experimental investigation of wall confluent jets ventilation and comparison with wall displacement ventilation, *Building and Environment* 43(6), pp. 1091-1100.

Chow, W.K., Yin R., 2004, A new model on simulating smoke transport with computational fluid dynamics. *Building and Environment* 39, pp. 611 – 620.

Dantec, Rules of thumbs for PIV, 2007, Dantec, Measurement Technology, Inc., NJ, USA.

Davidson, L., Nielsen P.V., Sveningsson A., 2003, Modification of the v2f model for computing the flow in a 3D wall jet. *Turbulence, Heat and Mass Transfer* 4, pp. 577-584.

Davidson, L., Nielsen P.V., 1996, Large eddy simulations of the flow in a three-dimensional ventilated room. In: Proceedings of the 5th International Conference on Air Distributions in Rooms (RoomVent 96), Yokohama, Japan, Vol. 2 pp. 161-168.

Deardorff, J.W., 1970, A numerical study of three-dimensional turbulent channel flow at large Reynolds numbers. *Journal of Fluid Mechanics* 42, pp. 453-480.

Durbin, P.A., 1995, Separated Flow Computations with the $k\text{-}\epsilon\text{-}v^2$ Model, *AIAA Journal* 33, pp. 659-664.

EH Price, 2007, Price Products for Sustainable Buildings, Winnipeg, Canada.

Elvsen P., Sandberg M., 2009, Buoyant jet in a ventilated room: Velocity field, temperature field and airflow patterns analysed with three different whole-field methods, *Building and Environment* 44(1), pp. 137-145.

Emvin, P. Davidson, L., 1996, A numerical comparison of three inlet approximations of the diffuser in case E1 Annex 20. In: Proceedings of the 5th International Conference on Air Distributions in Rooms (RoomVent 96), Yokohama, Japan, Vol. 1, pp. 219-226.

Etheridge D. Sandberg M., 1996, *Building ventilation: theory and measurement*, Wiley, United Kingdom.

Fatemi I., Wang B.C., Koupriyanov M., Tully B., 2013, Experimental study of a non-isothermal wall jet issued by a displacement ventilation system, *Building and Environment* 66, pp 131-140.

Flaktwood, 2010, Floormaster® DVPA flat terminals, www.flaktwoods.com/diffusers/displacement-diffusers/ last assessed 8th February 2011

Fontaine J., Rapp. R., Koskela H. Niem elä, R., 2005, Evaluation of air diffuser flow modelling methods experiments and computational fluid dynamics simulations, *Building and Environment* 40(3), pp. 377-389.

Haghighat F., Jiang J., Wang J.C.Y., Allard F., 1992, Air Movement in Buildings Using Computational Fluid Dynamics. Transactions of the ASAE 114, pp. 84-92.

Haghighat, F., Jiang, Z., Wang, J.C.Y., 1989, Natural Convection and Air Flow Pattern in a Partitioned Room with Turbulent Flow, ASHRAE Transactions 95(2a), pp. 600-610.

Hassani V.A. Stetz M., 1994, Application of infrared thermography to room air temperature measurements, ASHRAE Transactions 100(2), pp. 1238–1247.

Heikkinen, J., 1991, Modelling of a supply air terminal for room air flow simulation. In: Proceedings of the 12th AIVC Conference on Air Movement and Ventilation Control within Buildings, Ottawa, Canada, Vol. 3, pp. 213-230.

Heiselberg P., 1994, Stratified flow in rooms with a cold vertical wall. ASHRAE Transactions, 100(1), pp. 1155–1162.

Howell S. A., Potts I., 2001, On the natural displacement ventilation flow through a full scale enclosure, driven by a source of buoyancy at floor level, Proceedings of the Seventh International IBPSA Conference, Rio de Janeiro, Brazil, pp. 627-634.

Hu S., 2003, Airflow characteristics in the outlet region of a vortex room air diffuser, Building and Environment 38(4), pp. 553-561.

ISO, 2005, EN 7730 Moderate thermal environments - Determination of the PMV and PPD indices and specification of the conditions for thermal comfort". International Standards Organisation. Geneva.

Jiang, Y., Chen Q., 2001, Study of natural ventilation in buildings by large eddy simulation. Journal of Wind Engineering and Industrial Aerodynamics 89(13), pp. 1155-1178.

Jiang Z., Chen Q., Moser A., 1992, Comparison of displacement and mixing diffusers, *Indoor Air* 2(3), pp. 168-179.

Jouvray A., Tucker A.G., Liu Y., 2007, On nonlinear RANS models when predicting more complex geometry room airflows, *International Journal of Heat and Fluid Flow* 28, pp. 275–288.

Karimipannah T., Awbi H.B., Sandberg M., Blomqvist C., 2007, Investigation of air quality, comfort parameters and effectiveness for two floor-level air supply systems in classrooms. *Building and Environment* 42(2), pp. 647-655.

Kegel B. Schulz U.W., 1989, Displacement ventilation for office building, *AIVC 10th Conference* 1, pp. 393-412.

Kolmogorov A.N., 1941, The local structure of turbulence in incompressible viscous fluid for very large Reynolds number. *Doklady Akademii Nauk SSSR* 30, pp. 299–303.

Lau J., Chen Q., 2007, Floor-supply displacement ventilation for workshops, *Building and Environment* 42(4), pp. 1718-1730.

Launder B.E., Spalding D.B., 1974, *The Numerical Computation of Turbulent Flows*, *Computer Methods in Applied Mechanics and Energy* 3, pp. 269-289.

Lee K.S., Zhang T., Jiang Z., Chen Q., 2009, Comparison of airflow and Contaminant distributions in rooms with traditional displacement ventilation and under-floor air distribution systems (RP-1373), *ASHRAE Transactions* 115(2), pp. 306-321

Li Y., Fuchs L., Sandberg M., 1993, Numerical prediction of airflow and heat-radiation interaction in a room with displacement ventilation, *Energy and Buildings* 20(1), pp. 27-43.

Lin Y.J.P., Lin C.L., 2014, A study on flow stratification in a space using displacement ventilation, *International Journal of Heat and Mass Transfer* 73, pp 67-75.

Magnier, L., Zmeureanu, R., Derome, D., 2012, Experimental assessment of the velocity and temperature distributions in an indoor displacement ventilation jet, *Building and Environment* 47, pp. 150-160.

Magnier L., Zmeureanu R., Derome D., 2011, Experimental study of the temperature and velocity fields produced by a displacement ventilation diffuser, *ASHRAE Transactions*, Montreal.

Magnier, L., Zmeureanu, R., Rimmer, J. and Derome, D., 2010, Experimental models for the determination of the Length of the Adjacent Zone for Displacement Ventilation diffusers, *CLIMA 2010*, Turkey, May.

Mateus N. M., Carrilho da Graça G., 2015, A validated three-node model for displacement ventilation, *Building and Environment* 84, pp 50-59.

Melikov A., Pitchurov G., Naydenov K., Langkilde G., 2005, Field study on occupant comfort and the office thermal environment in rooms with displacement ventilation, *Indoor Air* 15(3), pp. 205-214.

Menter F.R., 1992, Improved two-equation k-w turbulence model for aerodynamic flows. *ASA TM-103975*.

Menter F.R., 1994, Two-equation eddy-viscosity turbulence models for engineering applications. *AIAA Journal* 32, pp. 1598-1605.

Morrison B.I., 2000, The adaptive coupling of heat and air flow modeling within dynamic whole-building simulation, Ph.D. Thesis, University of Strathclyde, Glasgow, United Kingdom.

Moureh J., Flick D., 2003, Wall air-jet characteristics and airflow patterns within a slot ventilated enclosure, *International Journal of Thermal Sciences* 42(7), pp. 703-711.

Mundt E., 1995, Displacement ventilation systems--Convection flows and temperature gradients. *Building and Environment* 30(1), pp.129-133.

Neely, A., 2008. Mapping temperature distributions in flows using radiating high-porosity meshes, *Experiments in Fluids* 45(3), pp.423-433.

Neely A., Young J., 2007, Upstream Influence of a Porous Screen on the Flow Field of a Free Jet, In *Proceedings of the 16th Australasian Fluid Mechanics Conference (AFMC)*, pp. 174 179.

Nielsen P.V., Hoff L., Pedersen L.G., 1988, Displacement diffuser by different types of diffusers, in *Proceedings of the 9th AIVC Conference*, pp. 13-29.

Nielsen P.V., 1994, Stratified flow in a room with displacement ventilation and wall-mounted air terminal devices, *ASHRAE Transaction* 100, pp. 1163–1169

Nielsen P.V., 2000, Velocity distribution in a room ventilated by displacement ventilation and wall-mounted air terminal devices, *Energy and Buildings* 31(3), pp. 179-187.

Nordtest method, 1990, Air terminal devices: Aerodynamic testing and rating at low velocity, NT VVS:083, Nordtest, Espoo, Finland.

Nordtest method, 2009, Air terminal devices: Aerodynamic testing and rating at low velocity, NT VVS:083, Nordtest, Espoo, Finland.

Novoselac A., Burley B.J., Srebric J., 2006, Development of new and validation of existing convection correlations for rooms with displacement ventilation systems, *Energy and Buildings* 38(3), pp. 163-173.

Rajaratnam N., 1976, *Turbulent Jets*, Elsevier Publishing Co., Amsterdam and New York.

Rees S. J., Haves P., 2013, An experimental study of air flow and temperature distribution in a room with displacement ventilation and a chilled ceiling, *Building and Environment* 59, pp 358-368

Sandberg M., Blomqvist C., 1989, Displacement ventilation systems in office rooms, *ASHRAE Transactions* 95(2), pp. 1041-1049.

Schild P.G., Sandberg M., Lundrsöm H., Measurement and characterization of gravity current from displacement ventilation terminals, Norges Byggeforskningsinstitut Internal report

Shaw C. Y., Barakat S. A., Newsham G. R., Veitch J. A., Bradley J. S., 1995, NRC indoor environment research facility, In proceedings of the 16th AIVC Annual Conference on Implementing the Results of Ventilation Research 1, pp. 209-220.

Shih, T., Liou W., Shabbir A., Yang Z., Zhu J., 1995, A new k–e eddy viscosity model for high reynolds number turbulent flows, *Journal Computer Fluids* 24, pp. 227-238.

Skåret E., 1998, A semi-empirical flow model for low-velocity air supply in displacement ventilation, *Proceedings of 19th AIVC conference*, pp. 1-9.

Smagorinsky, J., 1963, General circulation experiments with the primitive equations I: the basic experiment. *Monthly Weather Review* 164, pp. 91- 99.

Skistad H., 1994, *Displacement Ventilation*, Research Studies Press, John Wiley & Sons, Ltd., West Sussex, UK.

Skistad H., Mundt E., Nielsen P.V., Hagstrom K., Railio J., 2002, *Displacement ventilation in non-industrial premises*, Guidebook No. 1, REHVA.

Srebric J., Chen Q., 2002, Simplified numerical models for complex air supply diffusers, *international Journal of HVAC&R Research* 8(3), pp. 277-294.

Srebric J., Chen Q., Glicksman L.R., 1999, Validation of a zero-equation turbulence model for complex indoor airflows, *ASHRAE Transactions* 105(2), pp. 414-427.

Tian Z.F., Tu J.Y., Yeoh G.H., Yuen R.K.K., 2006, On the numerical study of contaminant particle concentration in indoor airflow, *Building and Environment* 41(11), pp. 1504-1514.

Trzeciakiewicz Z., Popiolek Z., Mierzwinski S., 1999, Displacement ventilation forming at different air flow rates, in: *Proceedings of the 8th International Conference Indoor Air'99*, Edinburgh, Scotland, VIII, pp. 8–13.

Turner J.S., 1973, *Buoyancy Effects in Fluids*, Cambridge University Press, Cambridge, UK.

Van Maele K., Merci B., 2006, Application of two buoyancy-modified $k-\epsilon$ turbulence models to different types of buoyant plumes, *Fire Safety Journal* 41, pp. 122–138.

Wilcox D.C., 1988, Reassessment of the Scale-Determining Equation for Advanced Turbulence Models, *AIAA Journal* 26, pp. 1299-1310.

Wulff D.L., 2006, PIV measurements in pumps, *Design and Analysis of High Speed Pumps*, pp. 1–36, Educational Notes RTO-EN-AVT-143, Neuilly-sur-Seine, France: RTO.

Yakhot V., Orszag S.A., 1986, Renormalization group analysis of turbulence, *Journal of Scientific Computing* 1, pp. 3-51.

Xu W., Chen Q., Nieuwstadt F.T.M., 1998, A New Turbulence Model for near-Wall Natural Convection, *International Journal of Heat and Mass Transfer* 41(21), pp. 3161-3176.

Xu Y., Yang X., Yang C. Srebric J., 2009, Contaminant dispersion with personal displacement ventilation, Part I: Base case study, *Building and Environment* 44(10), pp. 2121-2128.

Zhang J., 2008, *Investigation of Airflow and Heat Transfer in Earth-to-Air Heat Exchangers*, PhD Thesis, Concordia University, Canada.

Zhou L., Haghighat F., 2008, Optimization of ventilation systems in office environment. Part I. methodology, *Building and Environment* 44, pp. 651–656

Zhou L., 2007, Optimization of Ventilation System Design and Operation in Office Environment, PhD Thesis, Concordia University, Canada.

7.APPENDIX

Measurements on diffuser DF1W size 0.6 m x 0.6 m for an under-temperature of 2.4°C

Table 7-1: Air speed measured at 0.05 m from the diffuser for the 0.6 m x 0.6 m diffuser for a supply under-temperature of 2.4°C [m/s]

Distance from the longitudinal axis [m] / height [m]	-	-	-	-	-	-	0	0.05	0.10	0.15	0.20	0.25	0.30
0.10													
0.15							0.06						
0.20	0.07	0.06	0.42	0.33	0.33	0.32	0.33	0.35	0.35	0.35	0.39	0.45	0.04
0.25							0.26						
0.30							0.24						
0.35							0.20						
0.40	0.05	0.04	0.25	0.18	0.18	0.17	0.18	0.19	0.18	0.18	0.22	0.13	0.03
0.45							0.18						
0.50													
0.55							0.15						
0.62	0.02	0.04	0.16	0.18	0.19	0.19	0.18	0.18	0.18	0.19	0.21	0.26	0.03
0.65							0.01						
0.70							0.02						

Table 7-2: Temperature measured at 0.05 m from the diffuser for the 0.6 m x 0.6 m diffuser for a supply under-temperature of 2.4°C [°C]

Distance from the longitudinal axis [m] / height [m]	- 0.30	- 0.25	- 0.20	- 0.15	- 0.10	- 0.05	0	0.05	0.10	0.15	0.20	0.25	0.30
0.10							20.2						
0.15	20.9	20.5	19.6	19.3	19.2	19.4	19.5	19.5	19.4	19.2	19.3	20.0	20.9
0.20							19.3						
0.25							19.6						
0.30							19.6						
0.35	21.2	20.4	19.6	19.6	19.6	19.4	19.2	19.4	19.6	19.6	19.5	19.9	20.7
0.40							19.8						
0.45													
0.50							19.5						
0.55	21.0	20.5	19.8	19.8	19.6	19.5	19.7	19.7	19.8	19.6	19.4	20.0	20.8
0.62							20.3						
0.65							20.8						
0.70							20.2						

Table 7-3: Air speed measured in the longitudinal plane for the 0.6 m x 0.6 m diffuser for a supply under-temperature of 2.4°C [m/s]

Height [m] / Distance from the diffuser [m]	0.02	0.03	0.04	0.05	0.06	0.07	0.08	0.1	0.2	0.26

0.16	0.17	0.11	0.09	0.09	0.05	0.05	0.05	0.05	0.42	0.34
0.36	0.14	0.13	0.12	0.11	0.12	0.13	0.11	0.19	0.37	0.34
0.56	0.13	0.15	0.17	0.20	0.24	0.25	0.28	0.33	0.35	0.28
0.76	0.24	0.25	0.28	0.28	0.31	0.32	0.33	0.34	0.28	0.21
0.96	0.30	0.34	0.34	0.33	0.34	0.34	0.35	0.35	0.21	0.14
1.16	0.34	0.34	0.35	0.36	0.36	0.35	0.36	0.33	0.16	0.07
1.36	0.34	0.35	0.36	0.36	0.35	0.34	0.33	0.29	0.09	0.07
1.56	0.33	0.34	0.35	0.35	0.33	0.33	0.30	0.25	0.08	0.07
1.76	0.30	0.32	0.33	0.31	0.30	0.29	0.27	0.23	0.08	0.07
1.96	0.29	0.30	0.29	0.30	0.29	0.27	0.26	0.20	0.07	0.07
2.16	0.25	0.26	0.26	0.26	0.24	0.24	0.22	0.18	0.07	0.06
2.36	0.22	0.23	0.24	0.23	0.22	0.22	0.18	0.16	0.06	0.06
2.56	0.19	0.20	0.19	0.20	0.20	0.17	0.18	0.16	0.06	0.05
2.76	0.16	0.18	0.17	0.19	0.18	0.17	0.17	0.13	0.07	0.05
2.96	0.16	0.14	0.17	0.17	0.13	0.15	0.14	0.13	0.07	0.05
3.16	0.12	0.12	0.14	0.13	0.13	0.13	0.13	0.11	0.06	0.04

Table 7-4: Air temperature measured in the longitudinal plane for the 0.6 m x 0.6 m diffuser for a supply under-temperature of 2.4°C [°C]

Height [m] / Distance from the diffuser [m]	0.02	0.03	0.04	0.05	0.06	0.07	0.08	0.1	0.2	0.26
0.16	20.8	20.8	20.8	20.7	20.8	20.8	20.8	20.8	19.6	19.7
0.36	20.7	20.8	20.8	20.5	20.4	20.5	20.5	20.2	19.7	19.4
0.56	20.2	20.4	20.4	20.3	20.2	20.1	19.9	19.7	19.4	19.7
0.76	20.2	19.9	19.9	20.1	19.9	20.0	19.5	19.9	19.9	20.3

0.96	20.0	19.7	19.7	19.8	19.6	19.8	19.8	19.8	20.4	20.6
1.16	19.8	20.0	20.0	19.8	19.8	19.8	19.9	19.9	20.5	21.0
1.36	19.9	19.9	20.0	20.0	19.9	19.9	19.9	20.0	20.7	21.0
1.56	20.1	19.9	20.0	20.1	20.0	19.9	20.0	20.2	20.8	21.1
1.76	20.0	20.1	20.0	20.0	20.1	20.1	20.2	20.3	20.8	21.0
1.96	20.3	20.2	20.2	20.3	20.2	20.2	20.3	20.2	20.7	21.0
2.16	20.4	20.2	20.3	20.4	20.2	20.3	20.2	20.3	20.6	21.0
2.36	20.4	20.4	20.3	20.4	20.4	20.3	20.4	20.5	20.8	20.9
2.56	20.5	20.5	20.5	20.5	20.5	20.5	20.5	20.5	20.8	21.0
2.76	20.7	20.6	20.7	20.4	20.4	20.6	20.6	20.5	20.7	21.0
2.96	20.8	20.6	20.7	20.6	20.6	20.6	20.6	20.6	20.7	21.0
3.16	20.8	20.8	20.7	20.7	20.7	20.6	20.7	20.7	20.9	21.0

Table 7-5: Air speed measured in the transversal plane for the 0.6 m x 0.6 m diffuser for a supply under-temperature of 2.4°C
[m/s]

Height [m] / Distance from the axis [m]	0.02	0.03	0.04	0.05	0.06	0.07	0.08	0.1	0.2
-0.90	0.15	0.16	0.17	0.17	0.18	0.15	0.15	0.14	0.07
-0.70	0.19	0.20	0.20	0.19	0.20	0.19	0.17	0.15	0.06
-0.50	0.22	0.23	0.22	0.22	0.21	0.20	0.18	0.16	0.06
-0.30	0.24	0.24	0.25	0.24	0.22	0.22	0.19	0.18	0.05
-0.10	0.26	0.27	0.26	0.26	0.24	0.24	0.21	0.18	0.07
0.10	0.27	0.27	0.28	0.28	0.27	0.25	0.24	0.20	0.07
0.30	0.25	0.26	0.26	0.25	0.25	0.22	0.21	0.18	0.07
0.50	0.23	0.23	0.23	0.23	0.22	0.21	0.19	0.17	0.07

0.70	0.19	0.21	0.22	0.21	0.19	0.19	0.17	0.16	0.06
0.90	0.15	0.16	0.18	0.18	0.17	0.17	0.15	0.16	0.07

Table 7-6: Air temperature measured in the transversal plane for the 0.6 m x 0.6 m diffuser for a supply under-temperature of 2.4°C [°C]

Height [m] / Distance from the axis [m]	0.02	0.03	0.04	0.05	0.06	0.07	0.08	0.1	0.2
-0.90	20.8	20.7	20.6	20.7	20.6	20.6	20.7	20.6	20.9
-0.70	20.7	20.5	20.4	20.4	20.5	20.4	20.5	20.6	20.9
-0.50	20.5	20.5	20.4	20.5	20.4	20.5	20.6	20.6	20.9
-0.30	20.4	20.4	20.4	20.4	20.2	20.5	20.4	20.5	20.9
-0.10	20.4	20.3	20.3	20.3	20.3	20.3	20.4	20.3	20.8
0.10	20.4	20.3	20.2	20.3	20.3	20.2	20.3	20.5	20.8
0.30	20.4	20.4	20.3	20.3	20.3	20.4	20.5	20.5	20.8
0.50	20.5	20.5	20.5	20.4	20.3	20.5	20.5	20.4	20.8
0.70	20.5	20.4	20.5	20.4	20.5	20.4	20.4	20.5	20.9
0.90	20.7	20.6	20.5	20.4	20.6	20.5	20.6	20.6	20.7

Table 7-7: Air speed measured in the horizontal plane at a height of 0.05 m for the 0.6 m x 0.6 m diffuser for a supply under-temperature of 2.4°C [m/s]

Distance from the axis [m] / Distance from the diffuser [m]	-0.9	-0.7	-0.5	-0.3	-0.1	0.1	0.3	0.5	0.7	0.9
0.16	0.05	0.05	0.04	0.06	0.05	0.07	0.04	0.04	0.04	0.05
0.36										

0.56	0.09	0.07	0.06	0.08	0.19	0.14	0.06	0.07	0.08	0.07
0.76										
0.96	0.14	0.14	0.19	0.29	0.32	0.30	0.22	0.20	0.15	0.13
1.16										
1.36	0.18	0.22	0.27	0.32	0.35	0.36	0.31	0.26	0.22	0.17
1.56										
1.76	0.18	0.21	0.26	0.29	0.32	0.32	0.30	0.26	0.23	0.19
1.96	0.17	0.21	0.24	0.25	0.29	0.28	0.27	0.25	0.21	0.17
2.16	0.17	0.19	0.22	0.24	0.26	0.28	0.25	0.23	0.21	0.18
2.36	0.17	0.17	0.18	0.20	0.24	0.25	0.23	0.21	0.20	0.18
2.56	0.15	0.15	0.18	0.18	0.20	0.20	0.21	0.20	0.19	0.18
2.76	0.13	0.14	0.16	0.17	0.18	0.19	0.20	0.17	0.17	0.15

Table 7-8: Air temperature measured in the horizontal plane at a height of 0.05 m for the 0.6 m x 0.6 m diffuser for a supply under-temperature of 2.4°C [°C]

Distance from the axis [m] / Distance from the diffuser [m]	-0.9	-0.7	-0.5	-0.3	-0.1	0.1	0.3	0.5	0.7	0.9
0.16	21.2	21.3	21.3	21.2	21.0	21.0	21.1	21.1	21.1	21.1
0.36										
0.56	20.9	21.0	21.1	20.9	20.3	20.6	20.9	20.9	20.9	21.0
0.76										
0.96	20.7	20.7	20.4	20.0	19.7	20.1	20.3	20.3	20.5	20.8
1.16										
1.36	20.7	20.4	20.2	20.2	20.0	19.8	20.1	20.4	20.5	20.5

1.56										
1.76	20.7	20.6	20.5	20.2	20.1	20.3	20.4	20.3	20.5	20.7
1.96	20.6	20.5	20.4	20.3	20.1	20.3	20.4	20.3	20.5	20.7
2.16	20.7	20.4	20.5	20.4	20.3	20.3	20.3	20.4	20.4	20.4
2.36	20.8	20.5	20.5	20.6	20.5	20.3	20.4	20.5	20.6	20.5
2.56	20.7	20.8	20.6	20.4	20.5	20.5	20.5	20.4	20.6	20.6
2.76	20.8	20.7	20.8	20.8	20.5	20.6	20.7	20.5	20.6	20.6

Measurements on the DF1W diffuser size 0.6 m x 0.6 m for an under-temperature of 5.0°C

Table 7-9: Air speed measured at 0.05 m from the diffuser for the 0.6 m x 0.6 m diffuser for a supply under-temperature of 5.0°C [m/s]

Distance from the longitudinal axis [m] / height [m]	-	-	-	-	-	-	0	0.05	0.10	0.15	0.20	0.25	0.30
	0.30	0.25	0.20	0.15	0.10	0.05	0	0.05	0.10	0.15	0.20	0.25	0.30
0.10	0.07	0.11	0.08	0.04	0.05	0.05	0.06	0.06	0.08	0.09	0.10	0.10	0.07
0.15	0.06	0.08	0.13	0.05	0.05	0.06	0.06	0.07	0.07	0.06	0.09	0.22	0.05
0.20	0.04	0.03	0.48	0.40	0.39	0.38	0.38	0.39	0.39	0.39	0.45	0.05	0.04
0.25	0.04	0.03	0.39	0.30	0.28	0.27	0.27	0.28	0.29	0.29	0.35	0.05	0.04
0.30	0.03	0.02	0.36	0.28	0.25	0.24	0.24	0.26	0.25	0.28	0.35	0.04	0.02
0.35	0.03	0.03	0.32	0.24	0.23	0.22	0.22	0.22	0.23	0.24	0.32	0.03	0.03
0.40	0.02	0.03	0.28	0.19	0.19	0.18	0.18	0.18	0.18	0.19	0.28	0.03	0.04
0.45	0.03	0.04	0.23	0.17	0.18	0.17	0.17	0.17	0.17	0.17	0.23	0.04	0.03
0.50	0.03	0.03	0.18	0.15	0.16	0.16	0.16	0.16	0.16	0.16	0.15	0.20	0.03
0.55	0.03	0.04	0.15	0.16	0.16	0.16	0.16	0.15	0.17	0.17	0.13	0.19	0.05

0.62	0.02	0.10	0.21	0.12	0.09	0.12	0.09	0.15	0.14	0.12	0.26	0.28	0.03
0.65	0.02	0.05	0.05	0.05	0.04	0.03	0.03	0.03	0.04	0.04	0.04	0.05	0.02
0.70	0.00	0.00	0.00	0.00	0.00	0.00	0.00	0.00	0.00	0.00	0.00	0.00	0.00

Table 7-10: Temperature measured at 0.05 m from the diffuser for the 0.6 m x 0.6 m diffuser for a supply under-temperature of 5.0°C [°C]

Distance from the longitudinal axis [m] / height [m]	-	-	-	-	-	-	0	0.05	0.10	0.15	0.20	0.25	0.30
	0.30	0.25	0.20	0.15	0.10	0.05	0	0.05	0.10	0.15	0.20	0.25	0.30
0.10	19.8	19.7	19.5	19.5	19.2	19.1	19.1	19.1	19.3	19.4	19.4	19.4	19.5
0.15	19.8	19.0	18.3	18.7	18.6	18.4	18.5	18.6	18.7	18.7	18.5	18.8	19.6
0.20	20.1	19.4	17.8	17.2	17.2	17.3	17.3	17.3	17.3	17.3	17.3	18.6	19.8
0.25	20.3	19.6	17.9	17.2	17.2	17.3	17.3	17.3	17.3	17.2	17.4	18.6	19.9
0.30	20.1	19.4	17.8	17.3	17.3	17.3	17.3	17.3	17.3	17.3	17.5	18.9	19.9
0.35	20.2	19.5	17.9	17.3	17.3	17.3	17.3	17.3	17.3	17.3	17.5	18.9	19.9
0.40	20.3	19.3	17.7	17.4	17.4	17.4	17.4	17.4	17.4	17.4	17.6	19.0	20.0
0.45	20.3	19.1	17.6	17.4	17.4	17.4	17.4	17.4	17.4	17.4	17.4	18.6	19.9
0.50	20.5	19.5	17.9	17.5	17.6	17.5	17.6	17.6	17.6	17.5	17.6	18.4	20.0
0.55	20.6	19.5	18.1	17.7	17.7	17.7	17.8	17.7	17.7	17.7	17.7	18.5	20.2
0.62	20.4	19.2	18.4	19.3	19.7	19.7	19.7	19.7	19.6	19.6	19.1	18.9	19.7
0.65	20.5	20.3	20.2	20.2	20.2	20.3	20.3	20.2	20.2	20.2	20.2	20.2	20.3
0.70	16.9	16.9	16.9	16.9	16.9	16.9	16.9	16.9	16.9	16.9	16.9	16.9	16.9

Table 7-11: Air speed measured in the longitudinal plane for the 0.6 m x 0.6 m diffuser for a supply under-temperature of 5.0°C [m/s]

Height [m] / Distance from the diffuser [m]	0.02	0.03	0.04	0.05	0.06	0.07	0.08	0.1	0.2	0.26
0.16	0.11	0.12	0.11	0.10	0.09	0.08	0.09	0.08	0.43	0.33
0.36	0.10	0.12	0.17	0.21	0.24	0.26	0.29	0.32	0.36	0.31
0.56	0.28	0.29	0.30	0.32	0.34	0.35	0.35	0.36	0.31	0.23
0.76	0.36	0.37	0.38	0.38	0.38	0.38	0.38	0.38	0.18	0.07
0.96	0.40	0.41	0.41	0.41	0.40	0.39	0.39	0.34	0.09	0.08
1.16	0.41	0.42	0.42	0.40	0.39	0.36	0.34	0.29	0.08	0.09
1.36	0.39	0.40	0.39	0.36	0.35	0.32	0.29	0.21	0.08	0.10
1.56	0.36	0.37	0.36	0.34	0.31	0.28	0.27	0.21	0.08	0.10
1.76	0.33	0.33	0.33	0.31	0.28	0.26	0.25	0.18	0.07	0.09
1.96	0.27	0.27	0.28	0.26	0.25	0.23	0.19	0.17	0.07	0.08
2.16	0.24	0.25	0.24	0.24	0.23	0.19	0.18	0.15	0.05	0.07
2.36	0.19	0.23	0.21	0.21	0.20	0.18	0.17	0.14	0.07	0.06
2.56	0.18	0.18	0.19	0.18	0.17	0.17	0.16	0.14	0.06	0.07
2.76	0.15	0.17	0.17	0.16	0.16	0.14	0.15	0.12	0.06	0.06
2.96	0.13	0.13	0.14	0.14	0.14	0.14	0.13	0.11	0.07	0.05
3.16	0.12	0.13	0.13	0.14	0.12	0.11	0.12	0.11	0.07	0.04

Table 7-12: Air temperature measured in the longitudinal plane for the 0.6 m x 0.6 m diffuser for a supply under-temperature of 5.0°C [°C]

Height [m] / Distance from the diffuser [m]	0.02	0.03	0.04	0.05	0.06	0.07	0.08	0.1	0.2	0.26
--	-------------	-------------	-------------	-------------	-------------	-------------	-------------	------------	------------	-------------

0.16	19.4	19.3	19.4	19.4	19.4	19.3	19.3	19.1	17.4	17.3
0.36	18.6	18.6	18.5	18.4	18.3	18.2	18.1	18.0	17.4	17.5
0.56	17.9	17.8	17.7	17.7	17.6	17.6	17.5	17.5	17.8	18.8
0.76	17.8	17.6	17.6	17.6	17.5	17.5	17.5	17.5	19.3	19.8
0.96	17.7	17.7	17.6	17.6	17.6	17.8	17.8	18.2	19.7	20.1
1.16	17.7	17.7	17.8	17.9	17.9	18.3	18.4	18.7	19.9	20.0
1.36	18.0	18.0	18.1	18.3	18.3	18.5	18.6	18.9	19.8	20.0
1.56	18.3	18.2	18.4	18.4	18.6	18.6	18.8	19.0	19.7	19.9
1.76	18.6	18.6	18.6	18.6	18.7	18.8	18.9	19.1	19.7	19.9
1.96	19.0	18.8	18.8	18.9	18.9	18.9	19.1	19.2	19.7	19.8
2.16	19.2	19.1	19.0	19.0	19.0	19.1	19.2	19.2	19.8	19.8
2.36	19.4	19.2	19.1	19.1	19.2	19.2	19.3	19.4	19.8	19.8
2.56	19.6	19.5	19.3	19.3	19.3	19.3	19.4	19.4	19.8	19.9
2.76	19.8	19.6	19.4	19.5	19.4	19.5	19.5	19.6	19.8	20.0
2.96	19.9	19.8	19.7	19.6	19.6	19.6	19.7	19.7	19.9	20.0
3.16	20.1	19.9	19.7	19.8	19.7	19.7	19.8	19.8	20.0	20.0

Table 7-13: Air speed measured in the transversal plane for the 0.6 m x 0.6 m diffuser for a supply under-temperature of 5.0°C

[m/s]

Height [m] / Distance from the axis [m]	0.02	0.03	0.04	0.05	0.06	0.07	0.08	0.1	0.2
-0.90	0.17	0.18	0.17	0.16	0.17	0.16	0.15	0.13	0.06
-0.70	0.20	0.20	0.20	0.19	0.19	0.18	0.15	0.13	0.04
-0.50	0.21	0.22	0.21	0.21	0.19	0.18	0.17	0.14	0.05
-0.30	0.22	0.23	0.23	0.23	0.20	0.20	0.18	0.13	0.05

-0.10	0.24	0.26	0.26	0.23	0.22	0.21	0.20	0.15	0.06
0.10	0.23	0.25	0.25	0.24	0.23	0.21	0.19	0.18	0.07
0.30	0.25	0.26	0.26	0.25	0.24	0.23	0.20	0.18	0.05
0.50	0.24	0.26	0.26	0.24	0.23	0.21	0.20	0.17	0.06
0.70	0.22	0.24	0.23	0.22	0.21	0.19	0.18	0.16	0.07
0.90	0.18	0.19	0.20	0.18	0.17	0.17	0.17	0.15	0.06

Table 7-14: Air temperature measured in the transversal plane for the 0.6 m x 0.6 m diffuser for a supply under-temperature of 5.0°C [°C]

Height [m] / Distance from the axis [m]	0.02	0.03	0.04	0.05	0.06	0.07	0.08	0.1	0.2
-0.90	19.6	19.5	19.5	19.5	19.4	19.4	19.4	19.4	19.8
-0.70	19.4	19.4	19.3	19.3	19.2	19.3	19.3	19.3	19.8
-0.50	19.2	19.2	19.2	19.2	19.2	19.2	19.2	19.3	19.9
-0.30	19.1	19.2	19.1	19.1	19.1	19.1	19.1	19.3	19.9
-0.10	19.1	19.0	19.0	19.1	19.0	19.0	19.1	19.2	19.8
0.10	19.1	19.0	19.0	19.0	19.0	19.0	19.0	19.1	19.7
0.30	19.1	19.0	19.0	19.0	19.0	19.0	19.1	19.1	19.7
0.50	19.2	19.0	19.0	19.0	19.1	19.1	19.1	19.2	19.7
0.70	19.3	19.2	19.2	19.1	19.2	19.2	19.2	19.2	19.6
0.90	19.5	19.4	19.3	19.3	19.3	19.3	19.2	19.3	19.7

Table 7-15: Air speed measured in the horizontal plane at a height of 0.05 m for the 0.6 m x 0.6 m diffuser for a supply under-temperature of 5.0°C [m/s]

Distance from the axis [m] / Distance from the diffuser [m]	-0.9	-0.7	-0.5	-0.3	-0.1	0.1	0.3	0.5	0.7	0.9
0.16	0.09	0.08	0.07	0.05	0.07	0.07	0.07	0.07	0.07	0.07
0.36										
0.56	0.13	0.14	0.16	0.14	0.31	0.29	0.15	0.14	0.13	0.11
0.76										
0.96	0.20	0.27	0.32	0.39	0.38	0.40	0.35	0.30	0.23	0.17
1.16										
1.36	0.22	0.25	0.30	0.36	0.39	0.38	0.34	0.28	0.23	0.20
1.56										
1.76	0.20	0.23	0.25	0.27	0.29	0.31	0.30	0.28	0.24	0.20
1.96	0.19	0.20	0.24	0.25	0.26	0.28	0.27	0.27	0.23	0.19
2.16	0.16	0.19	0.21	0.23	0.23	0.24	0.25	0.24	0.22	0.18
2.36	0.16	0.17	0.18	0.19	0.19	0.22	0.22	0.22	0.20	0.18
2.56	0.14	0.16	0.17	0.18	0.19	0.18	0.19	0.18	0.19	0.18
2.76	0.12	0.13	0.15	0.16	0.16	0.16	0.16	0.17	0.16	0.16

Table 7-16: Air temperature measured in the horizontal plane at a height of 0.05 m for the 0.6 m x 0.6 m diffuser for a supply under-temperature of 5.0°C [°C]

Distance from the axis [m] / Distance from the diffuser [m]	-0.9	-0.7	-0.5	-0.3	-0.1	0.1	0.3	0.5	0.7	0.9
0.16	19.8	19.8	19.9	20.0	19.3	19.4	19.6	19.7	19.8	19.8

0.36										
0.56	19.6	19.5	19.2	18.8	17.6	18.0	18.9	19.4	19.5	19.6
0.76										
0.96	19.3	18.9	18.5	17.8	17.5	17.6	18.2	18.6	19.0	19.3
1.16										
1.36	19.1	19.0	18.7	18.2	18.1	18.2	18.5	18.8	19.0	19.1
1.56										
1.76	19.2	19.0	18.8	18.8	18.7	18.7	18.7	18.9	19.1	19.2
1.96	19.3	19.2	19.0	18.9	18.8	18.8	18.9	18.9	19.1	19.3
2.16	19.5	19.3	19.2	19.1	19.1	19.0	19.0	19.0	19.1	19.3
2.36	19.6	19.4	19.3	19.3	19.2	19.1	19.2	19.1	19.2	19.4
2.56	19.6	19.5	19.4	19.4	19.3	19.3	19.3	19.3	19.3	19.4
2.76	19.8	19.8	19.6	19.6	19.5	19.5	19.4	19.4	19.5	19.5

Measurements on the DF1W diffuser size 0.6 m x 0.6 m for under-temperatures of 1.5°C, 3.7°C, and 6.3°C

Table 7-17: Air speed and temperature measured at 0.05 m from the diffuser on a vertical axis passing through the center of the diffuser for the 0.6 m x 0.6 m diffuser for several supply under-temperature

Under-temperature [°C]	1.5		3.7		6.3	
Height [m]	Speed [m/s]	Temperature [°C]	Speed [m/s]	Temperature [°C]	Speed [m/s]	Temperature [°C]
0.10	0.04	21.7	0.05	20.9	0.07	18.7
0.15	0.05	21.4	0.03	20.4	0.06	17.8
0.20	0.36	20.6	0.36	18.9	0.37	16.2

0.25	0.26	20.4	0.26	19.0	0.27	16.1
0.30	0.23	20.5	0.23	18.9	0.24	16.0
0.35	0.20	20.9	0.20	19.1	0.22	16.1
0.40	0.18	20.5	0.18	19.0	0.19	16.2
0.45	0.16	20.8	0.16	19.0	0.18	16.4
0.50	0.15	20.9	0.15	19.2	0.16	16.5
0.55	0.14	20.9	0.14	19.3	0.17	16.7
0.62	0.17	21.0	0.19	19.7	0.21	17.3
0.65	0.03	21.8	0.04	21.3	0.04	19.6
0.70	0.02	22.0	0.03	21.4	0.03	19.9

Table 7-18: Maximum air speed and minimum temperature measured in the longitudinal plane for the 0.6 m x 0.6 m diffuser for several supply under-temperature

Under-temperature [°C]	1.5		3.7		6.3	
	Speed [m/s]	Temperature [°C]	Speed [m/s]	Temperature [°C]	Speed [m/s]	Temperature [°C]
0.66	0.13	21.4	0.29	19.5	0.36	16.4
0.76	0.20	21.3	0.33	19.3	0.38	16.3
0.86	0.24	21.2	0.33	19.5	0.40	16.4
0.96	0.25	21.1	0.36	19.3	0.41	16.5
1.06	0.29	21.0	0.37	19.4	0.41	16.7
1.16	0.28	21.3	0.36	19.4	0.40	16.9
1.26	0.30	21.0	0.37	19.4	0.40	17.0

1.36	0.32	20.9	0.36	19.6	0.38	17.3
1.46	0.32	21.1	0.35	19.7	0.37	17.3
1.56	0.32	21.0	0.34	19.8	0.35	17.5
1.66	0.32	21.1	0.33	19.8	0.33	17.7
1.76	0.32	20.9	0.31	20.0	0.32	17.8
1.96	0.30	21.1	0.28	20.1	0.29	18.0
2.16	0.27	21.1	0.25	20.3	0.25	18.2
2.36	0.24	21.2	0.23	20.4	0.22	18.4

Table 7-19: Table 7-20: Air speed and temperature at different heights at the end of the primary zone for the 0.6 m x 0.6 m diffuser for several supply under-temperature

Under-temperature [°C]	1.5		3.7		6.3	
	Speed [m/s]	Temperature [°C]	Speed [m/s]	Temperature [°C]	Speed [m/s]	Temperature [°C]
0.02	0.30	21.0	0.35	19.5	0.39	16.5
0.03	0.31	21.0	0.37	19.4	0.41	16.4
0.04	0.32	21.1	0.37	19.4	0.41	16.7
0.05	0.32	20.9	0.36	19.6	0.41	16.6
0.06	0.32	20.9	0.35	19.7	0.39	16.8
0.08	0.30	20.9	0.30	19.9	0.35	17.4

0.10	0.27	21.1	0.26	20.0	0.29	17.4
0.20	0.11	21.4	0.08	21.1	0.09	19.1

Table 7-21: Air speed and temperature measured on the transversal axis at height of maximum air speed at the end of the primary zone for the 0.6 m x 0.6 m diffuser for several supply under-temperature

Under-temperature [°C]	1.5		3.7		6.3	
	Speed [m/s]	Temperature [°C]	Speed [m/s]	Temperature [°C]	Speed [m/s]	Temperature [°C]
-0.9	0.15	21.5	0.20	20.6	0.21	18.5
-0.7	0.17	21.4	0.24	20.3	0.28	18.2
-0.5	0.21	21.2	0.29	20.1	0.34	17.8
-0.3	0.26	21.1	0.35	19.6	0.42	16.8
-0.1	0.30	21.1	0.36	19.6	0.41	16.6
0.1	0.32	21.0	0.37	19.4	0.41	16.8
0.3	0.27	21.2	0.33	20.0	0.37	17.6
0.5	0.22	21.4	0.28	20.2	0.30	18.0
0.7	0.18	21.4	0.23	20.6	0.24	18.2
0.9	0.14	21.5	0.19	20.8	0.16	18.5

Measurements on the diffuser DF1W size 1.2 m x 0.6 m for an under-temperature of 2.5°C

Table 7-22: Air speed measured at 0.05 m from the diffuser for the 1.2 m x 0.6 m diffuser for a supply under-temperature of 2.5°C [m/s]

Distance from the	-	-	-	-	-	-	0	0.05	0.10	0.15	0.20	0.25	0.30
-------------------	---	---	---	---	---	---	---	------	------	------	------	------	------

longitudinal axis [m] / height [m]	0.30	0.25	0.20	0.15	0.10	0.05							
0.10							0.09						
0.15	0.06	0.16	0.16	0.13	0.13	0.14	0.13	0.14	0.15	0.16	0.18	0.21	0.06
0.20							0.10						
0.25							0.10						
0.30							0.09						
0.35							0.09						
0.40							0.09						
0.45							0.09						
0.50							0.09						
0.55							0.09						
0.60							0.09						
0.65	0.02	0.03	0.10	0.10	0.09	0.09	0.09	0.09	0.09	0.08	0.09	0.15	0.02
0.70							0.10						
0.75							0.10						
0.80							0.10						
0.85							0.09						
0.90							0.05						
0.95							0.06						
1.00							0.04						
1.05							0.04						
1.10							0.15						
1.15	0.02	0.02	0.15	0.17	0.18	0.19	0.18	0.18	0.18	0.15	0.18	0.03	0.01
1.20							0.02						

1.25							0.01						
1.30							0.09						

Table 7-23: Air temperature measured at 0.05 m from the diffuser for the 1.2 m x 0.6 m diffuser for a supply under-temperature of 2.5°C [°C]

Distance from the longitudinal axis [m] / height [m]	-	-	-	-	-	-	0	0.05	0.10	0.15	0.20	0.25	0.30
	0.30	0.25	0.20	0.15	0.10	0.05							
0.10							20.3						
0.15							20.2						
0.20	20.5	20.2	19.8	19.8	20.0	19.9	19.9	19.7	19.7	19.9	19.8	20.1	20.3
0.25							19.9						
0.30							19.9						
0.35							20.0						
0.40							20.0						
0.45							20.0						
0.50							20.0						
0.55							19.9						
0.60							19.9						
0.65							19.9						
0.70	21.5	20.7	19.9	20.0	19.9	19.9	19.9	19.8	19.9	20.0	19.9	20.5	21.2
0.75							20.0						
0.80							19.8						
0.85							20.0						
0.90							20.1						

0.95							20.2						
1.00							20.4						
1.05							20.5						
1.10							20.5						
1.15							19.9						
1.20	21.7	21.5	20.2	19.8	20.1	19.9	19.9	20.1	20.1	20.3	20.0	20.9	21.6
1.25							20.7						
1.30							21.8						

Table 7-24: Air speed measured in the longitudinal plane for the 1.2 m x 0.6 m diffuser for a supply under-temperature of 2.5°C [m/s]

Height [m] / Distance from the diffuser [m]	0.02	0.03	0.04	0.05	0.06	0.07	0.08	0.1	0.2	0.26
0.16	0.17	0.15	0.14	0.09	0.09	0.09	0.09	0.07	0.11	0.11
0.36	0.04	0.04	0.05	0.05	0.05	0.06	0.07	0.08	0.13	0.16
0.56	0.13	0.12	0.15	0.17	0.17	0.19	0.18	0.23	0.17	0.15
0.76	0.28	0.30	0.30	0.29	0.29	0.23	0.23	0.20	0.08	0.04
0.96	0.29	0.30	0.29	0.27	0.27	0.23	0.21	0.17	0.05	0.03
1.16	0.29	0.29	0.27	0.25	0.25	0.20	0.19	0.15	0.04	0.03
1.36	0.28	0.28	0.26	0.23	0.23	0.18	0.17	0.12	0.04	0.03
1.56	0.25	0.26	0.23	0.22	0.22	0.16	0.15	0.12	0.06	0.03
1.76	0.23	0.23	0.23	0.22	0.22	0.18	0.17	0.14	0.05	0.04
1.96	0.20	0.20	0.21	0.19	0.19	0.16	0.16	0.13	0.05	0.05
2.16	0.18	0.19	0.19	0.18	0.18	0.17	0.16	0.14	0.07	0.05
2.36	0.16	0.17	0.17	0.18	0.18	0.15	0.15	0.14	0.08	0.05

2.56	0.17	0.17	0.16	0.17	0.17	0.16	0.16	0.15	0.09	0.06
2.76	0.13	0.15	0.15	0.15	0.15	0.14	0.13	0.13	0.08	0.06
2.96	0.12	0.14	0.14	0.15	0.15	0.15	0.13	0.12	0.09	0.07
3.16	0.11	0.11	0.12	0.13	0.13	0.11	0.12	0.12	0.09	0.07

Table 7-25: Air temperature measured in the longitudinal plane for the 1.2 m x 0.6 m diffuser for a supply under-temperature of 2.5°C [°C]

Height [m] / Distance from the diffuser [m]	0.02	0.03	0.04	0.05	0.06	0.07	0.08	0.1	0.2	0.26
0.16	20.1	20.1	20.2	20.3	20.3	20.2	20.3	20.3	20.0	20.0
0.36	19.9	20.1	20.1	20.1	20.1	20.1	20.0	19.9	19.9	20.0
0.56	20.0	19.9	19.9	19.9	19.9	20.1	20.2	20.2	20.6	20.7
0.76	20.1	20.1	20.3	20.4	20.4	20.5	20.5	20.7	21.1	21.2
0.96	20.3	20.3	20.4	20.6	20.6	20.6	20.8	20.9	21.2	21.3
1.16	20.2	20.4	20.6	20.6	20.6	20.7	20.8	20.9	21.3	21.3
1.36	20.5	20.4	20.6	20.6	20.6	20.8	20.9	21.0	21.2	21.3
1.56	20.4	20.5	20.7	20.7	20.7	20.8	20.9	20.9	21.2	21.4
1.76	20.7	20.7	20.6	20.7	20.7	20.9	20.8	20.9	21.1	21.3
1.96	20.7	20.7	20.7	20.8	20.8	20.8	20.9	20.9	21.2	21.3
2.16	20.9	20.8	20.8	20.8	20.8	20.8	21.0	21.0	21.1	21.2
2.36	20.9	20.9	20.9	20.9	20.9	20.9	20.9	20.9	21.1	21.2
2.56	21.0	21.0	20.8	20.9	20.9	21.0	20.9	20.9	21.0	21.1
2.76	21.0	21.0	21.0	21.0	21.0	21.0	21.0	21.0	21.1	21.2
2.96	21.2	21.1	21.0	21.0	21.0	21.0	21.1	21.1	21.0	21.1
3.16	21.2	21.2	21.1	21.1	21.1	21.1	21.1	21.0	21.1	21.1

Table 7-26: Air speed measured in the transversal plane for the 1.2 m x 0.6 m diffuser for a supply under-temperature of 2.5°C

[m/s]

Height [m] / Distance from the axis [m]	0.02	0.03	0.04	0.05	0.06	0.07	0.08	0.1	0.2
-0.90	0.14	0.14	0.14	0.14	0.14	0.14	0.13	0.12	0.07
-0.70	0.16	0.17	0.17	0.16	0.16	0.15	0.14	0.12	0.07
-0.50	0.18	0.18	0.18	0.18	0.17	0.16	0.16	0.12	0.07
-0.30	0.19	0.19	0.19	0.16	0.19	0.17	0.15	0.15	0.05
-0.10	0.18	0.19	0.18	0.18	0.16	0.16	0.16	0.12	0.06
0.10	0.19	0.19	0.20	0.17	0.18	0.15	0.14	0.13	0.05
0.30	0.20	0.20	0.19	0.19	0.18	0.17	0.15	0.13	0.06
0.50	0.19	0.19	0.19	0.17	0.19	0.16	0.15	0.15	0.07
0.70	0.19	0.18	0.19	0.18	0.16	0.15	0.15	0.13	0.07
0.90	0.15	0.16	0.16	0.15	0.15	0.13	0.13	0.12	0.06

Table 7-27: Air temperature measured in the transversal plane for the 1.2 m x 0.6 m diffuser for a supply under-temperature of 2.5°C [°C]

Height [m] / Distance from the axis [m]	0.02	0.03	0.04	0.05	0.06	0.07	0.08	0.1	0.2
-0.90	20.9	20.8	20.9	20.9	20.9	20.8	20.8	20.8	21.1
-0.70	20.9	20.7	20.8	20.9	20.8	20.8	20.8	20.8	21.0
-0.50	20.8	20.8	20.9	20.7	20.8	20.7	20.8	20.9	21.1
-0.30	20.8	20.8	20.8	20.8	20.7	20.8	20.9	20.8	21.2

-0.10	20.9	20.8	20.9	20.9	20.9	20.8	20.9	20.9	21.1
0.10	20.9	20.8	20.8	20.9	20.8	20.9	20.9	20.9	21.2
0.30	20.7	20.8	20.9	20.7	20.8	20.8	20.8	20.9	21.2
0.50	20.7	20.7	20.7	20.8	20.7	20.8	20.8	20.7	21.1
0.70	20.6	20.6	20.8	20.8	20.7	20.7	20.7	20.7	21.0
0.90	20.8	20.7	20.8	20.8	20.6	20.7	20.7	20.7	21.0

Table 7-28: Air speed measured in the horizontal plane at a height of 0.05 m for the 1.2 m x 0.6 m diffuser for a supply under-temperature of 2.5°C [m/s]

Distance from the axis [m] / Distance from the diffuser [m]	-0.9	-0.7	-0.5	-0.3	-0.1	0.1	0.3	0.5	0.7	0.9
0.16	0.10	0.09	0.09	0.10	0.07	0.05	0.12	0.12	0.11	0.09
0.36	0.14	0.15	0.15	0.13	0.09	0.04	0.13	0.16	0.14	0.09
0.56	0.17	0.20	0.18	0.17	0.14	0.17	0.19	0.22	0.16	0.12
0.76	0.17	0.21	0.24	0.24	0.27	0.26	0.28	0.22	0.18	0.14
0.96	0.18	0.20	0.24	0.27	0.27	0.29	0.27	0.21	0.18	0.17
1.16	0.17	0.18	0.21	0.26	0.25	0.25	0.26	0.20	0.16	0.16
1.36	0.17	0.18	0.21	0.25	0.23	0.22	0.24	0.21	0.18	0.15
1.56										
1.76	0.15	0.17	0.20	0.22	0.22	0.22	0.22	0.21	0.18	0.15
1.96	0.15	0.16	0.19	0.20	0.20	0.20	0.20	0.20	0.18	0.15
2.16	0.14	0.16	0.18	0.16	0.18	0.17	0.19	0.17	0.18	0.15
2.36	0.14	0.15	0.16	0.15	0.17	0.17	0.17	0.18	0.17	0.16
2.56	0.11	0.14	0.14	0.13	0.16	0.15	0.15	0.17	0.16	0.14

2.76	0.11	0.10	0.11	0.11	0.13	0.12	0.13	0.12	0.13	0.12
-------------	------	------	------	------	------	------	------	------	------	------

Table 7-29: Air temperature measured in the horizontal plane at a height of 0.05 m for the 1.2 m x 0.6 m diffuser for a supply under-temperature of 2.5°C [°C]

Distance from the axis [m] / Distance from the diffuser [m]	-0.9	-0.7	-0.5	-0.3	-0.1	0.1	0.3	0.5	0.7	0.9
0.16	20.7	20.6	20.6	20.4	20.6	20.4	20.4	20.4	20.6	20.8
0.36	20.5	20.6	20.1	20.1	19.9	20.1	20.2	20.5	20.6	20.8
0.56	20.4	20.3	20.0	19.9	19.9	20.1	19.9	20.2	20.4	20.6
0.76	20.5	20.4	20.1	20.2	20.5	20.4	20.3	20.4	20.5	20.6
0.96	20.5	20.4	20.4	20.5	20.5	20.4	20.3	20.6	20.6	20.5
1.16	20.6	20.6	20.6	20.6	20.7	20.6	20.5	20.7	20.6	20.6
1.36	20.7	20.7	20.7	20.5	20.7	20.9	20.7	20.5	20.7	20.6
1.56										
1.76	20.8	20.8	20.8	20.6	20.8	20.8	20.7	20.6	20.7	20.6
1.96	20.7	20.8	20.7	20.8	20.8	20.8	20.8	20.7	20.7	20.8
2.16	20.9	20.9	20.7	20.8	20.9	20.9	20.7	20.8	20.8	20.8
2.36	21.1	21.0	20.9	21.0	21.0	21.0	20.9	20.9	20.9	20.8
2.56	21.1	21.1	21.0	21.0	21.0	21.1	21.0	20.9	20.9	21.0
2.76	21.1	21.1	21.1	21.0	21.1	21.1	21.0	20.9	20.9	20.9

Measurements on the diffuser DF1W size 1.2 m x 0.6 m for an under-temperature of 5.5°C

Table 7-30: Air speed measured at 0.05 m from the diffuser for the 1.2 m x 0.6 m diffuser for a supply under-temperature of 5.5°C [m/s]

Distance from the longitudinal axis [m] / height [m]	-	-	-	-	-	-	0	0.05	0.10	0.15	0.20	0.25	0.30
	0.30	0.25	0.20	0.15	0.10	0.05	0	0.05	0.10	0.15	0.20	0.25	0.30
0.10	0.11		0.09		0.06		0.08		0.08		0.08		0.12
0.15							0.19						
0.20	0.17		0.18		0.17		0.16		0.18		0.25		0.09
0.25							0.12						
0.30	0.04		0.14		0.11		0.10		0.11		0.11		0.00
0.35							0.10						
0.40	0.03		0.15		0.10		0.10		0.11		0.13		0.00
0.45							0.10						
0.50	0.03		0.16		0.11		0.11		0.12		0.13		0.01
0.55							0.12						
0.60	0.02		0.14		0.12		0.12		0.12		0.12		0.01
0.65							0.12						
0.70	0.02		0.14		0.13		0.13		0.13		0.12		0.01
0.75							0.15						
0.80	0.02		0.13		0.14		0.15		0.14		0.12		0.01
0.85							0.15						
0.90	0.03		0.12		0.18		0.13		0.19		0.13		0.01
0.95							0.10						
1.00	0.02		0.01		0.15		0.08		0.17		0.03		0.01
1.05							0.08						

1.10	0.02		0.16		0.06		0.04		0.13		0.16		0.01
1.15							0.18						
1.20	0.02		0.19		0.19		0.19		0.15		0.16		0.01
1.25							0.01						
1.30	0.02		0.01		0.01		0.01		0.01		0.01		0.04

Table 7-31: Air temperature measured at 0.05 m from the diffuser for the 1.2 m x 0.6 m diffuser for a supply under-temperature of 5.5°C [°C]

Distance from the longitudinal axis [m] / height [m]	-	-	-	-	-	-	0	0.05	0.10	0.15	0.20	0.25	0.30
	0.30	0.25	0.20	0.15	0.10	0.05	0	0.05	0.10	0.15	0.20	0.25	0.30
0.10	18.5		18.3		18.3		18.2		18.4		18.5		18.7
0.15							18.0						
0.20	18.6		17.7		17.7		17.7		17.6		17.6		19.1
0.25							17.7						
0.30	19.7		17.7		17.7		17.8		17.7		17.7		20.2
0.35							17.9						
0.40	20.6		17.7		17.8		17.8		17.7		17.7		20.3
0.45							17.8						
0.50	20.8		17.7		17.7		17.7		17.7		17.8		20.4
0.55							17.6						
0.60	21.0		17.8		17.7		17.7		17.6		17.7		20.6
0.65							17.7						
0.70	21.0		18.2		17.7		17.6		17.7		17.7		20.3
0.75							17.8						

0.80	20.9		17.7		17.8		17.8		17.8		17.8		20.7
0.85							18.1						
0.90	21.2		18.1		17.9		18.1		18.1		18.0		20.6
0.95							18.2						
1.00	21.4		19.6		17.9		18.2		18.0		19.5		21.2
1.05							18.2						
1.10	21.4		20.5		18.5		18.4		18.0		19.5		21.3
1.15							17.9						
1.20	21.7		17.9		18.0		18.0		18.1		18.7		21.6
1.25							20.9						
1.30	21.9		21.3		21.4		21.5		21.5		21.4		21.7

Table 7-32: Air speed measured in the longitudinal plane for the 1.2 m x 0.6 m diffuser for a supply under-temperature of 5.5°C [m/s]

Height [m] / Distance from the diffuser [m]	0.02	0.03	0.04	0.05	0.06	0.07	0.08	0.1	0.2	0.26
0.16	0.22	0.21	0.20	0.19	0.18	0.14	0.11	0.06	0.15	0.09
0.36	0.07	0.09	0.10	0.14	0.12	0.13	0.14	0.19	0.23	0.17
0.56	0.32	0.36	0.33	0.36	0.29	0.26	0.23	0.19	0.06	0.03
0.76	0.39	0.40	0.35	0.35	0.29	0.25	0.22	0.15	0.03	0.03
0.96	0.37	0.37	0.33	0.32	0.25	0.22	0.18	0.13	0.04	0.04
1.16	0.33	0.34	0.30	0.29	0.23	0.21	0.18	0.12	0.05	0.05
1.36	0.31	0.30	0.28	0.27	0.22	0.20	0.18	0.16	0.06	0.04
1.56	0.26	0.28	0.27	0.25	0.23	0.21	0.19	0.16	0.07	0.05
1.76	0.24	0.25	0.26	0.25	0.22	0.21	0.20	0.18	0.08	0.06

1.96	0.21	0.22	0.24	0.22	0.21	0.20	0.20	0.17	0.09	0.07
2.16	0.20	0.20	0.22	0.22	0.21	0.19	0.19	0.17	0.09	0.07
2.36	0.17	0.20	0.20	0.20	0.19	0.19	0.19	0.16	0.09	0.07
2.56	0.16	0.18	0.18	0.18	0.18	0.18	0.18	0.16	0.09	0.08
2.76	0.15	0.16	0.17	0.18	0.17	0.16	0.16	0.16	0.08	0.07
2.96	0.14	0.15	0.16	0.16	0.15	0.16	0.15	0.15	0.09	0.08
3.16	0.12	0.13	0.14	0.14	0.13	0.14	0.14	0.13	0.09	0.08

Table 7-33: Air temperature measured in the longitudinal plane for the 1.2 m x 0.6 m diffuser for a supply under-temperature of 5.5°C [°C]

Height [m] / Distance from the diffuser [m]	0.02	0.03	0.04	0.05	0.06	0.07	0.08	0.1	0.2	0.26
0.16	18.3	18.3	18.3	18.3	18.6	18.6	18.5	18.2	17.8	18.0
0.36	18.1	18.1	18.0	18.0	17.9	17.9	18.0	17.9	18.3	19.0
0.56	18.1	18.2	18.5	18.9	18.9	19.1	19.4	19.8	20.5	20.8
0.76	18.6	18.9	19.2	19.4	19.6	19.7	20.0	20.3	20.7	21.2
0.96	18.9	19.1	19.5	19.6	19.8	19.9	20.1	20.2	20.7	21.2
1.16	19.2	19.3	19.5	19.6	19.8	19.9	20.0	20.1	20.6	21.2
1.36	19.4	19.6	19.6	19.7	19.8	19.9	20.0	20.0	20.6	20.9
1.56	19.7	19.7	19.8	19.8	19.9	19.9	19.9	20.0	20.5	20.6
1.76	20.0	19.9	19.9	19.8	19.9	19.9	19.9	20.0	20.4	20.5
1.96	20.3	20.1	20.0	20.0	20.0	20.0	20.0	20.0	20.4	20.5
2.16	20.4	20.3	20.2	20.1	20.1	20.1	20.1	20.1	20.3	20.5
2.36	20.5	20.4	20.3	20.2	20.2	20.1	20.1	20.1	20.4	20.4
2.56	20.6	20.6	20.5	20.3	20.2	20.3	20.2	20.2	20.4	20.4

2.76	20.7	20.7	20.5	20.4	20.4	20.4	20.4	20.3	20.4	20.4
2.96	20.7	20.7	20.7	20.5	20.5	20.4	20.4	20.4	20.5	20.4
3.16	20.9	20.8	20.7	20.5	20.6	20.5	20.5	20.5	20.5	20.4

**Table 7-34: Air speed measured in the transversal plane for the 1.2 m x 0.6 m diffuser for a supply under-temperature of 5.5°C
[m/s]**

Height [m] / Distance from the axis [m]	0.02	0.03	0.04	0.05	0.06	0.07	0.08	0.1	0.2
-0.90	0.15	0.16	0.16	0.16	0.16	0.16	0.16	0.14	0.09
-0.70	0.16	0.17	0.17	0.17	0.17	0.17	0.16	0.13	0.06
-0.50	0.18	0.19	0.19	0.19	0.18	0.18	0.16	0.14	0.07
-0.30	0.19	0.20	0.21	0.20	0.19	0.19	0.18	0.16	0.07
-0.10	0.19	0.20	0.22	0.21	0.22	0.20	0.19	0.18	0.09
0.10	0.20	0.21	0.22	0.22	0.21	0.21	0.20	0.18	0.08
0.30	0.21	0.22	0.23	0.23	0.23	0.22	0.21	0.18	0.08
0.50	0.21	0.22	0.23	0.22	0.21	0.20	0.19	0.17	0.08
0.70	0.17	0.19	0.20	0.19	0.19	0.19	0.18	0.17	0.10
0.90	0.14	0.16	0.16	0.16	0.16	0.16	0.15	0.14	0.10

**Table 7-35: Air temperature measured in the transversal plane for the 1.2 m x 0.6 m diffuser for a supply under-temperature
of 5.5°C [°C]**

Height [m] / Distance from the axis [m]	0.02	0.03	0.04	0.05	0.06	0.07	0.08	0.1	0.2
-0.90	20.5	20.5	20.3	20.3	20.2	20.2	20.3	20.3	20.4

-0.70	20.5	20.4	20.3	20.2	20.2	20.1	20.2	20.2	20.5
-0.50	20.4	20.3	20.2	20.2	20.1	20.0	20.2	20.2	20.5
-0.30	20.5	20.3	20.2	20.2	20.1	20.1	20.2	20.2	20.5
-0.10	20.5	20.4	20.2	20.2	20.1	20.1	20.2	20.2	20.5
0.10	20.4	20.4	20.2	20.1	20.1	20.1	20.1	20.2	20.5
0.30	20.3	20.3	20.1	20.0	20.0	19.9	20.0	20.1	20.4
0.50	20.2	20.1	20.0	19.9	19.9	19.9	20.0	20.0	20.3
0.70	20.3	20.2	20.1	20.0	20.0	19.9	20.0	20.0	20.1
0.90	20.4	20.3	20.2	20.1	20.1	20.0	20.0	20.0	20.1

Table 7-36: Air speed measured in the horizontal plane at a height of 0.05 m for the 1.2 m x 0.6 m diffuser for a supply under-temperature of 5.5°C [m/s]

Distance from the axis [m] / Distance from the diffuser [m]	-0.9	-0.7	-0.5	-0.3	-0.1	0.1	0.3	0.5	0.7	0.9
0.16	0.13	0.13	0.13	0.15	0.19	0.13	0.18	0.12	0.10	0.10
0.36	0.19	0.24	0.27	0.18	0.12	0.17	0.14	0.19	0.12	0.11
0.56	0.16	0.21	0.26	0.33	0.35	0.36	0.34	0.23	0.14	0.12
0.76	0.17	0.19	0.22	0.32	0.35	0.36	0.33	0.21	0.16	0.14
0.96	0.19	0.21	0.26	0.32	0.33	0.35	0.33	0.25	0.20	0.17
1.16										
1.36	0.19	0.21	0.25	0.29	0.29	0.30	0.30	0.26	0.21	0.17
1.56										
1.76	0.17	0.20	0.22	0.25	0.25	0.27	0.27	0.24	0.20	0.17
1.96	0.17	0.19	0.21	0.22	0.23	0.24	0.25	0.23	0.21	0.17

2.16	0.16	0.17	0.19	0.20	0.21	0.22	0.23	0.22	0.19	0.16
2.36	0.17	0.17	0.18	0.19	0.19	0.19	0.20	0.21	0.19	0.17
2.56	0.16	0.16	0.17	0.18	0.19	0.19	0.19	0.20	0.18	0.16
2.76	0.15	0.15	0.16	0.17	0.18	0.18	0.18	0.18	0.17	0.14

Table 7-37: Air temperature measured in the horizontal plane at a height of 0.05 m for the 1.2 m x 0.6 m diffuser for a supply under-temperature of 5.5°C [°C]

Distance from the axis [m] / Distance from the diffuser [m]	-0.9	-0.7	-0.5	-0.3	-0.1	0.1	0.3	0.5	0.7	0.9
0.16	19.4	19.5	19.3	18.7	18.3	18.6	18.6	19.1	19.2	19.1
0.36	19.0	18.8	18.1	17.9	18.0	18.0	17.9	18.2	19.3	19.2
0.56	19.2	19.1	19.2	18.8	18.7	18.8	19.0	19.3	19.3	19.2
0.76	19.4	19.3	19.4	19.3	19.2	19.3	19.3	19.5	19.4	19.3
0.96	19.4	19.4	19.4	19.3	19.4	19.5	19.3	19.4	19.3	19.3
1.16										
1.36	19.7	19.7	19.6	19.5	19.7	19.7	19.5	19.5	19.6	19.6
1.56										
1.76	19.9	19.9	19.8	19.8	19.8	19.8	19.7	19.7	19.7	19.8
1.96	20.1	20.0	19.9	19.9	20.0	19.9	19.9	19.8	19.9	20.0
2.16	20.3	20.2	20.2	20.2	20.2	20.1	20.0	19.9	20.0	20.1
2.36	20.3	20.2	20.2	20.2	20.2	20.2	20.1	20.0	20.0	20.2
2.56	20.3	20.3	20.2	20.3	20.3	20.3	20.2	20.1	20.1	20.2
2.76	20.3	20.4	20.3	20.3	20.3	20.4	20.2	20.1	20.1	20.1